


UNIVERSITY OF ALBERTA

**UDP-glucose dehydrogenase: A gene involved in the biosynthesis of
heparin-like GAGs is required for *dpp* signaling in
Drosophila melanogaster.**

by

Sam E. Scanga 

A thesis submitted to the Faculty of Graduate Studies and Research in partial fulfillment of the
requirements for the degree of Doctor of Philosophy

in

Molecular Biology and Genetics

Department of Biological Sciences

Edmonton, Alberta
Fall 2002



National Library
of Canada

Acquisitions and
Bibliographic Services

395 Wellington Street
Ottawa ON K1A 0N4
Canada

Bibliothèque nationale
du Canada

Acquisitions et
services bibliographiques

395, rue Wellington
Ottawa ON K1A 0N4
Canada

Your file Votre référence

Our file Notre référence

The author has granted a non-exclusive licence allowing the National Library of Canada to reproduce, loan, distribute or sell copies of this thesis in microform, paper or electronic formats.

The author retains ownership of the copyright in this thesis. Neither the thesis nor substantial extracts from it may be printed or otherwise reproduced without the author's permission.

L'auteur a accordé une licence non exclusive permettant à la Bibliothèque nationale du Canada de reproduire, prêter, distribuer ou vendre des copies de cette thèse sous la forme de microfiche/film, de reproduction sur papier ou sur format électronique.

L'auteur conserve la propriété du droit d'auteur qui protège cette thèse. Ni la thèse ni des extraits substantiels de celle-ci ne doivent être imprimés ou autrement reproduits sans son autorisation.

0-612-81261-8

Canada

UNIVERSITY OF ALBERTA

Library Release Form

Name of Author: Sam E. Scanga

Title of Thesis: UDP-glucose dehydrogenase: A gene involved in the biosynthesis of heparin-like GAGs is required for *dpp* signaling in *Drosophila melanogaster*.

Degree: Doctor of Philosophy

Year this Degree Granted: 2002

Permission is hereby granted to the University of Alberta Library to reproduce single copies of this thesis and to lend or sell such copies for private, scholarly or scientific research purposes only.

The author reserves all other publication and other rights in association with the copyright in the thesis, and except as herein before provided, neither the thesis nor any substantial portion thereof may be printed or otherwise reproduced in any material form whatever without the author's prior written permission.



Sam E. Scanga
727 Drury Lane,
Burlington,
Ontario, Canada
L7R 2X9

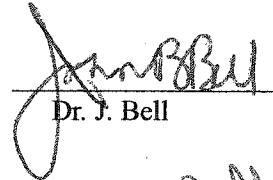
Sept 23/2002

UNIVERSITY OF ALBERTA
FACULTY of GRADUATE STUDIES and RESEARCH

The undersigned certify that they have read, and recommend to the Faculty of Graduate Studies and Research for acceptance, a thesis entitled " UDP-glucose dehydrogenase: A gene involved in the biosynthesis of Heparin-like GAGs which is required for *dpp* signalling in *Drosophila melanogaster*" submitted by Sam E. Scanga in partial fulfillment of the degree of Doctor of Philosophy in Molecular Biology and Genetics, Department of Biological Sciences.



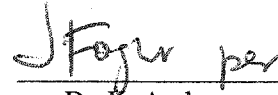
Dr. M. A. Russell



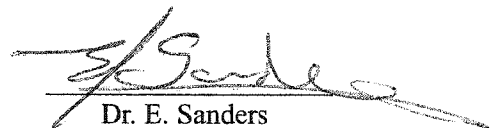
Dr. J. Bell



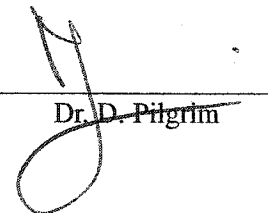
Dr. W. Gallin



Dr. K. Anderson



Dr. E. Sanders



Dr. D. Pilgrim

Aug 25 / 2002

To my wife Deanna
Thanks for your patients

ABSTRACT

In the fruit fly *Drosophila melanogaster* imaginal discs are the precursors of adult epidermal structures. The determination of cell fate and pattern in imaginal discs is believed to be specified by a positional information system involving cell-cell interactions. Pattern regulation during regeneration of imaginal discs provides a useful experimental model system with which to identify genes involved in pattern formation for developing cellular systems. I identify a P-element line (*A64*) from an enhancer trap screen during regeneration of the imaginal discs (Brook et al., 1993); this P-element is inserted in the gene for the *Drosophila* homolog of UDP-glucose dehydrogenase (UDP-GlcDH). Here I demonstrate, by genetic and expression analysis, a novel function for UDP-GlcDH. The evidence suggests that UDP-GlcDH is required in mediating the *dpp* signaling pathway during *Drosophila* development. *Dpp* is a member of the Transforming Growth Factor- β /Bone Morphogenetic Protein (TGF β /BMP) superfamily of growth factors, which are required for both dorsal-ventral axis patterning of the embryo and pattern formation in imaginal discs. UDP-GlcDH is a cytoplasmic enzyme required for the production of UDP-glucuronate. UDP-glucuronate is a precursor required for the biosynthesis of various glycosaminoglycans (GAGs) in the Golgi body of a cell after synthesis, these GAGs are exported to the extracellular matrix (ECM). Heparan sulfate is a complex heparin-like glycosaminoglycan (GAG) that is covalently linked to the protein core of various glycoproteins called proteoglycans. Proteoglycans are integral components of the ECM that are either bound to the outer surface of the cell membrane or are secreted into the ECM. Heparan sulfate proteoglycans (HSPGs) have been implicated in regulating the signaling of various growth factors, such as TGF β /BMP in vertebrates. In this study, I demonstrate that UDP-GlcDH is critical in mediating cellular responses to *dpp* signaling, both in dorsal-ventral axis specification of the embryo and in axial patterning of imaginal discs. I also show that the loss of UDP-GlcDH function during regeneration in imaginal leg discs prevents pattern respecification. Lastly, I present preliminary evidence that suggests this regulation by UDP-GlcDH may be due to its involvement in the biosynthesis of heparan sulfate GAGs.

ACKNOWLEDGEMENTS

First, I would like to acknowledge my supervisor, Dr. Mike Russell, for his patience and guidance throughout my time in his laboratory. Also, I would like to thank him for the freedom he gave me in doing my work, as well as for his insight and help in discussing the work. In addition, I would like to thank my committee members, Dr. J. Bell and Dr. W. Gallin, for their input and for their constructive criticism of my experiments. I would also like to thank Dr. D. Pilgrim and Dr. E. Sanders for their helpful suggestions on the thesis.

I also wish to thank the people in the lab. In particular, I acknowledge Ariel Finkielstein for his help with techniques and numerous discussions about the data, Lisa Ostafichuk for her help in the lab and for making it a pleasure to come to work, and Don Price, John Higgins, and Dave Dansereau for their enthusiasm and discussions on scientific matters. I would like to thank all these people for the great environment they cultivated in the laboratory.

Further thanks are due to Dr. Armen Manoukian and the members of his laboratory. In particular, Dr. Rich Binari and Norman Anthopoulos provided me with several reagents and shared unpublished data that were indispensable in helping me reach conclusions. Thanks is due to Norm for help on the computer. A special thank you is also due to Eugene Chomey and Dr. Bill Addison for their technical help in the molecular analysis and to Elaine Street for editorial assistance.

Finally, I would like to express my gratitude to the rest of those who directly or indirectly helped me in my research, with material or useful advice, and made my stay enjoyable. An incomplete list includes: Bill Clark, Gary Ritzel, Daralen Hodgetts, Dr. Dave Nash, Dr. John Locke, Effie Woloshlyn, Scott Hanna, John Osborne, Dave Hansen, Ali Riazi, Song Hu, Kelly Soanes, Gwen Jewett, Dawna, and the confocal guys. To everyone I have mentioned and to those whom, regrettably, I may not have mentioned, I sincerely thank you.

TABLE OF CONTENTS

I. INTRODUCTION	1
I-1 Pattern formation	1
I-2 <i>Drosophila</i> : a genetic model system for pattern formation	5
I-3 The imaginal disc as a model for pattern formation in a cellular system	7
I-3i Determination of imaginal discs	7
I-3ii Regulative properties of imaginal discs	11
I-4 Models for positional information	14
I-4i The gradient of developmental capacity model	14
I-4ii The polar coordinate model	16
I-4iii The compartment boundary model	19
I-5 The genetic and molecular basis of pattern formation in imaginal discs in <i>Drosophila</i>	21
I-5i Segment polarity genes required to specify both the imaginal disc primordia in the embryo and the larval segmentation pattern	22
I-5ii Segment polarity genes and the compartment boundary model in imaginal discs	25
I-6 Morphogen gradients in imaginal discs	33
I-6i <i>Decapentaplegic</i> acts as a morphogen to specify positional information in imaginal discs	35
I-7 Regeneration, a model for discovering new genes involved in pattern formation	37
I-8 Objectives	40
I-8i Specification of the dorsal-ventral axis in the <i>Drosophila</i> embryo	40
I-8ii UDP-glucose dehydrogenase, a gene required in pattern formation	52
I-8iii The HSPGs in the ECM and their role in regulating growth factor signaling	53
I-8iv The biological roles of HSGAGs and their biosynthetic enzymes in development	57
 II. MATERIALS and METHODS	 63
II-1 <i>Drosophila</i> culture	63
II-2 <i>Drosophila</i> lines	63
II-3 Bacterial and phage stocks	66
II-4 Screening of PZ-enhancer trap lines using the <i>su(f)¹²</i> temperature-sensitive autonomous cell lethal mutation	66
II-5 Screen for ectopic activation of <i>Gal4</i> insertions during <i>su(f)¹²</i> induced regeneration in imaginal leg discs	68
II-6 Genetic analysis of the PZ-lethal phenotype of the UDP-GlcDH mutant <i>sgl</i>	70
II-6i Cuticle preparations	70
II-6ii Crosses to generate embryos heterozygous for <i>sgl</i> (UDP-GlcDH) and mutations in the <i>dpp</i> pathway	70

II-6iii	Crosses made to analyze ectopic heparinase III effects in the embryo	70
II-6iv	Epistasis analysis of <i>sgl</i> ^{P1731} with <i>dpp</i>	71
II-6v	Analysis of <i>sgl</i> ^{P1731} interactions with <i>dpp</i> in trans-heterozygous adults.....	71
II-6vi	Mosaic analysis of <i>sgl</i> ^{P1731} (UDP-GlcDH) mutations in the adult wing and leg	71
II-6vii	Analysis of the effects of ectopic heparinase III expression on the adult phenotype	72
II-6viii	Analysis of the effects of ectopic UDP-GlcDH expression on the embryonic and adult phenotypes	72
II-7	Histochemical techniques	72
II-7i	Staining for β -galactosidase activity in imaginal discs and disc fragments	72
II-7ii	Staining of embryos for β -galactosidase activity	73
II-7iii	Immunostaining of imaginal discs	73
II-7iv	Immunostaining of embryos	74
II-7v	<i>In situ</i> hybridization of embryos	75
II-7vi	<i>In situ</i> hybridization of imaginal discs	76
II-7vii	Photomicroscopy of tissues	77
II-7viii	<i>In situ</i> hybridization of polytene chromosomes	77
II-8	DNA extractions and manipulations	78
II-8i	Plasmid purification	78
II-8ii	Restriction digests	78
II-8iii	DNA fragment purification	79
II-8iv	Southern blotting	79
II-8v	Plasmid rescue of <i>A64 PZ</i> -lethal insertion line	79
II-8vi	Subcloning of rescued genomic DNA fragment into pBS-KS+ plasmids	83
II-9	Molecular cloning of the <i>Drosophila</i> UDP-glucose dehydrogenase	83
II-9i	Plating and screening of a <i>Drosophila lambda gt10</i> embryonic cDNA library	81
II-9ii	Isolation of cDNA from <i>lambda gt10</i> clones	83
II-9iii	Subcloning and sequencing of <i>Drosophila</i> UDP-GlcDH cDNA	83
II-10	Developmental Northern analysis.....	85
II-10i	Isolation of mRNA	85
II-10ii	Northern blotting	85
II-11	DNA Labeling	85
II-11i	Labeling by random priming with Digoxigenin dUTP.....	85
II-11ii	Digoxigenin-dUTP labeling by PCR run-off	85
II-11iii	Labeling DNA with P ³² by random priming	86
II-11iv	P ³² labeling of DNA by PCR run-off	86

III. RESULTS	87
III-1 Identifying genes involved in imaginal disc patterning	87
III-1i LacZ misexpression screen of PZ-lethal insertions	87
III-1ii PZ-lethal insertion lines selected for further analysis based on lethal embryonic mutant phenotypes	89
III-1iii A64, the PZ-lethal insertion line selected for further analysis.....	90
III-2 Genetic analysis of the A64 insertion	96
III-2i Segregation analysis of the A64 insertion	96
III-2ii Physical mapping of the A64 P{lacZ ry+} insertion using polytene chromosomes	99
III-2iii Reversion of the A64 embryonic lethal phenotype by excision of the P{lacZ ry+} insertion	99
III-2iv Genetic mapping and complementation analysis of A64.....	99
IV-2v Genetic analysis of A64 alleles	103
III-3 Molecular analysis of the A64 PZ-lethal insertion line	107
III-3i Cloning of flanking DNA by P-element rescue.....	107
III-3ii Isolation of <i>Drosophila</i> UDP-GlcDH cDNA	111
III-3iii Rescue of the A64 zygotic embryonic lethal phenotype by <i>Drosophila</i> UDP-glucose dehydrogenase cDNA expression.....	116
III-3iv Expression pattern of UDP-GlcDH in the <i>Drosophila</i> embryo and imaginal discs	118
III-4 Developmental effects of the UDP-GlcDH gene in <i>Drosophila</i> embryos	121
III-4i <i>Drosophila</i> UDP-GlcDH zygotic mutations result in loss of dorsal specific gene expression	121
III-4ii Genetic interactions between UDP-GlcDH and <i>dpp</i> signaling pathway genes	123
III-4iii Regulation of <i>dpp</i> expression by UDP-GlcDH	129
III-4iv Epistasis analysis of UDP-GlcDH and <i>dpp</i> mutations	132
III-4v Mosaic analysis of UDP-GlcDH function in imaginal discs	134
III-4vi Ectopic expression of heparinase III in cellularized embryos	140
III-4vii Ectopic expression of UDP-GlcDH results in dorsalized embryos	143
III-5 Role of UDP-GlcDH function in imaginal disc pattern formation	145
III-5i Regulation of <i>dpp</i> signaling by UDP-GlcDH during imaginal disc patterning	145
III-5ii Ectopic expression of heparinase III in imaginal discs causes adult patterning defects.....	148
III-5iii Ectopic expression of UDP-GlcDH in imaginal discs	150
III-6 UDP-GlcDH organizer-like function is required during pattern regulation in regenerating imaginal leg discs in <i>Drosophila</i>	153
III-6i Misexpression of <i>hh</i> , <i>ptc</i> , <i>wg</i> , and <i>dpp</i> in duplicating imaginal discs	153
III-6ii UDP-GlcDH and heparan sulfate GAGs are ectopically expressed during pattern regulation of leg imaginal discs in <i>su(f)¹²</i> mutants	158

III-6iii	UDP-GlcDH is required for distal organizer function in imaginal leg discs	160
IV.	Discussion	165
IV-1	Isolating novel genes involved in pattern formation	165
IV-2	Isolation of the <i>Drosophila</i> homolog of UDP-glucose dehydrogenase	167
IV-2i	Loss of UDP-glucose dehydrogenase inhibits <i>dpp</i> signaling in the embryo	168
IV-2ii	Role of UDP-GlcDH in <i>dpp</i> signaling during <i>Drosophila</i> embryo development	171
IV-3	The role of heparan sulfate proteoglycans in <i>dpp</i> signaling in the <i>Drosophila</i> embryo	176
IV-3i	Heparan sulfate GAGs and their role in <i>dpp</i> signaling in <i>Drosophila</i> embryos	176
IV-3ii	Models for heparan sulfate GAG modulation of <i>dpp</i> signaling in <i>Drosophila</i> embryos	183
IV-4	The role of heparan sulfate GAGs in regulating the DPP morphogen in imaginal discs in <i>Drosophila</i>	187
IV-4i	ECM molecules that regulate WG and HH diffusion: an analogous mechanism for the DPP morphogen gradient in imaginal discs	187
IV-4ii	Heparan sulfate GAGs may regulate the ECM distribution of DPP in imaginal discs	194
IV-5	Role of the ECM during regeneration	200
V.	Summary	205
VI.	References	207
Appendix I.	Synthesis pathway for the formation of UDP-sugars	253
Appendix II.	The structure of disaccharide residues of different glycosaminoglycan chains	254
Appendix III.	The heparin and heparan sulfate biosynthetic pathway	255
Appendix IV.	Sequence of the 1.8 kb {A64(1-1)(3R)} rescued genomic DNA fragment containing the 5' translation start site for <i>Drosophila</i> UDP-GlcDH	256

LIST OF FIGURES

Figure 1.	Wolpert's model for the operation of positional information	3
Figure 2.	Fate map for domains of the mesothoracic imaginal leg disc	9
Figure 3.	Pattern regulation of two complementary imaginal leg disc fragments	12
Figure 4.	Pattern regulation in terms of the gradient of developmental capacity model ...	15
Figure 5.	The polar coordinate model of positional information during axial patterning in imaginal leg discs.....	17
Figure 6.	The boundary model for the specification of positional information to explain pattern formation in imaginal leg discs	20
Figure 7.	Establishing the imaginal disc primordia during <i>Drosophila</i> embryogenesis	23
Figure 8.	Genetic model for specifying A/P and D/V compartment identity in the imaginal leg disc	26
Figure 9.	Model for establishing the proximal-distal organizer in the imaginal leg disc	29
Figure 10.	The effects of ectopic <i>hh</i> expression on proximal-distal axis formation in an imaginal leg disc	31
Figure 11.	The effects of ectopic expression of <i>wg</i> and <i>dpp</i> on proximal-distal axis formation in an imaginal leg disc	34
Figure 12.	Duplication of adult legs in <i>Drosophila melanogaster</i> caused by the <i>su(f)¹²</i> temperature-sensitive autonomous cell-lethal mutation	39
Figure 13.	Maternal regulatory pathway that determines D-V polarity in the <i>Drosophila</i> oocyte	41
Figure 14.	Maternal regulatory pathway of dorsal group genes that determine D-V polarity in the <i>Drosophila</i> embryo	43
Figure 15.	Expression of early zygotic genes required to determine D-V polarity in the <i>Drosophila</i> embryo	47
Figure 16.	Current model for the canonical <i>dpp</i> /TGF β /BMP signal pathway in <i>Drosophila</i>	49
Figure 17.	<i>In vivo</i> models of cell surface HS proteoglycan function	55
Figure 18.	Proteoglycans and glycosaminoglycan biosynthetic pathway enzymes identified in <i>Drosophila</i> and <i>C. elegans</i> genetic mutant screens	61
Figure 19.	<i>P</i> { <i>lacZ ry+</i> }-plasmid element used in the regeneration enhancer trap screen in this study	67

Figure 20.	A screen for <i>Gal4</i> lines that are activated upon <i>su(f)¹²</i> -induced regeneration in imaginal leg discs	69
Figure 21.	Plasmid rescue of left and right genomic flanking DNA sequence from the <i>A64</i> PZ insertion line	82
Figure 22.	Expression of lacZ in leg discs following 29°C heat treatment of <i>su(f)¹²/+</i> ; <i>A64/+</i> mutant larvae.	93
Figure 23.	LacZ expression in an <i>A64</i> 3/4+EK lateral leg disc fragment	93
Figure 24.	<i>A64</i> PZ-lethal zygotic embryonic mutant phenotype.....	95
Figure 25.	LacZ expression pattern of <i>A64</i> PZ insertion during embryonic development	97
Figure 26.	Segregation analysis of the lethal phenotype of <i>A64</i>	98
Figure 27.	Cytological mapping of the PZ insert in the <i>A64</i> line using polytene chromosome squashes	100
Figure 28.	Generation of revertants of the <i>A64</i> PZ-lethal phenotype	101
Figure 29.	Cuticle phenotype of embryos homozygous for <i>sgl</i> alleles	104
Figure 30.	Schematic alignment of the <i>A64</i> (1-1) (3R) rescued genomic fragment with the 5.8 kb genomic clone at 65D	109
Figure 31.	<i>In situ</i> hybridization of Digoxigenin-labeled <i>A64</i> (1-1) (3R) genomic DNA flanking sequence onto Ore-R polytene chromosome squashes	110
Figure 32.	Lambda gt10 clones isolated from a <i>Drosophila</i> embryonic cDNA library (Huynh et al., 1985)	112
Figure 33.	Cytological mapping of the 7-A3 cDNA clone to <i>Ore-R</i> polytene chromosomes	113
Figure 34.	Comparison of the deduced amino acid sequence of various UDP-GlcDH proteins	115
Figure 35.	Developmental Northern blot showing the expression profile of UDP-GlcDH RNA in <i>Drosophila melanogaster</i>	119
Figure 36.	Expression of the UDP-GlcDH transcripts in <i>Drosophila</i> embryos	120
Figure 37.	Expression of the UDP-GlcDH transcript in the imaginal leg disc	120
Figure 38.	Loss of UDP-GlcDH blocks <i>dpp</i> signaling	122
Figure 39.	Genetic interactions among <i>sgl^{P1731}</i> , <i>dpp</i> , <i>thv</i> , and <i>punt</i> mutants	125
Figure 40.	Expression of the UDP-GlcDH transcript in WT and <i>dpp²⁷</i> mutant embryos	130
Figure 41.	Expression of <i>dpp</i> in WT and <i>sgl^{P1731}</i> mutant embryos	131
Figure 42.	Suppression of the ectopic effects of <i>dpp</i> by the <i>sgl^{P1731}</i> mutation	133
Figure 43.	Somatic clonal analysis of <i>sgl^{P1731}</i> mutation in the imaginal leg disc	136

Figure 44.	Effects of <i>sgl</i> ^{P1731} somatic clones in adult legs and wings	137
Figure 45.	Expression of heparinase III degradative enzyme inhibits <i>dpp</i> signaling in the embryo	141
Figure 46.	Effects of ectopic expression of UDP-GlcDH in the embryo	144
Figure 47.	Genetic interactions between <i>sgl</i> ^{P1731} mutant and <i>dpp</i> disc mutant alleles in the wing and leg	146
Figure 48.	Morphological abnormalities induced by heparinase III expression in imaginal discs	149
Figure 49.	Morphological defects in adult legs induced by ectopic expression of UDP-GlcDH in imaginal discs	152
Figure 50.	Misexpression of segment polarity genes during pattern regulation of imaginal leg discs induced in the <i>su(f)</i> ^{I2} mutant	154
Figure 51.	Overlapping ectopic expression of <i>wg</i> and <i>dpp</i> during pattern regulation of imaginal discs in the <i>su(f)</i> ^{I2} mutant	157
Figure 52.	UDP-GlcDH transcript and heparan sulfate GAG misexpression during pattern regulation of imaginal leg discs in the <i>su(f)</i> ^{I2} mutant	159
Figure 53.	Identification of <i>Gal4</i> lines that are ectopically activated during pattern regulation of imaginal leg discs in the <i>su(f)</i> ^{I2} mutant	162
Figure 54.	Adult defects induced by the expression of heparinase III degradative enzyme in imaginal leg discs during pattern regulation in the <i>su(f)</i> ^{I2} mutant	163
Figure 55.	Models for <i>dpp</i> signaling cascade involving HSPG regulation	184

LIST OF TABLES

Table 1.	<i>Drosophila</i> and <i>C. elegans</i> mutants affecting proteoglycan and glycosaminoglycan biosynthesis	59
Table 2.	<i>Drosophila</i> strains used in this study	63
Table 3.	<i>E. coli</i> and phage strains used in this study	66
Table 4.	Autosomal <i>Gal4</i> insertion lines	68
Table 5.	List of primers used to sequence the 7-3 <i>lambda</i> gt10 cDNA clone	84
Table 6.	Selection of <i>PZ</i> -lethal lines showing differential expression during pattern respecification	88
Table 7.	<i>PZ</i> -lethal insertion lines selected for differential expression during regeneration induced by the <i>su(f)¹²</i> mutant	89
Table 8.	Zygotic embryonic mutant phenotypes of <i>PZ</i> -lethals from the regeneration screen	91
Table 9.	Segregation analysis with the <i>A64</i> <i>PZ</i> -lethal phenotype	98
Table 10.	Complementation analysis of the <i>A64</i> <i>PZ</i> -lethal insertion	102
Table 11.	Percentage of <i>sgl</i> mutant embryos that failed to hatch that showed a U-shaped phenotype	105
Table 12.	Cytological positions of the cDNA clones on <i>Oregon-R</i> polytene chromosomes	113
Table 13.	Rescue of the <i>sgl^{A64}</i> and <i>sgl^{P1731}</i> zygotic embryonic mutant phenotype with ectopic expression of full-length <i>sgl</i> cDNA	117
Table 14.	Results of trans-heterozygous genetic interactions among <i>sgl</i> and the <i>dpp</i> pathway mutant alleles	126
Table 15.	Mosaic analysis of <i>sgl^{P1731}</i> somatic clones in the adult wing and leg	138
Table 16.	Frequency of lethal phenotype in heparinase III treated embryos	142
Table 17.	Number of lethal and dorsalized phenotypes generated by ectopic expression of UDP-GlcDH (<i>sgl</i> cDNA) during embryogenesis	144
Table 18.	Frequency of dominant negative genetic interaction between <i>sgl^{P1731}</i> and <i>dpp</i> loss-of-function disc mutants in the adult wing and leg	147
Table 19.	Frequency of defects observed with heparinase III treatment of imaginal discs	149

ABBREVIATIONS

3/4L-EK	three-quarter lateral leg imaginal disc fragment with end-knob
1/4UM	one-quarter upper medial lateral leg disc fragment
<i>al</i>	<i>aristaless</i>
AP	alkaline phosphatase
A/P	anterior/posterior compartment boundary
A-P	anterior-posterior axis
<i>arm</i>	<i>armadillo</i>
as	amnioserosa
bp	base pair
cDNA	complementary DNA
<i>cact</i>	<i>cactus</i>
<i>ci</i>	<i>cubitus interruptus</i>
c.i.	confidence interval
CyO	Curly of Oster (a second chromosome balancer)
<i>dally</i>	<i>division abnormally delayed</i>
<i>Dfz2</i>	<i>Drosophila frizzled-2</i>
DIG	Digoxigenin
<i>dl</i>	<i>dorsal</i>
<i>Dll</i>	<i>Distalless</i>
D/V	dorsal/ventral compartment boundary
D-V	dorsal-ventral axis
DMSO	dimethylsulphoxide
DNA	deoxyribonucleic acid
<i>dpp</i>	<i>decapentaplegic</i>
EDTA	ethylene-diamine-tetra-acetic acid
ECM	extracellular matrix
<i>en</i>	<i>engrailed</i>
<i>eve</i>	<i>evenskipped</i>
FLP	P-insertion carrying a Flip recombinase gene
FM7,c	First Multiple 7 (an X chromosome balancer)
FRT	P-insertion carrying a Flip recombinase target sequence
GAGs	glycosaminoglycans
GAL4	Galactose 4 (a yeast transcriptional activator)
<i>gb</i>	<i>glass bottom boat</i>
GPI	glycosylphosphatidylinositol
grk	<i>gurken</i>
HS	heparan sulfate
<i>hh</i>	<i>hedgehog</i>

kb	kilobases
kbp	kilobasepair
Kr	<i>Kruppel</i>
lacZ	<i>E. coli</i> lactose Z gene
NBT	nitroblue tetrazolium chloride
ndl	<i>nudel</i>
omb	<i>optomotor blind</i>
Ore-R	<i>Oregon-R</i> (wild-type fly strain)
PCR	polymerase chain reaction
PBS	phosphate-buffered saline
PBT	0.1% Tween 20 in 1X PBS
P/D	proximal/distal compartment boundary
P-D	proximal-distal axis
pfu	plaque-forming unit
pip	<i>pipe</i>
ps	posterior spiracles
prd-dpp	<i>pairedGAL4; UASdpp</i> line
ptc	<i>patched</i>
RNA	ribonucleic acid
RT	room temperature
thv	<i>thickveins</i>
sax	<i>saxophone</i>
sgl	<i>sugarless</i>
sfl	<i>sulfateless</i>
shn	<i>schnurri</i>
sog	<i>short gastrulation</i>
spz	<i>spatzle</i>
smo	<i>smoothened</i>
TAE	Tris-acetate EDTA
tin	<i>tinman</i>
tld	<i>tolloid</i>
TM3	Third multiple inverted (a third chromosome balancer)
top	<i>torpedo</i>
UAS	Upstream Activation Sequence (the <i>Gal4</i> binding site)
UDP-GlcDH	UDP-glucose dehydrogenase
UDP	uridine diphosphate
wg	<i>wingless</i>
wind	<i>windbeutel</i>
X-Gal	5-Bromo, 4-chloro, 3-indolyl galactose
X-phosphate	5-Bromo, 4-chloro, 3-indolyl phosphate

I. INTRODUCTION

Development is the process that mediates the transformation of a single-celled zygote into a complex multicellular metazoan. This involves the regulation of growth, cell division and cell differentiation based on differential gene expression. The mechanism by which these processes are coordinated to generate a spatially-organized pattern of cells with different developmental fates is called pattern formation. Elucidating the mechanism of pattern formation is a basic goal of developmental biology.

I-1. Pattern formation.

Pattern formation is the process by which a genetically identical group of cells can adopt distinct fates that are appropriate for their positions in a cellular field or in a cell lineage. This leads to the differentiation of an organized pattern of diversified cells. Classical embryologists showed that the fate of a cell in many but not all organisms, depended on its position in the embryo. In some experimental systems, when certain fragments of an embryo were isolated and cultured, the cells differentiated according to their normal fates. Thus these embryos were thought to behave as "mosaics" consisting of self-differentiating parts that have fixed cell fates. Based on this observation, it was hypothesized that the cytoplasm of the fertilized egg might contain a pre-existing distribution of localized cytoplasmic determinants (reviewed in Slack, 1991). These cytoplasmic determinants would be segregated into different cell lineages at cleavage and could therefore determine the fates of cells based on a cell's position in the embryo, so that cell fate would be fixed prior to cell division. Models of this kind are called neo-preformationist (Davidson, 1968).

However, many embryos showed different behaviors. When cells were ablated at post-cleavage stages, the remaining cells acted in a coordinated manner that compensated for the missing cells, leading to the complete reestablishment of the normal pattern in the embryo. This phenomenon was called pattern regulation. Further investigations showed that cell fates in these embryos were not always fixed by cell lineage. The grafting experiments of Spemann and Mangold in 1924 (cited in Slack, 1991) using the embryos of the amphibian *Triturus* showed that ectopically-positioned cells from the dorsal blastopore lip in ventral regions of the embryo could trigger ectopic gastrulation, thus producing a secondary dorsal-anterior body axis. The secondary axis consisted of cells from both the host and grafted tissue, showing that the dorsal blastopore lip had organizing activity that was able to exert a long-range influence on the adjacent ventral cells to specify a new axis. Thus the fates of the ventral cells were not fixed. This could not be explained by a pre-localized set of cytoplasmic determinants. Spemann (1938) proposed that the long-range influence of the dorsal blastopore lip was a result of cell-cell interactions involving a series of induction events. In this case, a secreted molecule would stimulate neighboring cells to express a second factor, which in turn would stimulate the expression of additional factors in other cells, thereby generating a chain of inductive signals. The recipient cells somehow are able to sense and interpret their environment, perhaps responding to inductive signals from the dorsal lip that act as cell fate determinants. This suggested that some "epigenetic" mechanism must be

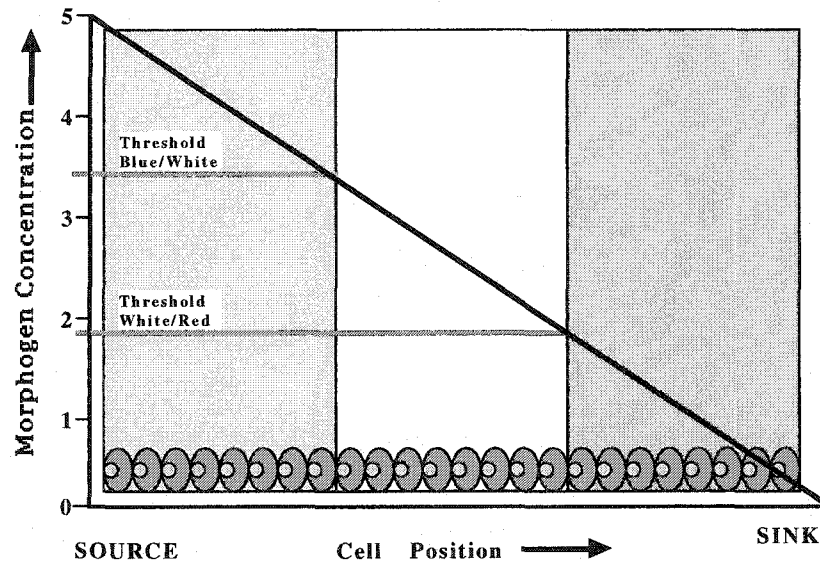
necessary in development, implying that interaction between constituents of the egg can give rise to patterns not initially present (Waddington, 1959). Today, this is understood as a problem of how the information for pattern encoded in the genome is decoded during development.

These properties of embryos suggested that development may proceed by a regulative process. For example, an early embryo, or part of a later embryo, possesses regulative properties which may be explained if the cells' fates are defined by their positions in the field relative to a signal source like the Spemann organizer (dorsal blastoderm lip). From studies that demonstrated the local autonomy of pattern mutations in genetic mosaics, Stern (1968) postulated that the competence of a cell to differentiate a pattern element was dependent on the ability of its genome to correctly respond to local singularities (e.g. peaks of morphogen concentration) in a global prepattern. Wolpert (1969) then formulated an alternative hypothesis, referred to as the positional information model. This model described in formal terms how cells within a regulative field may adopt particular fates that are appropriate for their positions. He argued that, in a regulative field, cells respond not to singularities in a pre-pattern, but acquire positional information (values) about their locations within a developing field according to an underlying global coordinate system. A field in this model is a set of cells that have their position specified by the same global coordinate system. The cells may collectively establish these global positional values by means of a smoothly-changing variable, giving every cell a unique value to specify its position. In this model, each cell would interpret its local coordinate values and differentiate as a specific cell type. This model left open the question of the nature of the biochemical mechanism responsible for generating the positional information to which the cells responded.

One popular hypothesis at the time was that spatial information is formed within a tissue by a group of cells that express an extracellular factor that diffuses over a long distance within a developmental field. Such a diffusible factor would accumulate in the form of a gradient and act as a morphogen capable of triggering distinct responses at different distances from the localized source of the signal as a function of its changing concentration, influencing the behavior of cells in a developmental field (Lawrence, 1966; Stumpf, 1966; Lawrence, 1972; Sander, 1975; Tickle et al., 1975). This was an alternative to Spemann's (1938) earlier model in which he proposed that spatial information in a field could be specified by a series of local short-range inductive signals (reviewed by Jacobson and Sater, 1988; Tomlinson, 1988).

Morphogen concentration gradients were proposed as early as the 1930s by Child to explain the properties of several developing and regenerating systems (cited in Wolpert, 1969). Turing (1952) defined a morphogen as a form-generating substance that is expressed by a group of cells in a field which moves through the field providing neighboring cells with information about their relative position. While Wolpert's positional information model does not absolutely require that a morphogen gradient must be used to generate positional information, this has remained the most attractive version of the model (**Figure 1**). Wolpert illustrated this idea by imagining a flat layer of cells, which differentiates a one-dimensional pattern of a French flag. In such a system, the concentration of the morphogen

Figure 1. Wolpert's model for the operation of positional information.



According to the Wolpert model, positional information is delivered by a gradient of a diffusible morphogen from a source to a sink. A soluble substance (morphogen) diffuses from a source where it is produced, to a sink where it is degraded, thereby establishing a continuous range of concentrations within a cellular field. In this French flag model, a source is postulated to exist on the left hand margin of the blue stripe, and the sink is located at the right hand margin of the red stripe. A concentration gradient is thus formed, with the highest concentration at one end of the tissue and the lowest concentration at the other. All cells are assumed to be pluripotent, so that the specification of cell fate is accomplished by the concentration of the morphogen. In other words, each cell would interpret the gradient of information by measuring the local concentration of the morphogen. This would specify a developmental response that is restricted by the position of a cell in the gradient, thus activating genes required for a specific developmental pathway. For example, cells receiving a large amount of morphogen would become (or differentiate into) a blue cell. However, there are threshold concentrations of a morphogen below which cells would become white or red (Wolpert, 1969).

declines in a continuous fashion with distance from the cells that express the morphogen at the edge of a field. This provides a graded series of local concentrations that elicit specific responses by cells as a function of their distances from the source. In the second stage of this process, each cell would measure the local morphogen concentration which is translated into positional values that specify different cell identities in a field in a concentration dependent manner (reviewed by Wolpert, 1989). Thus, the position of a specific cell and its fate is determined by a cell's response to the concentration gradient, activating a specific developmental program (gene expression) at discrete thresholds. This model uncouples positional information from the final differentiation behavior of cells. Thus interpretation of a positional value (cell differentiation) will depend on the genetic constitution (or competency) of a cell which in turn is determined by its developmental history. Therefore, the same positional information (global coordinate system) could be used by different fields in different developmental contexts, to produce different patterns.

In addition to the experiments in *Triturus* by Spemann (1938), that defined the Spemann organizer, other studies indicated similar examples of organizing centers in other biological systems. One early piece of evidence was illustrated in the regeneration of *Hydra* (cited in Sang 1984). *Hydra* differentiates as a one-dimensional linear array of cells, which contains a head (apical hypostome), a stalk and a basal disc. The arrangement of these three organs reflects a polarity (directionality) in the pattern of cell fates along the apical-basal axis. When a hydra is cut in half the fragments behave as a regulative field. Specifically, the half containing the basal disc will form a new apical structure, and the apical half will generate a new base. If a hydra is cut perpendicular to the body axis into several pieces, every region of the stalk can regenerate into an entire proportionally-correct organism, with both a basal disc and an apical hypostome. Yet, the basal disc and apical hypostome only form at the basal and apical ends, respectively, of any excised piece of tissue. Thus, the spatial information in this case appears to have directionality. One way to explain this property is to argue that the positional information is defined by a diffusible factor that forms a gradient of information with a polarity defined by its origin at one pole. In any fragment, there must be a re-establishment of the original gradient (positional information), cued by the remaining polarity in the fragment, to explain the regeneration of the lost tissue. A model involving two interacting morphogens was found to be minimally sufficient to account for this regulative behavior (Webster and Wolpert, 1966). This hypothesis was further tested in grafting experiments, which showed that when hypostome tissue was transplanted into the middle of another hydra, it formed a new apical-basal axis with the hypostome extending outward. Conversely, when the basal disc cells were grafted into the middle of the hydra, a new axis formed, but with opposite polarity, extending a basal disc outward from the stalk (Hicklin and Wolpert, 1973; MacWilliams and Kafatos, 1968). It was proposed that the cells in the hypostome secrete a head activator, which behaves as a morphogen (Schaller, 1976). This activator would form a gradient, decreasing continuously from a high level at the apical end toward the basal disc. Although any part of the hydra was able to regenerate a head, multiple heads were clearly not formed. Therefore, it was reasoned that

extra heads do not normally form because an existing head also produces a diffusible inhibitor that prevents the formation of another head, except where head activator is found at the highest level. When the head is removed, the inhibitor disappears and a new head can form at the high end of the gradient in the remaining fragment. A similar activity gradient model incorporating an activator and inhibitor was proposed to explain the formation of the basal disc.

In another example, experiments on limb development in the chick suggested that a group of cells that comprise the "zone of polarizing activity" (ZPA) in the posterior mesenchyme of a limb bud may be the source of a morphogen (see review by Brickell and Tickle, 1989). These cells were found to act as an organizing center to determine anterior-posterior pattern formation in the chick limb bud. When the cells from the ZPA are ectopically grafted in the anterior compartment of a host limb, a mirror image duplication of the posterior limb digits are generated. Results showed that cells of the ZPA have the ability to influence cell fate in the surrounding limb tissue, resulting in the reorganization of cell pattern. Grafting experiments in insects were also interpreted as revealing the existence of a gradient of positional information that organizes pattern within insect segments (Stumpf, 1966; Lawrence, 1966).

Despite the explanatory value of morphogen gradients, considerable controversy remained over whether such gradients actually operated during animal development and, if so, how they precisely organized cellular pattern. Early candidates for signaling molecules have been suggested for some of the systems that have been described above, for example, retinoic acid and Sonic hedgehog for the ZPA in vertebrate limbs (Tickle et al., 1982; Thaller and Eichele, 1987; reviewed by Eichele, 1989; Riddle, 1993; Tickle et al., 1997), activin and noggin for the Spemann organizer in *Xenopus* (Green and Smith, 1990; Smith and Harland, 1992), and small secreted peptides that show activating and inhibitory functions in the head and basal disc in *Hydra* (Schmidt and Schaller, 1976; Schaller, 1978; Bodenmuller and Schaller, 1981). However, in each case, uncertainties remain about whether the relevant factor is expressed in the appropriate cells at the relevant time and whether its activity is normally responsible for organizing the pattern of surrounding cells.

I-2. *Drosophila*: a genetic model system for pattern formation.

The *Drosophila* embryo is a compelling genetic model system, since it enables one to perform large-scale mutagenesis screens to identify genes involved in specific developmental processes (Nusslein-Volhard and Wieschaus, 1980; reviewed in Ashburner, 1989; Nusslein-Volhard et al., 1987; Ingham, 1988; Hooper and Scott, 1992). The seminal work done by Lewis (1978), as well as Nusslein-Volhard and Wieschaus (1980), identified a set of genes that affected early embryonic patterning. Since then, a combination of genetic and molecular biological tools have been used to identify a large number of genes that determine pattern formation during embryogenesis. This work led to a detailed understanding of the molecular basis of positional information and pattern formation during *Drosophila*

embryogenesis (Anderson, 1987; Tautz, 1988; review by Ingham, 1988; St. Johnston and Nusslein-Volhard, 1992). Some of the strongest evidence for the establishment of positional information involving morphogen gradients has come from studies on the specification of the anteroposterior (A-P) axis of the *Drosophila* embryo (reviewed by St. Johnston and Nusslein-Volhard, 1992).

The concept of positional information being established by a morphogen was first validated by studies of the *bicoid* (*bcd*) gene. Mothers homozygous for *bcd* loss-of-function mutant alleles cause a maternal-effect lethal phenotype resulting in the loss of anterior structures in the embryo. These were replaced by an anterior expansion of the posterior pattern. Transplantation of cytoplasm from the anterior to the posterior pole of a wild-type embryo resulted in the specification of an ectopic anterior pattern. *Bcd*⁺-dosage-dependent cytoplasmic rescue of the *bcd* mutant phenotype suggested that anterior-posterior positional polarity is initially specified by the *bcd* gene, suggesting that it may encode a morphogen required for anterior identity and patterning (Driever and Nusslein-Volhard, 1988a; Berleth et al., 1988). The Bicoid protein (BCD) was shown to exhibit the attributes expected of a classical morphogen (reviewed by St. Johnston and Nusslein-Volhard, 1992). Molecular data showed that maternal *bcd* mRNA was localized to the anterior pole of an oocyte (St Johnston et al., 1989). Upon fertilization, the *bicoid* mRNA is translated into its protein product (BCD) which diffuses posteriorly through the syncytial pre-blastoderm embryo and forming a concentration gradient. This gradient organizes the segmentation of the head and thoracic primordia in the embryo (Driever and Nusslein-Volhard, 1988b). BCD acts as a DNA-binding transcription factor and regulates the expression of downstream segmentation genes in a concentration-dependent manner (Driever et al., 1989; Struhl et al., 1989). These genes constitute the zygotically-expressed genetic program that interprets the maternally-specified positional information that is established by the BCD gradient morphogen. Their expression is activated in restricted domains along the A-P axis of the embryo, thus establishing the pattern of metameric segments and different embryonic domains (Ingham, 1988; reviewed by Pankratz and Jackle, 1990; Cohen and Jurgens, 1991; Hooper and Scott, 1989).

Expression of the gap (Nusslein-Volhard and Wieschaus, 1980), pair-rule (Kuroiwa et al., 1984; Harding et al., 1986), and segment polarity (Desplan and Theis, 1985; Baker, 1987; Rijsewijk and Schuermann, 1987) genes subdivides the action of the BCD gradient into successively smaller domains, that specify the parasegments, which define the metameric repeating pattern along the A-P axis of the embryo. The homeotic selector genes (Lewis, 1978) are also regulated by the segmentation genes, which restrict the expression of the homeotic genes to specific domains in the embryo (reviewed by Ingham, 1988), specifying segmental identity (Duncan, 1987; Peifer et al., 1987; Mahaffey and Kaufmann, 1988). Thus the role of the segmentation and homeotic selector genes is to translate the local level of the BCD signal into different heritably-determined cell states. In this way, the positional information provided transiently by the BCD gradient in the early embryo can specify pattern differences in the remote clonal descendants of the embryonic blastoderm cells.

The early *Drosophila* embryo is an unusual system because it involves the establishment and

interpretation of the BCD gradient in a syncytium. Therefore, cytosolic proteins such as BCD, can freely diffuse throughout a common cytoplasm to form a gradient. This is not typical of systems where patterning mechanisms operate within fully cellularized tissues. Therefore, this system is not a useful model for the sort of morphogen gradient that may operate in cellular tissues, such as in a vertebrate embryo, where the developmental process is cellular from its inception. Despite the explanatory value of morphogen gradients, at the time considerable controversy remained over whether such gradients actually operate during animal development, how they might be established, and how they might organize fields with regulative properties. The imaginal discs, unlike the embryo, however, provide an alternative experimental paradigm for pattern formation, which may allow investigators to dissect and elucidate the molecular mechanism of pattern specification within a fully-cellularized tissue.

I-3. The imaginal disc as a model for pattern formation in a cellular system.

The adult fly possesses ventral (leg) and dorsal (eye-antenna and wing) sets of appendages; these are derived from the imaginal discs of a larva (reviewed by Bryant and Schneiderman, 1969). Each adult appendage in *Drosophila* consists of a shell of integument composed of an outer cuticle which is secreted by an underlying epidermis at metamorphosis (during the pupal period). The epidermis is a simple cellular monolayer bounded apically by cuticle, and basally, by a basement membrane. The intricate cuticle pattern produced during differentiation provides a large number of structural markers so that individual parts of the exoskeleton can be identified separately with a high degree of resolution. In addition, as in the embryo, pattern formation in imaginal discs is highly amenable to genetic analysis using large-scale mutagenesis screens that select directly for any changes in the morphology of the adult epidermis.

I-3i. Determination of the imaginal discs.

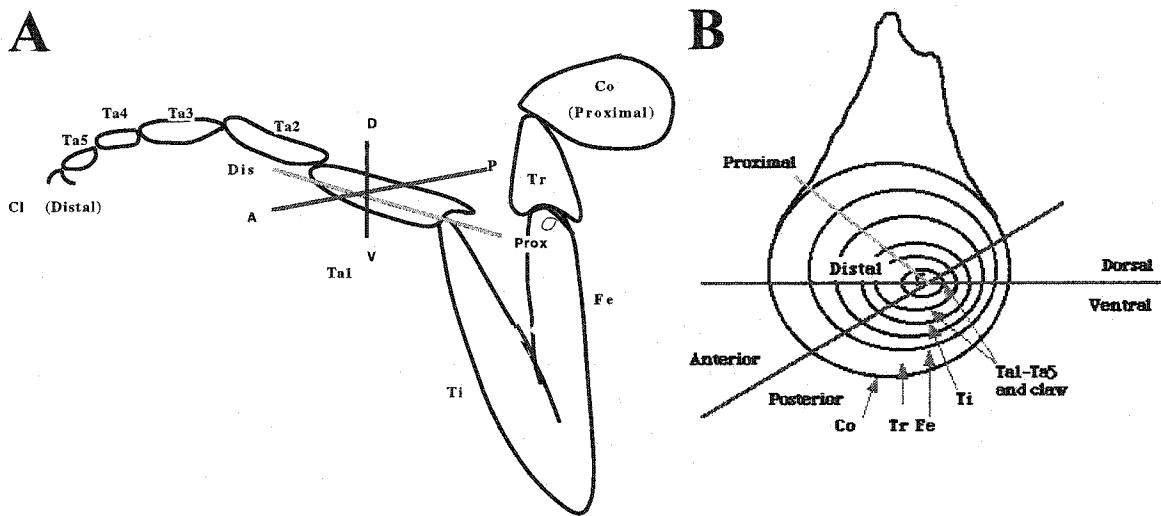
An early approach used to understand imaginal disc development sought to ascertain when and where the imaginal disc primordia are initially determined for specific adult structures. Adult cuticle structures and appendages differentiate at metamorphosis, during the pupal period, but the commitment to form specific imaginal structures occurs early in development. Discs are specified shortly after embryonic segmentation as small groups of cells (referred to as polyclones) that are already determined for different imaginal fates (Chan and Gehring, 1971; Postlethwait and Schneiderman, 1973; Crick and Lawrence, 1975; Bryant, 1976; Simcox and Sang, 1982). Chan and Gehring (1971) showed that cells from the anterior and posterior halves of a bisected blastoderm embryo were heritably committed to form only anterior and posterior imaginal structures, respectively. By transplanting small groups of these cells to ectopic positions in a host embryo, Sang and Simcox (1983) further tested the specificity of these commitments. Their results showed that at syncytial blastoderm stage, donor cells were already determined to differentiate structures that are specified by their original segmental location in the donor embryo. In addition, the corresponding segmental structures were often deleted in the surviving donors. This showed that imaginal disc cells were able to maintain their developmental com-

mitments to an individual metamere from as early as the blastoderm stage. This kind of heritable commitment is referred to as determination, and the experimental demonstration of a heritable commitment is used as a specific criterion for a state of determination (Hadorn, 1965; Gehring, 1966 and 1973).

Using gynandromorph analysis, it was estimated that the imaginal disc primordia initially consist of 10-40 founder cells which map to the prospective ectoderm of the blastoderm embryo (Janning, 1978; Madhavan and Schneiderman, 1977). Bate and Martinez-Arias (1991) showed that the imaginal disc primordia could be identified visually as early as germband extended embryos (stage 11) (Ashburner, 1989) as they segregated from the embryonic epidermis. By stage 13 in germband retracted embryos (Ashburner, 1989), a group of ectodermal cells within the embryonic segments can be identified to form the disc precursors. These cells then undergo invaginations to form epithelial sacs that remain connected to the larval epidermis by a thin peripodial stalk during larval development. The surrounding larval cells cease to divide and are polyploid, whereas disc cells remain diploid and divide mitotically throughout larval development. By late third instar, growth and pattern formation within the discs are essentially complete, and each disc consists of tens of thousands of cells making up a characteristically-folded columnar epithelium enclosed by, and connected to, the larval body wall (Ashburner, 1989). During pupariation, the discs finally evert to form external appendages and differentiate to form the evaginated adult exoskeleton (Condic and Fristrom, 1991). The larvae from *discless* mutants of *Drosophila* can develop normally to pupariation, but never undergo metamorphosis, so the adults never eclose. This result indicates that the larval system is autonomous and develops independently of the disc cells, which seem to have no essential role in the larva (Shearn and Garen, 1974). Earlier experimental findings by Ephrussi and Beadle (1936) showed that, following *in vivo* culture of third instar imaginal discs in the abdomen of a larval female host, the discs can differentiate along with the host at metamorphosis. These experiments demonstrated that each imaginal disc gives rise to an invariant set of adult cuticular structures depending on its segmental origin. This also implied that the determination of disc fates must occur in late blastoderm embryos prior to the onset of larval formation. This suggested that the determination of the fate of a disc is independent of its position in the larva by first instar.

Early attempts to understand pattern specification in imaginal discs came from fate mapping experiments. Disc fragments cultured in larval female hosts were only able to make a fraction of the adult structures that the whole disc forms normally during metamorphosis. Using the characteristic epithelial folds as markers, Schubiger and Hadorn (1968) constructed a fate map of the leg disc by culturing discrete disc fragments. They were able to show that each fragment differentiates a particular part of the leg. Conversely, when groups of cells were removed from a disc, specific pattern elements were missing when the disc differentiated, indicating that a late-stage imaginal disc was a composite or mosaic of specified pattern elements. The center of a leg disc corresponds to the presumptive distal tip of a leg and the periphery of a disc to its base (see **Figure 2**), so that the radial coordinates of the disc define the proximal/distal (P/D) axis of a leg (Schubiger, 1971). Thus, cells in late 3rd instar imaginal discs had already acquired commitments which were specific to their particular positions within the

Figure 2. Fate map for domains of the mesothoracic imaginal leg disc.



Schematic representation of the adult leg in **(A)** is shown with a corresponding imaginal leg disc fate map in **(B)** derived from disc fragment culture experiments (Schubiger and Schubiger, 1978). The leg disc in **(B)** is represented as a series of concentric rings, telescoped segment by segment. The concentric folds (rings) depicted in **(B)** represent the corresponding segments of the leg in **(A)** (in a proximal to distal direction): coxa (**Co**), trochanter (**Tr**), femur (**Fe**), tibia (**Ti**), tarsal segments 1-5 (**Ta1-5**), and claw (**Cl**). The D/V axis [dorsal (**D**), ventral (**V**)] is represented by the red line, the A/P [anterior (**A**), posterior (**P**)] by the blue line and the D/P [distal (**Dis**), proximal (**Prox**)] by the yellow line. **(A)** and **(B)** are modified from Schubiger and Schubiger (1978).

disc (Bryant, 1975; Poodry et al., 1971).

Imaginal disc fragments were shown to grow independently by mitosis when cultured in an adult female host, but do not differentiate (Nothiger and Schubiger, 1966; Schubiger and Hadorn, 1968). Hadorn (1965, 1969) then went on to show, by serial transfer of imaginal disc fragments through *in vivo* culture in a series of adult female hosts, that the determination of discs to form specific adult segments was indefinitely stable. For example, when wing fragments were subdivided and subcultured repeatedly in adult hosts, and finally transferred to a larval host to differentiate, the tissue was still capable of forming the original determined structure. Hadorn showed in these experiments that the early embryonic developmental commitments of cells to particular discs can be bequeathed to their mitotic progeny during growth indefinitely through many cell divisions before it was allowed to differentiate.

Using mosaic analysis, experimenters showed that cell fate determination in the imaginal discs was acquired by a progressive restriction of the developmental potential of cells (Bryant and Schneiderman, 1969; Garcia-Bellido and Merriam, 1969, 1971; Garcia-Bellido and Santamaria, 1972) to regions called compartments (Garcia-Bellido et al., 1973). These compartmental restrictions subdivided the imaginal disc in a simple geometric, anterior-posterior (A/P), dorsal-ventral (D/V) and proximal-distal (P/D) pattern, reflecting heritable commitments of cells and leading to specific final states of determination (Garcia-Bellido et al., 1973; Crick and Lawrence, 1975). For example, somatic clones produced in wing discs as early as first larval instar defined a compartment boundary that separated the anterior and posterior compartments of a wing (Garcia-Bellido et al., 1973). Clones induced later were restricted to either upper or lower parts of a wing, thus defining a new compartment boundary that separates dorsal cell fates from ventral ones (Garcia-Bellido et al., 1973; Crick and Lawrence, 1975). These experiments suggested that successive compartmentalization events progressively subdivide cell populations to create more specific cell fates. Since these are clonal properties, these cell fate restrictions must be heritably maintained. Based on these results Garcia-Bellido et al. (1973 and 1976) proposed the compartment model, an alternative to the positional information model proposed by Wolpert (1969) in **Figure 1**, as a mechanism to explain how cell fate is determined in imaginal discs.

Studies of *engrailed* (*en*), a gene encoding a nuclear transcription factor that is required to specify the posterior compartment identity in imaginal discs, provided further evidence for the basis of compartmentalization. Flies mutant for *en* showed a mirror-image transformation of structures in the posterior compartment of the wing into those of the anterior compartment (Garcia-Bellido and Santamaria, 1972; Lawrence and Morata, 1976). The anterior compartment remained unaffected. Mutant clones of *en* induced in the anterior compartment of the wing disc showed that the mutant phenotype never crossed the A/P compartment boundary. However, mutant clones of *en* induced in the posterior compartment often did display mutant phenotype across both sides of the A/P boundary (Garcia-Bellido and Santamaria, 1972; Morata and Lawrence, 1975). Clonal cells possessing of *en/en* in the posterior compartment autonomously differentiated structures which are seen normally seen in

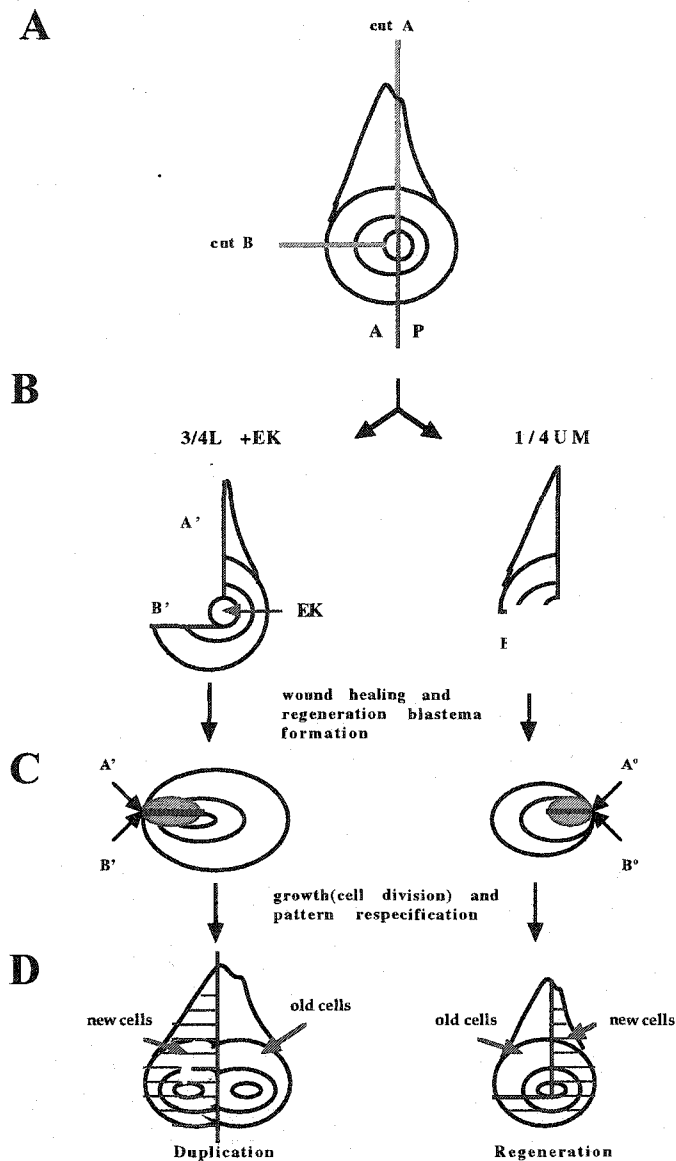
the anterior compartment. This suggests that wild-type *en* function is required for posterior cell fate, and that *en* must be activated in all the cells of the posterior compartment, and repressed in cells of the anterior compartment, where it is not required. This led to Garcia-Bellido's hypothesis for the basis of determined cell states, which he called the selector gene model (Morata and Garcia-Bellido, 1976). According to the model, a selector gene is one that selects a particular developmental pathway for a cell. Each different selector gene, acting as a binary switch, would be turned ON or OFF at each compartmental subdivision. The resulting combination of active selector genes in each cell of the compartment would encode the determined state of a cell. The expression of these genes would have to be maintained clonally in the compartments that they specify, so that the determined states would be heritably transmitted. The combination of selector genes expressed in a particular compartment activates a specific set of downstream target genes leading to the specification of a distinctive developmental fate. The formation of the compartment boundary results from cells expressing different selector genes. This model, however, was not able to explain how selector genes are switched ON or OFF in a position-specific manner as the compartments are being formed, or how patterning within each compartment is later accomplished. However, the regulative properties of imaginal discs during development provided an approach to this problem since the regulative behavior implied that specification of disc cell fates was also positionally dependent.

I-3ii. Regulative properties of imaginal discs.

Although compartmental commitments in mature imaginal discs are clonally heritable during normal development (and therefore interpreted as cell determination), Schubiger (1971) showed that these commitments could be re-specified during regeneration. When undifferentiated disc fragments were implanted for a prolonged time period into an adult female abdomen to permit their growth, and then allowed to differentiate in a larval female host, they formed structures that transcended those expected from the fate map predictions (see **Figure 3**). For example, upper-medial-quarter (UM1/4) fragments in leg discs could regulate to form the entire leg pattern when cultured in the adult host for seven days. The complementary 3/4 lateral fragment with the distal endknob (3/4L+EK) also regulated to duplicate the pattern specified by the fate map (Schubiger and Hadorn, 1968; Schubiger, 1971). More importantly, this experiment showed that regeneration of the entire pattern was possible even from a small fragment derived entirely from the anterior compartment. Thus, under these conditions the fragments behaved as if a disc was a regulative field, meaning that the normal cell fate commitments represented by the compartments could be re-specified. Therefore, states of cell determination which are normally fixed can be changed after tissue injury, under specific experimental conditions (Bryant, 1971).

Haynie and Bryant (1976) showed that pattern regulation of imaginal disc fragments occurred by filling in the missing tissue from the cut edges that had fused to form a wound heal, by a process called intercalation. They found that certain fragments from the edge of a disc, when cultured alone, only formed duplications. However, when grafted to a fragment from the opposite edge of a disc, the

Figure 3. Pattern regulation of two complementary imaginal leg disc fragments (described in Schubiger, 1971).



Regulation of two complementary leg disc fragments. (A) Two cuts (red, cut A and cut B) are made in the imaginal leg disc producing two complementary fragments in; (B) shows the 1/4 upper medial (1/4UM) and 3/4 lateral plus distal endknob (3/4L+EK). (C) Once the 1/4UM and 3/4L+EK fragments are implanted into an adult female host abdomen, the cells at the cut edge of each fragment (A' and B' for 3/4L+EK.; A° and B° for 1/4UM), fuse to form a wound heal [red line in (C)]. Following wound healing, a small group of cells (blue) on both sides of the wound heal start to proliferate. These groups of cells are referred to as the regeneration blastema, which marks the region of regulative growth and development of each fragment. (D) The 1/4UM fragments will normally regenerate the missing disc tissue, and the 3/4L+EK fragment will regenerate a mirror image duplicate of itself. A and P mark the anterior and posterior compartment respectively.

same fragments regenerated intervening structures. This showed that the fate of a duplicating fragment could be changed by interaction with another fragment from an opposite edge of the disc. Reinhardt et al. (1977) showed directly by scanning electron microscopy of *in vivo* cultured wing disc fragments, that prior to any cell division, the cut edge of the disc epithelium first heals by folding and fusion of the cut edges so that the cells from different positions confront each other. This subsequently stimulates intercalary cell division adjacent to the wound heal. It was suggested that this cell division leads to a restoration of the continuity of positional information by filling in the intervening positional values across the wound heal (Reinhardt and Bryant, 1981). Moreover, these experiments taken together suggested that the re-specified pattern during regulative growth depended on the positional values of the cells on both sides of the wound that were brought together during the process of wound healing. This showed that cell-cell interactions across the wound heal were instructive in determining the pattern regenerated by a disc fragment.

Abbott et al. (1981) used marked clones of cells to study the A/P compartmental restriction in a leg disc fragment undergoing regeneration. Clones of cells labeled prior to transplantation of the UM1/4 fragment, crossed the A/P compartment boundary, while clones induced later did not. Therefore clonal restriction was initially lost and then re-established during regeneration. This implies that a re-specification of compartmental cell fate takes place to generate a new posterior compartment when cells from that compartment are separated from the anterior UM1/4 fragment. In addition, marked clones in the regenerated posterior part of the leg did not usually extend from the original anterior UM1/4 of the leg, but only extended from the site of the cut edges of the disc fragment. This means that regeneration does not derive by cell migration from the original fragment (Postlethwait et al., 1971), but rather from cells at the cut edges in the wound heal (Abbott et al., 1981). Haynie and Bryant (1976) had noted that previously, a small number of cells from a specific region adjacent to the wound heal were needed to produce the new pattern. These cells, which defined a new region of cell division, that were able to produce the new pattern, were referred to as the regeneration blastema. Bromodeoxyuridine (BrdU) incorporation experiments used to mark cells in S-phase showed that the incorporation of the BrdU label was most intense in cells adjacent to the cut edges that had fused to form the wound heal (Dale and Bownes, 1980 and 1985). This indicated that these cells possess a high mitotic activity, consistent with the postulated regenerative ability of cells at the cut edge.

Using a different experimental approach, Girton and Russell (1980) were able to estimate the number of cells that make up the blastema. Larval heat treatment of a temperature-sensitive cell autonomous lethal mutation, *suppressor of forked 12 (su(f)¹²)*, induced limited cell death in the imaginal discs (Clark, 1976; Russell, 1974; Clark and Russell, 1977). When these heat treated larvae were shifted back to the permissive temperature and allowed to recover, a number of the adults which eclosed exhibited a high frequency of duplications of leg, antenna, and other head structures (Russell, 1974; Russell, et al., 1977). Using this system, in combination with clonally-marked cells, Girton and Russell (1980) estimated that the average number of cells that form the duplicate leg was only about seven, consistent with the formation of a localized blastema after cell death.

The regeneration blastema consists of a dividing population of cells which have lost their previous compartmental commitments. Ultimately, the blastema gives rise to intercalated structures. The unique nature of blastema cells was shown in experiments in which the blastema was removed from a normally-duplicating disc fragment following wound healing. The blastema was able to regenerate an entire disc pattern (Karpen and Schubiger, 1981). Such cells were thus able to transcend their normal compartmental restrictions, suggesting that blastema cells had a high level of developmental plasticity. Normally in disc fragments, such as the UM1/4 or 3/4L+EK fragments, the surrounding cell environment must limit the developmental potential of a blastema. This implies that the cells from a blastema, in the context of the fragment with which it is associated, can somehow "sense" the positional values of neighboring cells. Thus, the process of pattern formation (including, in the case of the UM1/4 leg fragment), the specification of a new compartments, may be regulated by a mechanism which involves the intercalation of positional information by cell-cell interactions (Bryant et al., 1978; Schubiger and Karpen, 1983).

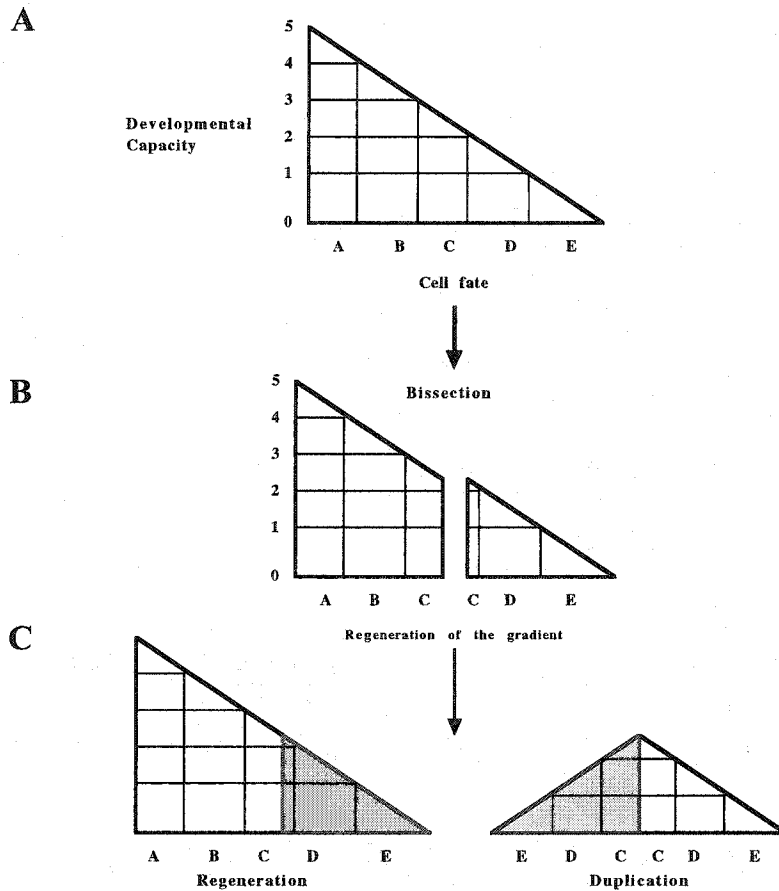
In summary, clonal labeling of cells during both normal disc development and regeneration suggest that patterning involves at least two processes: heritable determination of cell fate by compartmental specification, and specification of positional values by local cell-cell interactions that leads to regulative re-patterning of compartmental fates. Re-specification was never considered by the selector gene model, which also does not explain how the compartmental states originate during normal development. The rules of re-patterning in regeneration do suggest that a positional information system may underlie compartment formation in normal development. Several models, which try to explain pattern formation in the context of either heritable or regulative properties of imaginal discs have been proposed. All postulate a hypothetical positional information system in a disc, that show how the cells within a disc would have to change to account for the observed regulative properties. These models will be explained in detail, below.

I-4. Models for positional information.

I-4i. The gradient of developmental capacity model.

Bryant (1971) proposed that the ability of two complementary leg disc fragments to either regenerate or duplicate distal structures is due to a proximal-distal gradient of developmental capacity of cells in an imaginal disc. According to this idea, cells exposed by a cut at a particular level could only regenerate structures associated with the lower levels of this gradient (**Figure 4**). For example, the UM1/4 fragment is able to regenerate all lower lateral pattern elements. Based on this model, Schubiger (1971) postulated that an UM1/4 fragment must include cells of the highest developmental capacity. Conversely, the remaining 3/4L+EK fragment could only duplicate lateral pattern elements at levels lower than the cells at the cut edge which represents the low end of developmental capacity in a disc (Schubiger and Schubiger, 1978). Thus, both fragments produce the same pattern elements, leading to either regeneration or duplication, because the cells at both cut edges represent similar cells that

Figure 4. Pattern regulation in terms of the gradient of developmental capacity model.



The interpretation of duplication and regeneration in terms of a gradient of developmental capacity in disc fragments. (A) The 'source' of the gradient substance is (5), and the 'sink' is (0), giving a regular slope of gradient positions. (B) When the continuity of the gradient is disrupted, it is assumed that only the lower, not higher, gradient levels can be re-established from the edge of the bisected disc fragments (C) (blue and red shaded regions). Therefore, regeneration and duplication fragments will be produced. In this case, the new growth is identical in each of the two fragments.

have the same developmental capacity. The model then implies that there is a gradient of developmental capacity with a boundary, or region, specifying the high point and another specifying a low point, where growth can generate only cells with lower positional levels. The utility of this model is that it can explain the regeneration and duplication of complementary disc fragments using a single (simple) rule. However, the model cannot be used to explain the behavior of all disc fragments.

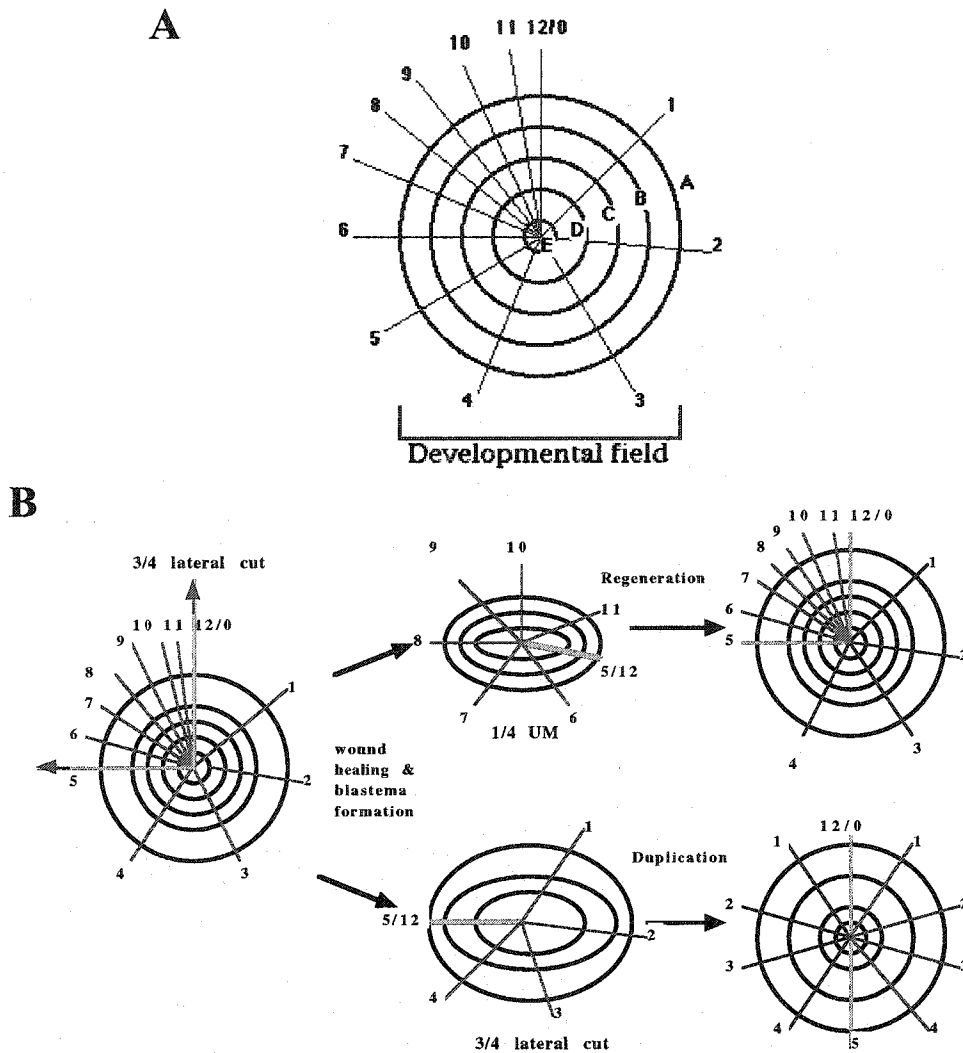
Bryant (1975) observed that, in wing discs subdivided into two fragments by single cuts in different positions, a region in the center of a disc was included in all regenerating fragment, but this central region was absent in duplicating fragments. Thus, this model implies that a smaller fragment containing only the center of the disc should regenerate all the missing pattern elements, whereas, the complementary (edge) fragment should always duplicate. He found, instead, that the center fragment duplicated itself and the complementary peripheral fragment regenerated the central pattern elements. Thus, the gradient of developmental capacity model is not sufficient to account for all experimentally observed results.

I-4ii. The polar coordinate model.

Bryant et al. (1981), applied the polar coordinate positional information model, initially proposed by French (1976) to explain regulative behavior of amputated and grafted cockroach limbs, to explain the regulative behavior observed in most regenerating imaginal disc fragments (**Figure 5**). French et al. (1976) proposed that a continuous positional information system is specified by polar coordinates in two dimensions, so that each cell has both a radial positional value specifying position along the P/D axis, and a circumferential (angular or "clockface") value specifying position around the circumference of the leg (**Figure 5A**). In cockroach legs, removal of a longitudinal stripe of epidermis and cuticle from around the circumference of the femur created a situation where distant cells from both cut edges were juxtaposed. This initiated the mitotic division of cells at the wound heal producing a blastema that differentiated the missing intermediate structures by intercalary regeneration. Therefore, interpolation of circumferential positional values between the initial values of cells at the two cut edges may facilitate regeneration of the missing tissue. This further shows that the re-specification of cell fate after injury depends on local cell-cell interactions as observed in imaginal disc fragments in *Drosophila*.

The model postulates two rules that describe how new positional values are assigned to the cells comprising a blastema (**Figure 5B**). In cockroach legs or imaginal discs, when cells with different positional values become juxtaposed upon wound healing, the discontinuity in positional values is "sensed", leading to cell division. A blastema is formed and new cells adopt the missing fates by smoothing out the discontinuity between the positional values of the pre-existing neighboring cells through local cell interactions. Therefore, if cells that are normally in non-adjacent positions in the disc epithelium are juxtaposed by grafting or fusion of two cut edges (wound healing), cell interactions will lead to intercalation of intermediate circumferential positional values. In addition, these observa-

Figure 5. The polar coordinate model of positional information during axial patterning in imaginal leg discs (French et al., 1976).



(A) The polar coordinates of positional information in a developmental field are represented by a circumferential clockface (0-12) and radial (A-E) values. The field of an imaginal leg disc is depicted as a flat 2-dimensional layer of cells, with the proximal part (A) at the edge and the distal part (E) in the center. Each cell would then have precise information as to its position in surface space determined by its circumferential and radial values. (B) Shows the results of culturing the 1/4UM and 3/4L+EK (see Figure 3 for description) fragments as explained by the polar coordinate model. The regulative behavior of each fragment can be explained best if the circumferential values are assumed not to be uniformly distributed around the disc, but mostly clustered in the upper medial quarter (UM1/4). The values 5 and 12 (red) heal together. Then, by intercalary growth (red lines), the 1/4UM fragment having more than half the positional values is the one that regenerates; the physically larger 3/4L+EK fragment, which possesses less than half the positional values, duplicates.

tions show, that the intermediate structures are always filled in by the shortest of the two possible routes, implying that angular positional values are arranged around a (clockface) circle in a continuum with no points of discontinuity. This means that there is no singularity at the position of 12/0 (o'clock) or at any other point around the (imagined clock face) circle, thus ruling out a gradient model for specification of the angular coordinate. This rule accounts for the duplication of a fragment that contains less than half of the circumferential values, and the regeneration of one that contains more than half of those same values (Figure 5B).

The second rule of distalization in the model, states that distal regeneration occurs whenever a complete circle of circumferential positional values is present at the cut edge (Schubiger and Schubiger, 1978; Bryant et al., 1981). For example, when a cockroach leg is amputated, structures distal to the site of the amputation are all generally regenerated. Thus, cells at a cut edge at a certain proximo-distal level (radial value) regenerate all the missing distal structures (lower radial values). This rule accounts for the observed duplication of a central wing disc fragment and the regeneration of the complementary edge fragment, that could not be explained by the gradient of developmental capacity model.

However, the polar coordinate model had to be modified since it does not explain the regeneration behavior observed by all disc fragments. For example, based on the regulative behavior of wing disc fragments, the angular values are assumed to be distributed equally. Conversely, the angular values around the leg disc must be compressed into the upper medial quarter of a disc so as to explain the regeneration of the UM1/4 fragment as well as the duplication of the remaining 3/4 fragment (French et al., 1976). Karlsson (1980) attempted to map the distribution of circumferential values required to explain the data using the polar coordinate model. She observed that wing discs also show a non-uniform distribution of angular (clockface) values. According to her data, 7 or 8 of the twelve clockface values were clustered very close to the two ends of the A/P boundary. This supported the possibility (see below) that the A/P compartment boundary might act as a source for angular positional information. Finally, according to this model, normal development in discs could proceed by the same intercalation of positional values as observed in regeneration. However, the question of how initial positional values are determined in the imaginal disc primordia needs to be addressed. In addition, the relationship between the binary "decision" mechanism postulated in the selector gene model in the formation of compartmental restrictions in imaginal discs, and the continuous positional information system in imaginal discs implied by regulative behavior of regenerating discs, needs to be explained.

In regenerating discs fragments it was shown that cells from one compartment were able to give rise to cells of another compartment (Schubiger, 1971). For example, an UM1/4 fragment, consisting of cells whose fates are all anterior, can regenerate an entire posterior compartment. This implies that the heritable commitment of a cell to anterior fates is lost in cells that regenerate. Szabad et al. (1979) showed that the A/P compartment boundary may be transgressed by clones that are induced soon after damage to the imaginal disc, while clones induced 24hrs after cell death respected the A/P compart-

ment boundary. In addition, this clonal restriction appears to be established before regenerative cell division begins (Girton and Russell, 1981, Abbott et al., 1981). This implies that cells that give rise to the new pattern lose their initial compartmental commitments but are re-assigned new ones before cell division first occurs in the blastema. Thus, although cells in the leg disc normally have heritably-restricted compartmental fates, they are not irreversibly committed to form these structures when cell interactions across the wound heal re-assign positional values.

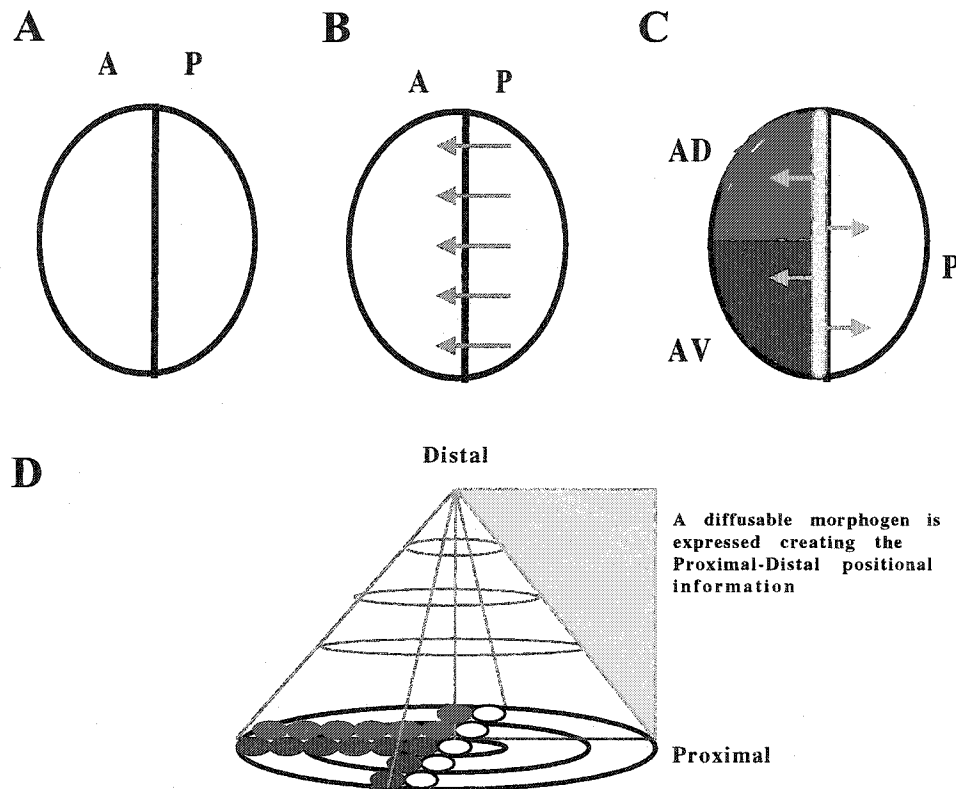
Subsequent work by Schubiger and Schubiger (1978), implicated compartments and compartment boundaries in distal regeneration. Distal regeneration of proximal fragments of imaginal leg discs is observed in the absence of complete circumferential values, which is contradictory to the complete circle rule of the polar coordinate model. Girton (1981), looking at distal duplications in the leg induced with the mutation *su(f)*¹², also noticed that distally-complete duplications generally contain cells from all compartments (posterior, anterior-dorsal and anterior-ventral). These results suggest that the ability of fragments to regenerate distally may depend on cooperation between cells of different compartments rather than a complete circle of angular positional values. The relationship between compartment boundaries and positional information is addressed by a model in which the compartment boundaries are organizers of positional coordinates (Meinhardt, 1983a).

I-4iii. The compartment boundary model.

Crick and Lawrence (1975) proposed the idea that compartment boundaries in a cellular field may function as reference axes in a Cartesian coordinate system, where the cells along the boundary produce a morphogen that specifies that positional information for the adjacent cells. Meinhardt (1983b, 1984, 1986, and 1989) proposed a different model which also related compartments and positional fields. Using the theory of pattern formation proposed by Turing (1952), he described how two morphogens could form a pattern of equally-spaced peaks (singularities) that develop spontaneously by reaction-diffusion (e.g. a short-range autocatalytic process coupled with a long-range inhibitory process involving the diffusion of two morphogens). Autocatalysis is one way to maintain a determined state, and this could be the basis for compartments. In this model (**Figure 6**) a second interaction between cells across the compartment boundary generate a morphogen, so that the boundary is the high point of a gradient of positional information.

To generate a proximal/distal (P/D) axis, Meinhardt proposed that a third interaction between A/P, D/V and P compartments could create a local singularity at the point of intersection of the compartment boundaries. The model postulates that the site where the A/D, A/V and P compartment boundaries intersect, specifies the presumptive distal/proximal pattern of a leg by acting as a source (or high point) of a third diffusible morphogen. The conical concentration gradient of positional information generated would provide a radial coordinate for all cells in the disc, and would both induce out-growth and presumably, specify fate along the P/D axis. The radial and circumferential positional values are thought to be integrated into the conical gradient. In general, the discrete compartmental states

Figure 6. The boundary model for the specification of positional information to explain pattern formation in imaginal leg discs (Meinhardt, 1983a).



According to the compartment boundary model, the interaction between cells of different compartmental fates at the compartment boundary acts as organizing centers for imaginal discs. **(A)** The primary process involves defining anterior (A) and posterior (P) compartmental fates by establishing new cell lineages. **(B)** A diffusible asymmetric signal (green arrow) from the posterior to the anterior compartment defines the anterior-dorsal (AD) (blue) and anterior-ventral (AV) (red) sub-compartments. **(C)** The intersection between cells along the anteriodorsal, anteroventral and posterior borders define a unique point at the center of the disc. Topographically, the three compartments are sufficient to specify the center of the disc. As a result of the interaction among cells of the AD, AV and P compartments at their point of intersection, an organizer region (yellow) is established. This is defined as a local morphogen source. **(D)** By diffusion and decay into the surrounding sheet of cells, a gradient morphogen profile results, thus specifying the positional information along the proximal-distal axis of the disc. The circularly arranged primordia of the leg disc segments correspond to the contour lines of this cone-shaped distribution. In agreement with this model, the most distal structures, the claw and tarsus, are formed around the intersections of the compartment borders.

act as sources of information so that the compartmental boundaries might act as cardinal positional values between which intermediate positional values are subsequently interpolated to establish a Cartesian coordinate system that specifies pattern. Unlike all previous models, this would place compartmentalization upstream of positional information in the hierarchy of information flow. Observations by Karlsson (1981) support the idea that the polar coordinate description of positional values is specified with reference to the compartment boundaries. The polar coordinate model explains the regulative behavior of imaginal discs by assuming the intercalation of an existing continuous positional value system, while the boundary model may describe the mechanism by which such a system of positional information could be generated. Meinhardt and Gierer (1980) had earlier observed that the ability of proximal fragments to regenerate distal structures is associated merely with the presence of cells from the anterior-dorsal, anterior-ventral, and posterior compartments. On the other hand, fragments which contain only the posterior or anterior compartment failed to regenerate distal structures. To explain this, Meinhardt proposes that cooperative interactions between cells of different compartments can create a distal organizer at their boundary. Another prediction of the model is that distal transformation (duplication) will occur if a new intersection of A/P and D/V boundaries is created. Thus, Meinhardt suggests a modification of French et al. (1976) in which compartment boundaries in imaginal discs act as discrete local organizers of continuous global gradients of positional information. Recent evidence fully supports this prediction (see below). The boundary model, however, is unable to explain several surgical results in imaginal discs (reviewed by Blair, 1996). For example, the UM1/4 fragment of a leg disc that lacks cells from the posterior compartment (and therefore an A/P boundary to act as a gradient source) is able to regenerate a structurally and functionally complete pattern. This model can neither explain the intercalation of ablated structures within a compartment, nor the duplication of complementary fragments (see review by Blair, 1996). Therefore, the explanatory value of these models remain incomplete-possibly because the genetic and molecular mechanisms that determine the regulative behavior and positional information in imaginal discs was yet to be determined.

I-5. The genetic and molecular basis of pattern formation in *Drosophila* imaginal discs.

During the past three decades, insights into the molecular components of the positional information system in imaginal discs started to emerge (Shearn et al., 1971; Shearn and Garen, 1974; Kiss, 1976; Shearn, 1977; James and Bryant, 1981). By 1991, studies of embryonic pattern formation (reviewed by Ingham, 1988; St. Johnston and Nusslein-Volhard, 1992; and Ingham and Martinez-Arias, 1992) were beginning to furnish some clues as to the way in which many of the genes involved in late segmental patterning in an embryo might also participate in patterning adult structures. Pattern transformations similar to those observed in an embryo, due to mutations in segment polarity genes, are also found in excision and grafting experiments using insect abdominal segments (Locke, 1959; Wright and Lawrence, 1981) as well as with regenerating imaginal disc fragments (Schubiger and Schubiger, 1978). This suggested that a common basis for positional information may exist in both an embryo and imaginal discs (Meinhardt, 1983a, 1986; Russell, 1985; Martinez-Arias, 1989). Based on the

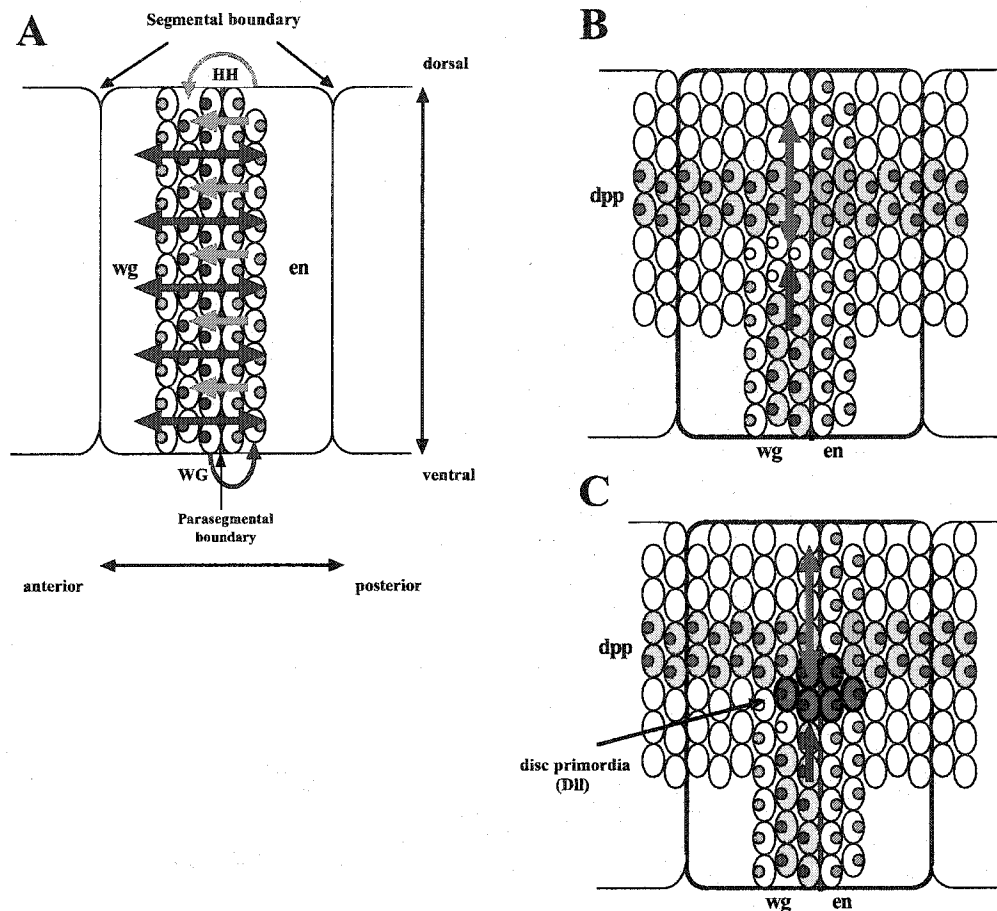
mutant phenotypes and the expression patterns of segment polarity genes in imaginal discs, Wilkins and Gubb (1991) reason that these genes are instrumental in assigning positional information in discs.

I-5i. Segment polarity genes specify both imaginal leg disc primordia in an embryo as well as segmental pattern in a larva.

Early clonal analysis experiments provide support for the idea that the determination and patterning of imaginal discs involves some of the same genes required for segmentation in the embryo. Genetically-marked clones induced in wild-type blastoderm stage embryos indicate that the imaginal disc primordia are divided into two groups of cells—one committed to form the anterior, and the other the posterior, adult structures of a particular segment (Wieschaus and Gehring, 1976; Lawrence and Morata, 1977).

The determination or allocation of cells to imaginal disc primordia in thoracic segments of an embryo depends on *wingless* (*wg*) and *engrailed* (*en*) function. Embryos mutant for either of these genes fail to develop thoracic imaginal disc primordia (Simcox et al., 1989). The *wingless* gene encodes a member of the Wnt family of secreted extracellular signaling molecules (reviewed in Nusse and Varmus, 1992). Several findings have shown that *wingless* protein (WG) acts as an intercellular signal involved in pattern formation during embryogenesis (Gonzalez et al., 1991). Mutations that reduce or eliminate *wg* function have global effects on the pattern of cell differentiation within embryonic segments, even though WG expression is restricted to a subset of cells within each segment primordium (Baker, 1987; Martinez-Arias et al., 1988; van den Heuvel et al., 1989a; Peifer et al., 1991). The A/P compartmental restriction in each segment primordium originates with the formation of the parasegmental boundaries in the embryo, determined by the adjacent stripes of expression of WG and EN (see **Figure 7**). This precedes, and is critical for, allocation of disc precursor cells from the epidermis of an embryo during metamerization (Madhavan and Schneiderman, 1977). Restricted expression of WG and EN in thoracic and abdominal segments of an embryo is initially established by gap and pair-rule genes during A/P axis pattern formation during germband extension in an embryo (stage 9). Expression of *engrailed*, which encodes a homeodomain-containing transcription factor (van den Heuvel et al., 1989a; DiNardo et al., 1988; Vincent and Lawrence, 1994), defines posterior cell fate of embryonic segments. *Engrailed* protein (EN), in a cell-autonomous fashion, activates the expression of *hedgehog* (*hh*), which encodes a secreted growth factor. *Hedgehog* protein (HH) is a transmembrane protein that is autoproteolytically cleaved to generate a diffusible product (Lee et al., 1992 and 1994) (**Figure 7A**). The HH protein diffuses anteriorly to neighboring cells stabilizing the expression of *wg*. WG in turn, secreted by adjacent anterior cells, acts as a long-range signal that diffuses anteriorly to determine anterior cell fate. WG acts also as a short-range signal that diffuses posteriorly to maintain the expression of *en* in the immediate neighboring cell. Formation of this regulatory loop between *wg* and *en* creates the parasegmental boundary in an embryo (reviewed in Martinez-Arias, 1993, see **Figure 7A**). Later, *en* expression becomes independent of *wg* and *vice versa*. Their expressions are maintained by an autoregulatory loop. *Engrailed* expression becomes cell-heritable upon formation of

Figure 7. Establishing the imaginal disc primordia during *Drosophila* embryogenesis (reviewed by Martinez-Arias 1993; and Cohen, 1993).



Schematic diagram depicting the spatial relationship among the discfounder cell population and the forming parasegment boundary in the embryo. (A) In stage 10 embryos *Engrailed* expressing cells (green cells) activate and maintain *wingless* expression (red cells) in adjacent anterior cells by activating and secreting *hedgehog* protein (HH) (yellow arrow). *Wingless* expressing cells in turn, secrete *wg* protein (WG) (red double arrow) which diffuses posteriorly to maintain *engrailed* expression in adjacent cells, thus defining the parasegmental boundary in each segment of the embryo, and anteriorly to specify the naked cuticle pattern of the anterior compartment of each segment. (B) By stage 12 in germband retracting embryos, DPP (blue double arrow) and WG (red arrow) protein secreted from *dpp* (dorsal lateral cells, blue) and *wg* (ventral cells, red) expressing cells intersect at cells in the lateral region of each trunk segment of the embryo. (C) The nuclear target gene *Distalless* (*Dll*) (purple cells) is activated in adjacent non-expressing cells in response to both the WG and DPP signals, thus specifying the leg disc primordium (Cohen, 1993).

disc primordia from ectodermal cells that straddle the parasegmental boundary in germband extended embryos (stage 10-11). Therefore, posterior compartment identity in disc primordia appears to be acquired through the embryonic activity of EN in the posterior half of a segment. EN expression subsequently maintains posterior compartment identity in a disc during larval stages (Vincent and O'Farrell, 1992; reviewed by Cohen, 1993; Lawrence and Morata, 1994; Lawrence and Sanson, 1996; Blair, 1996).

The *decapentaplegic* (*dpp*) growth factor, is required to specify the dorsal-ventral (D-V) axis in the blastoderm embryo (for a review see; Anderson, 1987; Gelbart, 1989). During germband retraction (stage 11-13) in the embryo, *dpp* expression is restricted to a longitudinal stripe on each side of an embryo, along the length of the embryo in the dorsal-lateral ectoderm. In addition, *wg* expression fades in the dorsal ectodermal half of an embryo and is restricted to a transverse set of cells in the ventral-lateral ectoderm of each segment in the embryo (**Figure 7B**) (reviewed in Martinez-Arias, 1993). *Dpp* protein (DPP) and WG are thought to diffuse from the longitudinal stripes of *dpp*-expressing cells in the dorsal half, and the transverse rows of *wg*-expressing cells, in the anterior compartment of an embryonic segment (stage 12) respectively (**Figure 7B**). Both DPP and WG are then thought to affect adjacent cells dorsal to *wg*-expressing cells and ventral to *dpp*-expressing cells. The intersection of DPP and WG causes the activation of *Distalless* (*Dll*) expression in these cells (**Figure 7C**) (review by Cohen, 1993). *Dll* is a gene whose activity is required for the specification of the proximal/distal (P-D) axis in leg and wing discs (Cohen et al., 1989; Cohen and Jurgens, 1991). Cohen (1990) showed that the earliest *Distalless* expression coincides with the position where the thoracic disc primordia originate in an embryo. *Distalless* was most strongly expressed at the point of intersection between *wg* expressing cells at the parasegmental boundary, and the longitudinal stripe of cells expressing *dpp*. Mutations in both *dpp* and *wg* result in a loss of *Dll* expression and the failure of cells to form disc primordia (Cohen 1990; review by Cohen, 1993). These experiments indicate that the origin and patterning of imaginal discs is closely linked to A/P parasegmental and dorso-ventral positional information generated in an embryo (Cohen et al., 1993; Couso and Gonzalez-Gaitan, 1993). The disc primordia are made up of *en*-expressing and *wg*-expressing cells from both sides of the parasegmental boundary. This system generates borders characterized by neighboring cells with different states of determination. This coincides with the A/P lineage restriction in the imaginal discs and is probably the first step in imaginal disc patterning (Cohen, 1993; Cohen et al., 1993; Couso et al, 1993). This spatial relationship suggests that the two morphogens (WG and DPP) that establish the A/P and D/V pattern in an embryo also serve as the source of A/P and D/V positional signals which provides an orthogonal coordinate system to position imaginal disc primordia. Thus, WG and DPP are not only involved in A/P and D/V patterning of imaginal discs later during larval development (see below), but are also responsible for the earlier allocation of embryonic cells to disc primordia (Cohen et al., 1993). These experiments confirm the association of imaginal disc patterning with that of the larval epidermis. This supports Meinhardt's (1983a, 1989) earlier speculation that secondary developmental fields (like disc primordia) might be established in a naive field of cells at the boundaries of stripes of cells expressing different genes, such as adjacent *en*- and *wg*- or *dpp*-expressing cells that specify the A-P or D-V axes in an

embryo. This would be a way to initiate a determined state leading to the formation of compartments.

It has been shown that *wg*, *dpp* and other genes such as *hh* and *en* continue to play key roles during larval stages in specifying positional information in imaginal discs. Viable mutant alleles of these genes that are sufficient for normal embryonic development cause position-specific pattern defects, including polarity reversals, in adult disc derivatives, analogous to the effects seen in embryos that are mutant for the same segment polarity genes (Baker, 1987; Ingham, 1988; Wilkins and Gubb, 1991; Held, 1993). These included deficiency-duplication phenotypes in which either the ventral or dorsal portion of a leg was missing and was replaced by a mirror-image copy of the remaining portion (Held, 1993). For example, a pupal-lethal allele of *wg* causes loss of ventral tissue, resulting in a double-dorsal phenotype in the adult leg. Adult-viable mutations in *dpp* sometimes delete the dorsal side and cause a double-ventral phenotype in a leg, along with loss of distal structures in the wing and leg. Null alleles of *wg* and *dpp* cause similar phenotypes in genetic mosaic studies, showing that *wg* and *dpp* are required for specification of ventral and dorsal cell fates, respectively.

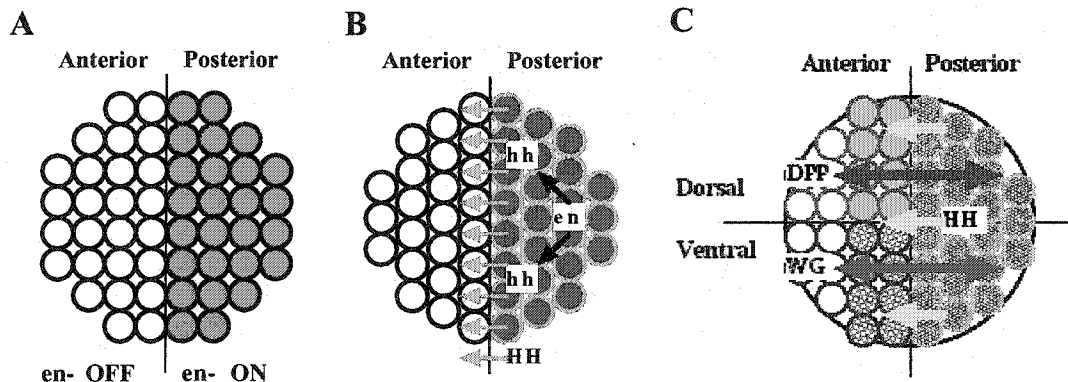
I-5ii. Segment polarity genes and the compartment boundary model in imaginal discs.

Several studies on signaling molecules have provided both genetic and molecular support for some aspects of Meinhardt's boundary model and the role of segment polarity genes in imaginal disc pattern formation. To explain pattern formation in secondary fields (imaginal discs), Meinhardt (1983a) combined Wolpert's idea that positional information is acquired by the cell's interpretation of a morphogen gradient with the concept of compartmentalization based on differential selector gene activation (Garcia-Bellido et al., 1976). The cell-cell interactions across the compartment boundaries created between gene expression domains would specify the source of the required morphogen gradient.

The A/P compartment boundary is the primary organizer in imaginal discs.

An anterior/posterior compartment boundary bisects every *Drosophila* imaginal disc. According to the boundary model, the initial requirement for the generation of positional information would be the formation of a boundary by means of an initial compartmentalization event. For the thoracic discs, this occurs when segment polarity genes are first activated in an embryo to form parasegment boundaries. This system generates a lineage restriction (compartment boundary) in disc primordia (**Figure 8A**). The leg disc, for example, is divided into two lineage compartments (Steiner, 1976; Lawrence and Morata, 1977) which abut along an extended interface. Neighboring cells with different determined cell fates specify the A/P boundary generated in imaginal disc. The cells of the anterior and posterior compartments are defined by, *engrailed/invented* (*en/inv*)-expressing cells that specify the posterior cell fate, and *cubius-interruptus* (*ci*) (or non-*engrailed*)-expressing cells that define the anterior cell fate (Kornberg et al., 1985; Eaton and Kornberg, 1990; Lee et al., 1992; Tabata et al., 1992; Simmonds et al., 1995). Short-range interactions between cells in adjacent compartments trigger the patterning of the imaginal discs of *Drosophila* (reviewed in, Lecuit et al, 1996; Brook et al., 1996;

Figure 8. Genetic model for specifying A/P and D/V compartment identity in the imaginal leg disc.



Genes implicated in specifying anterior/posterior (A/P) and dorsal/ventral (D/V) compartment formation. (A) *Engrailed* (green cells) expression is activated and establishes posterior identity in the disc primordia in embryos following germband retraction. Conversely, *en* non-expressing cells (white) establish the anterior compartmental fates in the disc. (B) *Engrailed* protein activates the expression of *hedgehog* (*hh*), in the posterior compartment. The HH protein (yellow arrow) defines the asymmetric signal that originates in the posterior compartment and diffuses across the A/P compartment boundary, into the anterior compartment. (C) The diffusion of HH protein (yellow arrow) into the anterior compartment, leads to the activation of *dpp* (blue cells) and *wg* (red cells) expression in cells of the anterior-dorsal and anterior-ventral compartment respectively, that are adjacent to the A/P compartment boundary. DPP (blue double arrow) and WG (red double arrow) protein are then secreted, and go on to specify anterior-dorsal and anterior-ventral cell fate respectively in both anterior and posterior compartments of the leg disc (adopted from a review by Brook et al., 1996).

Lawrence and Struhl, 1996). The compartment-specific expression of *ci* and *en/in* is critical for the regulation of *hedgehog* (*hh*), resulting in the expression of the *hh* transcript only in the posterior compartment (Lee et al., 1992; Mohler and Vani, 1992; Tabata et al., 1992; Aza-Blanc et al., 1997; Dominguez et al., 1996; Hepker et al., 1997). En protein expression activates *hh* expression in the posterior compartment. HH protein is then secreted by the posterior cells, diffuses across the A/P compartment boundary (**Figure 8B**) into the adjacent anterior compartment. Here it specifies a specialized group of anterior cells that express *wg* and *dpp* in a stripe of cells adjacent to the A/P boundary in the anterior compartment (Basler and Struhl, 1994; Tabata and Kornberg, 1994; Aza-Blanc et al., 1997; Methot and Basler, 1999) (**Figure 8C**). This supports the model proposed by Meinhardt in which he postulates that cells at the boundary would generate a morphogen that would diffuse in opposite directions into anterior and posterior compartments. Their distances from the border could then partly determine positional values of cells.

Genetic studies demonstrate that *en* promotes the expression of *hh* and inhibits the expression of both *dpp* and *wg* in the posterior compartment (Tabata et al., 1992; Sanicola and Sekelsky, 1995; Schwartz et al., 1995). By inducing *en*⁻ clones, it was shown that abolishing EN activity in the posterior compartment caused both a decline in *hh* expression and ectopic expression of *dpp* and *wg* in those cells that had lost *en* function (Tabata and Kornberg, 1994). The consequence is a complete anterior transformation of posterior cells lacking *en* function, thus creating two new compartments - an anterior compartment consisting of *en*⁻ posterior cells, and a posterior compartment consisting of the remaining *en*⁺ cells. This created a new compartment boundary, marked by the ectopic expression of *dpp* and *wg* in cells mutant for *en*. In some cases, the new compartment formed a new axis of A/P polarity, indicating that juxtaposition of *en*-expressing (posterior compartment) cells with non-*en*-expressing cells alone provides sufficient information to create a new compartment border. When properly situated, such an ectopic border can initiate formation of an appropriately-patterned ectopic imaginal appendage. These results demonstrate that the A/P compartment border is the critical organizational feature of disc patterning.

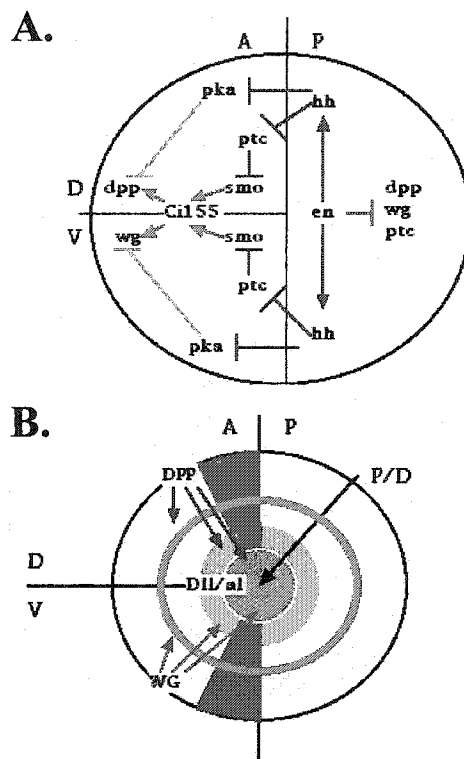
Creating the dorsal-ventral axis in imaginal leg discs.

HH diffusion into the anterior compartment from the A/P boundary causes differential activation of *wg* (Basler and Struhl, 1994) and *dpp* (Blair, 1992; Capdevilla et al., 1994; Basler and Struhl, 1994; Tabata and Kornberg, 1994; Massucci et al., 1990; Posakony et al., 1990) in cells near the A/P compartment boundary (**Figure 8C**). The dorsal cells in the anterior compartment that abut the posterior compartment express *dpp* (Massucci et al., 1990; Raftery et al., 1991; Padgett et al., 1987), whereas the corresponding ventral cells express *wg* (Struhl and Basler, 1993; Couso et al., 1993; Baker, 1987; Hepker et al., 1997; Sanicola and Sekelsky, 1995). HH binds to the *Patched* (*Ptc*)/*Smoothed* (*smo*) receptor complex, counteracting the inhibition of *smo* and Protein Kinase A (*pka*), thereby allowing activation of *wg* and *dpp* in the anterior compartment (Chen and Struhl, 1996, Stone et al., 1996; Marigo et al., 1996; Chen and Struhl., 1998) (see **Figure 9A**). In addition to transducing the HH sig-

nal, PTC also impedes movement of HH thereby limiting the region of *wg* and *dpp* activation to a narrow stripe abutting the A/P boundary (Chen and Struhl, 1996; Chen and Struhl, 1998). *Cubitus interruptus* (*Ci*) which is expressed in the anterior compartment, is proteolytically processed into two different forms - CI^{75} a repressor and CI^{155} an activator (Alexander et al., 1996; Dominguez et al., 1996). At the A/P boundary HH signaling causes *Ci* to be converted to the activator of *wg* and *dpp* expression (Aza-Blanc et al., 1997; Chen et al., 1998; Ohlmeyer and Kalderon, 1998; Hepker et al., 1997). In cells in the anterior compartment that do not receive the HH signal, CI^{75} predominates and represses *wg* and *dpp* (Dominguez et al., 1996; Aza-Blanc et al., 1997; Ohlmeyer and Kalderon, 1998). Therefore, the localized expression of *dpp* and *wg* transcripts are tightly regulated. *EN/INV* represses the expression of *dpp* and *wg* in the posterior compartment (Sanicola and Sekelsky, 1995; Tabata et al., 1995) whereas CI^{75} acts as a transcriptional repressor of *dpp* in anterior cells outside the range of the HH signal (Aza-Blanc et al., 1997).

Wg is expressed in the anterior ventral (A/V) quadrant and, *dpp* is expressed mainly in the anterior-dorsal (A/D) quadrant of a leg disc in cells adjacent to the A/P boundary (Capdevilla and Guerrero, 1994). It was proposed that the asymmetric expression of *wg* and *dpp* signals the initial specification of D/V cell fate (Figure 8C). Earlier studies showed that disc mutants of *wg* result in loss of ventral structures and their replacement by symmetric duplications of dorsal structures (Baker, 1987; Couso et al., 1993, Held et al., 1994, Held and Hempf, 1996; Theisen et al., 1996). Ectopic expression of *wg* in the dorsal compartment of a leg disc results in re-specification of dorsal cells to ventral cells, causing ventral axis duplications (Struhl and Basler, 1993; Diaz-Benjumea and Cohen, 1993). Conversely, *dpp* activity is needed to specify dorsal cell fates. Disc mutations of *dpp* result in ventralization of dorsal structures and symmetric duplication of ventral structures (Held, 1993). Ectopic expression of *dpp* in the ventral compartment results in a ventral-to-dorsal cell fate transformation that causes dorsal axis duplications (Diaz-Benjumea et al., 1994). This D/V restriction of *wg* and *dpp* function is further supported by experiments in which clones ectopically expressing *hh* in the disc are able to induce ectopic expression of *dpp* only in the dorsal quadrant of the anterior compartment (Masucci et al, 1990; Basler and Struhl, 1994) and *wg* in the ventral anterior quadrant (Basler and Struhl, 1994). In these experiments, ectopic *wg* or *dpp* expression is never observed in either the dorsal or ventral quadrants of the anterior compartment. Restricted expression of both *wg* and *dpp* was possibly due to the fact that cells in the dorsal quadrant are only competent to express *dpp*, whereas cells in the ventral compartment are only competent to express *wg*. Later studies illustrate that *dpp* could be expressed in the ventral compartment in the absence of *wg*. Conversely, *wg* could be expressed in the dorsal quadrant in the absence of *dpp*. This study concluded that *wg* and *dpp* might mutually antagonize one another's expression in the anterior compartment, thus restricting their functions to the ventral and dorsal quadrants (Brook and Cohen, 1996; Theisen et al., 1996; Jiang and Struhl, 1996; Penton and Hoffmann, 1996; Heslip et al., 1997). These authors suggest that this localized expression of *wg* and *dpp* is maintained by a combination of autoactivation and lateral inhibition. Thus, restriction of *wg* and *dpp* expression in the A/V and A/D quadrants correlates with the genetic evidence suggesting that *wg* and *dpp* function are required to specify the A/V and A/D cell fates, by mutually inhibit the others expres-

Figure 9. Model for establishing the proximal-distal organizer in the *Drosophila* imaginal leg disc.



Schematic diagram describing the genetic circuitry implicated in forming the proximal-distal organizer in a leg disc. **(A)** Initially, the anterior-posterior pattern is inherited from the embryonic ectoderm by the localized expression of the selector gene *engrailed* (*en*) (see **Figure 7**). This leads to the activation of *hedgehog* (*hh*). Diffusion of HH into the anterior compartment activates the expression of *wingless* (*wg*) and *decapentaplegic* (*dpp*) by repressing *protein kinase A* (*pka*) and *patched* (*ptc*). The repression of *ptc* by HH leads to the activation of the *smoothened* (*smo*) receptor, which allows the *cubitus interruptus* activator, *Ci*¹⁵⁵, to activate *dpp* and *wg* expression in the anterior cells adjacent to the A/P boundary. Dorsal/ventral cell fates are established by the restricted expression of *dpp* and *wg* that is maintained by autoactivation of *dpp* and *wg* expression and by their mutual lateral inhibition. **(B)** Subsequently, the interaction between adjacent cells of AD, AP and P compartments, which intersect at a unique point in the disc, defines the most distal extremity of the leg disc. The interactions between adjacent cells from these compartments defines the distal organizer, and the distal most extremity of the leg disc. The interaction between these adjacent cells is mediated by *wg* and *dpp* expression, in which the overlapping expressions of diffusible DPP (blue) and WG (red) morphogens at the center of the imaginal leg disc are thought to act as organizing signals to pattern cells along the proximal-distal axis. The integration of high levels of DPP and WG signaling in the center of the disc leads to the activation of *Dll* (yellow) (Cohen, 1993) and *aristaless* (*al*) (brown) (Campbell and Tomlinson, 1998), genes that specify distal cell fates in the leg disc. Anterior compartment (A), posterior compartment (P), dorsal compartment (D), ventral compartment (V), and proximo-distal axis (P/D).

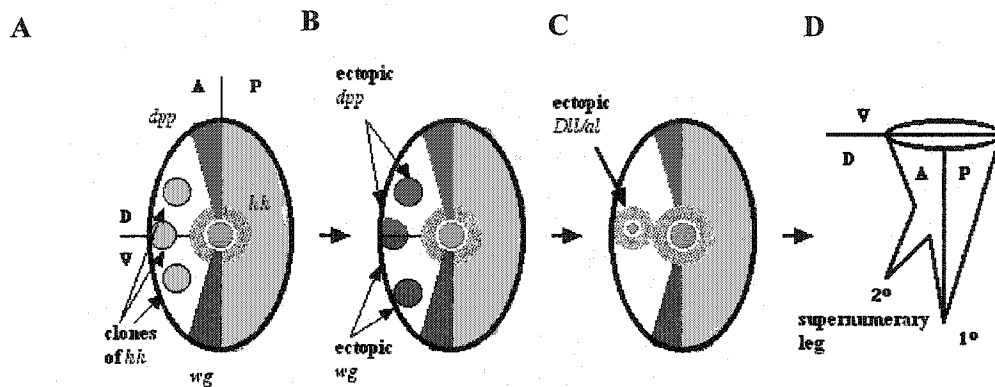
sion, such that *dpp* expression remains localized in the anteriodorsal quadrant and *wg* is expressed in the anteroventral quadrant. The differential response to HH signal in the dorsal and ventral anterior quadrants reflects the subdivision of the anterior compartment of a leg disc into dorsal and ventral cell identities. This supports earlier cell lineage evidence that a D/V boundary subdivides the anterior compartment of a leg into dorsal and ventral subcompartments (Steiner, 1976). The complementary AD and AV domains, which are defined by a hidden competence to express *wg* and *dpp*, buttress Meinhardt's assumption of a second (D/V) compartment boundary in a leg disc. In this case, a second compartment restriction in a leg disc is regulated by HH function along the A/P compartment boundary. Therefore, control of gene expression in the anterior compartment by *en* via HH functionally links the A/P boundary with regulation of D/V axis formation. The A/P compartment boundary, established by *en* expression, acts as a source for a short-range HH signal, which leads to the asymmetrical expression of two other secreted growth factors, the products of *wg* and *dpp*, which provide spatial information that specifies dorsal/ventral compartment fate.

The A/P and the D/V boundaries generate an organizing center for proximal/distal axis specification.

A feature that distinguishes the patterning of discs from that of the embryo is a requirement to superimpose organization of a proximal-distal axial pattern on underlying anterior-posterior and dorsal-ventral patterns. The current model, based on Meinhardt's boundary model (Meinhardt, 1983a), proposes that the established intercellular signaling machinery involving segment polarity genes, which transmit positional cues within a disc primordium to establish the A-P and D-V axes, is later co-opted in the disc to establish a radial proximal-distal pattern.

The activation of *dpp* and *wg* by *hh* was shown to be important not only for specifying the D-V axis in a leg disc, but also for inducing distalization in a leg (Basler and Struhl, 1994; Capdevilla and Guerrero, 1994; Kojima et al., 1994; Campbell and Tomlinson, 1995; Held, 1995) (**Figure 9B**). Basler and Struhl (1994) showed that clones ectopically expressing *hh* in the anterior compartment of a leg disc can exert a non-autonomous influence on surrounding cells that can lead to axis duplication in a leg (**Figure 10**). Distal duplications in an adult leg induced by ectopic HH expression contain only anterior compartment structures and occur only when *hh*-expressing clones occupy both dorsal and ventral anterior quadrants. The authors suggest that axis duplications in a leg are due to the juxtaposed expression of *wg* and *dpp* in dorsal and ventral cells of the anterior compartment. The adjacent expression of *wg* and *dpp* is thought to induce an ectopic distal organizer as suggested by Meinhardt (see above). Basler and Struhl (1994) further speculate, based on Meinhardt's boundary model (Meinhardt, 1983a, 1986, 1989), that the apposition of cells expressing high levels of *wg* and *dpp* at the conjunction of the AD/AV and A/P boundaries triggers activation of another morphogen in the same cells. This morphogen would then diffuse radially from the organizing center in the middle of a disc, providing proximo-distal positional values. Further support for this hypothesis came from studies showing that clones ectopically expressing *wg* or *dpp* in a imaginal leg disc result in the activation of an ectopic dis-

Figure 10. The effects of ectopic expression of *hh* on proximal-distal axis formation in a leg disc.



(A) A small clone of cells ectopically expressing *hh* (yellow circle) in the dorsal/anterior or ventral/anterior region of a leg disc will induce ectopic expression (B) of *dpp* (blue circle) or *wg* (red circle) respectively. These clones will typically result in the overgrowth of dorsal or ventral anterior quadrants. Cells ectopically expressing *hh* in the medial-lateral region of the leg disc (A), straddling the D/V boundary in the anterior compartment, will induce juxtaposing ectopic expression of both *dpp* and *wg* (blue and red circles) (B). (C) In the case in which clones of *wg* and *dpp* are closely situated in the same leg disc, this will result in the ectopic expression of *al* (brown) and *Dll/al* (grey). (D) In the case of medial lateral clones, a supernumerary leg will be generated from the anterior compartment in the adult leg. *Decapentaplegic* (*dpp*), *distalless* (*dll*), *hedgehog* (*hh*), *wingless* (*wg*), *aristaless* (*al*), primary axis (1^o), secondary axis (2^o). *Hedgehog* (*hh*) expression is depicted in yellow, *dpp* in blue, and *wg* in red. Anterior compartment (A), posterior compartment (P), dorsal compartment (D), and ventral compartment (V).

tal organizer, causing axis duplications in the adult legs (Struhl and Basler, 1993; Campbell et al., 1993; Capdevilla and Guerrero, 1994; reviewed in Campbell and Tomlinson, 1995, see also **Figure 9B**). When clones ectopically express *wg* in cells that are in close proximity to cells that express *dpp* endogenously in the AD quadrant, an ectopic distal organizer forms, leading to the formation of supernumerary distal leg structures (Struhl and Basler, 1993; Campbell et al., 1993). Similarly, ectopic expression of *dpp* in the anterior (or posterior) compartment(s), close to the D/V boundary where *wg* is expressed, induces a distal leg duplication (Capdevilla and Guerrero, 1994). The various ectopic expression experiments using *hh*-, *dpp*- or *wg*-expressing clones provide compelling evidence that the A/P and D/V boundaries direct P-D axis formation by acting as a source for activation of one or more inductive signals.

Dll (first identified by Cohen et al., 1989) was initially proposed as a candidate morphogen responsible for P-D axis formation. *Distalless* mutations resulted in distal truncation or entire deletions of the P/D axis of a leg (Cohen et al., 1989). *Distalless* is expressed throughout leg disc development, and is first detected at the intersection of perpendicular *wg* and *dpp* stripes along the A/P and D/V axes of an embryo where epidermal cells are first allocated to a leg disc primordia (**Figure 8C**). Later in development, *Distalless* expression becomes centrally localized in mature leg discs (**Figure 9B**) (Cohen, 1993). However, cloning of *Dll* showed that the gene encoded a protein containing a homeobox domain, characteristic of a nuclear transcription factor. This is inconsistent with the notion of *Dll* being the diffusible morphogen postulated for patterning of the P/D axis according to the Meinhardt boundary model (Cohen and Jurgens, 1991). The authors hypothesized that *Dll* protein (DLL) might specify positional information along the P/D axis of a leg in response to another P/D morphogen. This was supported by earlier genetic analysis which showed that hypomorphic alleles of *Dll* can be ordered in a series wherein varying amounts of distal leg material are missing (Cohen et al., 1989).

The idea that *Dll* expression is dependent on the activity of *wg* and *dpp* is consistent with earlier genetic data. Reduction of *wg* and *dpp* activity caused by certain viable mutations results in the loss of distal leg structures (Sharma and Chopra, 1976; Spencer et al., 1982; Baker, 1987; Gelbart, 1989; Diaz-Benjumea et al., 1994). This is seen with *Dll* mutations as well. In addition, genetic interaction studies show that the phenotypes of weak *Dll* mutations are enhanced in the presence of *wg* and *dpp* mutations, supporting the idea that these genes work in a common pathway (Held et al., 1994).

Clones ectopically expressing *hh* close to (or overlapping) the D/V boundary result in ectopic activation of *Dll* in the clone and surrounding cells (Basler and Struhl, 1994; **Figure 10C**). Ectopic activation of *Dll* is also found straddling the AD/AV boundary between the ectopic *wg*-expressing and *dpp*-expressing domains (Diaz-Benjumea et al., 1994). This shows that *Dll* activation, responsible for P/D axis specification, is the result of juxtaposed expressions of *wg* and *dpp*. Using a *wg* Flp-out construct to ectopically express *wg* (Struhl and Basler, 1993), supernumerary legs are seen only when *wg*-expressing clones are made adjacent to endogenous *dpp*-expressing cells in the AD quadrant of leg disc (**Figure 11A**). This coincides with ectopic *Dll* expression seen in ectopic patches of *wg*-expressing

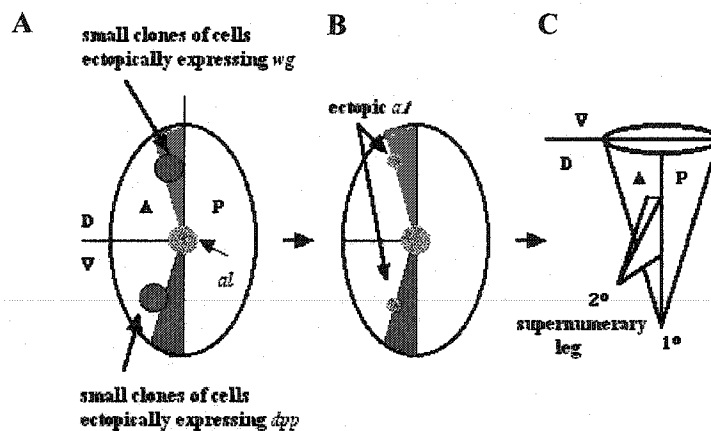
cells that are in close proximity to endogenous *dpp*-expressing cells in the dorsal-anterior quadrant of a leg disc (**Figure 11B**). Diaz-Benjumea et al. (1994) also report that *Dll* expression is activated upon ectopic expression of *wg* or *dpp* in the AD or AV quadrants, respectively. Therefore, ectopic expression of *Dll* confirms that *dpp* and *wg* are both functionally active at ectopic sites where *dpp* and *wg* expression are juxtaposed. The authors conclude from this that the initial specification of the P/D axis is governed by interactions among the diffusible factors HH (A/P compartment), WG (AV compartment) and DPP (AD boundaries) in accordance with the Meinhardt boundary model of positional information. This may lead to the activation of another diffusible factor, acting as a morphogen, which in turn either regulates the expression of *Dll* or is regulated by *Dll* itself (Campbell and Tomlinson, 1995).

I-6. Morphogen gradients in imaginal discs.

Morphogens were originally postulated as form-generating substances that are capable of organizing surrounding tissues into distinct territories of specific cell types (Turing, 1952). The precise molecular and cellular mechanisms of molecules with morphogenic properties remained sketchy. The model postulates that a morphogen forms a long-range concentration gradient (Stumpf, 1966; Lawrence, 1966, 1972; Slack, 1987; Wolpert, 1969, 1989 and 1996) that emanates from a localized source, diffuses across a cellular field, and provides a series of thresholds that specify the fates of neighboring cells (Gurdon et al., 1995; Neumann and Cohen., 1997b; Gurdon, 1998). From insects to vertebrates, signaling molecules of the Wnt (Wingless and Int-1) and TGF β (transforming growth factor β) families are proposed to act as *bona fide* morphogens with long-range organizing properties. These morphogens bind to receptors that activate a specific intracellular signal transduction cascades (see reviews, Wodarz and Nusse, 1998; Massague, 1998). For example, in *Xenopus*, activin, a TGF β family member that was originally characterized as a dorsal mesoderm inducer (Green and Smith, 1990; Smith et al., 1990; Gurdon et al., 1994), is known to behave as a potent morphogen. Different thresholds of activin produce distinct effects on mesoderm gene expression and cell type. For example, high levels of activin induce notochord, and low levels induce haemopoietic tissue (Green and Smith, 1990; Green et al., 1992; Gurdon et al., 1997). Activin-induced gene expression was examined by implanting beads soaked in different concentrations of activin into the animal cap of *Xenopus* embryos (Gurdon et al., 1994, 1995; Gurdon and Mitchell, 1996). The authors showed that striking changes in gene expression and cell type are induced depending on the concentration used.

Despite the appeal of the concentration gradient hypothesis, there are some unresolved issues. Even though experiments suggest that cellular responses to a given secreted factor are a function of its concentration, it has never been established if the secreted factor acts directly on the target cells. Recent studies using the imaginal discs in *Drosophila* have suggested that secreted factors such as WG (Zecca et al., 1996; Neumann et al., 1997; Cadigan et al., 1998) and DPP (Nellen et al., 1996; Lecuit et al., 1996; Lecuit and Cohen, 1997 and 1998) protein behave diffusible morphogens to specify cell fate over long distances (see section IV-5ii in the Discussion for a detailed description). In addition, the mechanism by which a cell can detect and discriminate between different threshold concentrations of a

Figure 11. The effects of ectopic expression of *wg* and *dpp* on the proximal-distal axis formation in an imaginal leg disc.



(A) Small clones of cells ectopically expressing *wingless* (*wg*) (red circle) or *decapentaplegic* (*dpp*) (blue circle) in the leg disc will induce a secondary P/D axis (C) only if the *wg* expressing clone (red circle) or the *dpp* expressing clone (blue circle) are situated in the dorsal or ventral compartment adjacent to the endogenous stripe of *dpp* (blue) or *wg* (red) expression respectively. (B) Ectopic *aristaless* (*al*) (gray circle) expression is induced where cells expressing *dpp* juxtapose those expressing *wg*, marking the presumptive tip of the supernumerary leg (C). For the *dpp* clones, the supernumerary axis is formed on the ventral side. For *wg* clones, the extra axis forms on the dorsal side. Anterior compartment (A), posterior compartment (P), dorsal compartment (D), ventral compartment (V), primary axis (1°), and secondary axis (2°).

morphogen remains unknown. In this case, putative morphogens such as WNT and TGF β were shown to bind to specific receptors, which may or may not be solely responsible for detecting threshold concentrations.

Positional information systems mediated by gradients of diffusible morphogens that can account in principle for imaginal disc patterning in *Drosophila* (but not necessarily for duplication and regeneration), have been postulated, but molecular evidence has remained elusive. *Decapentaplegic* protein (a TGF β family member in *Drosophila* (Padgett et al., 1987), for example, has been proposed as a candidate morphogen. Spencer et al. (1982) suggest that disc alleles of *dpp* alter the gradient of positional information. Mutations of *dpp* affect an array of positional information values as a result of non-autonomous effects, which would be predicted for genes encoding a molecule with the properties of a morphogen. The non cell-autonomous behavior of a gene describes the ability of a mutant of a gene to influence the behavior not only of cells that contain the mutation, but also their wild-type neighbors. Even though *dpp* is transcribed in only a small portion of the wing and leg discs, mutations affecting *dpp* signaling have phenotypic effects on pattern well beyond its expression domain. Such a discrepancy between a small domain of transcription and a large area of influence would be expected if the gene product was functioning as a diffusible morphogen. Spencer et al. (1982) show that various alleles of *dpp* could be arranged in a phenotypic series, with an increasing severity of effects from distal to proximal segments of adult legs. Distal structures are abnormal or absent in all mutants, and damage from more extreme mutant alleles extends progressively to include more proximal structures. Different mutant alleles of *dpp*, that vary in strength, are associated with position-specific effects on disc development, showing that *dpp* affects positional information in a gradient-like manner.

Despite the explanatory value of morphogen gradients, much of the evidence over whether such gradients actually operate during imaginal disc development, or how they organize cell behavior remains indirect. Much of the available experimental data up to 1996 seem to argue against the view that secreted proteins such as HH, WG and DPP function as gradient morphogens. HH, for example, seems to be propagated indirectly by its ability to act as a short-range inducer of DPP and WG (Basler and Struhl, 1994; Capdevila and Guerrero, 1994; Ingham and Fietz, 1995; Zecca et al., 1995; Jiang and Struhl, 1995; Li et al., 1995; Pan and Rubin, 1995). In the case of WG and DPP there is compelling evidence that these serve as local inducers as described in the embryo (Ferguson and Anderson, 1992a; Vincent and Lawrence, 1994; Bienz, 1994). However in a few apparent cases of longer-range organizing activity of WG, DPP and HH, the evidence that these molecules normally exert a direct influence on responding cells is not compelling (Struhl and Basler, 1993; Hoppler and Bienz, 1995; Zecca et al., 1995). The failure to obtain such evidence had left uncertain whether any extracellular signaling molecules actually function as a bona fide gradient morphogen.

I-6i. *Decapentaplegic* acts as a morphogen to specify positional information in imaginal discs.

In two elegant papers Zecca et al. (1996) and Nellen et al. (1996) showed that both WG and

DPP behaved as gradient morphogens that had both direct and long-range action on patterning in the imaginal wing disc. In the case of DPP the authors (Nellen et al., 1996) compared the consequences of ectopically expressing DPP with that of ectopically activating the receptor system that transduces the DPP signal. They hypothesized that if DPP operated indirectly through the induction of other signals, then the ectopic activity of the receptor system alone should be as effective in exerting a long-range influence on surrounding cells as the ectopic expression of the DPP ligand. Conversely, if DPP operates as a gradient morphogen, only the ectopic expression of the DPP ligand should have this property. In the developing wing disc, *dpp* is expressed in a narrow stripe of cells that are adjacent to the A/P compartment boundary. Nellen et al (1996) demonstrated in the wing that *dpp*-expressing cells can influence the behavior of surrounding cells, up to 20 cell diameters away from the A/P boundary. The activated form of the *dpp* receptor *thv* failed to induce this response non-autonomously in the surrounding cells. This implied that the long-range organizing activity must be attributed solely to the direct action of DPP on responding cells. Secreted DPP must translocate either through or across the tissue over many cell diameters, acting directly on cells from the DPP-secreting cells. Different threshold concentrations of DPP would then elicit distinct molecular responses of its nuclear target genes *optomotorblind* (*omb*) and *spalt* (Nellen et al., 1996; Lecuit et al., 1996). This suggested to the authors that DPP may form a long-range activity gradient necessary for the activation of its target genes. The edges of the domains of both *omb* and *spalt* induction extended over a range of a few cell diameters as a function of distance from the DPP-secreting cells, showing different threshold concentrations of DPP elicited distinct expression of target genes. Although the authors did not show the distribution of secreted DPP in this experiment, DPP appeared to exert a long-range influence on wing development, acting as a morphogen organizing the domains of *spalt* and *omb* expression at different concentration thresholds, rather than as a short-range inducer of other signals. The authors inferred from the results that the spatial gradient of DPP activity determines both the range and level of target gene activation, where different threshold concentrations of DPP elicit distinct molecular outputs (Nellen et al., 1996).

In another study Lecuit and Cohen (1997) show that DPP also functions as a gradient morphogen to specify the P/D axis in the leg disc. They showed that DPP could act directly and at long range to induce *Dll* and *dachsund* (*dac*) expression respectively. *Dac* is induced at a greater distance from a clone of DPP-expressing cells than *Dll*, which suggests that *dac* can be induced at levels of DPP activity that are not sufficient to induce *Dll*. They proposed that the DPP signal is required in a spatially-graded manner to define distinct proximal-distal domains of target gene expression that define differences in cell identity along the proximal-distal axis of the leg (Lecuit and Cohen, 1997). The kinetics of gradient formation were analyzed indirectly via the expression of the DPP target genes *omb* and *sal*. Lecuit and Cohen (1998) showed that small clones of cells expressing DPP, were able to organize gene expression over broad domains of surrounding cells. Ectopic expression of low levels of DPP results in the differential expression of *omb* and *sal*: *omb* is turned on within 24 hr of clone formation, while *sal* expression is first observed after 72 hr. These results suggest that receptors sense the amount of DPP, and transcriptional output may be the result of stable ligand accumulation on the target cell surface over time. By contrast, clones ectopically expressing high levels of DPP induce both *sal*

and *omb* expression within 24 hr, but both genes are expressed in the same spatial domain. By 50 hr after clone formation, the transcriptional boundary of *omb* becomes measurably wider than that of *sal*. These results suggest that the diffusion of DPP is initially restricted, resulting in a steep gradient, and only after a period of time does the slope of the gradient lessen to allow differential expression of *sal* and *omb*. These studies support the hypothesis that DPP may act as a diffusible morphogen, acting through THV, to specify all positional values in a field of cells in a dose-dependent fashion. The extracellular gradient of DPP then directs distinct cellular responses over many cell diameters, in a concentration dependent manner. If this so, regulating the graded distribution of DPP in the ECM would be critical to its role in specifying positional information in imaginal discs during development.

Maximal DPP activity in imaginal discs require synergistic signaling from a second ligand, *glass bottom boat* (*gbb*), acting exclusively through the SAX receptor, adding another level of complexity to the morphogen model (Khalas et al., 1998). *Gbb* represents another TGF β - like signal in imaginal wing discs, and provides a constant level of DPP activity across the imaginal disc (see **Figure 16** page 49). *Gbb* is normally expressed uniformly throughout the wing pouch of the disc, and the patterning defects observed in hypomorphic *dpp* mutant wings are exacerbated by a small reduction in *gbb* activity. This suggests that *gbb* protein (GBB) elevates DPP signaling through its receptor, most noticeably in regions of low signaling strength away from the site of DPP expression (Khalas et al., 1998). It was also shown that SAX, the receptor for GBB, is required to obtain normal levels of DPP signaling in imaginal discs (Penton et al., 1994; Nellen et al., 1994; Brummel et al., 1994; Singer et al., 1997). The question of how the morphogen gradient involving DPP and GBB is physically formed remained unknown. However, recent findings have shed some light on how the diffusion of DPP might be regulated to establish a gradient of DPP activity. In the discussion (section IV-4) I will describe the current evidence, and how the results from this study might be incorporated with present model.

I-7. Regeneration, a model for discovering new genes involved in pattern formation.

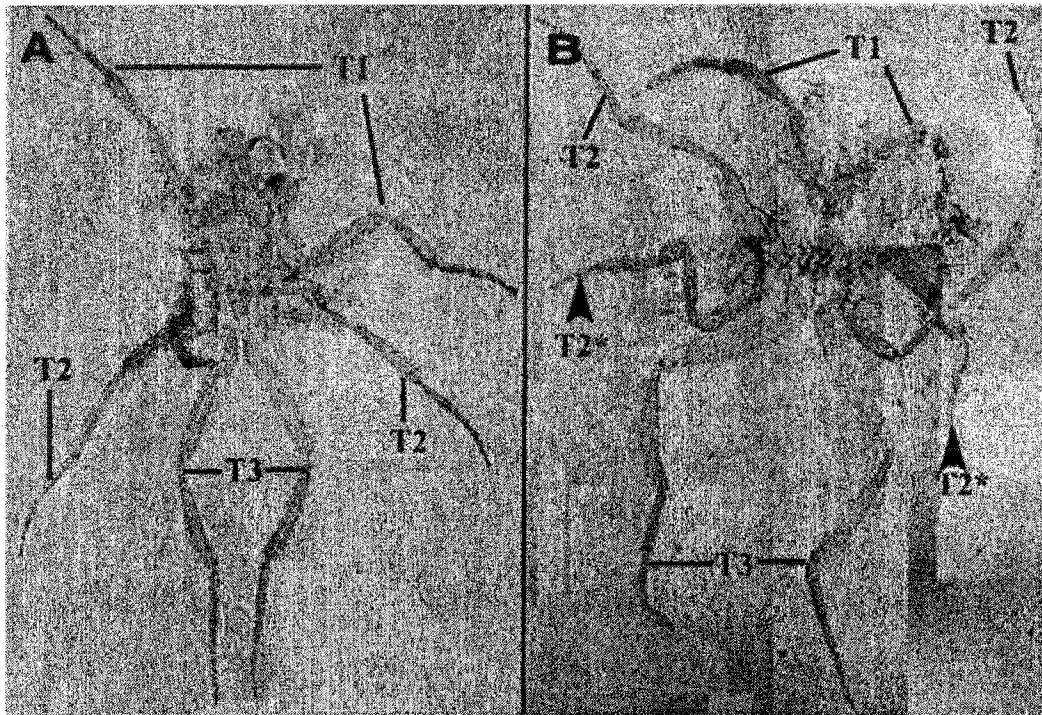
When the endeavors documented in this thesis were initiated, there was no evidence concerning *Drosophila* limb development regarding the molecular mechanism of the distal organizer beyond the required activity of the secreted growth factors HH, WG and DPP. Cells expressing these genes were known to have potent organizing activity that could affect the fates of neighboring cells and result in secondary axis formation in the leg and wing discs. However, there was only a limited understanding at the time of how these genes may function. For example, it was not known whether they act directly or as short- or long-range signals. WG is not detectable at distances greater than a few cell diameters beyond the domain of transcription of *wg* in the AV quadrant. *Wingless*-expressing clones in the AD region can recruit neighboring cells to form extra ventro-lateral pattern elements. Such a non-autonomous organizing ability could be explained either by an indirect inductive process whereby WG behaves as a local signal which goes on to trigger a lateral cascade of short-range inductions (Struhl

and Basler, 1993; Siegfried and Perrimon, 1994; Siegfried et al., 1994; Wilder and Perrimon, 1995), or by a direct role as the WG morphogen, which would depend on the diffusion of WG over a long distance.

The current literature reviewed here remained insufficient to describe fully the mechanism of insect imaginal disc pattern formation at both the cellular and molecular levels. Most of the genes involved in disc patterning were originally discovered because of their roles in embryonic patterning. Evidence to this point implicates signaling molecules like HH, DPP and WG in the initial events of imaginal disc patterning. However, relatively little is known about the mechanism by which they interact to provide patterning information in a dividing cell population or about other genes that may be involved. Thus, additional screens were needed to identify new genes affecting disc patterning. Imaginal discs provide a multicellular model system in a genetically-tractable organism by which one can utilize the extensive genetic and molecular techniques in *Drosophila* to identify new genes involved in the patterning process. Identification of novel genes will inevitably shed light on the mechanism of patterning that could be of general relevance to patterning and regeneration in other biological systems.

One way to dissect the genetic basis of positional information in imaginal discs is to utilize the regeneration/duplication phenomenon. The regulative re-patterning events during regeneration of imaginal discs involves the formation of a regeneration blastema (distal organizer), the reassignment of compartmental commitments, and the re-specification of cell fates. This provides several basic cellular and molecular events that can be studied genetically, providing a useful experimental paradigm for pattern formation. One approach is to identify genes misexpressed in duplication events during regeneration of imaginal leg discs in *Drosophila melanogaster* (Brook et al., 1993). It is speculated that the duplication of the leg pattern would require not only developmental cues to initiate a secondary axis but also the same positional cues used in normal leg development to create a new leg pattern. Duplications can be induced *in situ* by using a temperature-sensitive cell-autonomous lethal mutation, *suppressor of forked 12* (*su(f)¹²*) (Russell, 1974; Russell et al., 1977; Clark and Russell, 1977; Girton and Kumor, 1985) (**Figure 12**). Using an enhancer-trap strategy (O'Kane and Gehring, 1987; Bellen et al., 1989) in conjunction with the *su(f)¹²* mutation, Brook et al. (1993) devised a screen that identified a set of enhancer-trap lines which were ectopically misexpressed during imaginal disc re-patterning following cell death. The enhancer-trap system is useful for identifying a desired class of genes on the basis of their expression patterns (Cooley et al., 1988; Grossniklaus et al., 1989; Hartenstein and Jan, 1992). The expression of a *lacZ* reporter gene by an enhancer-trap insertion putatively indicates the expression pattern of an endogenous gene (Wilson et al., 1989; Jacob et al., 1989). In this case, the enhancer-trap system is employed instead of a direct mutational approach, owing to the extreme technical difficulty of identifying mutations in genes required for pattern respecification. This is because most of these mutations would be homozygous lethal, and also because regeneration phenotypes are difficult to score. Using the enhancer-trap screen, over 800 random autosomal inserts of a transposable *P-lacZ*, *ry+* construct were initially screened (Brook et al., 1993), followed subsequently by 500 PZ-

Figure 12. Duplication in adult legs in *Drosophila melanogaster* caused by the temperature-sensitive autonomous cell-lethal mutation $su(f)^{12}$ (this study; Russell, 1974; Russell et al., 1977).



(A) Legs of adult wild-type female. (B) Heat-treated *suppressor of forked*¹² ($su(f)^{12}$) adult female showing a duplication of both mesothoracic (T2) legs. Prothoracic legs (T1), mesothoracic legs (T2), and metathoracic legs (T3). Mesothoracic (second thoracic) leg duplications are indicated as (T2*) (see arrowheads).

lethal insertion lines (Russell et al., 1998). Positive fly lines in which the *lacZ* reporter gene was ectopically misexpressed in regenerating discs were maintained and designated as identifying putative regeneration and patterning genes. Several lines that showed differential *lacZ* expression were re-tested for the same behavior in regenerating disc fragments cultured *in vivo*. Specific expression was often seen at the sites of wound healing, where the regeneration blastema subsequently forms (Brook et al., 1993).

I-8. Objectives.

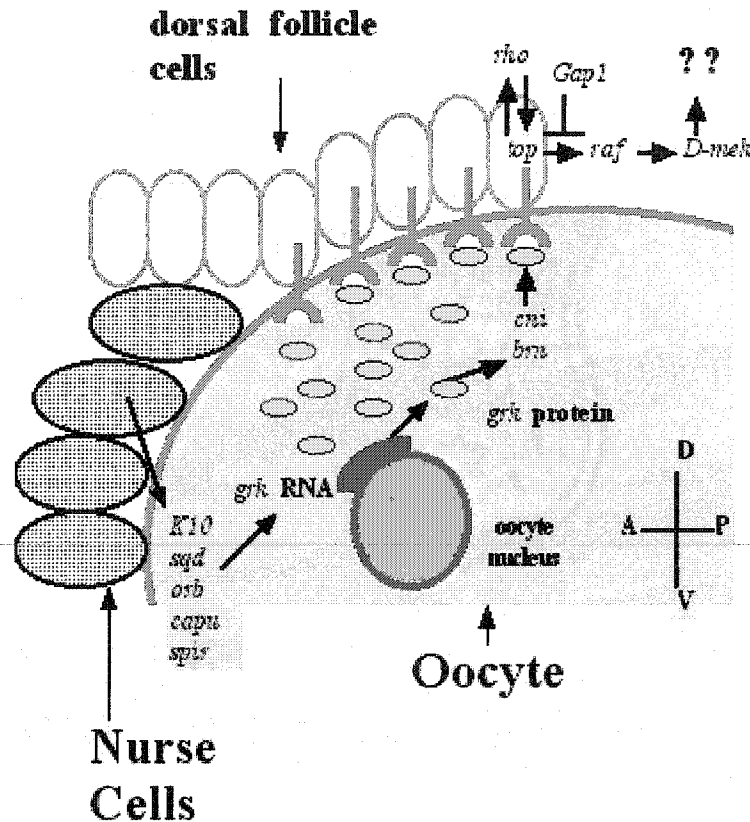
My objective was to identify genes that may have been isolated in the regeneration enhancer-trap screen, and to characterize their roles in the context of pattern formation in *Drosophila*. Based on the previous evidence demonstrating that genes which regulate pattern formation in an embryo are also required in imaginal disc patterning, the embryonic mutant phenotypes associated with the lethal insertions were analyzed by looking at embryonic cuticle preparations. Therefore, I decided to screen for embryonic lethal effects that resulted in patterning defects, caused by the PZ-lethal insertion lines isolated from the regeneration screens by Brook et al. (1993) and Russell et al. (1998).

The zygotic lethal mutation of *PZ A64*, that was chosen from the screen for analysis, generates embryos that exhibit a loss of dorsal pattern elements. Head involution and germband retraction is disrupted, and the dorsal-most epidermis is significantly reduced or lost. In embryos that show partial germband retraction, dorsal closure fails to occur, resulting in a small opening on the dorsal side. These phenotypic effects are similar to those caused by mutations in genes that regulate the *dpp* signaling pathway and dorsal-ventral patterning of the embryo. This phenotype, led me to further characterize the role of *PZ A64* in dorsal-ventral pattern formation. The specification of the dorsal-ventral (D-V) axis in *Drosophila* embryo unfolds by the sequential action of three signaling pathways, and the challenge is to determine which pathway is affected in a particular mutant.

I-8i Specification of the dorsal-ventral axis in the *Drosophila* embryo.

The initial signaling cue for D-V asymmetry is determined by a group of maternal genes expressed in the germline and soma during oogenesis (**Figure 13**), which cooperate to progressively define the D-V axis. D-V patterning requires communication within the ovary between the germline-derived oocyte and the surrounding somatically derived follicle cells, which secrete the chorion and vitelline membrane of the eggshell. The oocyte nucleus (germline), located in the dorsal anterior corner of the oocyte, produces an asymmetric dorsalizing signal that is received by neighboring follicle cells (soma), thereby defining the polarity of both the embryo and eggshell. The ligand and receptor in this pathway are encoded by the genes *gurken* (germline), the *Drosophila* TGF-alpha like protein, and *torpedo* (soma), the *Drosophila* EGF receptor homolog, respectively (Schupbach, 1987; Schupbach et al., 1991; Rouhola-Baker et al., 1994). *Gurken* and *torpedo* are required for the specification of dorsal fates in the eggshell and embryo (Schupbach, 1987; Roth et al., 1995). The spatial regulation of the

Figure 13. Maternal regulatory pathway that determines D-V polarity in the *Drosophila* oocyte.



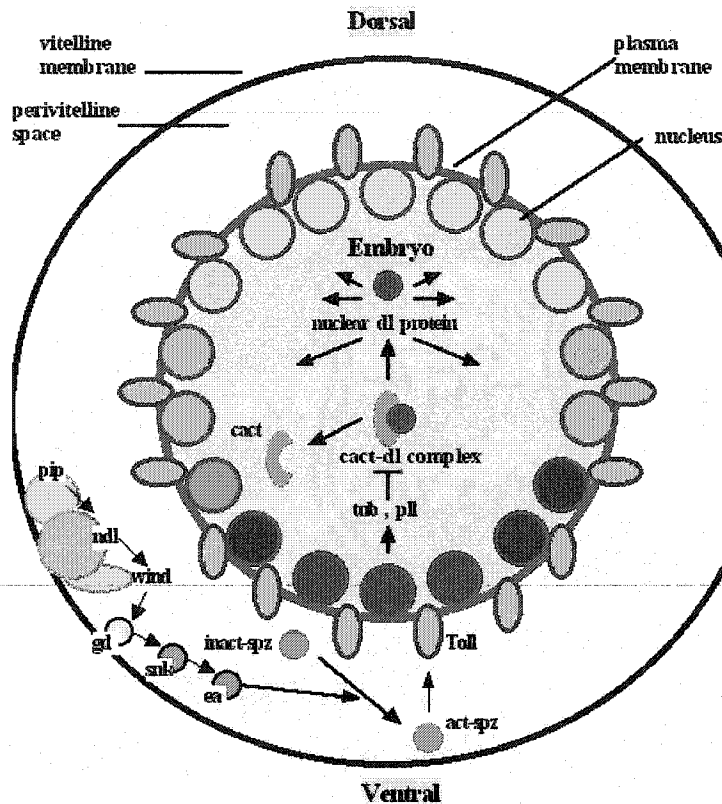
A schematic of the *gurken-torpedo* maternal regulatory pathway required for D-V pattern formation during oogenesis. The drawing shows the dorsal anterior region of the egg chamber with nurse cells (germline) and follicle cells (soma) epithelium surrounding the oocyte. The genes *fs(1)K10*, *squid* (*sqd*), *orbital* (*orb*), *cappuccino* (*capu*), and *spire* (*spir*) are required for the localization of *gurken* (*grk*) RNA to the dorsal anterior corner of the oocyte in close proximity to the oocyte nucleus. The production of an active *gurken* protein signal requires *cornichon* (*cni*), and *brainiac* (*brn*). *Gurken* protein binds to the *torpedo* receptor (*top*) expressed on the cell surface on the neighboring follicle cells. Binding of *gurken* protein to its receptor activates an intracellular Ras signaling pathway which involves the genes, *ras*, *gap1*, *raf* and *D-mek*, within follicle cells. This is modulated by the gene *rho* in dorsal follicle cells, which somehow enhances the signal, leading to proper dorsal cell differentiation. It also leads to the repression of the pattern-forming processes that establish the ventral pre-pattern of the embryo. These pattern-forming processes are active in the ventrally situated follicle cells. (Modified from Schupbach and Roth, 1994). Anterior (A), Posterior (P), Dorsal (D), and Ventral (V).

gurken signal is achieved by localizing *gurken* RNA to the dorsal side of the oocyte. The dorsalizing signal, *gurken* (expressed in the oocyte), is interpreted by *torpedo* (expressed in the follicle cells), inducing the closest neighboring follicle cells to adopt a dorsal fate. Follicle cells that are located ventrally receive little or no signal, and thus enter a ventral fate by default (Manseau and Schupbach, 1989; Schupbach et al., 1991).

The localization of *gurken* RNA is crucial in defining the spatial asymmetry of the oocyte and egg chamber. The localization of *gurken* RNA to the dorsal anterior side of the oocyte nucleus correlates with the similar displacement of the oocyte nucleus to the dorsal anterior corner of the oocyte. This marks the earliest visible dorsal-ventral asymmetry in the egg chamber (Mahowald and Kambysellis, 1989, Schupbach et al., 1991). Soon thereafter, *gurken* protein (GRK) accumulates in the cytoplasm and the plasma membrane on the dorsal side of the oocyte (Roth et al., 1995). The production of an active signal requires the downstream activation of *cornichon* and *brainiac* in the oocyte (germline) (Ashburner et al., 1990; Goode et al., 1992). *cornichon* encodes a hydrophobic protein that could be involved in the membrane localization of GRK (Roth et al., 1995). *fs(1)K10*, *spire*, *cappuccino*, and *squid* are genes that function upstream of *gurken*, and may regulate the production of an activity required for the localization of *gurken* RNA in the oocyte. Maternal-effect mutations in these genes cause the dorsalization of the egg chamber and embryo. Activation of *torpedo* (a receptor tyrosine kinase) in the follicle cells, transmits the germline dorsalizing signal by using the *Ras* pathway (van der Geer et al., 1994; Heldin, 1995). The GTPase activating protein Gap1, the serine/threonine kinase *Raf*, and the threonine/tyrosine kinase MEK are required downstream of *torpedo* (Brand and Perrimon, 1994; Hsu and Perrimon, 1994). This signaling pathway leads to dorsal follicle cell differentiation, presumably by regulating the activity of unidentified transcription factors. The follicle cells might eventually signal back into the oocyte to establish embryonic polarity, because loss of *torpedo* receptor (TOP) activity causes ventralization of the embryonic pattern in addition to the ventralization of the eggshell. The activation of TOP also induces the expression of *rhomboid* (Neuman-Silberberg and Schupbach, 1994). The rhomboid protein is a putative transmembrane protein, that appears to enhance the interaction between GRK and TOP.

The dorsal-ventral asymmetry initiated during oogenesis is transmitted to the embryo by a second signaling pathway through the activity of 12 maternal-effect genes: 11 dorsal group genes and *cactus* (see **Figure 14**) (St Johnston and Nusslein-Volhard, 1992; Chasen and Anderson, 1993). Mutations in these genes perturb the dorsal-ventral polarity of the embryo, but they have no effect on the shape of the eggshell. Females that lack the activity of any one of the dorsal group genes produce dorsalized embryos (Schupbach and Wieschaus, 1989) that lack lateral and ventral pattern elements. On the other hand, mutations in *cactus* cause an opposite phenotype resulting in ventralized embryos encircled by ventral denticle belts (Roth et al., 1991, Schupbach and Wieschaus, 1989). In contrast to the dorsalizing signal produced by the oocyte nucleus during oogenesis, the polarity of the embryo is defined by a ventral signal that promotes ventral fates. The production of this ventral signal is controlled by the ventral follicle cells, which are defined by their failure to receive the GRK signal and thus to activate

Figure 14. Maternal regulatory pathway of dorsal group genes that determines D-V polarity in the *Drosophila* embryo.



A schematic representation of *spatzle-Toll* maternal signaling pathway that establishes D-V polarity in the syncytial embryo. Early events during oogenesis in the germline and soma generate a somatic signal on the ventral side of the embryo in the perivitelline space. The cues that contribute to this signal are encoded by the somatically required dorsal group genes *nudel* (*ndl*), *pipe* (*pip*) and *windbeutel* (*wind*), all of which are contributed by the maternal soma (follicle cells). The ventral signal is transmitted through the perivitelline space by a series of zymogen activation steps encoded by the dorsal genes *gastrulation defective* (*gd*), *snake* (*snk*), and *easter* (*ea*), all of which are contributed by the germline (nurse cells). The zymogen activation steps lead to the localized proteolytic processing of *spatzle* protein (*spz*) (origin germline) and the graded activation of the transmembrane receptor *Toll* (*Tl*) (origin germline) on the ventral side of the syncytial embryo. The graded activation of *Tl* by *spz* ligand results in degradation of *cactus* protein (*cact*) and the graded nuclear import of *dorsal* protein (*dl*) (origin, germline). Localization of *dl* protein is mediated by the activities of cytoplasmic factors *pelle* (*pll*) (origin germline) and *tube* (*tub*) (origin germline). (Modified from Govind and Steward, 1991).

TOP receptor during oogenesis.

The ligand and receptor in this pathway are encoded by the genes *spatzle* and *Toll* (both germline factors) respectively. The *Toll* receptor (TOLL) encodes a transmembrane protein that shares sequence similarity with the vertebrate interleukin-1 receptor (Hashimoto et al., 1988; Gay and Keith, 1991; Schneider et al., 1991). Toll protein is distributed uniformly on the surface of the embryo indicating that dorsal-ventral asymmetry does not arise from the spatially restricted expression of *Toll*. Instead, TOLL activity is confined to the ventral side of the embryo by the ventral localization of the ligand *spatzle* (SPZ), in the perivitelline space, which activates TOLL to promote ventral cell fate (Chasen et al., 1992; Morisato and Anderson, 1994). The perivitelline space is the fluid-filled compartment that lies between the vitelline membrane and embryonic plasma membrane (see **Figure 14**). *Spatzle* encodes a secreted protein, that shows sequence similarity to a family of vertebrate growth factors that include NGF, TGF β and PDGF β (McDonald and Hendrickson, 1993; Morisato and Anderson, 1994). Consistent with its proposed role as a signaling molecule, the level of SPZ can determine the dorsal-ventral fate of an embryo (Morisato and Anderson, 1994). Spatzle protein is secreted as an inactive precursor, and diffuses freely as it becomes distributed uniformly within the perivitelline space. The spatially restricted production of active SPZ ligand is achieved by a localized proteolytic processing reaction on the ventral side of the egg chamber in the perivitelline space, generating the asymmetric signal on the ventral side of the embryo.

The proteolytic processing of SPZ, which defines the ventral polarizing activity, requires the function of seven dorsal group genes that act upstream of *spatzle* and *Toll* in the genetic pathway (Anderson et al., 1985; Chasen and Anderson, 1989; Stein and Nusslein-Volhard, 1992; Hecht and Anderson, 1992; Roth, 1994). The processing machinery that converts the precursor to the active form is tightly regulated. Ventral production of active SPZ appears to be regulated by a spatially restricted extracellular protease cascade in the perivitelline space. The *snake* and *easter* (germline factors) genes both encode proteins that are members of the trypsin family of serine proteases (Anderson et al., 1985; Chasen and Anderson, 1989; Hecht and Anderson, 1992; Stein and Nusslein-Volhard, 1992; Roth, 1994). *Snake* (SNK) and *easter* (EA) proteins are secreted into the perivitelline space as zymogens (Chasen and Anderson, 1992; Stein and Nusslein-Volhard, 1992; Smith and DeLotto, 1994), that require proteolytic cleavage for protease activity. EA is the protease directly responsible for processing precursor SPZ to its active form (Chasen and Anderson, 1992; Morisato and Anderson, 1994). SNK functions immediately upstream to cleave the EA zymogen (Smith and DeLotto, 1994). In turn *gastrulation defective* (a germline factor) encodes a trypsin serine protease that acts upstream of *snake*, to cleave and activate the SNK zymogen.

The extracellular protease cascade is regulated by *nudel*, *pipe* and *windbeutel*. These are somatic factors transcribed in the ovarian follicle cells that provide the earliest ventral cue for embryonic polarity (Stein et al., 1991). The *nudel* gene encodes a large modular protein resembling an extracellular matrix protein that contains a serine protease domain (Hong and Hashimoto, 1995). The *pipe* gene

has been shown to encode a 2-O-sulfotransferase, an enzyme localized in the Golgi apparatus, that modifies the functional properties of glycosaminoglycans, complex polysaccharide chains found associated with the extracellular domains of proteoglycans (Sen et al., 1998). The *windbeutel* gene encodes a putative resident protein of the endoplasmic reticulum, and may be responsible for the folding and or modification of a specific factor that participates in the activation of the ventralizing signal (Konsolaki and Schupbach, 1998). Spatial restriction of nudel (NDL) and pipe (PIP) protein activity occurs at the level of their expression. PIP synthesis is inhibited in dorsal follicle cells when GRK binds to TOP. The activation of the NDL zymogen is believed to be localized through the ventrally restricted activity of another protease which may involve the function of a proteoglycan regulated by PIP. Thus SPZ the D-V "polarizing activity" in the embryo is activated by a spatially localized protease activity on the ventral side of the vitelline membrane, that may represent a zymogen cascade complex (Hecht and Anderson, 1992; Roth, 1994; Hong and Hashimoto, 1995). It was shown that different concentrations of processed SPZ lead to a gradient of TOLL activity (Schneider et al., 1991), suggesting that active SPZ diffuses from its ventral site of activation to form a gradient within the perivitelline space, defining the D-V polarity of the embryo.

The activation of TOLL initiates an intracellular signaling pathway in the embryo that shows similarities to NF-KB and I κ B signaling in mammalian cells. The *dorsal* gene is homologous to NF-kB (Steward, 1987) and whereas *cactus* is related to I κ B (Geisler et al., 1992; Kidd, 1992) (**Figure 14**). The activation of Toll disrupts the cytoplasmic complex between dorsal protein (DL) and its antagonist cactus (CACT). This leads to the ventral-to-dorsal graded nuclear localization of DL (Kidd, 1992; Steward and Govind, 1993; Wasserman, 1993; Whalen and Steward, 1993) and rapid degradation of CACT (Belvin et al., 1995). The inhibition of CACT and release of DL requires the activity of *pelle*, a serine/threonine kinase and *tube* (unknown) (Letsou et al., 1991; Hecht and Anderson, 1993; Shelton and Wasserman, 1993).

Therefore, the principal effect of *gurken*, the initial asymmetric dorsalizing signal in the oocyte, on embryonic polarity is to repress the production of the active TOLL ligand, SPZ, on the dorsal side of the oocyte. The *gurken* signal then acts to restrict and orient the dorsal-ventral patterning events that act later following fertilization in the embryo. The graded activation of the TOLL receptor by the diffusion of processed SPZ results in the graded nuclear translocation of the transcription factor DL in a ventral-to-dorsal nuclear concentration gradient (Roth et al., 1989; Rushlow et al., 1989; Steward, 1989). High levels of DL are present in ventral nuclei, progressively lower levels in lateral nuclei, and no detectable protein in dorsal nuclei. This gradient culminates in the transcriptional activation and repression of a set of zygotic group genes which subdivide the axis into distinct domains by setting expression limits of key zygotic regulatory genes (Pan and Courey, 1992; Jiang et al., 1992; Kirov et al., 1993; Huang et al., 1993; Jiang et al., 1993; Kirov et al., 1994) (**Figure 15**). These genes are responsible for initiating the differentiation of various tissues along the D-V axis. High levels of DL present in the ventral region establish the mesoderm by activating the expression of *twist* and *snail*, two transcription factors (Jiang et al., 1991; Pan et al., 1991; Thisse et al., 1991; Ip et al., 1992), and in turn

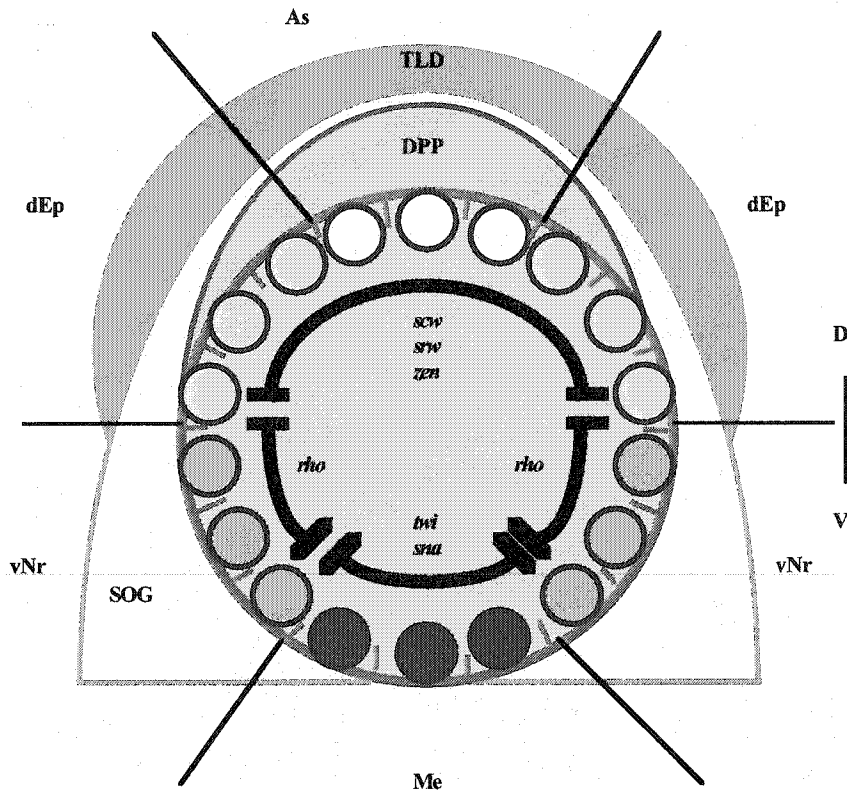
control the formation of dorsal ectoderm and amnioserosa by repressing *decapentaplegic* (*dpp*), *zerknüllt* (*zen*), and *tolloid* expression in ventral regions (St Johnston and Gelbart, 1989; Ip et al., 1991; Shimell et al., 1991). Intermediate levels of DL in the lateral regions specify neuroectoderm, which is marked by *rhomboid* expression (Ip et al., 1992). *Snail* acts to repress *rhomboid* in the mesoderm, and defines the boundary between the presumptive mesoderm and neuroectoderm (Kosman et al., 1991; Jiang et al., 1992; Gray et al., 1994; Leptin et al., 1991). Thus, the continuum of spatial information contained in the DL gradient is interpreted by the embryo to subdivide the axis into discrete regions.

As no DL protein is detectable in nuclei in the dorsal 40% of the embryo, the development of this region is not directly determined by the DL gradient. Patterning in the dorsal half of the embryo requires a set of zygotically active genes that are activated by default including *dpp*, *screw* (*scw*), *short gastrulation* (*sog*), *shrew* (*srw*), *tolloid*, *twisted gastrulation* (*tsg*) and *zerknüllt* (*zen*) (Figure 15) (Ferguson and Anderson, 1992; Arora and Nusslein-Volhard, 1992). Loss-of-function mutants of these genes typically produce a variety of related mutant phenotypes, characterized by the expansion of lateral and ventrolateral pattern elements at the expense of more dorsal structures like the amnioserosa. Thus, a third signaling pathway defines patterning on the dorsal side of the embryo in which the *dpp* plays a critical role (Arora and Nusslein-Volhard, 1992). Genetic analysis suggests that these genes establish a gradient of dorsalizing activity encoded by *dpp*.

The *dpp* gene in *Drosophila* encodes a secreted molecule of the Transforming Growth Factor- β (TGF β)/Bone morphogenetic protein (BMP) superfamily (Padgett et al., 1987). The DPP/TGF β /BMP superfamily represents an important class of signaling molecules diversified throughout evolution with functions that range from the determination of distinct cell fates to the control of cell division (Kingsley, 1994; Hogan, 1996). *Dpp* encodes the primary dorsalizing signal that is required for specifying cell fate along the dorsal-ventral axis of the embryo (Irish and Gelbart, 1987; Ferguson and Anderson, 1992b; Wharton et al., 1993). *Dpp* is expressed at a uniform intensity over the dorsal 40% of the embryonic circumference that gives rise to the amnioserosa and dorsal ectoderm by stage 9 of embryogenesis (St. Johnston and Gelbart, 1987). *Dpp* seems to act early in the hierarchy of events that regulate dorsal development, since *dpp* expression remains unaltered in any of the zygotic mutants (Ray et al., 1991). Loss of *dpp* function produces the most severe phenotype among the zygotic mutants in which cells in the dorsal half behave as ventral epidermal cells differentiating ventral denticle belts (Irish and Gelbart, 1987).

While the absence of *dpp* activity results in the loss of all dorsal tissues (Irish and Gelbart, 1987), the phenotypes caused by partial loss-of-function mutations in *dpp* indicate that there is a graded requirement for *dpp* activity in the specification of dorsal fates (Ferguson and Anderson, 1992a; Wharton et al., 1993). This allelic series showed that *dpp* is an essential component of a dorsal-to-ventral gradient of positional information in the embryo. Ferguson and Anderson (1992a), also showed that injection of increasing quantities of *dpp* mRNA into lateralized syncytial embryos, which lack all dorsal-ventral polarity, restores dorsal structures in a dose-dependent fashion. The deposition of *dpp*

Figure 15. Expression of early zygotic genes required to determine D-V polarity in the *Drosophila* embryo.

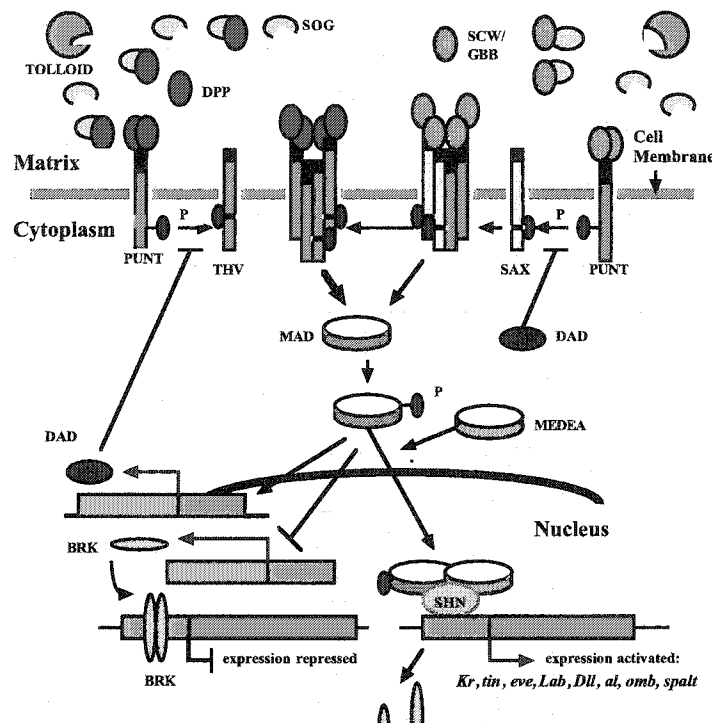


A schematic representation of a cross-section fate map of a blastoderm embryo illustrating the initial expression patterns of zygotic target genes regulated by the maternal signaling pathway of the dorsal group genes. The nuclear gradient of *dorsal* protein is depicted by the circles showing different shades of red. The relative expression pattern and activity of *tolloid* (TLD), *short gastrulation* (SOG) and *decapentaplegic* (DPP) are shown in the cross section of the embryo. Uniform levels of TLD are expressed in dorsal regions (As and dEp), of the embryo, as SOG shows a gradient expression from ventrolateral to dorsal regions (vNr to As). DPP shows increasing activity from dorsal lateral to dorsal regions, representing the presumptive dorsal epidermis (dEp) and amnioserosa (As) respectively. *Twist* (*twi*) and *snail* (*sna*) are expressed in the presumptive mesoderm, *rhomboid* (*rho*) is expressed in the presumptive ventral neurogenic region. *Zerknullt* (*zen*), *screw* (*scw*) and *shrew* (*srw*) are expressed uniformly in dorsal region (As and dEp) of the embryo. Amnioserosa (As), dorsal epidermis (dEp), mesoderm (Me), and ventral neurogenic (vNr). (Modified from Govind and Steward, 1991; Mullins, 1994).

RNA defined the dorsal-most point of the rescued pattern. These embryos went on to differentiate nearly all of the dorsal pattern elements of the ectoderm (Ferguson and Anderson, 1992a). This showed that asymmetric DPP activity is capable of promoting detailed ectodermal pattern, in the absence of any other asymmetric signal. Therefore it was proposed that the D-V axis in the embryo is determined by a gradient of DPP activity established in the syncytial blastoderm prior to cellularization (between stages 2-4), and which is formed by spatially-restricted modulation of DPP activity over its domain of expression. Whereas ventral ectodermal cells that lack DPP activity differentiate a mesoderm and neurogenic ectoderm, different levels of DPP activity can elicit two distinct epidermal cell fates (St. Johnston and Gelbart, 1987; Irish and Gelbart, 1987; Ferguson and Anderson, 1992; Wharton et al., 1993). The dorsal-most cells in the ectoderm nearest the dorsal midline of the embryo differentiate into the extra-embryonic amnioserosa and require high levels of DPP activity, whereas the dorsal lateral cells of the ectoderm differentiate into dorsal epidermis, and are specified by progressively lower levels of DPP activity (Ferguson and Anderson, 1992a, Wharton et al., 1993). Because *dpp* transcript is expressed at uniform intensity within its dorsal domain (St Johnston and Gelbart, 1987), the DPP activity gradient must be formed by post-translational mechanisms that can modulate DPP distribution and enhance DPP signaling activity on the dorsal side, while repressing DPP activity on the ventral side of the embryo.

The genes *tolloid* and *screw* genetically act upstream of *dpp* to increase DPP activity, whereas diffusible *sog* protein (SOG) is required to inhibit DPP activity (Ferguson and Anderson, 1992) (Figure 16). DPP activity is thought to be positively regulated by tolloid protein (TLD) indirectly by protein-protein interaction through another component of the *dpp* pathway. *Tolloid* is expressed in the dorsal 30% of the embryo (Shimell et al., 1991). Genetic evidence consistent with this model showed that antimorphic mutants of *tolloid* lead to dorsal defects that show a concomitant expansion of the ventrolateral ectoderm, and are able to act as dominant enhancers of *dpp* loss-of-function mutants (Ferguson and Anderson, 1992b). However, interaction is not direct since loss of *tolloid* activity is suppressed by increasing *dpp* dosage. On the other hand, *sog* loss-of-function mutants, which lead to loss of ventrolateral ectoderm and a corresponding expansion of the dorsal ectoderm, are enhanced by increasing *dpp* dosage (Ferguson and Anderson, 1992b). This is consistent with *sog* acting as an antagonist of DPP activity. *Sog* is expressed in a broad lateral stripe of cells that abuts the *dpp*-expression domain (Francois et al., 1994). The *tolloid* gene encodes a member of the *astacin* family of metalloproteases closely related to the procollagen protease BMP-1 (Shimell et al., 1991). The *sog* gene encodes a protein with a type I transmembrane domain and a large extracellular domain (Francois et al., 1994), which shows sequence similarity to *Xenopus chordin*, a dorsalizing factor expressed in the Spemann organizer (Sasi et al., 1994; Francois et al., 1995). In fact, *sog* and *chordin* are functionally equivalent, as assayed by the injection of *chordin* RNA into *Drosophila* embryos and *sog* RNA into *Xenopus* embryos (Holley et al., 1995). The data reveal a double inhibition mechanism is used to generate a gradient of DPP activity along the dorsal-ventral axis of the embryo. TLD and SOG both act by inhibitory mechanisms. SOG functions upstream of DPP in dorsal and ventral regions to inhibit DPP signaling, by binding to DPP (Ferguson and Anderson, 1992), thus abrogating receptor-ligand interac-

Figure 16. Current model for the canonical *dpp*/TGF β /BMP signaling pathway in *Drosophila*



A schematic diagram showing the canonical *dpp* signaling pathway. The zygotic gene *tolloid* enhances *dpp* activity on the dorsal side, while *sog* inhibits *dpp* activity on the ventral side of the embryo. Activation of the *dpp* protein (DPP) is achieved by *tolloid* protein (TOLLOID) cleaving the *sog* protein (SOG), thus releasing the *dpp* ligand (DPP). The DPP ligand then binds and activates its receptors *punt* (PUNT) and *thickveins* (THV) which encode receptor serine-threonine kinases. Two more TGF β -like ligands, *screw* (SCW) in the embryo, or *glass bottom boat* (GBB) in imaginal disc, act through their receptor *saxophone* (SAX), to synergistically enhance signaling by DPP through THV. Receptor clustering between PUNT and THV or PUNT and SAX upon ligand binding leads to the formation of activated receptor complexes between THV/PUNT and SAX/PUNT. These receptor complexes then transduce the signals from their ligands through the receptor specific cytoplasmic factors, *mothers against dpp* (MAD) and *medea* (MED). The integration between the THV and SAX signaling pathways is thought to formally occur at any of three levels: at the receptor level between THV and SAX, at the cytoplasmic levels between MAD and MEDEA, or at the transcriptional activation level in the nucleus. The expression of *brinker* (BRK), a constitutive repressor of DPP target genes, is repressed by the activated MAD and MEDEA complex following its translocation into the nucleus following their activations by the THV/PUNT and SAX/PUNT receptor complexes. *Daughters against dpp* (DAD) expression is activated by *dpp* signaling. DAD represents a negative feedback inhibitor that is thought to prevent the activation of THV receptor by the PUNT receptor. *Schnurri* (SHN) a transcriptional activator of *dpp* signaling, helps to promote MAD/MEDEA binding to the transcriptional promoter sites of the DPP target genes. DPP target genes include, *Kruppel* (*Kr*: embryo amnioserosa), *tinman* (*tin*: dorsal mesoderm of embryo), *evenskipped* (*eve*: in pericardial cells of mesoderm in the embryo), *Labial* (*Lab*: in endodermal midgut of embryo), and *Distalless* (*Dll*), *aristaless* (*al*), *optomotor blind* (*omb*), and *spalt* in imaginal the imaginal discs. (Modified from Podos and Ferguson, 1999).

tion and transmission of the DPP signal. SOG is expressed in the ventral-lateral half of the embryo, where it is thought to be cleaved and released from the cells surface and secreted into the ECM, and diffuses to the opposite dorsal pole where it reduces DPP activity in a graded manner. TLD protease, in turn, acts upstream of the DPP/SOG inhibitory complex, to cleave SOG thus releasing DPP so that it can bind its receptor (Letsou et al., 1995; Singer et al., 1997) (Figure 16). Uniform dorsal expression of TLD (Singer et al., 1997) results in degradation in dorsal regions of SOG in SOG/DPP complexes. It was also shown that SOG proteolysis is greatly enhanced by the presence of DPP, presumably in a DPP/SOG complex source. The consequence is increasing the concentration of free DPP in the direction opposite to that of the SOG inhibitory gradient, generating a signal activity which patterns the dorsal-ventral axis. A simple model for the formation of a DPP activity gradient is that a ventral source of the SOG inhibitor, coupled with a dorsal sink for SOG, provided by TLD, results in a ventral-to-dorsal gradient of SOG, that causes a reciprocal dorsal-to-ventral gradient of DPP activity.

However, additional complexity was uncovered by findings that suggest that SOG inhibits DPP signaling primarily by blocking *screw* protein (SCW) function (Neul and Ferguson, 1998; Nguyen et al., 1998). The *screw* gene encodes a second BMP ligand of the TGF β family in *Drosophila*, which is required for the elaboration of the full dorsal pattern. The *screw* gene is expressed around the embryonic circumference in the dorsal half of the embryo at the syncytial blastoderm stage (Arora et al., 1994). *Screw* null mutant embryos result in a loss of amnioserosa and dorsal ectoderm with a concomitant transformation to ventral ectoderm (Arora et al., 1994). *Screw* loss-of-function mutants can be partially suppressed by an increase in *dpp* dosage, as antimorphic alleles of *screw* act as dominant enhancers of *dpp* loss-of-function mutants (Arora et al., 1994). This suggests that *screw* is required for maximal DPP activity, and normally acts to increase *dpp* activity at the dorsal-most side of the embryo. In fact, *screw* has been found to interact with the signal transduction components of the *dpp* signaling pathway. Thus, the graded dorsalizing signal in a wild-type embryo is thought to be generated by the combined action of both DPP and SCREW (Arora et al., 1994).

The transmission of the DPP signal is integrated downstream through a family of transmembrane serine/threonine kinases. The genes *thickveins* (*thv*) and *saxophone* (*sax*) encode two members of the type I receptor family in *Drosophila* (Brummel et al., 1994; Nellen et al., 1994a and b; Penton et al., 1994; Xie et al., 1994). The loss of maternal and zygotic *thv* activity causes strong ventralization of the embryos that are comparable to effects caused by null *dpp* alleles (Nellen et al., 1994a and b; Terracol and Lengyel, 1994), while loss of *sax* function results in a weaker phenotype limited to the amnioserosa (Nellen et al., 1994a and b). *Sax* receptor (SAX) is required to interpret peak levels of DPP or SCW signal to specify amnioserosal cell fates. Overexpression of *thv* can bypass the requirement for *sax* (Brummel et al., 1994), suggesting that the two receptors could use the same intracellular signal-transduction machinery. The *punt* a typeII receptor that is the *Drosophila* homolog of a mouse activin receptor (Childs et al., 1994; Letsou et al., 1995; Ruberte et al., 1995), can bind the DPP ligand independently, whereas the type I receptors require an association with the type II receptor for ligand binding. Removal of maternal and zygotic *punt* function causes phenotypes indistinguishable from loss

of *dpp* or loss of *thv* activity. Analysis of genetic phenotypes suggest that *dpp* signaling requires both *thv* and *punt* activity, whereas *scw* signaling requires *sax* and *punt* function.

Response to the DPP signal is mediated by a heteromeric complex containing the type II receptor *punt* (PUNT) and the type I receptor *thv* or *sax*, both serine/threonine receptor kinases (THV, SAX) (Brummel et al., 1994; Nellen et al., 1994a and b; Penton and Hoffmann, 1994; Xei et al., 1994; Letsou et al., 1995; Ruberte et al., 1995). The DPP signal is thought to initially bind to the type II receptor (PUNT), which then recruits the type I receptor (THV) into a heteromeric signaling complex (Wrana et al., 1992; Wrana et al., 1994a and b; Derynck and Feng, 1997; Heldin et al., 1997). The type II kinase receptor phosphorylates the type I kinase receptor, which transduces the signal to downstream components (Childs et al., 1994; Penton et al., 1994; Wrana et al., 1994). While PUNT and THV are essential for all DPP signaling (Penton et al., 1994; Nellen et al., 1994; Brummel et al., 1994; Letsou et al., 1995; Ruberte et al., 1995), the second type I receptor SAX along with PUNT is essential to transduce the limited SCW signal (Figure 16). It was shown that SAX acts synergistically to elevate the biological response of THV (Neul and Ferguson, 1998; Ngyuyen et al., 1998). Thus, dorsal pattern of the embryo is established by the combination of DPP and SCW signals which act through two different type I receptors, THV and SAX respectively, to transmit distinct intracellular signals that must be integrated downstream, for the accurate interpretation of dorsal positional values in the embryo.

The current paradigm that describes the transmission of the DPP signal from the cell surface to the nucleus of target cells involves a single class of proteins known as SMADs which couples receptor activation to the control of target-gene transcription (Heldin et al., 1997). Upon activation of type I receptors THV and SAX, by a receptor specific SMADs, referred to as *Mothers against dpp* (*Mad*), are phosphorylated (Raftery et al., 1995; Newfeld et al., 1996 and 1997). Activated *Mad* protein (MAD) then associates with a cytoplasmic factor called *Medea* (*Med*) (Wisotzkey et al., 1998; Hudson et al., 1998). MAD and *Medea* protein (MED) possess direct and specific DNA-binding capacity and can form a complex (Heldin et al., 1997). The MAD/MED complex is then translocated into the nucleus where it functions with other transcription regulators such as *schnurri* (*shn*) (Arora et al., 1995), to regulate tissue specific target-gene expression such as *tinman* (*tin*) and *evenskipped* (*eve*) (Azpiazu and Frasch, 1993). The simplicity of this pathway allows for the tight coupling of external ligand concentration to transcriptional responses, with the sensitivity of an individual target gene being dependent upon the arrangement and/or affinities of MAD-MED binding sites within its enhancer.

Recently, it has been shown that DPP signal transduction does not involve a simple linear cascade, but involves a series of negative feed back loops that allow for the establishment of sharp thresholds to the DPP activity gradient. *Brinker* (*brk*), represents a novel gene whose transcription is repressed by DPP and which functions to repress DPP target-gene expression in the absence of the DPP signal (Jazwinska et al., 1999; Campbell and Tomlinson, 1999; Minami et al., 1999), such that *brk* expression is a direct reflection of the DPP activity gradient. *Brk* protein (BRK) expression is localized to the nucleus throughout its domain of expression, suggesting that it might function directly as a tran-

scriptional repressor. Loss of function mutants of *brinker* result in the inappropriate expression of DPP target genes, resulting in the dorsalization of the embryonic ectoderm. This indicated that the transcription of DPP target genes can be independent of transcriptional activation by the MAD-MED signaling complex. Therefore, BRK protein acts as an intracellular negative regulator of DPP signaling, and, as such, represents an integral component of the pathway that is necessary for proper transcriptional responses to the DPP gradient. *Daughters against dpp (Dad)*, encodes a second intracellular negative regulator of DPP signaling, which behaves differently from *brk* (Tsuneizumi et al., 1997; Inoue et al., 1998). The *Dad* protein (DAD), which has limited similarity with MADs, antagonizes DPP signaling by binding to, and inhibiting THV receptor activity, following its transcriptional activation by the MAD-MED complex. Integration of positive and negative inputs on DPP target gene expression in the syncytial blastoderm embryo, in response to the DPP activity gradient may be interpreted by a field of cells to produce sharp thresholds of target gene expression.

By stage 9 of embryogenesis (germband extension), *dpp* is expressed as a longitudinal stripe in cells along the dorsal ectodermal ridge. Here the *dpp* signaling pathway is co-opted for a later developmental process to specify the dorsal pattern of the underlying mesoderm and endoderm germ layers. Loss of *dpp* function results in the loss of dorsal mesodermal and endodermal pattern and the conversion of dorsal cells to ventral cells (Irish and Gelbart, 1987). Therefore, a dorsal-to-ventral gradient of DPP activity arises as a consequence of post-translational modulation of DPP signaling by a combination of diffusible enhancers (TOLLOID, SCREW) and repressors (SOG) of DPP activity. The spatial modulation of SCREW activity by the combined action of SOG and TOLLOID is also likely to be a major component of the generation of D-V positional information within the embryonic ectoderm.

Based on the genetic and molecular evidence, this study demonstrates that a novel mutation caused by the lethal *PZ A64* insertion can dominantly interact with mutant alleles of both *dpp* and its receptors in embryos and imaginal leg discs resulting in a direct block in *dpp* signaling. This suggested that a new component of the *dpp* signaling pathway may have been identified.

I-8ii. UDP-glucose dehydrogenase, a gene required in pattern formation.

As described later in this thesis, the molecular identification and characterization of the gene uncovered by the *PZ A64* lethal insertion showed that it is the *Drosophila* homolog of uridine-diphosphate-glucose dehydrogenase (UDP-GlcDH). It is important to give background to what is known about this system so that the results can be interpreted in the proper context. The UDP-GlcDH gene encodes an enzyme responsible for the production of UDP-glucuronate by catalyzing the reaction of UDP-glucose to yield UDP-glucuronic acid in the cytosol (Dougherty and van de Rijn, 1993). Specific transporters then translocate the UDP-glucuronate along with other UDP-sugars into the Golgi lumen (Hirschberg and Snider, 1987; Hirschberg et al., 1998) (**Appendix I**). In the Golgi lumen, the UDP-sugars are precursors for the synthesis of complex carbohydrate residues called glycosaminoglycans (GAGs) (reviewed in Prydz and Dalen, 2000) (**Appendix II**). Specific GAG chains are synthe-

sized in a regulated fashion from linker sequences covalently-linked to specific serine amino acids of glycoproteins (**Appendix III**). This is followed by enzymatic modifications of specific disaccharide residues, such as deacetylation, epimerisation and subsequent sulphur modifications of the sugar ring (reviewed in Prydz and Dalen, 2000) (**Appendix III**). These complex glycoproteins are referred to as proteoglycans (PGs). After synthesis, PGs are exported from the Golgi to the cell surface or extracellular matrix (ECM). At the cell surface, the GAGs remain associated with extracellular domain of membrane bound PGs or ECM PGs (reviewed in Prydz and Dalen, 2000). The GAG residues associated with the proteoglycan play an integral role in its function (Jackson et al., 1991; Lander et al., 1999). GAGs are highly negatively charged molecules, owing to the presence of acidic sugar residues and/or modifications by sulfate groups. The specific sugars and their modification patterns in the GAG chains are critical for the biological activity of the individual PG, such as its interaction with various growth factors or cell-surface molecules (Jackson et al., 1991, Lander et al., 1999).

I-8iii. The ECM, HSPGs and their role in regulating growth factor signaling.

Pattern formation of complex multicellular organisms requires information to be transferred between cells and tissues. Much of the processing necessary for the transfer of this information occurs in the extracellular environment. Growth factor molecules play a pivotal role in this intercellular communication. The binding of growth factors to the extracellular matrix (ECM) is a major mechanism regulating growth factor signaling (review, Taipale and Keski-Oja, 1997). The ECM is a fibrillar meshwork of proteins, proteoglycans, and glycosaminoglycans, that is believed to constitute a barrier for diffusion and convection of growth factors (review, Taipale and Keski-Oja, 1997). For example, the association of growth factors to the matrix allows storage of large quantities of signaling molecules in a readily available form, allowing extracellular signaling to proceed in the absence of new protein synthesis. Proteolytic release and activation of matrix stored growth factors can generate rapid and highly localized signals (Lyons et al., 1988; Hecht and Anderson, 1992; Taipale et al., 1995; Miyazawa et al., 1996). The association of signaling molecules with matrix decreases loss of information by slowing diffusion. Although some developmental signals are restricted to adjoining cells, others are thought to form long range "gradients." The formation of the signal gradient could involve the diffusion of the growth factor to the low affinity receptor complexes, defined by proteoglycans, at the cell-surface and relaying the factors to receptors on other cells. The storage of growth factors in the matrix makes it possible for cells to transmit signals to cells in contact with the same matrix later.

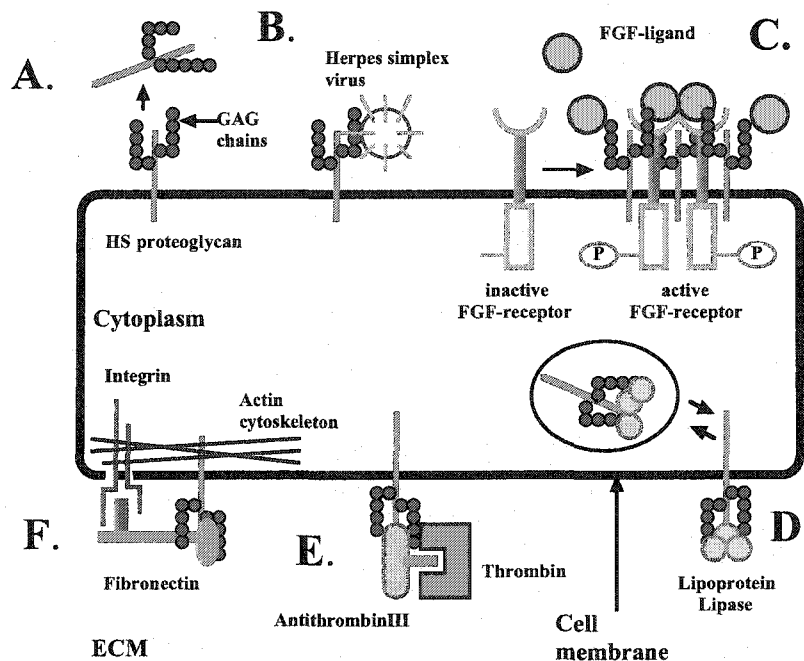
Proteoglycans play important roles in various cellular processes: control of growth and differentiation by regulating growth factor signalling, receptor turnover, protease and protease inhibitor activity, cell-cell adhesion and cell-matrix interactions (Kjellen and Lindahl, 1991; Esko, 1991; Bourin and Lindahl, 1993; Schlessinger et al., 1995; Werb 1997; Matrisian, 1997; Iozzo, 1998; Woods and Couchman, 1998; Baeg and Perrimon, 2000; Lander and Selleck, 2000; Selleck, 2000). The largest group of growth factor ECM interactions involve the binding of growth factors to heparan sulfate proteoglycans (HSPG). UDP-glucuronate (UDP-GlcA) along with UDP-N-acetylglucosamine (UDP-GlcNAc) forms the basic repeating disaccharide units required for the biosynthesis of the heparin and heparan sulfate

GAGs. Heparin and heparan sulfate are synthesized by the sequential and alternating addition of GlcA and GlcNAc to the non-reducing end of a tetrasaccharide primer that is initiated on specific serines of specific core proteins (Salmivirta et al., 1996; Hiroko et al., 1998) (see **Appendix III**). The heparan sulfate polymer then undergoes a series of modifications that involve deacetylation, epimerization and N-linked or O-linked sulfation steps (Kjellen and Lindahl, 1991; Salmivirta et al., 1996). Structurally, heparan sulfate GAGs are complex and heterogeneous (Lindahl and Lindahl, 1997; Lindahl et al., 1998). Discrete variants are achieved during synthesis since not all of the saccharides are subjected to all of the modification steps (review by Kornfeld and Kornfeld, 1980). The HS GAG chains are bound to the protein core region, that is associated with the extracellular domain of PGs on the surface of a cell. Core proteins have been classified in three distinct families. The syndecans include four members which are membrane spanning proteins (reviewed in Rapraeger, 2001), the Glypican family contain at least six members that are bound to the cell-surface membrane by a glycosylphosphatidylinositol-anchor (GPI) (David et al., 1990; Filmus et al., 1995; Karthikeyan and Maurel, 1992; Litwack et al., 1994; Stumpf et al., 1994; Watanabe et al., 1995; reviewed in DeCat and David, 2001), and finally the basement membrane proteoglycans, a major member being Perlecan, that are secreted into the ECM. The heparan sulfate GAG residues are ubiquitous macromolecules that may be either associated with cell-surface proteoglycans or found as an unbound form in the extracellular matrix (Kjellen and Lindal, 1991; Bernfeld et al., 1992; David, 1993).

The heparan sulfate GAG residues and the HSPGs have been implicated in regulating the biological activities of a variety of growth factors (Capdevilla and Belmonte, 1999; reviewed in Bernfield et al., 1999 and Perrimon and Bernfield, 2000). It is thought that cell-surface HS proteoglycans (HSPGs) act as low affinity co-receptors to modulate growth factor binding to its primary receptors (Mason and Konrad, 1994; Ortiz and Leder, 1992; Ortiz et al., 1992; Schlessinger et al., 1995; Sasisekharan et al., 1997; Yanagishita and Hascall, 1992) (**Figure 17**). Tissue culture studies have shown that cell-associated HSPGs can affect signaling that is mediated by Fibroblast Growth Factors (FGFs) (Olwin and Rapraeger, 1992; reviewed Ornitz, 2000), Wnt/Wingless (WG) (Reichsman et al., 1996; reviewed by Cumberledge, 1997) and the Transforming Growth Factor- β (TGF β) (Lopez-Casillas and Cheifez, 1991; Lopez-Casillas et al., 1993; Lopez-Casillas et al., 1994). For example, betaglycan, a molecule identified on the basis of its affinity for TGF- β , is a transmembrane proteoglycan that potentiates the response of TGF β in transfected cells by promoting the interaction of TGF β with its receptors (Lopez-Casillas and Cheifez, 1991; Lopez-Casillas et al., 1993; Lopez-Casillas et al., 1994). Betaglycan represents an example of a low affinity type III receptor that is a HS modified PG (Lopez-Casillas et al., 1993). In this case, however, TGF- β appears to bind directly to the core protein itself rather than to the carbohydrate side chains (Lopez-Casillas et al., 1994).

Glypicans have been shown to modulate responses of tissue culture cells to FGF (Mali et al., 1993; Steinfield et al., 1996). In the vertebrate model, two mechanisms have been proposed by which GAGs can regulate FGF signaling. In one model, the association of FGF with HS-proteoglycans may result in protection of the growth factor from degradation, and may reduce ligand diffusion by allowing

Figure 17. *In vivo* models of cell surface HS proteoglycan function.



A schematic diagram describing the various functions of cell surface heparan sulfate proteoglycans (HSPG) that have been characterized. (A) Soluble paracrine effectors are produced by shedding of the heparan sulfate proteoglycan (HSPG) ectodomains from the cell surface. Shedding can instantly changes the function of the HSPG, such as co-receptor function for growth factors, reducing the levels of a cell surface ligands and its activity. For example, the shedding of syndecan ectodomains leaves a potentially interactive peptide that could for example behave as a direct inhibitor of growth factors. (B) Intracellular pathogens, such as the herpes simplex virus, use HSPG as co-receptors to mediate entry of the pathogen into host cells. (C) HSPGs can act as co-receptors for soluble ligands (e.g. growth factors like FGF, cytokines) that form part of a signaling complex with their signal transducing receptors. (D) Internalization receptors for soluble ligands such as serpins like lipoprotein lipase, can present ligands at the cell surface and take ligands into cells via either coated pits or caveolae for degradation, recycling, or transcytosis. (E) HSPGs can also activate protease inhibitors and promote association of inhibitor with the protease. Conversely, HSPG can also inhibit protease inhibitor function by either blocking the access of the inhibitor to the protease, or binding directly to the inhibitor and internalizing it for degradation in cell. For example, thrombomodulin (TM), an HSPG, potentiates the inhibition of thrombin by antithrombin III (AT III) and prevents the cleavage of fibrinogen and the activation of Factor V, inhibiting blood coagulation near vascular endothelial cells. Alternatively, soluble ectodomains of syndecan bind neutrophil elastase, reducing the enzyme's affinity for its plasma-derived inhibitor, serpin alpha-1-antiprotease (Kainulainen et al., 1998). Elastase remains active in wound fluids because it is protected from its protease inhibitor. (F) HSPGs can also act as co-receptors for insoluble ligands (e.g., extracellular matrix molecules) which immobilize the receptor complex in the plane of the membrane causing it to associate with actin microfilaments. (For reviews on this subject see Kjellen and Lindahl, 1991; Bernfield et al., 1992; Bernfield et al.,

it to bind to the cell surface via interactions with low affinity proteoglycans (Bernfield et al., 1992). This would increase the local concentration of the ligand, thus enhancing the probability of a productive interaction with a high affinity receptor (Aviezer et al., 1994). The heparan sulfate side chains of cell-surface glypican, or syndecan (another proteoglycan molecule), may perform this function in mediating FGF signalling (Bernfield and Hooper, 1991, 1993; Schlessinger et al., 1995; Steinfield et al., 1996; Ornitz et al., 1995; Ornitz, 2000). Initially, heparin-like GAGs are thought to tether FGF in the ECM so as to create a reservoir of FGF. A stable FGF-GAG complex is first formed at the surface of the cell. By proteolysis the complex is released from the membrane surface and diffuses to activate the FGF receptor at a site distant from the release site (Jackson et al., 1991). Thus, the GAG acts as a chaperone for the ligand, and possibly as a stabilizing factor against proteases in the ECM.

A second model is called the dual receptor model. According to this model, the function of heparin-like GAG is to oligomerize the FGF ligand, thus inducing receptor clustering. In the case of FGF, the high affinity receptors have intracellular tyrosine kinase domains, which are activated by transphosphorylation as a result of ligand-induced receptor dimerization. Since FGF binds to the extracellular domain of its high affinity receptor as a monomer (Spivak-Kroizman et al., 1994) which is not capable of inducing receptor dimerization on its own, it has been proposed that a multimeric heparan-sulfate-FGF complex is required in order to produce a biologically-active signal (Mason and Konrad, 1994; Ornitz and Leder, 1992; DiGabriel, 1998; Faham et al., 1996; Herr et al., 1997). The heparin-like GAGs would participate in a dual receptor system as low affinity receptors to facilitate the interactions of FGF with its high affinity receptors (Klagsburn and Baird 1991; Yayon et al., 1991; Schlessinger et al., 1995; Pantoliano et al., 1994). The binding of heparin to FGF causes FGF oligomerization, leading to clustering of FGF receptors for signal transduction (Ornitz and Leder, 1992; Ornitz et al., 1992; Kan et al., 1993).

Other roles of HSPG(s) on growth factor activity include storage of latent forms of growth factors in the ECM or activation of latent growth factors by specific proteases. For example, the hepatocyte growth factor (HGF) is stored as a latent single chain form in the ECM by binding to a HSPG factor (Mizuno et al., 1994). The conversion to its biologically active form is mediated by hepatocyte growth factor (Shimomura et al., 1995) HS residues that interact with the specific proteases and help target them to cleavage site in HGF, following injury in organs such as the liver or kidney (Miyazawa et al., 1996). Hematopoietic stem cell differentiation into multiple blood cell lineages, is dependent on two cytokines, interleukin-3 (IL-3) and granulocyte macrophage-colony stimulating factor (GM-CSF). These cytokines require associated HS residues on stromal cell-surface HSPG(s) like syndecans, and in bone marrow ECM-HSPG like perlecan for presentation of the cytokines to the cells (Roberts et al., 1998; Klein et al., 1995). It has also been shown that one or more of the ECM proteins can bind to the active form of TGF β once it is released upon proteolytic cleavage from its latent form when bound to latent TGF β binding proteins (LTBPs) at the cell surface (Taipale et al., 1994; Saharinen et al., 1996). These ECM proteins include the HSPG (s) decorin and biglycan (Ruoslahti et al., 1992; Schultz-Cherry et al., 1993). For example, thrombospondin induces the activation of the latent form of TGF β , as in

turn decorin functions as a negative regulator to attenuate TGF β activity once it is released in its active form in the ECM (Ruoslahti et al., 1992).

Other functions of heparan sulfate proteoglycans are summarized in **Figure 17**. Cells interact with fibronectin in the ECM via syndecan-1 (through the HS residues) and β -1 integrin found on the surfaces of cells (Saunders and Bernfield, 1988). Fibronectin can induce signals through their receptors, such as integrins, which interact with the cytoskeleton of the cell (Clark and Brugge, 1995). In this case information might be transferred from the ECM to the inside of the cell directly, via mechanical forces, that are mediated by ECM associated factors like HSPGs (Ingber, 1993). Therefore, HSPG(s) can act as matrix receptors, responsible for normal actin filament organization (Woods et al., 1986; LeBaron et al., 1988), controlling the shape and organization of cells in a tissue.

In another example, HSPGs have been shown to activate protease inhibitors, like antithrombin III and promote association of inhibitor with proteases (Taipale et al., 1995) (see **Figure 17**). Antithrombin III binds to syndecan-1 and -4, which enables formation of a ternary complex with thrombin that has reduced protease activity and is proposed to provide endothelial cells with non-thrombogenic surfaces (Kojima et al., 1992). As well, HSPG can remove protease inhibitors from the cell surface, providing a mechanism for the activation of a protease, as in the case of uptake and degradation of tissue factor pathway inhibitor-coagulation factor Xa complexes (Falcone et al., 1993). In another example, lipoprotein lipase is anchored to the cell surface, potentially by a syndecan, on which it cycles to a non-degradative intracellular compartment (Saxena et al., 1990). Herpes simplex viruses can bind to the cell surface, using a cell-surface HSPG, via the gC and gB viral coat proteins. This enables uptake of viral particles upon infection, by fusion of the viral envelope with the plasma membrane (Wu Dunn and Spear, 1989; Shieh et al., 1992). Finally, the cleavage of the syndecan extracellular domain at a protease susceptible site adjacent to the plasma membrane can release bound ligands from the cell surface and possibly provide competitive binding sites in the extracellular matrix (Bernfield and Sanderson, 1990). These studies have shown that cell-surface HSPGs can affect growth factor signaling, but they do not address the role that these molecules play *in vivo* during development.

I-8iv. The biological roles of HS GAGs and their biosynthetic enzymes in development.

In the context of development, the importance of heparan sulfate GAG residues with respect to the functional role of proteoglycans has garnered much interest over the last decade or so (Bernfield et al., 1992; David, 1993; Rapraeger, 1993; Carey, 1997). The heparan sulfate GAG residues on the proteoglycan play a critical role in modulating the interactions with various ECM and growth factor proteins. The HSGAG chain structure and the modifications of its sugar residues determines its functional specificity (see Lindahl et al., 1998 and references therein). This heterogeneity in structure is due to the presence or absence of multiple modifications in the chain, which are carried out by various enzymes that are found in the Golgi apparatus during GAG biosynthesis (see **Figure 18**, **Table 1**, and references therein). Modifications include, N-acetylation or deacetylation, N-sulfation, 3-O-sulfation,

and 6-O-sulfation of the glucosamine, and epimerization or 2-O-sulfation of glucuronic acid. The overall sulfation patterns, are typically organized into regions of 2-20 disaccharides. Tissue-specific isoforms of the biosynthetic enzymes can produce enormous heterogeneity in the glycosaminoglycan chains with distinct sequences and macroscopic organization generating different ligand-binding properties (Ernst et al., 1995). For example, 2-O-sulfate of glucuronic acid promotes the high affinity binding to FGF-2, whereas N- or 6-O-sulfation of glucosamine that promotes HGF binding (Lyon et al., 1994; Faham et al., 1996). The expression of specific isoforms of these enzymes that create HS domains that bind to specific growth factors is thought to be determined by the proteoglycan core protein or by the differentiation state of the producing cell (Nurcombe et al., 1993; Aviezer et al., 1994).

Screens for mutations that affect development in *Drosophila*, *C.elegans* and mouse have uncovered genes involved in HS GAG synthesis or expression of HS proteoglycans (see **Figure 18** and **Table 1**) These mutations have been shown to affect the function of various enzymes that are required for biosynthesis and modification of their associated HS GAG chains with specific HSPG molecules (Baeg and Perrimon, 2000; Selleck 2000, 2001). In *C. elegans*, *unc-52*, a homolog of a basement membrane ECM associated proteoglycan, disrupts myofilament assembly during embryogenesis (Rogalski et al., 1993; Moerman et al., 1996; Mullen et al., 1999). *Squashed vulva-3 (sqv-3)*, a galactosyl transferase, and *squashed vulva-8 (sqv-8)*, a glucuronyl transferase are enzymes that are required for the synthesis of the tetrasaccharide linker that joins GAG polymers to the serine residues of the proteoglycan core protein (Herman et al., 1999; Herman and Horovitz, 1999; Bulik et al., 2000).

Squashed vulva-7 (sqv-7), encodes a nucleotide-sugar transporter, suggesting that this mutant affects the transport of the nucleotide-sugar substrates from the cytoplasm into the Golgi (Herman and Horvitz, 1999). All three mutants are maternal-effect lethals that affect GAG biosynthesis, and result in defects in the invagination of the vulval epithelium (Herman et al., 1999). In *Drosophila* the mutations identify genes that encode proteins that participate in different steps in GAG biosynthesis or gene that encodes a specific HSPG. In the mouse and human, mutations in HSPG(s) or in genes of HS biosynthetic enzymes, can result in morphological abnormalities or disease. Targeted disruption of Syndecan-1 in mouse results in defective repair of skin and corneal lesions. Lack of Syndecan-1 (a transmembrane HSPG) prevents keratinocyte migration into the wound and restoration of stable cell-cell and cell-matrix contacts. This results in a marked delay in reconstitution of normal epithelium. Genetic lesions in HS 2-O-sulfotransferase result in mice which die during the neonatal period exhibiting bilateral renal agenesis, bilateral coloboma of the iris, skeletal fusions and ectopic ossifications in the mouse embryo (Bullock et al., 1998). Mutations in the EXT-1 and EXT-2 genes that encode the human HS polymerase enzymes (Lind et al., 1998; McCormick et al., 1998), cause Hereditary Multiple Exostoses. These are tumors derived from the growth plate of endochondral bones which occasionally undergo malignant transformation into chondrosarcomas and most rarely to osteosarcomas (Stickens et al., 1996). These genes have been reported to have a general tumor suppressor function (Hecht et al., 1995). Mutations in the glypican-3 family of genes (a membrane associated HSPG), results in a rare X-linked syndrome, called Simpson-Golabi-Behmel-Syndrome (Pilia et al., 1996). These mutants are characterized as both pre- and postnatal overgrowths, with a distinct facial appearance, a predisposition

Table 1. *Drosophila* and *C. elegans* mutants affecting proteoglycan or glycosaminoglycan biosynthesis

Genes	Vertebrate homolog	Function and mutant phenotype	References
<i>squashed vulva-3 (sqv-3): C. elegans</i>	Galactosyl transferase	Affects GAG linker biosynthesis, vulval invagination defects	Bulik et al., 2000; Herman et al., 1999; Herman and Horvitz, 1999
<i>squashed vulva-8 (sqv-8): C. elegans</i>	Glucuronyl transferase I	Affects GAG linker biosynthesis, disrupts vulval epithelial invagination	Bulik et al., 2000; Herman et al., 1999; Herman and Horvitz, 1999
<i>sugarless (sgl): Drosophila</i>	UDP-glucose dehydrogenase	Affect HSGAG biosynthesis, defects in <i>wg</i> , <i>FGF</i> receptor and <i>dpp</i> signaling	Hacker et al., 1997; Haerry et al., 1997; Binari et al., 1997
<i>tout-velu (tiv): Drosophila</i>	HS co-polymerase : Ext1 and EXT2 genes	Heparan sulfate co-polymerase, defects in <i>hh</i> signaling distribution	Toyoda et al., 2000; Bellaiche et al., 1998; The et al., 1999; Toyoda et al., 2000
<i>sulfateless (sfl): Drosophila</i>	N-deacetylase/N-sulfotransferase : NDST genes	Heparan sulfate modifications, defects in <i>wg</i> , <i>FGF</i> receptor, and <i>dpp</i> signaling	Lin et al., 1999
<i>pipe (pip): Drosophila</i>	HS-2-O-sulfotransferase : HS2ST genes	Controls generation of ventral signal, results in defects in dorsal-ventral patterning in embryo	Sen et al., 1998
<i>squashed vulva-7 (sqv-7): C. elegans</i>	putative nucleotide sugar transporter	Affects heparan sulfate biosynthesis, vulval invagination defects	Bulik et al., 2000; Herman et al., 1999; Herman and Horvitz, 1999
<i>dally : Drosophila</i>	Glypicans: cell surface HSPG	Cell surface HS proteoglycan, defects in <i>wg</i> and <i>dpp</i> signaling	Nakato et al., 1995; Tsuda et al., 1999; Jackson et al., 1997; Lin and Perrimon 1999
<i>dally-like(dyl): Drosophila</i>	Glypicans: cell surface HSPG	Cell surface HS proteoglycan, defects in <i>wg</i> signaling and <i>WG</i> extracellular distribution	Baeg et al., 2001
<i>Drosophila syndecan</i>	Syndecan: integral membrane HSPG	Unknown	Spring et al., 1994
<i>wic-52 : C. elegans</i>	Perlecan : ECM HSPG	myofilament assembly	Moerman et al., 1996; Rogalski, et al., 1993

Genetics of proteoglycan and glycosaminoglycan biosynthesis in *Drosophila* and *C. elegans*. The table shows the various genes and their mutants affecting different steps in glycosaminoglycan biosynthesis, along with their *in vivo* mutant effects and their vertebrate homologs.

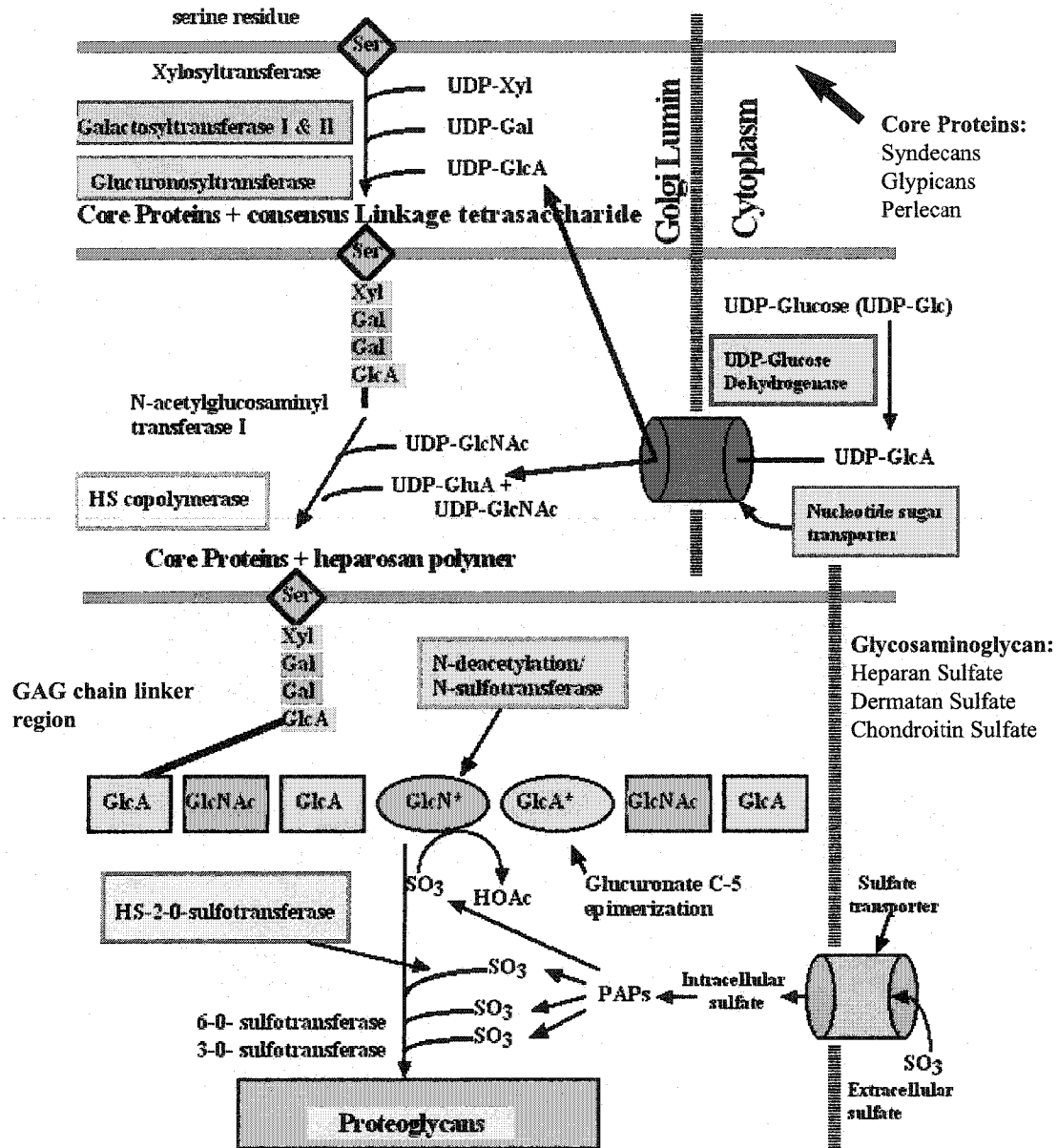
Figure 18 Legend:

A schematic that shows genes isolated in *Drosophila* and *C. elegans* that encode enzymes involved in GAG biosynthesis. Core proteins have been classified into three distinct families based on studies in mammals. The syndecan family includes four members; these are membrane spanning proteins. The glypican family contains at least six members bound to the cell surface membrane by a glycosylphosphatidylinositol-anchor. The final group, basement membrane proteoglycans are secreted (e.g., perlecan). Glycosaminoglycans (of which heparin, heparan, dermatan and chondroitin sulfates are the most common) are attached to the core protein by a consensus linker region at a serine amino acid residue. Multiple biosynthetic enzymes are involved in the polymerization of the various polysaccharide chains: A specific sugar nuclear transporter localizes UDP-modified sugars by UDP-GlcDH into the Golgi lumen from the cytosol. UDP-GlcDH, N-acetylglucosaminyl transferase I and HS co-polymerases synthesis the polysaccharide GAG chains onto the core protein. During GAG synthesis, the the sugar residues in the polysaccharide chains are selectively modified by the following set of specialized enzymes: N-deacetylase/N-sulfotransferase, Glucuronate C-5 epimerase, HS-2-O-sulfotransferase; 3-O-sulfotransferase, and 6-O-sulfotransferase. The sulfotransferase adds sulfate moieties in a specific pattern on the GAG chains. The sulfate substrate 3'Phosphoadenosine-5'phosphosulfate (PAPS) is produced in the cytosol and is then actively transported into the Golgi lumen by a sulfur transporter. The sugar residues in GAG chains depicted in **Figure 18**: Glucuronic acid (GlcA), modified Glucuronic acid (GlcA*), N-acetyl Glucosamine (GlcNAc), modified N-acetyl Glucosamine (GlcNAc*).

Figure 18 Key

Colour Key	Genes	Vetebrate homolog
	<i>squashed vulva-3 (sqv-3): C. elegans</i>	Galactosyl transferase
	<i>squashed vulva-8 (sqv-8): C. elegans</i>	Glucuronyl transferase I
	<i>sugarless (sgl): Drosophila</i>	UDP-glucose dehydrogenase
	<i>tout-velu (tiv): Drosophila</i>	HS co-polymerase : Ext1 and EXT2 genes
	<i>sulfateless (sif): Drosophila</i>	N-deacetylase/N-sulfotransferase : NDST genes
	<i>pipe (pip): Drosophila</i>	HS-2-O-sulfotransferase : HS2ST genes
	<i>squashed vulva-7 (sqv-7): C. elegans</i>	putative nucleotide sugar transporter
	<i>dally : Drosophila</i>	Glypicans: cell surface HSPG
	<i>dally-like (dyl): Drosophila</i>	Glypicans: cell surface HSPG
	<i>Drosophila syndecan</i>	Syndecan: intergral membrane HSPG
	<i>unc-52 : C. elegans</i>	Perlecan : ECM HSPG
GAG sugar residues		
	GlcA - Glucuronic Acid	
	Modified GlcA - Glucuronic Acid	
	GlcNAc - N-acetyl Glucosamine	
	Modified GlcNAc - N-acetyl Glucosamine	

Figure 18. Proteoglycans and the glycosaminoglycan biosynthetic pathway enzymes identified in *Drosophila* and *C. elegans* genetic mutant screens (reviews in Lander et al., 1999; Prydz and Dalen 2000; Selleck, 2000 and 2001)



to embryonal tumors, and variable morphological anomalies such as polydactyly, renal defects, vertebrate and rib fusions and congenital heart disease (Neri et al., 1998). The pathogenesis of these syndromes is unknown, but cell-surface HSPGs are known to interact with a variety of ligands involved in growth control, which may act to inhibit or enhance growth factor function.

In two concurrent independent studies involving a screen for maternal-effect mutations in *Drosophila* embryos, it was shown that germline clone mutants of *P1731*, a PZ- lethal insertion (Spradling et al., 1995), resulted in a *wingless*-like mutant phenotype in embryos, referred to as *kiwi* (Binari et al., 1997) and *sugarless* (Hacker et al., 1997) (see **Figure 18**). In a third study, *SG9*, a second P-element lethal insertion line (isolated in a disc screen by Shearn and Garen, 1974), was identified as a modulator of *wingless* signaling by its ability to enhance a weak *dishevelled* (*dsh^w*) adult phenotype (*suppenkasper*; Haerry et al., 1997). The mutant phenotypes attributed to the *P1731* and *SG9* insertions were identified as mutations in the *Drosophila* homolog of UDP-glucose dehydrogenase. Binari et al. (1997) and Haerry et al. (1997) correlated the *wg* mutant phenotype caused by the UDP-GlcDH mutation in embryos with a loss in heparan sulfate GAG production. Characterization of these mutations in UDP-GlcDH, referred to as alleles of *sugarless* (*sgl*), has not implicated heparin-like GAGs in *decapentaplegic* (*dpp*) signaling in the embryo, even though Haerry et al. (1997) also showed that *SG9* and *P1731* mutants suppress the adult wing mutant phenotype caused by an activated mutation of *thickveins* (*thvA*) (Hoodless et al., 1996).

During the same period, I demonstrated in this study that the embryonic lethal mutation *A64*, that resulted in a dorsal-ventral patterning defects in the embryo, was caused by the insertion of a P-element in the *sugarless* gene. The evidence suggested that the dominant negative effects, caused by the loss-of-function mutants of UDP-GlcDH on normal DPP activity, is the result in the loss of heparan sulfate GAG production. Furthermore, similar evidence has correlated the possible involvement of heparan sulfate GAGs with pattern regeneration in the imaginal discs of *Drosophila*. In the course of this study, genes encoding other enzymes involved in HSGAG biosynthesis have been identified in *Drosophila* by various other labs, implicating their gene functions in the specific regulation of various signaling pathways involving WG, HH and FGF signaling (reviewed in Selleck 2000, 2001). For a description of these mutations and a summary of their functions in *Drosophila* (see **Figure 18**). A more comprehensive description of the roles of these genes is provided in the various sections of the discussion in the context of the results found in this study.

II. MATERIALS AND METHODS

II-1. *Drosophila* culture.

Drosophila cultures were reared on medium containing: 10 g agar, 100 g sucrose, 100 g brewer's yeast, 100 mg chloramphenicol, 4.3 g sodium phosphate dibasic, 2.7 g sodium phosphate monobasic, and 10 ml propionic acid, in 1 L of distilled water (pH 7.4) (Nash and Bell, 1968). Fly stocks and crosses were kept at room temperature (between 20°C - 22°C) or in a 25°C incubator, unless otherwise indicated. Three percent agar-apple juice plates for egg collections were made as follows: 50% apple juice, 50% distilled water by volume in a 500 ml solution, with 15 grams of bacto-agar.

II-2. *Drosophila* lines.

TABLE 2. *Drosophila* strains used in this study.

A full description and explanation of the genetic markers and balancers used in this study can be found in "The genome of *Drosophila melanogaster*" (Lindsley and Zimm, 1992; Flybase 2001; <http://www.flybase.com>) and as individually referenced in Table 1 below.

STOCK	SOURCE
1. <i>y v f su(f)</i> ¹²	M. A. Russell, University of Alberta
PZ-lethal inserts:	
2. <i>A64 P{lacZ:Hsp70, ry+} / T(2;3)CyO-TM3, Sb ry⁵⁰⁶</i>	M. A. Russell, University of Alberta
3. <i>A64 P{lacZ:Hsp70, ry+} ry⁵⁰⁶/TM3, Sb ry⁵⁰⁶</i>	S. Scanga (this study)
4. <i>l(3)08310^{P1731}{ry+t7.2=PZlacZ ry+} ry⁵⁰⁶/TM3, ry⁵⁰⁶ Sb^{RK}</i>	Kathy Matthews, Indiana of University
sugarless alleles:	
5. <i>sgl^{A31} /TM3, Sb e</i>	A. M., University of Toronto
6. <i>sgl^{A64} / TM3, Sb e</i>	S. Scanga (this study)
7. <i>sgl^{N71} /TM3, Sb e</i>	A. M., University of Toronto
8. <i>sgl^{P1731}{ry+t7.2=PZlacZ} / TM3, Sb e</i>	A. Manoukian, University of Toronto
dpp pathway mutants:	
9. <i>dpp^{H46} / CyO</i>	Kathy Matthews, Indiana University
10. <i>dpp²⁷ / CyO</i>	R. Warrior, University of Southern California (Capdevilla et al., 1994)
11. <i>thv⁷ / CyO</i>	Kathy Matthews, Indiana University
12. <i>thv str-1 / CyO</i>	K. M., Indiana University
13. <i>sax¹ / CyO</i>	K. M., Indiana University
14. <i>punt¹³⁵ e¹ / TM3, Sb e</i>	K. M., Indiana University
15. <i>dpp^{d5}/CyO</i>	K. M., Indiana University
16. <i>dpp^{d6}/CyO</i>	K. M., Indiana University
17. <i>dpp^{hr4}/CyO</i>	K. M., Indiana University

Wildtype strains :

18. Canton S
19. *Ore-R*

M. A. Russell, University of Alberta
M. A. Russell, University of Alberta

Balancer lines:

20. *Sp/ CyO; ry/ry*
21. *TM3, Sb e/TM6, Tb Hu ry e*
22. *TM3, Sb e/TM6, Tb Hu e*

M. A. Russell, University of Alberta
M. A. Russell, University of Alberta
M. A. Russell, University of Alberta

LacZ lines :

23. *wg^{P[lacZ, en2]}/CyO*
24. *P[BS3.0dpp-lacZ] / TM3 Sb*
25. *hh^{P[lacZ]2033} / TM3 Sb*
26. *ptc^{P[lacZ, w⁺]H3} / CyO*
27. *P[en-lacZ, jryXho25.1] / CyO*

A. Manoukian, University of Toronto
(Kassis et al., 1992)
R. Blackman, University of Washington
(Blackman et al., 1991)
Kathy Matthews, Indiana University
(Tabata et al., 1992)
Kathy Matthews, Indiana University
(Hooper and Scott, 1989)
T. Kornberg, University of California, San
Francisco (Hama et al., 1990)

FRT recombinant lines:

28. *w; l(3)08310^{P{ry⁺t7.2=PZlacZ}}P{FRT 2A, w⁺}/TM3, Sb e*
29. *y w¹¹¹⁸; P{ry⁺, Hsp70: neo FRT<FRT< Hsp70:
neo=neoFRT}82B P{w⁺m Hsp70:N:c-myc=NM}88C*
30. *y w ; P {Tub(alpha)1>FRT y+>FRT hh}*
31. *y w; P{y⁺ FRT2A}/TM3, Sb e*

A. Manoukian, University of Toronto
Kathy Matthews, Indiana University (Xu, T., and
Rubin, G. M., 1993)

Kathy Matthews, Indiana University
A. Manoukian, University of Toronto
(Basler and Struhl, 1994)

FLPase source lines:

32. *y w ; P{w⁺mC^{hs70-FLP1}}*
33. *y w f su(f)¹², P{hs70-FLP1} / FM7c*

Kathy Matthews, Indiana University
(Xu, T. and Rubin, G. M., 1993)
S. Scanga (this study)

UAS transgenic lines:

34. *w; P{w⁺mC^{UASkiwi5.1}} / CyO; Ki / TM3, Sb e*
35. *w; P{w⁺mC^{UAS-heparinase III}}*
36. *w; P{w⁺mC^{=UASdpp}}*
37. *w; P{w⁺mC^{=UAS-dpp}};
l(3)08310^{P1731{ry⁺t7.2=PZlacZ}} / TM3, Sb*
38. *w; P{w⁺mC^{=UAS-lacZ.B}4-2-4B}*
39. *y,v f su(f)¹²/FM7c; P{w⁺mC^{=UAS-lacZ.B}4-2-4B}*
40. *w; P{w⁺mC^{=UAS-kiwi}5.1/CyO}*

A. Manoukian, University of Toronto
A. M., University of Toronto
A. M., University of Toronto
S. Scanga (this study)
Kathy Matthews, Indiana University
S. Scanga (this study)
A. Manoukian, University of Toronto

Gal4 transgenic lines:

41. *w; P{w⁺mC^{=Gal4-Hsp70.PB}89-2-1}*

Kathy Matthews, Indiana University

42. $w; P\{w^+mC=prd-GAL4\};$
 $P173]P\{ry+t7.2=PZlacZ\} / TM3, Sb e$
43. $w; P\{w^+mC=GAL4\} C5 / CyO$
44. $w; P\{w^+mC=GAL4\} C52/CyO$
45. $y v f su(f)^{12}/FM7c;$
 $P\{w^+mC=GAL4\} C5 / CyO$
46. $y v f su(f)^{12}/FM7c;$
 $P\{w^+mC=GAL4\} C52/CyO$

S. Scanga (this study)

G. Boulianne, University of Toronto

G. Boulianne, University of Toronto

S. Scanga (this study)

S. Scanga (this study)

Lines with a transposase source:

47. $Sp / CyO; ry Sb P[\Delta 2-3, ry^+](99B)/TM6, Ubx e$
48. $w; Sb ry e P[\Delta 2-3, ry^+](99B) ry^{506}/ TM6A, Ubx e ry^{506}$
49. $w; Sb ry e P[\Delta 2-3, ry^+](99B)/ TM6A, Ubx e ry$

R. Hodgetts, University of Alberta

R. Hodgetts, University of Alberta

R. Hodgetts, University of Alberta

Deficiencies:

50. $Df(3L) CH39 /TM3, Sb e$
51. $Df(3L) ZN47/ TM3, Sb e$
52. $Df(3L) XA596 /TM3, Sb e$
53. $Df(3L) Vn /TM3, Sb e$
54. $Df(3L) v65n / TM3, Sb e$
55. $Df(3L) w5.4 /TM3, Sb e$
56. $Df(3L) CH12 /TM3, Sb e$
57. $Df(3L) XBB70 /TM3, Sb e$
58. $Df(3L) RM5-2 /TM3, Sb e$
59. $Df(3L) pbl-X1 /TM3, Sb e$
60. $Df(3L) w5.4/TM3, Sb$

K. Anderson, University of California Berkeley

K. A., University of California Berkeley

K. A., University of California Berkeley

K. A., University of California Berkeley

K. A., University of California Berkeley

A. Manoukian, University of Toronto

K. Anderson, University of California Berkeley

K. A., University of California Berkeley

K. A., University of California Berkeley

K. A., University of California Berkeley

A. Manoukian, University of Toronto

EMS-induced mutation:

61. $A31 /TM3, Sb e$
62. $A99 /TM3, Sb e$
63. $C76 /TM3, Sb e$
64. $C88 /TM3, Sb e$
65. $E82 /TM3, Sb e$
66. $J82 /TM3, Sb e$
67. $J83 /TM3, Sb e$
68. $N71 /TM3, Sb e$
69. $SG9 /TM3, Sb e$

A. Manoukian, University of Toronto

K. Anderson, University of California Berkeley

K. A., University of California Berkeley

K. A., University of California Berkeley

K. A., University of California Berkeley

K. A., University of California Berkeley

K. A., University of California Berkeley

A. Manoukian, University of Toronto

A. Manoukian, University of Toronto

X-ray induced mutation:

70. $XAJ36 99 /TM3, Sb e$

K. Anderson, University of California Berkeley

For a list of the *PZ* enhancer-trap lines identified in the *su(f)¹²* screen, see Brook et al. (1993) and Russell et al. (1998).

II-3. Bacterial and Phage stocks.

Escherichia coli (*E. coli*) strains were grown in LB or superbroth prepared according to Sambrook et al. (1989). The three bacterial and one phage strain used in this study are shown in Table 3.

TABLE 3.
E. coli and Phage strains used in this study

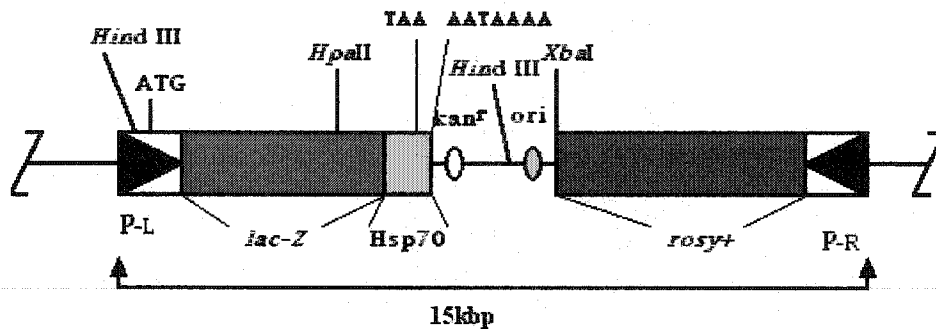
Strain	Genetic description	Source
XL-1 blue (bacteria)	endA1 hsdR17 supE44 thi-1 recA1 gyrA96 relA1 Δ (argF-lacZYA)U169 ϕ 80dlacZ Δ M15	Eugene Chomey, University of Alberta (Stratagene)
Q358 (bacteria)	hsd ⁻ R, hsdM ⁺ K, supE, ϕ 80 ^F	Eugene Chomey University of Alberta (Doherty et al., 1993)
PMC103 (bacteria)	mcrA Δ (mcrBC-hsdRMS-mrr)102 recD sbcC	Dr. W. D. Addison University of Alberta (Kam et al., 1980)
Lambda gt10 (phage)	<i>Drosophila</i> embryonic cDNA library at 3-12 hr and at 12-24 hr.	Eugene Chomey University of Alberta

II-4. Screening of PZ enhancer-trap lines using the *su(f)*¹² temperature-sensitive autonomous cell-death mutant.

The enhancer-trap lines used as the starting point for this study were PZ-lethal insertions generated from the enhancer-trap regeneration screen by Brook et al. (1993) and the autosomal PZ-lethal insertion lines of Spradling et al. (1995).

PZ (Flybase 1994; Flybase 2001, <http://www.flybase.com>) is a non-autonomous transposable P-element derivative, specifically, *P*{*ry*⁺, *P/T*:*lacZ*:*Hsp70* *Kmr* *ori*} carrying a *lacZ* reporter gene under the control of the weak P-transposase promoter (see Figure 19). The chromosomal locations of the autosomal PZ-lethal insertion lines from Spradling et al. (1995) are listed in Flybase (2001, Flybase <http://www.flybase.com>). The screen was performed with the help of Daralyn Hodgetts, Lisa Ostafichuk, and M. A. Russell. The suppressor of forked mutation, *su(f)*¹², is a temperature-sensitive, cell-autonomous, X-linked lethal mutation (Russell, 1974). A 48-hr 29°C treatment causes extensive cell death in imaginal discs of *Drosophila* resulting in regeneration and duplication repatterning events

Figure 19. PZ{lacZ, ry⁺} -plasmid element used in the regeneration enhancer trap screen in this study.



PZ enhancer-trap construct from Jacobs et al. (1989) used in the regeneration enhancer-trap screen. Shown are the inverted repeats of the P-element ends (black triangles), the translation start site (ATG), the *E. coli lacZ* reporter encoding the β -galactosidase gene and the *Drosophila melanogaster* HSP-70 terminator sequence containing the stop codon (TAA) and poly-A (AATAAAA) sites, the plasmid sequence containing the kanamycin resistance marker (*kan-r*) and the bacterial origin of replication (*ori*) required for plasmid rescue, and the *rosy⁺* marker which allows for the transposons in the fly crosses to be detected in the appropriate genetic background. The unique *Xba*I and *Hpa*II restriction sites allows for the cloning of the left (P-L) and right (P-R) flanking genomic sequences respectively.

(Clark, 1976; Clark and Russell, 1977; Girton and Russell, 1981). Males from the Spradling *PZ*-lethal insertion lines to be tested for ectopic misexpression of *lacZ* were crossed to homozygous *yellow* (*y*), *vermilion* (*v*), *forked* (*f*), *su(f)*¹² virgin females collected from a stock kept at the permissive temperature of 22°C (see Brook et al., 1993; Russell et al., 1998). The cross generated F1 progeny males that are *y v f su(f)*¹²/*Y*; *PZ*/+ (yellow phenotype), and female controls that are *y v f su(f)*¹²/+; *PZ*/+ (*y*⁺ phenotype). These progeny were reared at 22°C for 5-days until 3rd larval instar, shifted to 29°C for 2-days, and then returned to 22°C to allow the discs to initiate the pattern respecification process. After a 24-hr recovery period, late third instar ts-lethal male larvae were identified; their imaginal discs were dissected and stained for β-galactosidase activity using the X-gal staining reaction, then compared with discs from female controls at the same stage of development.

II-5. Screen for ectopic activation of *GAL4* insertions during *su(f)*¹² induced regeneration in imaginal leg discs.

A collection of random autosomal *GAL4* insertion lines was screened for ectopic activation of the *GAL4* insertion during *su(f)*¹² induced regeneration, using a the *UAS-lacZ* reporter transgene (see Brand and Perrimon, 1993). The autosomal *GAL4* insertion lines were obtained from G. Boulianne (unpublished), N. Perrimon (unpublished), and Kathy Matthews (Bloomington Stock Center, Indiana University); these are listed in Table 4.

TABLE 4.
Autosomal *GAL4* insertion lines

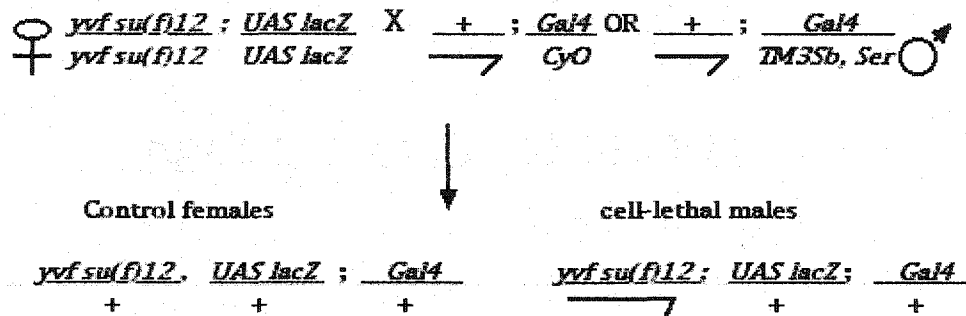
Stocks	Source
e41c, e4A, e9A,3IT/CyO, e26B, E27C/CyO, e33c/TM3, e29c/TM3, e49D, e32A, e43A/CyO, 350A, e7A, e33A/CyO, e33B, e8A, e55A, e21A/CyO, e74A/CyO, e26A, eE6, en1-2, e65A/CyO, e25A, e6A, e47A/CyO, e41A/TM3, e13C, e45A/TM3, eF2, e1A/CyO, e75B, e3B, e46A, e16, e16D/CyO, e1E1	Dr. N.Perrimon Harvard Medical School
1J3, 71B, 24B/TM3, 69B/TM3,32B/TM3, 30A/CyO, T80, RG1, 34B, e22c	Kathy Matthews Indiana University Bloomington Stock Center
A23, A40, A59, C41, C49, B41, B66, C15, C52, C89, C98, D14, D24, B51, B99, C5, C14,	G. Boulianne Hospital for Sick Children Toronto

*Y v f su(f)*¹²/*Y*; *Gal4*/*TM3* or *CyO* males were crossed to *y v f, su(f)*¹²/*y w f, su(f)*¹²; *UAS-lacZ*/*UAS-lacZ* females generating *y v f su(f)*¹²/+; *UAS-lacZ*/+; *Gal4*/+ or *y v f su(f)*¹²/+; *UAS-lacZ*/*Gal4* F1 male progeny (see Figure 20). These were reared at 22°C (the permissive temperature) for 5-days

Figure 20. A screen for *Gal4* lines that are activated upon *su(f)¹²* induced regeneration in imaginal leg discs.

Screening for Gal4 insertion lines on the 2nd and 3rd chromosomes.

(1). Cross at 22°C:



(2). Cultures shifted to 29°C for 48hr at mid 2nd instar larval stage.

(3). Cultures shifted to 22°C, and allow the larvae to develop for 24hr.

(4). Larvae separated by sex and imaginal discs stained for β-galactosidase activity.

Note: *UASlacZ - w*; *P{w[+mC]}=UASlac-Z}4-2-4B/* *P{w[+mC]}=UASlac-Z}4-2-4B* on the second.
Gal4 -w; *P{w[+mC]}=Gal4}* lines on the second and third chromosome.

Figure 20 describes the crossing scheme and selection of *Gal4* insertion lines that show ectopic misexpression in imaginal leg discs during regeneration, induced by the *su(f)¹²* mutant upon the heat-treatment of larvae.

until 3rd larval instar, shifted to 29°C for 2-days, and then returned to 22°C to allow the discs to initiate the pattern regeneration process. After a 48-hr recovery period, late third instar male (experimental) and female (controls) larvae were identified and imaginal discs dissected and stained for β -galactosidase activity, using X-gal staining reaction.

II-6. Genetic analysis of PZ-lethal phenotypes of an UDP-GlcDH mutant, *sgl*.

II-6i. Cuticle preparations.

The embryonic lethal phenotypes of the enhancer-trap PZ-insertions of UDP-GlcDH, *A64* and *P1731* were determined as described in Wieschaus and Nusslein-Volhard (1986). Males carrying the PZ insert over a balancer were crossed to *Oregon R* (*Ore R*) virgin females to out-cross the balancer chromosome. The F1 non-balancer siblings were mated (50 males to 100 females). Embryos were collected at 25°C for 20-hr on yeasted agar-apple juice plates and then counted while they were being replated onto fresh plates, where they were allowed to develop for 48-hr at 25°C. Unhatched embryos were dechorionated in 50% bleach, washed, mounted on slides, and cleared overnight on a slide warmer in Hoyers/15% lactic acid medium (Wieschaus and Nusslein-Volhard, 1986). Cuticles were then flattened with a weight on a slide warmer for 3- to 4-hr, before examination under a compound microscope.

II-6ii. Crosses used to generate embryos heterozygous for *sgl* (UDP-GlcDH) and mutations in the *dpp* signaling pathway.

To look for interactions between *sgl*^{*P1731*} and mutations in the *dpp* pathway, the balancer chromosomes were substituted from *sgl*^{*P1731*}/*TM3 Sb e*, *dpp*^{*27*}/*CyO*, *dpp*^{*H46*}/*CyO*, *thv*^{*7*}/*CyO*, and *punt*^{*135*}/*TM3 Sb e* by crossing to *Ore-R*. Transheterozygotes were then made by crossing *sgl*^{*P1731*}/*+* females to *dpp*^{*27*}/*+*, *punt*^{*135*}/*+*, *thv*^{*7*}/*+* and *dpp*^{*H46*}/*+* males. The resulting embryos were plated on fresh agar-apple juice plates and aged at 25°C until hatching. Cuticles from unhatched embryos were analyzed for patterning defects as described above. Samples of 8- to 10-hr old embryos from the above cross were also fixed and stained as described in section II-7iv for *evenskipped*, *Kruppel* and *tinman* protein expression. Controls involving embryos heterozygous for *dpp* pathway mutations only or *sgl*^{*P1731*} were also analyzed for differences in *evenskipped*, *Kruppel* and *tinman* protein expression in 8- to 10-hr (stage 11-13) embryos and for any discernable cuticle defects.

II-6iii. Crosses made to analyze ectopic heparinase III effects in the embryo.

The heparinase III enzyme (also referred to as heparanase), a heparan sulfate specific degradative enzyme, was ectopically expressed in the embryo by crossing *hsGal4* males with *UAShepIII* transgenic (Manoukian lab, unpublished) females. The heparinase III cloned from a bacteria (*Flavobacterium heparium*) (Sasisekharan, 1993) was subcloned into a pUAST expression vector

(Brand and Perrimon, 1993). The clone encoded an N-terminal signal sequence that allows for its proper secretion from the cell upon its expression (Manoukian lab, unpublished). Embryos were collected in food vials for 1 hr at 25°C, aged for 2-hr and then heat shocked at 37°C for 15-min in a water bath. Embryos were then transferred to fresh apple juice-agar plates and allowed to age for a further 24-hr at 25°C. Cuticles from unhatched embryos were prepared as described above. To visualize *Kruppel* and *tinman* expression in these embryos, heat treated embryos were aged 6- to 8-hr AEL at 25°C following heat treatment. The embryos were then fixed and stained as described in section II-7iv for *Kruppel*, *evenskipped* and *tinman* protein expression. Expression of stain in both experimental and controls were monitored in parallel until the appropriate intensity was observed in controls.

II-6iv. Epistasis Analysis of *sgl^{P1731}* with *dpp*.

PrdGal4/prdGal4; sgl^{P1731}/+ males were crossed to *UASdpp/UASdpp; sgl^{P1731}/TM3* females and embryos were collected on apple juice-agar plates for 2-hr. Half of the embryos were transferred to fresh plates and allowed to age at 25°C for 48-hr, after which cuticle preparations were made. The other half of the embryos were aged at 25°C until 8- to 10-hr after egg lay. They were then fixed and stained for *tinman* and *evenskipped* protein expression as described in section II-7iv. A control group of *prdGal4/prdGal4; sgl^{P1731}/+* and *UASdpp/UASdpp; sgl^{P1731}/+* embryos was also collected for cuticle analysis.

II-6v. Analysis of *sgl^{P1731}* interactions with viable *dpp* disc mutants in adult flies.

Dpp^{d6}/CyO; sgl^{P1731}/TM3 males were crossed to *dpp^{d5}/CyO* and *dpp^{hr4}/CyO* females; and F1 adults that had lost the balancer chromosome were preserved in 70% ethanol. Adult wings and legs were dissected in 70% ethanol, mounted in 50% Euparal/50% ethanol, and allowed to clear overnight. The wings and legs were then flattened with a weight overnight on a slide warmer.

II-6vi. Mosaic analysis of the *sgl^{P1731}* mutation in adult wings and legs.

For the generation of adult somatic clones in imaginal discs the FLP/FRT method was used (Xu and Rubin, 1993). The following cross was made: *y w P{w⁺m^C_{hs70}-FLP¹²}/y w, P{w⁺m^C_{hs70}-FLP¹²}; *sgl^{P1731} P[FRT 2A, w⁺] (80B)/TM3 Sb e* females were crossed to *y w P{w⁺m^C_{hs70}-FLP¹²}/Y; P[y⁺] FRT2A(80B)/TM3, Sb e* males. Embryos were collected in food vials for 12-hr at 25°C and shifted to 37°C for 2-hr at early second larval instar (60-hr after egg laying), to induce FLP activity. Larvae were then incubated at 25°C until eclosion. Adult legs from non-TM3 flies were then dissected and mounted as described above in II-6v. All crosses were performed at RT on standard medium (see above), except in those cases in which antibiotic was required for selection of the Neomycin resistance gene of recombinogenic FRT lines generated for this study (described in Xu and Rubin, 1993). The antibiotic G418 (Geneticin, GIBCO laboratories) was used as described in Xu and Rubin (1993); 300 µl of a freshly made solution of G418 (25 mg/ml) were added per 10 ml of medium. This antibiotic is toxic to eukaryotic cells, except, in flies that carry the P[ry⁺; hs-neo; FRT] cassette.*

II-6vii. Analysis of the effects of ectopic heparinase III expression on the adult phenotype.

UAShepIII/UAShepIII females were crossed to *hsGal4/hsGal4* males. Embryos were collected in vials for 12-hr at 25°C and aged until late second or early third larval instar (78-hr AEL). Larvae were then heat treated for 50 min at 37°C and aged until eclosion at 25°C. Adult legs and wings were then mounted as described in section II-6v.

II-6viii. Analysis of the effects of ectopic UDP-GlcDH expression on the embryonic and adult phenotypes.

w; UASkiwi5.1 (UDP-GlcDH-cDNA)/CyO (Manoukian lab, unpublished) females were crossed to *hsGal4/hsGal4* (chromosome III) males. Embryos were collected in food vials for 12-hr at 25°C and aged until mid second larval instar (72-hr AEL). Second instar larvae were then heat shocked at 37°C for 1-hr, allowed to recover for 24-hr and then heat shocked again for an additional 1-hr. The larvae were then incubated at room temperature (22°C) until eclosion, and adult wings and legs were mounted as described in II-6v.

II-7. Histochemical techniques.

II-7i. Staining for β -galactosidase activity in imaginal discs and disc fragments.

a. Dissection and X-gal staining of imaginal discs.

Using watchmaker's forceps, larval heads were dissected in cold (4°C) phosphate-buffered saline (PBS) (140 mM NaCl, 25 mM sodium phosphate buffer, pH 7.2) by separating the head and thoracic segments from the abdominal segments. The head and the thoracic half of the larvae contain the eye-antenna, wing, and first thoracic (T1), second thoracic (T2) and third thoracic (T3) leg discs; all remain attached to two optic lobes and the CNS stalk. The heads were everted using dissecting needles to expose the imaginal discs and were then transferred to microfuge tubes containing PBS. This allows for easier manipulation and identification of the imaginal discs during the fixation and staining process. The tissues were then fixed for 10-min at room temperature with freshly prepared 0.75% glutaraldehyde in PBS, washed three times with PBT (0.05% TritonX-100 in PBS), and then stained in 0.2% X-Gal (5-bromo, 4-chloro, 3-indolyl galactose dissolved in dimethyl formamide) in staining solution (10 mM sodium phosphate, pH 7.2, 150 mM NaCl, 1 mM MgCl₂, 5 mM potassium ferricyanide, 5 mM potassium ferrocyanide), freshly prepared from an 8% X-Gal stock solution in dimethyl formamide kept at -20°C (Bellen et al., 1989). Staining was performed for both controls and experimentals in parallel at 37°C in the dark for 12-hr and terminated with three washes in PBT. The tissues were then put in mountant (70% glycerol buffered with 0.03M Tris, pH 9.0) overnight at 4°C. The imaginal discs were then dissected in mountant and placed on microscope slides, flattened with cover slips, and observed with a compound microscope.

b. *In vivo* culture of imaginal disc fragments.

Preparation and injection of disc fragments for *in vivo* culture was performed with Lisa Ostafichuk, essentially as described by Ursprung (1967). Needles for injection were made by pulling 25 μ l Microcaps capillary tubes (Drummond Scientific Co.) over an alcohol burner by hand. The tips were broken in order to give them a beveled edge of the desired diameter (approximately the diameter of the imaginal disc fragments to be injected). The bevelled edge was sharpened on Saphire Film (Circon Corp.). Needles were attached to a mouth aspirator set (American Hospital Supply Corp.) with parafilm. The appropriate discs were dissected in Ringer's Solution (NaCl 7.5 g/L, KCl 0.35 g/L, 10 mM Tricine, pH 7.2, and 100 mg/ml streptomycin made up in sterile Milli-Q distilled water, then filter sterilized and kept at 4°C). Leg discs were fragmented in Ringer's on a slide using a sharpened insect pin. Mated Canton-S female hosts (24- to 48-hr post-eclosion) were anesthetized with diethylether and placed ventral side up on double-sided tape attached to a microscope slide. The disc fragment was aspirated with a small amount of Ringer's into the tip of the needle. Fine forceps were used to pinch the ventral abdominal cuticle and the fragment was injected in a posterior to anterior direction between the sternites. The host fly was then placed in a vial containing yeast-agar medium. The vial was laid on its side so that the host would not become stuck in the medium. The injected hosts were cultured for 2- to 5-days at 25°C; an incision was then made in the host abdomen in PBS. The implanted leg disc was recovered, fixed, stained for β -galactosidase activity, and mounted on slides as described in II-7i.a.

II-7ii. Staining of embryos for β -galactosidase activity.

Embryos were collected on yeasted apple-juice agar plates for 14-hr at 25°C. Embryos were then fixed and stained for β -galactosidase activity according to Ghysen and O'Kane (1989), with the following modifications. Both controls and experimental samples incubated in staining solution in a microfuge tube overnight (12- to 16-hr) at 37°C and monitored the next day in parallel. When the control embryos were sufficiently stained, the X-Gal solution was removed and embryos from both the experimentals and controls were rinsed three times in 1X PBS/0.2% Triton-X100. The wash medium was then replaced with mountant (70% glycerol, 0.1M Tris HCl pH 9.0), and the embryos were incubated overnight at 4°C. The embryos were then placed in a drop of mountant on a slide, flattened with a cover slip, and observed under a compound microscope.

II-7iii. Immunostaining of imaginal discs.

Imaginal discs were exposed as described above by inverting dissected larval heads in 1XTBS (50 mM Tris-HCl pH 7.6, and 150 mM NaCl, in MilliQ-H₂O). The heads were transferred to microfuge tubes containing 1XTBS on ice. The tissue was fixed for 7-min at room temperature (RT) in a TBS/4% formaldehyde fix solution [1XTBS, 4% formaldehyde, 1% Triton X-100, 0.1M Pipes, 2 mM MgSO₄, 1 mM EGTA (pH 6.9)]. The heads were then rinsed in methanol:fix (1:1 solution), and then washed three times in methanol for 5-min each. At this stage, the tissue was stored in methanol

overnight at -20°C. This step reduces background staining levels in discs. The following day, the discs were washed 3X with 1XTBST (1X TBS, 0.1% Triton X-100) for 5-min each. The tissue was then incubated in blocking (0.5% Blotto) solution (1XTBS, 0.5% Triton X-100, 0.5% Carnation dry skim milk) for 1-2 hr at RT. The discs were then incubated with primary (1^o) antibody (Ab), overnight at 4°C in blocking solution with gentle agitation on a rocker. The next day, three washes of 20-min each were performed at RT in 1X TBST. Following the washes the discs were incubated for 60-min at RT with the appropriate biotinylated secondary antibody (at a dilution of 1/500 from Vector Labs). This was followed by another three washes at RT for 10-min each. Discs were then incubated for 50-min in 1X TBST containing the streptavidin-alkaline phosphatase conjugate (Vector Labs) at a 1:500 dilution. Discs were then rinsed three times in 1X TBST for 20 min each. To stain for streptavidin-alkaline phosphatase activity, embryos were then rinsed twice in AP-developer solution (100 mM NaCl, 50 mM MgCl₂, 100 mM Tris-HCl, pH 9.5, 1 mM Levamisol, and 0.1% Tween-20). In the last wash, 4.5 µl of nitroblue tetrazolium chloride (NBT) and 3.5 µl of 5-bromo, 4-chloro, 3-indolyl phosphate (X-Phosphate) solution was added. The colour reaction was allowed to proceed in AP-developing buffer/NBT/X-phosphate (according to Boehringer Mannheim) at RT until the appropriate signal was observed in the control discs, but before the appearance of any visible background (non-specific stain) in the tissue. The colour signal was developed in parallel reactions for both the control and experimental embryo samples. The staining reaction was not allowed to proceed more than 1-hr at RT. The reaction was stopped at the same time in both experimental and control samples by washing several times in 1X TBST. The heads were then incubated in mountant (0.1M Tris-HCl pH 9 /70% glycerol) overnight at 4°C, then placed on slides for examination with the compound microscope. Discs were then dissected from the larval heads in mountant, placed on slides, and observed under the compound microscope.

II-7iv. Immunostaining of embryos.

Primary antibodies were provided by Dr. M. Frasch (rabbit anti-*evenskipped* and mouse anti-*tinman*), Dr. M. Hoffman (mouse anti-*dpp*), and Dr. K. Vorwerk (rabbit anti-*Kruppel*). Zero- to 8-hr embryos were collected at 25°C on yeasted agar-apple juice plates, dechorionated in 50% bleach and fixed in heptane /4% formaldehyde/ 1X TBS solution for 10-min, washed three times in methanol for 10-min each, rinsed three times in 1X TBST (10 mM Tris-HCl pH 7, 150 mM NaCl, 0.5% Tween-20) for 10min each, and blocked for 1-hr at room temperature in 1XTBST/ 0.5% BSA/ 0.5% Carnation dry skim milk powder. Incubation with primary antibody at the appropriate dilution in 1XTBST was carried out overnight at 4°C. Embryos were then washed four times in 1X TBST for 20-min each. This was followed with incubations at room temperature with the appropriate biotinylated secondary antibody (Vector Labs) for 1 hr. Embryos were again washed three times in 1X TBST for 10-min each, incubated with streptavidin-AP (alkaline phosphatase) conjugate at room temperature for 45-min, and then rinsed three times in 1X TBST for 10-min each. The colour reaction was allowed to proceed in AP-developing buffer/NBT/X-phosphate (according to Boehringer Mannheim) at RT until the appropriate signal was observed in the control embryos, before the appearance of any visible background in the

tissue. The colour signal was developed in parallel reactions for both the control and experimental embryo samples. The staining reaction was not allowed to proceed more than 1-hr at RT. The reaction was stopped at the same time in both experimental and control samples by washing several times in 1X TBST. The embryos were then incubated in mountant (Tris-HCl, pH 6.9/70% glycerol) overnight at 4°C and then placed on slides for examination with the compound microscope.

II-7v. *In situ* hybridization of embryos.

In situ hybridization of embryos was performed by using non-radioactive digoxigenin-labeled DNA probes. The protocol is from Tautz and Pfeifle (1989) with modifications given below:

a. Fixation.

Embryos were collected on yeasted apple juice-agar plates, transferred to a mesh basket where they were rinsed with wash (0.7% NaCl, 0.03% Triton X-100), dechorionated for 2- to-min in 50% bleach, and rinsed thoroughly with deionized water. For fixation, embryos were transferred to a scintillation vial containing a two-phase 1:1 mixture of heptane and fix (10% formaldehyde, 1X PBS, 50 mM EGTA, pH 7.4) for 20-min while shaking at RT. To devitellinize the embryos, they were transferred to microfuge tubes; and the fixative and heptane were then removed and replaced by 100% methanol and shaken vigorously during three methanol washes. Devitellinized embryos sink to the bottom of the tube. These embryos were then rinsed with 100% methanol, rinsed several times with 100% ethanol, and stored at -20°C until used.

b. Staining.

For staining, embryos were rinsed in 100% methanol and then in 50% methanol/50% PBT (1X PBS, 0.1% Tween-20) plus 5% formaldehyde mix, post-fixed for 20-min in PBT plus 5% formaldehyde at room temperature and rinsed in PBT three times for 2-min each. Proteinase K (PBT plus 50 µg/ml non-predigested Proteinase K) treatment was performed at 37°C for 3- to 5-min, and stopped by rinsing twice with 2 mg/ml glycine in PBT, followed by two rinses in PBT. Embryos were then post-fixed for 20-min in PBT plus 5% formaldehyde at room temperature, followed by five rinses in PBT. To hybridize the probe, embryos were washed in a 1:1 solution of PBT and hybridization solution (50% de-ionized formamide, 5X SSC, 100 µg/ml denatured sonicated salmon sperm DNA, 100 µg/ml yeast tRNA, 50 µg/ml heparin, and 0.1% Tween 20) and then rinsed in 100% hybridization solution. Prehybridization was performed for 2-hr at 48°C. Hybridization was done at 48°C overnight in a small volume (100 µl) with approximately 100 ng/ml denatured probe, washed for 20-min at 48°C in hybridization solution, for 20-min in 50% hybridization solution:50% PBT, and five times for 20-min each in PBT. To develop the colour signal, the anti-Digoxigenin-alkaline phosphatase-conjugated antibody was added to embryos in a 1:2000 dilution in PBT and incubated overnight at 4°C. Embryos were washed four times for 20-min each in PBT at RT, then rinsed twice in an AP-developer solution

(100 mM NaCl, 50 mM MgCl₂, 100 mM Tris-HCl pH 9.5, 1 mM Levamisol, 0.1% Tween 20). To develop, 500 µl of AP-developer solution was added to embryos, along with 2.3 µl NBT and 1.8 µl X-Phosphate. The staining reaction in both controls and experimental samples was monitored in parallel until the desired colour intensity was attained in the control sample. In this case, control discs were monitored for a maximum of 1-hr at RT or until the appearance of background (non-specific stain). At this point, both control and experimental staining reactions were stopped simultaneously by washing in PBT several times (5 times for 10 min each); the embryos were then placed in mountant, and observed under the microscope.

II-7vi. *In situ* hybridization of imaginal discs.

In situ hybridization of imaginal discs was performed using non-radioactive digoxigenin labeled DNA probes using the protocol of Manoukian and Krause (1993) with modifications.

a. Fixation.

Larval heads were dissected and everted (exposing the imaginal discs) in 1X PBS and transferred to a 500 µl microfuge tube containing cold 1X PBS. The 1X PBS was removed and replaced with 4% formaldehyde fix (4% formaldehyde, 1% Triton X-100, 0.1M Pipes pH 7, 2 mM MgSO₄, and 1 mM EGTA, pH 6.9, in MilliQH₂O) for 7-min at RT; the fix was then replaced with 100% methanol. The heads were then washed three times for 10-min each in 100% methanol. Properly fixed discs sink to the bottom of the tube. Heads were then stored in 100% methanol at -20°C until used.

b. Staining.

For staining, the heads were rinsed in 100% methanol, then in 50% methanol/50% PBT (1X PBS, 0.1% Tween-20) plus 5% formaldehyde. They were then post-fixed for 20-min in PBT plus 5% formaldehyde at room temperature and rinsed in PBT three times for 2-min each. Proteinase K (PBT plus 50 µg/ml non-predigested Proteinase K) treatment was performed at RT for 30-seconds. Proteinase treatment was stopped by rinsing twice with 2 mg/ml glycine in PBT, followed by two rinses in PBT. Heads were then post-fixed again for 20-min in PBT plus 5% formaldehyde at room temperature, followed by five rinses in PBT. To hybridize the probe, the heads were washed a solution of 1:1 PBT:hybridization solution (50% deionized formamide, 5X SSC; 100 µg/ml denatured sonicated salmon sperm DNA, 100 µg/ml yeast tRNA, 50 µg/ml heparin; and 0.1% Tween 20), and then rinsed in 100% hybridization solution. Prehybridization was performed for 2 hr at 48°C. Hybridization was done at 48°C overnight in a small volume (100 µl) of hybridization solution with approximately 100 ng/ml denatured probe. The heads were then washed for 20-min at 48°C in hybridization solution, for 20-min in 50% hybridization solution/50% PBT and five times for 20-min each in PBT. The anti-Digoxigenin-alkaline phosphatase-conjugated antibody was added to the heads in a 1:2000 dilution in PBT, incubated overnight at 4°C, washed four times for 20-min each in PBT at RT, and rinsed twice in

a AP-developer solution (100 mM NaCl, 50 mM MgCl₂, 100 mM Tris-HCl pH 9.5, 1 mM Levamisol, and 0.1% Tween 20). To develop the colour signal, 500 µl of AP developer solution was added to heads, along with 2.3 µl NBT and 1.8 µl X-Phosphate. The staining reaction, was monitored, in both controls and experimental samples in parallel until the desired colour intensity was attained in the control sample. In this case, control discs were monitored for a maximum of 1 hr at RT or just prior to the appearance of background (non-specific stain). At this point, both control and experimental staining reactions were stopped simultaneously by washing in PBT several times (five times for 10-min each). The imaginal discs were then dissected from heads in mountant and observed under the microscope.

II-7vii. Photomicroscopy of tissues.

Specimens were photographed with a Zeiss Axioskop photomicroscope using DIC optics (provided by Dr. D. Pilgrim, Biological Sciences Department, University of Alberta) using Kodak GOLD 35 mm film, ASA100.

II-7viii. *In situ* hybridization of polytene chromosomes.

The polytene *in situ* hybridization protocol used was taken from Dr. J. Locke (Biological Sciences, University of Alberta) and Ashburner (1989) and carried out with some modifications given below.

a. Preparation of polytene chromosomes.

Third instar larvae of the required genotype were grown at 18°C (allowing for more rounds of DNA replication) making the polytene chromosomes fatter and easier to see with the compound microscope. Late third instar larvae were then taken out of the food vials, washed in 1X PBS, and placed in a drop of 45% acetic acid solution. The salivary glands were dissected and transferred to a gelatinized slide containing another drop of 45% acetic acid. A siliconized coverslip was placed on top and the salivary glands were squashed and frozen in liquid nitrogen for 5-min. The coverslip was then flipped off with a razor blade. Chromosomes were fixed for 10 min in a solution of 3:1 acetic acid:ethanol, transferred to 70% ethanol for 5-min, then to 95% ethanol for 5 min and allowed to dry for 1-hr at RT. Slides containing the polytene chromosomes were then stored at 4°C until use.

b. Hybridization using Digoxigenin-AP-labeled DNA probe.

Slides were incubated for 30-min at 60°C in 2X SSC and rinsed at RT in 2X SSC. To dehydrate the chromosomes, slides were placed twice in 70% ethanol for 5-min, in 95% ethanol for 5-min, and then dried at RT for examination under the microscope for the presence of clear bands. Chromosomes were denatured by immersing the slides in freshly made 70 mM NaOH for 2-min at RT, then rinsed twice for 5-min in 2X SSC, immersed twice for 5 min in 70% ethanol, and immersed 5-min in 95% ethanol. The chromosomes were allowed to dry at RT and the chromosome region was marked with water-proof ink. The Dig-labeled DNA probe was then added to the hybridization solution (45%

deionized formamide, 6.5% dextran sulfate, 575 µg/ml yeast tRNA, 1.4 µg/ml sonicated salmon sperm DNA) to a final concentration of 30-50 ng/µl. The hybridization solution was heated at 75°C for 10-min to denature the probe and quenched on ice for 5-min. Ten to twenty µl was added per slide and a coverslip placed on top. Hybridization was performed in a humidified chamber at 37°C overnight. Following hybridization, the coverslips were removed and the slides were washed twice in 2X SSC for 10-min each at 42°C, then twice in 2X SSC at RT for 10 min, and finally twice in PBS at RT for 10 min. To detect the signal, slides were first blocked by immersion in blocking buffer I (100 mM Tris-HCl, 150 mM NaCl, pH 7.5, plus 0.5% blocking reagent) (Boehringer Mannheim) for 20 min at 42°C, then placed in blocking buffer for 10 min at RT, and finally rinsed briefly in buffer I and flicked dry. The anti-Digoxigenin-AP-conjugated antibody was diluted in buffer I at 1/1000; 40 µl of the dilution was added per slide, and covered with a 22-mm-square coverslip. Incubations were carried out in a humidified chamber at 4°C. Following incubation, the slides were rinsed once for 1-min in buffer I at RT to remove the coverslip, then three times for 10-min in buffer I at RT. To detect the probe, slides were immersed in buffer III (100 mM Tris-HCl, pH 9.5, 100 mM NaCl, 50 mM MgCl) for 2-min at RT. To develop the slides at RT, 40 µl of colour solution (4.5 µl NBT-solution, and 3.5 µl of X-phosphate in 1 ml of buffer III) was added per slide. The signal usually appeared between 0.5 and 1 hr later. Following the development of the signal, slides were rinsed for 2 min at RT in TE (100 mM Tris-HCl, 100 mM EDTA, pH 7.0) to stop the reaction. Lacto-orcein (Lactic acid plus orcein) (Sigma) was used as a counterstain to help visualize the banding patterns in the polytene chromosomes. In order to observe the chromosomes under the microscope, mountant (as above) was added to the slide and sealed with a coverslip and rubber cement. The *en-lacZ PZ* insertion line, in which the cytological location of the *PZ* insert is already determined, was used as a positive control, and the wild-type Canton S line, which contains no *PZ* insert, was used as a negative control for these experiments.

II-8. DNA extraction and manipulations.

II-8i. Plasmid purification.

a. Minipreps.

Small-scale plasmid DNA preparations were carried out according to Sambrook et al. (1989), along with the optional STE and phenol-chloroform extraction steps.

b. Midipreps.

Medium-scale preparations were performed according to the QiagenTM plasmid handbook (1995), using the Qiagen resin columns. Heat-treated RnaseA was added to a final concentration of 5 µg/ml.

II-8ii. Restriction digests.

Restriction enzymes were purchased from BRL or Boehringer-Mannheim. Digests were performed according to the manufacturer's suggestion with the buffers supplied. Digested genomic or

plasmid DNA was separated in 0.8-1.0% agarose gels in TAE buffer (40 mM Tris-acetate, 1 mM EDTA), that included 0.5 µg/ml of ethidium bromide. DNA samples were mixed in a 10:1 ratio with loading buffer (0.25% bromophenol blue, 0.25% xylene cyanol, 25% ficoll [type 400]) in MilliQ-water. The BRL 1 kb ladder was used as a size standard.

II-8iii. DNA fragment purification.

DNA fragments were excised from 0.8-1.0% TAE-agarose gels following electrophoresis. The desired DNA fragments were then purified from excised agarose plugs using the GlassmaxTM kit (BRL) according to the manufacturer's instructions.

II-8iv. Southern blots.

DNA samples electrophoresed on agarose-TAE gels were transferred to GenescreenPLUS membrane (Dupont) by capillary action. The protocol describing the transfer and hybridization using appropriate P³²-dCTP-labeled DNA probes is detailed in the manufacturer's manual. The blot was then exposed to Kodak X-ray film for 1 day at -70°C.

II-8v. Plasmid rescue of the *A64 PZ* insertion line.

The P-element construct that is inserted near the gene is designated *PZ*. *PZ* has specific molecular features that make it useful by using plasmid rescue, for cloning genomic sequences adjacent to the *PZ* insertion site. These features include a bacterial origin of replication, a kanamycin-resistance gene, and single *Xba*I and *Hpa*II cleavage sites (see **Figure 21**).

a. Genomic DNA extraction (protocol provided by Dr. Bill Addison, University of Alberta).

Total genomic DNA was extracted from *PZ A64/TM3* adults. Three hundred to 400 flies were placed in a chilled mortar containing liquid nitrogen, and ground to a powder using a pestle. Three ml of Extraction Buffer (0.1M NaCl, 0.1M Tris-HCl pH 8, 50 mM EDTA) were then added, and the mixture was transferred to a 10 ml polypropylene tube. Ten µl of 0.5M spermidine (20 mg/ml) and 40 µl of proteinase K (20 mg/ml) were added to the extraction mix. Two hundred µl of 10% SDS were then added to the extraction mix, which was then incubated for 30-min at 37°C. A further 40 µl of Proteinase K (20 mg/ml) were added and the mix was allowed to incubate overnight at 50°C. The following day, 100 µl of 1 mg/ml PMSF (phenylmethylsulfonylfluoride) were added and incubated at 50°C for 30-min. Five microliters of RNAse (10 mg/ml) was then added and incubated at 37°C for 10-min. Two extractions using 1 volume of (1:1) phenol:chloroform were carried out for 5-min each at RT. The mix was then spun for 5-min at 5000 rpm at 4°C. This was followed by two extractions with 1 volume of (24:1) chloroform:isoamylalcohol. The mix was then spun again at 5000 rpm for 5-min at 4°C. The aqueous phase was transferred to a fresh 10 ml polypropylene tube. Two ml of 1M ammoni-

um acetate were added to the DNA solution along with 6 ml of isopropanol to precipitate the DNA. The DNA was spooled onto a glass pipette, immersed in a solution of 70% ethanol and 300 mM (final concentration) potassium acetate (KOAc), pH 5.5 for 30 min, air dried at RT, and then resuspended overnight at 4°C in TE, pH 8, to a concentration of 1 µg/µl of DNA.

b. Ligations.

Seven µg of DNA were digested with 30 units of *Xba*I or *Hpa*II in a total volume of 100 µl for 6 hr. A phenol/chloroform extraction was performed to inactivate the enzyme. The *Xba*I and *Hpa*II DNA fragments were then allowed to circularize and ligate. The ligation reaction mix consisted of 50 mM Tris-HCl pH 7.7, 10 mM MgCl₂, 10 mM DTT, 1 mg/ml ATP, and 25 µg/ml acetylated BSA. Fifty µl (3 µg) of the *Xba*I-digested genomic DNA were added to 450 µl of the ligation reaction mix along with 2 units of T4 DNA ligase (BRL). Ligations were performed at 15°C for 48 hr. then placed at 65°C for 20-min to inactivate the enzyme. A spin vacuum was then used for 1.5-hr to reduce the volume of the sample from 500 µl to 50 µl. Ammonium acetate (NH₄OAc) was added to a final concentration of 340 mM along with three volumes of 100% ethanol, to precipitate the DNA overnight at -20°C. After centrifugation at 14000 rpm for 30 min, the pellet was washed with 70% ethanol, allowed to dry at RT, and then resuspended in 100 µl of distilled H₂O overnight at 4°C. The DNA was again precipitated with 10 µl 3M potassium acetate (KOAc) and 300 µl of isopropanol overnight at 20°C. Following centrifugation at 14000 rpm for 20-min, the pellet was washed three times with 70% ethanol, then resuspended in 7 µl of MilliQ-H₂O overnight at 4°C. The DNA solution was then stored at -20°C.

c. Competent Cells.

The preparation of competent cells for electroporation was carried out according to the instructions for the electroporation protocol for *E. coli* DH5alpha that were provided by the manufacturer of the ElectroCell Manipulator 600TM. Competent cells for electroporation were made by inoculating 1 L of L-Broth (10 g Bacto tryptone, 5 g bacto yeast extract, and 5 g NaCl per liter) with 2 ml of an overnight culture of PMC103. The culture was incubated at 37°C while shaking until an OD₆₀₀ reading of 0.5-1.0 (about 10¹⁰ cells/ml) was obtained. The culture was then placed on ice for 30 min, then divided into four equal volumes of 250 ml in containers and centrifuged at 1000 rpm, and resuspended and washed in ice-cold deionized H₂O. Cells were centrifuged and washed five times, resuspended in DMSO at 1/350 dilution, and stored at -70°C.

d. Transformation.

Electroporation was used to transform the ligated DNA into competent cells. Three ng/µl of ligated DNA was added to 40 µl of competent cells in a BTX Disposable Cuvette (3mm) and chilled on ice. The cuvette was then placed into the electroporater and exposed to an exponential pulse of 2.45

kV for 5.5 milliseconds. The cuvette was immediately removed and 1 ml of SOC was added. To allow the cells to recover, the mixture was then transferred to a 10 ml polypropylene tube and allowed to incubate for 1 hr at 37°C while shaking at 225 rpm. Approximately 250 µl of the mixture was then plated onto each of four LB plates supplemented with kanamycin (70 µg/ml) and incubated at 37°C for 12-to 16-hr to allow for the selection of plasmids containing the genomic flanking sequence, the kanamycin resistance marker, and the origin of replication.

e. Plasmid minipreps.

Colonies that grew were amplified in overnight cultures in LB kan broth at 37°C while shaking at 500 rpm. Plasmid DNA was then isolated as described above. The DNA samples were then digested with the enzymes *Xba*I and *Hind*III and the products were electrophoresed on an 0.8% agarose gel to determine the sizes of the ligated product and the genomic insert.

II-8vi. Subcloning of rescued genomic DNA fragment into pBS-KS+ plasmid.

a. Ligations.

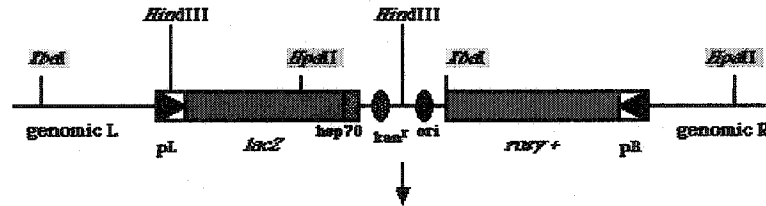
To excise the genomic sequence that flanked the left side of the P-element insert, the rescued plasmid was digested with *Hind*III, then gel purified (see **Figure 21**). The genomic fragment was then subcloned into a *Hind*III cut, dephosphorylated Bluescript II KS+ (Stratagene Cloning System) plasmid sequencing vector according to Sambrook et al. (1989), with some modifications. The ligation mix consisted of 10X T4 DNA Ligase Buffer (300 mM Tris-HCl, pH 7.5, 100 mM MgCl₂, 100 mM DTT, 10 mM ATP) diluted to 1X concentration, 60 ng Bluescript-KS+ *Hind*III cloning vector, 20 ng *Hind*III cut DNA fragment, and T4 DNA ligase (2U) in MilliQ-H₂O for a total volume of 30 µl. Ligation reactions were left overnight at 15°C, then stopped the next day by heating at 75°C for 10-min.

b. Transformations.

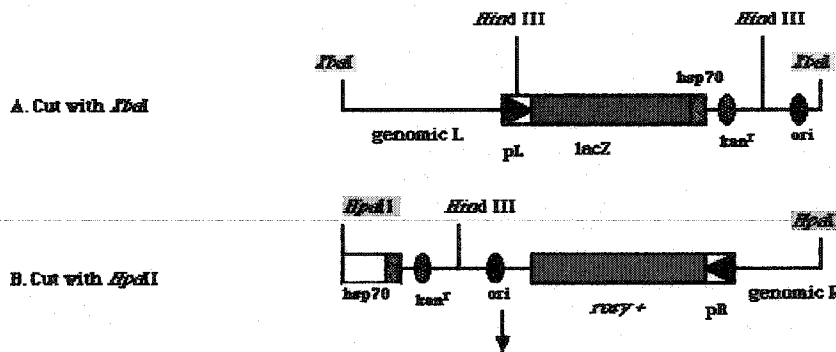
Ten µl of the ligation reaction was then used to transform electroporation-competent XL-1 blue cells prepared according to the Electroporation Manipulator 600TM electroporation protocol. Transformed cells were then plated on LB-agar/ampicillin/IPTG plates and incubated overnight at 37°C. Positive (white) colonies were then amplified in an overnight culture of LB-broth and ampicillin. A fresh cell culture was then used to carry out, using Qiagen resin columns, a medium-scale plasmid preparation according to the QiagenTM plasmid handbook (1995). The template was then prepared for sequencing. Sequencing of the 1.5 kb genomic fragment was performed in both directions using T3 and T7 primers (supplied by Stratagene) and subsequently with internal primers. The design of internal primers (see primer list in **Table 5**) and sequencing were carried out at the automated sequencing facility at the Biological Sciences Department, University of Alberta.

Figure 21. Plasmid rescue of left and right genomic flanking sequence from the *A64* PZ insertion line.

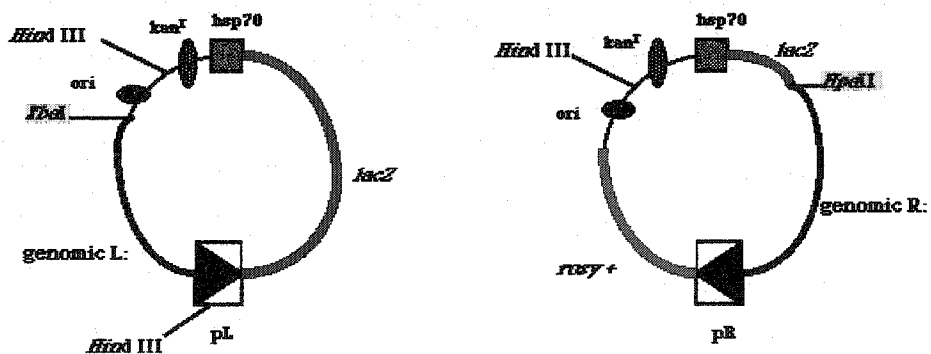
1. Isolation of genomic DNA from adult flies.



2. Restriction digest of genomic DNA to isolate the left and right arms of the plasmid with flanking genomic DNA.



3. Ligations: formation of plasmids containing the left or right genomic flanks with a “kan^r” gene and an “ori” site.



4. Plasmids are transformed into PMC103 cells, and transformants are selected on kanamycin supplemented plates.

II-9. Molecular cloning of *Drosophila* UDP glucose-dehydrogenase.

II-9i. Plating and screening of a *Drosophila lambda gt10* embryonic cDNA library.

A total of approximately 100,000 plaque-forming units from a *lambda gt10* embryonic cDNA library were plated over ten large LB + 10 mM MgSO₄ + 0.2% maltose agar plates for the primary screen. The cDNA library, which was provided by T. Kornberg (1981), consisted of cDNA isolated from 3- to 12-hr and 12- to 24-hr embryos (Huynh et al., 1985). The plating cells were strain Q358 grown in LB broth + 0.2% maltose. The top agarose consisted of 0.7% agarose, 20 mM MgSO₄, and 0.2% maltose. Large-scale phage preparation, preparation of plates, plating of cells, preparation of storage medium for phage, phage titring, and plaque isolation were performed according to Sambrook et al. (1989). Plaque lifts were performed using HybondTM-N nylon membranes (Amersham LIFE SCIENCE). Processing of the membranes and hybridizations using P³²-labeled probe were carried out in a Tyler hybridization oven according to the manufacturer's manual supplied with the membranes. After hybridization and washing, the membrane filters were allowed to air dry and were then exposed to Kodak X-ray film for 24-hr at -70°C. After positive plaques were identified by aligning the film on top of the agar plate from which the plaque had been lifted, a plug was picked up with the wide end of a Pasteur pipette, transferred to storage medium (Sambrook et al., 1989), and used for the next round of screening. The secondary and tertiary screens were performed as above until a single positive plaque was isolated.

II-9ii. Isolation of cDNAs from *lambda gt10* positive clones.

Large-scale phage particle isolation and lambda DNA purification of *lambda gt10* positives clones were performed according to WizardTM Lambda Preps DNA Purification System from Promega (© 1993).

II-9iii. Subcloning and sequencing of UDP-GlcDH *Drosophila* cDNA.

Purified *lambda gt10* DNA was digested with *EcoRI* to release the cDNA insert from the *lambda*-*da* vector. The *EcoRI* cDNA fragment was isolated from a 0.8% agarose gel and purified using a GlassmaxTM kit from BRL according to the manufacturer's specification. The *EcoRI* cDNA fragments were then subcloned into a BluescriptII KS+ (*EcoRI*-cut, dephosphorylated) sequencing vector (Stratagene Cloning Systems) according to Sambrook et al. (1989). Plasmids were transformed into XL1 Blue electrocompetent cells according to the Electroculture ManipulatorTM 600 electroporation protocol. Medium-scale plasmid preparations were performed using the QiagenTM plasmid midi prep kit for template preparation for sequencing of cDNA. Sequencing was performed, and primers (see Table 5) were synthesized by the automated sequencing facility at the Biological Sciences Department of the University of Alberta.

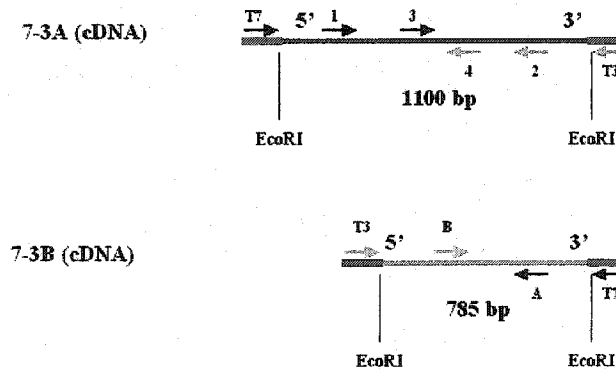
Table 5.

List of primers used to sequence the 7-3 *lambda* *gt10* cDNA clone.

A

Primer	Primer sequence
T7	5'GTAATACGACTCACTATAGGGC 3'
T3	5'AATTAACCCTCACTAAAGGG 3'
7-3A (1)	5'GACCTGCTAAATGCGGATCGT 3'
7-3A (2)	5' TTCTGGTACTCATTATGTCGAT 3'
7-3A (3)	5' CATACTCAGGACGAACACGTGGAGC 3'
7-3A (4)	5' GTAGGCGGCCACCTCGGGCAGATTG 3'
7-3B (A)	5' AACGAATAACTATAAGTTGTGGGA 3'
7-3B (B)	5'ACACCGCTATTCGTGCCTCGATTG3'

B



(A) List of DNA primers that were synthesized by the automated sequencing facility at the Department of Biological Sciences, University of Alberta. (B) A schematic diagram that shows the relative position of each primer that was used to sequence the cDNA clones 7-3A (1100 bp) and 7-3B (785 bp).

III. RESULTS

III-1. Identifying genes involved in imaginal disc patterning.

III-1i. LacZ misexpression screen of lethal PZ insertions.

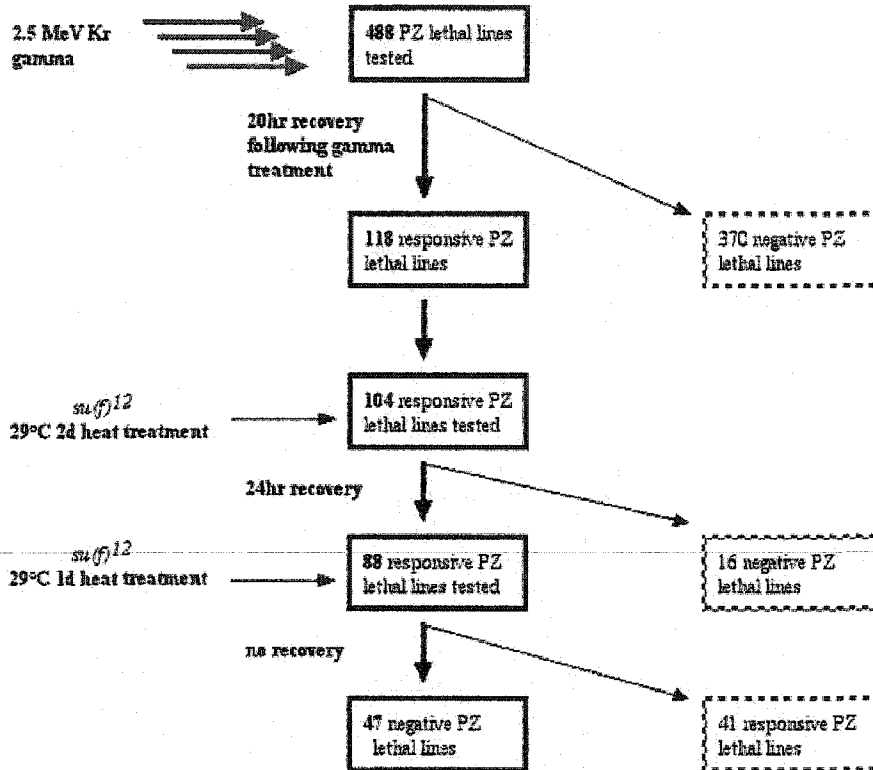
In an earlier study by Brook et al. (1993) over 800 independent autosomal $P\{lacZ\ ry^+ = PZ\}$ enhancer-trap lines were generated and screened for changes in *lacZ* expression during disc patterning regulation initiated by cell death. The temperature-sensitive (ts) cell lethal *suppressor of forked* (*su(f)¹²*) mutation was used to induce cell death in a fraction of disc cells and thus initiate disc repatterning. Differential *lacZ* expression during pattern respecification was observed in approximately 5% of all insertion lines tested. The number enhancer-trap lines that may represent genes required for the process of pattern respecification was not clear because the majority of the insertions that showed differential expression during pattern respecification were homozygous viable (a non-lethal PZ insertion). For this reason, a similar screen (Russell et al., 1998) was applied to another collection of PZ insertion lines that had been preselected for a lethal phenotype (Berkeley *Drosophila* Genome Project, Spradling et al., 1995; Flybase 2001; <http://www.flybase.com>).

The criteria used for selection was essentially as described in the previous study by Brook et al. (1993), in which the insertion lines were first screened for *lacZ* misexpression during recovery from cell death induced pattern regulation in the *su(f)¹²* cell lethal mutant. Each PZ-insertion line was then rescreened for *lacZ* misexpression using gamma radiation (2.5MeV) to induce cell death and pattern regulation, in order to eliminate lines reporting *su(f)¹²*-induced transcription unrelated to cell death and pattern respecification. This last screen proved to be the most stringent, eliminating approximately 80% of the lines retained to that point. Therefore, in the new screen of the lethal PZ insertion lines, the gamma treatment was first applied (see Table 6A Russell et al., 1998). A total of 488 PZ-lethal insertions were initially tested by gamma treatment. A longer recovery period after gamma irradiation was also used to avoid early expression that might be associated with cell death rather than the subsequent repatterning process. The 118 PZ-lethal lines that showed differential *lacZ* misexpression upon gamma treatment were then tested in a *su(f)¹²* mutant background for differential misexpression of *lacZ* during pattern respecification following a 24 hr recovery period. The 88 positives from this first *su(f)¹²* treatment were then put through a second *su(f)¹²* mutant screen. The PZ lines that showed *lacZ* activation soon after *su(f)¹²* heat treatment, with no recovery period allowed, were assumed to be directly responding to cell death initially induced by the *su(f)¹²* mutant. A total of 41 PZ-lethal lines showed this early response to *su(f)¹²* treatment, and were eliminated. The remaining 47 PZ-lethal lines, that showed *lacZ* activation, were retained as potential pattern respecification genes according to the criteria described in Table 6B (Russell et al., 1998). The expression pattern profile of these positive lines, in untreated and treated imaginal discs, was similar to those observed in the first screen by Brook et al. (1993). Differential expression ranged from general misexpression of *lacZ* in all imaginal discs, to restricted ectopic misexpression in specific regions of the disc. Sixty-four percent of the insertions

TABLE 6.

Selection of PZ lethal lines showing differential expression during pattern respecification.

A. Screening process for detecting regeneration response genes.



B. The resulting 47 lines that met all three criteria for enhancer traps detecting regeneration genes as described in the flow chart above.

Lethal insertions on chromosome 2 (1[2]):

P866, 1(2)0222; P936, 1(2)0255; P984, 1(2)01094; P1063, 1(2)01501; P1101, 1(2)01857; P1360, 1(2)03972; P1377, 1(2)04454; P1379, 1(2)04524; P1384, 1(2)04643; P1386, 1(2)04738; P1451, 1(2)05836; P1485, 1(2)06082; P2335, 1(2)07103; P2348, 1(2)08814.

Lethal insertions on chromosome 3 (1[3]):

P1491, 1(3)00274; P1510, 1(3)00945; P1522, 1(3)01152; P1523, 1(3)01164; P1524, 1(3)01207; P1529, 1(3)01319; P1530, 1(3)01344; P1532, 1(3)01436; P1533, 1(3)01453; P1536, 1(3)01470; P1542, 1(3)01658; P1543, 1(3)01673; P1555, 1(3)02102; P1563, 1(3)02281; P1565, 1(3)02331; P1582, 1(3)03076; P1586, 1(3)03346; P1595, 1(3)03539; P1609, 1(3)03834; P1615, 1(3)03928; P1623, 1(3)04091; P1630, 1(3)04449; P1633, 1(3)04556; P1642, 1(3)05014; P1669, 1(3)03712; P1671, 1(3)05820; P1686, 1(3)04490; P1765, 1(3)06924; P1711, 1(3)07013; P1715, 1(3)07117; P1717, 1(3)07172; P1721, 1(3)07351; P1737, 1(3)08645.

(A) Depicts the criteria used for selecting PZ-lethal lines from Spradling et al. (1995), in the *su(f)¹²* regeneration enhancer trap screen in imaginal discs as described by Russell et al. (1998).
 (B) The resulting 47 PZ-lethal lines that were selected as potential pattern respecification reporters.

selected as positive in the screen normally showed patterned *lacZ* expression in imaginal discs as opposed to only 13% in unselected lines, indicating a selection for genes with restricted expression patterns. This included annular or distal expression in the leg, wing pouch, wing margin, A/P compartment boundary, furrow and post-furrow expression in the eye disc, and patchy patterns in the wing and leg discs. These restricted expression patterns may indicate a role in a specific pattern formation process. However, 10% of the selected positive lines showed no detectable expression in the control discs. Most of the remaining selected lines showed general expression in control discs and increased levels of expression during regeneration, implying transcriptional up-regulation of genes during pattern regulation.

III-1ii. PZ-lethal insertion lines selected for further analysis based on a lethal embryonic mutant phenotype.

It was assumed that the *PZ* enhancer-trap screen identified putative genes expressed during pattern regulation based on the altered expression of the *lacZ* reporter gene. However, the functional relevance of this misexpression is not known. A lethal phenotype due to the insertion of the P-element indicates possibly that a gene (or genes) with some vital function has been identified. To identify genes required specifically for pattern formation, I decided to focus on the *PZ* insertions with lethal embryonic effects. Many genes with roles in embryonic patterning and segmentation are to be also crucial in imaginal disc pattern formation (see Introduction). For example, about 25% of the *PZ*-lethal lines that we scored as positive in the regeneration screen (Russell et al., 1998), also behave as maternal-effect mutants on embryonic patterning (Perrimon et al., 1996). A phenotype in the embryo may strengthen the chances of finding a gene with a role in imaginal disc patterning. Therefore, the 70 positive *PZ*-lethal insertion lines generated from Brook et al. (1993) (Table 7) along with 47 selected in the screen of the Spradling *PZ*-lethal insertion lines (Russell et al, 1998) (Table 6B), were examined for specific zygotic lethal effects on embryonic patterning. Insertion lines that are embryonically lethal

TABLE 7

PZ lethal insertion lines isolated from the regeneration screen (Brook et al., 1993) selected for analysis of embryonic cuticle phenotype.

A08, A11, A14, A34, A40, A44, A46, A56, A64, A72, B04, B28, B45, B56, B76, B82, B93, B98, C00, C08, C64, C82, C92, D09, D17, D23, D39, D42, D43, D46, D90, D96, E16, E20, E34, E43, E46, E48, E49, E55, E58, E59, E64, E97, F09, F22, F35, F45, F47, F62, F75, F89, F90, F91, G04, G11, G12, G15, G17, G19, G37, G62, G67, G69, G76, H04, H08, H35, H87, H21

PZ-lethal lines selected from the regeneration enhancer trap screen by Brook et al. (1993) for the analysis of the cuticle pattern of the embryonic zygotic lethal phenotype.

as homozygotes were identified by out-crossing each insertion line to *Oregon-R* (wild-type) flies to replace the balancer with a wild-type chromosome. Non-balancer F1 adult male and female sibs were then crossed to each other. Embryos from the cross were collected for a 12 hr period at 25°C, and permitted to develop for an additional 48 hr at 25°C. Of the 117 *PZ*-lethal lines tested, 98 lines displayed an embryonic lethal phase, possibly caused by the *PZ* insertion. The remaining 19 lines were lethal during later stages (larval or pupal), but the exact stage of death was not determined. To assess the embryonic lethal phenotypes, cuticle preparations were made from the dead embryos in each cross. Of the 98 embryonic lethal lines, 71 showed informative embryonic pattern defects. The remaining 27 lines showed no visible cuticle defects. **Table 8** catalogues the cuticle phenotypes that were observed, along with an example of a *PZ*-lethal line for each phenotypic category, and the number of *PZ* lines that showed similar phenotypes. The most commonly observed phenotypes was pair-rule segmentation defects, resulting in loss of alternate denticle belts, or fusion of adjacent denticle belts. Other frequently observed phenotypes included U-shaped embryos that had not completed germband retraction, or embryos that did not undergo dorsal closure, resulting in holes in the dorsal part of the cuticle. Typically, these phenotypes are an indication of defects in gastrulation or dorsal-ventral patterning. Thus, these lethal embryonic phenotypes allowed me to tentatively identify lines that might be defective for specific genetic pathways required in *Drosophila* embryogenesis. For example, the lines *A64*, *H87*, *P936*, and *P1386* all showed specific dorsal-ventral patterning defects typical of mutants observed from the *dpp* signaling pathway. Two of these lines carried insertion mutants in genes previously identified as nuclear targets of the *dpp* pathway, *schnurri* (*P1386*, Arora et al., 1995) and *short-sighted* (*P936*, Treisman et al., 1995). These results were of interest because *dpp* function is also required for imaginal disc primordium formation in the embryo, and later in imaginal disc pattern formation (see Introduction). Thus, 61% (71 of 117 of the positives) of the selected *PZ*-lethal lines from the disc regeneration screens may identify genes that also have a role in embryonic pattern formation, and might represent genes whose functions are co-opted for imaginal disc patterning. One of the goals of this study is to characterize the *PZ*-lethal lines from the regeneration screen using information from the embryo.

III-III. *A64*, the *PZ*-lethal insertion line selected for further analysis.

The *PZ*-lethal line selected for further analysis was *A64* based on two criteria. First, *A64* was scored as a positive in the enhancer-trap regeneration screen (see Brook et al., 1993). In *A64*, *lacZ* expression is activated at an early stage during pattern respecification induced by the *su(f)¹²* cell death mutant. Approximately 6 hr after heat treatment in a *su(f)¹²* mutant background, *lacZ* misexpression is observed in leg discs. It was hypothesized that this early activation of *lacZ* expression might indicate a gene that is activated for the initial respecification of cell fates required primarily for regeneration, rather than the later events which might be involved in the elaboration of normal disc pattern. Second, although the activation of *lacZ* misexpression during regeneration provides no direct evidence that *A64* has an important function during regeneration, the zygotic mutant phenotype in *A64* homozygous embryos suggests that it might play a role in regulating *dpp* signaling during embryogenesis. Since

Table 8.

Zygotic embryonic mutant phenotypes of PZ-lethals from the regeneration screen.

Cuticle phenotype	Representative PZ-lines showing cuticle phenotype	Gene	No. of PZ (<i>lacZ</i> , η) lethal insertion lines
gap-like segmentation defects	<i>H21</i>	unknown	4
pair-rule segmentation defects	<i>D42</i>	unknown	5
segment-polarity segmentation defects	<i>P1711</i>	unknown	5
incomplete germband retraction and segmentation defects	<i>E20</i>	unknown	14
incomplete germband retraction	<i>H87</i>	unknown	12
incomplete germband retraction and dorsal closure (dorsal open defect)	<i>A64</i>	<i>sugarless</i> this study	7
incomplete dorsal closure (dorsal open defect)	<i>P1386</i>	<i>schuuri</i>	6
ventralized cuticle	<i>P936</i>	<i>shorsighted</i>	3
head and tail defects	<i>E16</i>	unknown	11
necrotic mass in embryos	<i>P1595</i>	unknown	4
no visible cuticle pattern defects	<i>G15</i>	unknown	27
larval and pupal lethals	<i>P1533</i>	unknown	19

Categorization of embryonic cuticle pattern defects in PZ-lethal insertion lines isolated from the imaginal disc regeneration screens of Brook et al. (1993) and Russell et al. (1998). Given is a example of a PZ line that exhibits the cuticle pattern defects, along with the gene if known, and the number of PZ lines associated with a specific cuticle defect.

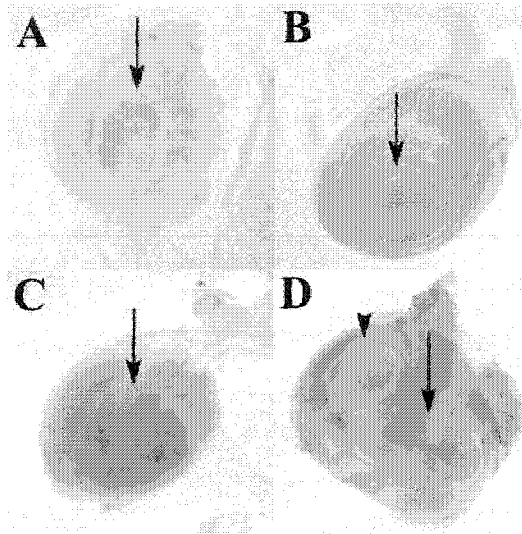
dpp has been shown to play a critical role in disc patterning, this suggests that the *A64* PZ insert may have uncovered a role for *dpp* in imaginal disc regeneration in *Drosophila*.

a. Characterization of *A64 lacZ* expression in regenerating leg discs in a *su(f)¹²* background .

Figure 22 shows the misexpression of *lacZ* of *A64* in regenerating second thoracic(T2) leg discs following heat treatment in the *su(f)¹²* mutant. *A64/+* male flies were crossed with homozygous *su(f)¹²* females at room temperature. Following a 2h egg collection, the progeny were allowed to develop for 60 hr at 25°C until mid-second instar. Larvae were shifted to 29°C for 48 hr to induce cell death in imaginal discs, then shifted back to 25°C and allowed to recover. During the recovery period *lacZ* expression in the imaginal leg disc was monitored at various time points following heat treatment. General ectopic activation of *lacZ* was first detected in regenerating imaginal leg discs at 6 hr after heat treatment (**Figure 22C**) confirming the initial characterization of *A64* (Brook et al., 1993). *LacZ* expression in non-heat-treated *su(f)¹²; A64/+* control discs that were at similar developmental stages are shown in **Figure 22A** and **B**. Heat treatment in a *su(f)¹²* background, which induces cell death, typically retards normal development (growth and cell division) of discs. Thus, discs at 6 hr following heat treatment, looked similar to mid-second instar discs (compare panel **A** and **C** in **Figure 22**). For example, at 6 hr after heat treatment, the imaginal leg disc shows a single concentric fold in the center of the disc (**arrow, Figure 22C**) - similar to what is observed in mid-second instar leg discs (see **arrow, Figure 22A**). Mid-second instar leg discs from non-heat-treated *su(f)¹²; A64/+* lines show low uniform levels of *lacZ* expression (**Figure 22A**). Mid-third instar discs from similar controls show again low uniform levels of *lacZ* expression (**Figure 22B**). In heat treated *su(f)¹²; A64/+* larvae, the leg discs showed elevated levels of uniform *lacZ* expression at 6 hr (**Figure 22C**), followed by patchy expression at 48 hr (**Figure 22D**) after heat treatment. In addition, a second distal axis (duplicate) has started to form at 48 hr, as indicated by the presence of a second distal endknob (see arrowhead, **Figure 22D**). In controls, with leg discs from *A64* PZ larvae in a background wild-type for *su(f)¹²*, no ectopic activation of *lacZ* expression was detected after a similar heat treatment (not shown). According to these results, *A64* generates ectopic misexpression before any morphological changes are detectable in the disc (such as outgrowths). This suggests that *A64* could represent a gene required for the initial events required in axis respecification during regeneration and duplication of imaginal discs. Such a gene may be involved in wound healing and the initiation of the regeneration blastema, or the respecification of compartmental restrictions, events that occur prior to any duplicate forming.

To further determine if *A64* identifies a gene, consistent with its involvement in the early regeneration response, cultured imaginal leg disc fragments were analyzed for the altered expression of *lacZ*. Disc fragments cultured *in vivo* undergo wound healing, which involves fusion of cut edges. This process is then followed by blastema formation, represented by proliferation of cells adjacent to the wound heal, and then growth and pattern respecification (see Introduction). T2 leg discs were dissected from mature late third instar *A64* larvae, fragmented as shown in **Figure 23A**, and the resulting 3/4L+EK disc fragments implanted into the abdomen of *Oregon-R* female hosts. This environment

Figure 22. Expression of *lacZ* in leg discs following 29°C heat treatment of *su(f)¹²; A64PZ/+* mutant larvae.



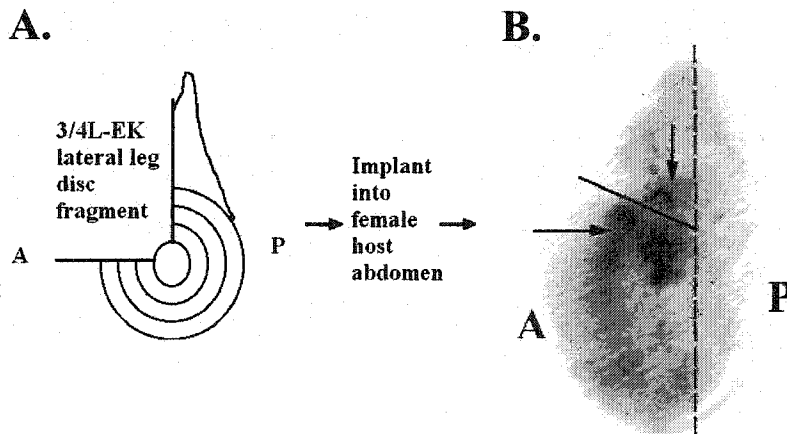
Controls (A) and (B) are non-heat treated *su(f)¹²; A64 PZ/+* imaginal leg discs. (C) and (D) depict heat treated *su(f)¹²; A64 PZ/+* experimental leg discs. *A64-lacZ* expression in (A) second and (B) third larval instar imaginal leg discs show very weak uniform *lacZ* expression. (C) *A64-lacZ* expression at 6 hr after heat-treatment is elevated, but remains uniform. (D) At 48 hr after heat-treatment a duplicate starts to form, indicated by a second distal endknob (see black arrowhead), and increased levels of *lacZ* expression become patchy. In all panels in the figure, the black arrow marks the position of the original distal endknob in the imaginal leg disc. The distal endknob represents the presumptive most distal segment of the adult leg.

Figure 23. *A64* A. *PZ* expression in an 3/4L+EK leg disc fragment

(A) Diagram of the 3/4L+EK fragment from a *A64 PZ T2* leg disc that was implanted into the female host abdomen.

(B) The T2 leg disc were dissected from the abdomen 24 hr after

implantation and stained for *lacZ* expression. *LacZ* expression is elevated in the anterior compartment, with higher levels of expression localized in cells on both sides of the wound heal (see black arrows) where the cut edges have fused (fusion indicated by the solid black line). The dashed black line marks the approximate A/P compartment boundary (A, anterior compartment; P, posterior compartment)



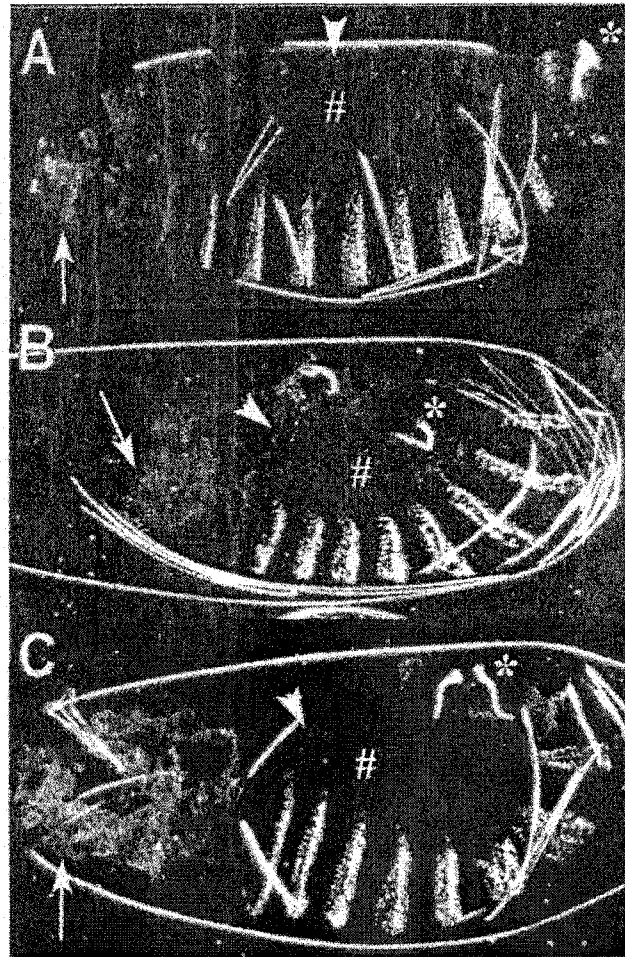
permits healing and subsequent pattern respecification of the disc fragment (Schubiger, 1971). Approximately 24 hr after implantation, allowing sufficient time for cut edges to fuse and form a wound heal (**Figure 23B**, see black line), the discs were recovered and stained for *lacZ* expression. Elevated levels of uniform *lacZ* expression were detected in the anterior compartment of the leg discs, with increased levels of expression in cells on both sides of the wound heal (the site of origin for cells of the regeneration blastema, where pattern respecification and axis duplication initiates (**Figure 23B**, see arrows). Leg discs that were cut but not implanted into the female abdomen, showed no alteration in the uniform levels of *lacZ* expression (not shown). Whole legs discs that were uncut and implanted into the female abdomen, and recovered and stained after 24 hr following implantation, showed no detectable changes in *lacZ* expression, when compared to fragmented discs (as in **Figure 22B**). Similar fragments (3/4L+EK) from the *dpp-lacZ* lines were used as a positive control for the misexpression of *lacZ*. *P1599*, a *PZ* line that did not respond in the gamma and *su(f)*¹² treatments in the screen, was used as a negative control in the disc culture analysis. Fragments (3/4L+EK) from *P1599* showed no ectopic misexpression of *lacZ*. This suggests that the *A64 PZ* insert may represent a gene that is required for events at wound healing that precede growth, such as the initiation of the regeneration blastema (distal organizer).

b. Characterization of the embryonic lethal phenotype of *A64*.

In a cross between *PZ A64/+* males and females, approximately 17% of the fertilized embryos, failed to hatch, turned brown and died. The predicted one quarter of dead embryos (based on Mendelian random segregation of chromosomes) was not observed. This suggested that the embryonic lethality caused by this mutation was not fully penetrant. These embryos, presumably homozygous for the *A64 PZ*-lethal insertion, were analyzed for cuticular patterning defects. The *A64* lethal phenotype showed embryos that fail to undergo complete germband retraction indicated by the dorsal medial position of the posterior spiracles (see * in **Figure 24B**) that is normally located at the posterior most end of the larva (see * in **Figure 24A**). Cuticles also showed a loss of dorsal and dorsal lateral cuticle (see #, compare **Figure 24A and 24B**). Because of the loss of dorsal tissue, these embryos were also unable to undergo dorsal closure, resulting in holes in the dorsal cuticle (arrowhead - compare **Figure 24A and Figure 24B**). Loss of dorsal tissue may contribute to incomplete germband retraction effects, resulting in the characteristic U-shaped embryos. In addition, embryos showed strong dorsal head defects, which result in loss of anterior head structures in the larva (see white arrow, compare **Figure 24A and Figure 24B**). These cuticle phenotypes are reminiscent of embryonic lethal phenotypes demonstrated by partial loss-of-function mutant effects of *dpp*, and its receptors, *thickveins* (*thv*) and *punt* (*pnt*). Embryos heterozygous for the haplo-insufficient mutant allele *dpp*^{H46/+} (**Figure 24C**), typically result in U-shaped embryos with a hole in the dorsal cuticle, as well as head defects, both of which are seen in *A64* homozygous embryos.

To further assess the role of *A64* in the embryo, *lacZ* expression pattern in staged *A64/+* embryos was examined (**Figure 25**). Initially, *lacZ* expression is detected in dorsal extraembryonic

Figure 24. *A64 PZ*-lethal zygotic embryonic mutant phenotype.



(A) A cuticle preparation of an unhatched 1st larval instar from a wild-type embryo. (B) Cuticle preparation of a dead 1st larval instar from the *A64 PZ*-lethal insertion line. The *A64 PZ* embryos show a failure of the germband to retract, which is indicated by the dorsal position of the posterior spiracles (*), along with a loss of anterior head segments (arrow) and dorsal cuticle (arrowhead). (C) A cuticle preparation of a 1st larval instar from a *dpp^{H46/+}* heterozygous embryo, shows anterior head defects and a dorsal open cuticle phenotype along with incomplete germband retraction. (white arrow = anterior head segment, white arrowhead = dorsal cuticle, * = posterior spiracles, # = dorsal lateral cuticle region). In all figures, anterior is to the left, and dorsal is up.

cells, the amnioserosa (as) during germband extension at around stage 9 of embryogenesis. Light expression also extends to the dorsal anterior side of the procephalon (pro) in head (**Figure 25A**). This expression is maintained in the amnioserosa during germband retraction (stages 11 and 12) (red arrow, **Figure 25B**). However, during this stage *lacZ* expression is also activated in the rudimentary head segments, such as: the hypopharyngeal (hy), mandible (md), labium (lb), and maxilla (mx) and intensifies in the procephalon (pro). In addition, expression is also detected in the most dorsal ectodermal cells that abut the amnioserosa (dorsal ectodermal ridge cells, arrow **Figure 25B**), and in a cluster of cells in the underlying mesoderm of each parasegment (possibly the pericardial cells, arrowheads, **Figure 25B**). In germband-retracted embryos (stage 13) (**Figure 25C**) expression in the ectoderm and mesodermal cells fades, but is maintained in the head (arrow) and amnioserosa (as). During dorsal closure (stage 15), the dorsal lateral and ectodermal ridge cells on both sides of the embryo migrate dorsally and fuse along the dorsal midline (dm) (**Figure 25D**). At this stage *lacZ* expression remains in the head segments and is strongly activated in cells of the ectodermal dorsal ridge. This *lacZ* expression pattern in the embryo described for the *A64 PZ* insertion line is consistent with head and dorsal cuticle defects observed in *A64* homozygous mutant embryos. Cells of the amnioserosa, dorsal ectoderm and mesoderm all require *dpp* function during normal development. It is well known that the formation of the pericardial cells in the dorsal mesoderm requires *dpp* signaling from the overlying ectodermal cells along the dorsal ridge (Frasch, 1995). Also, dorsal closure requires proper *dpp* function in cells from the dorsal ectoderm (Frasch, 1995). The *lacZ* expression pattern of *A64* appears to correlate with cells that were affected by *dpp* signaling during various stages of embryogenesis.

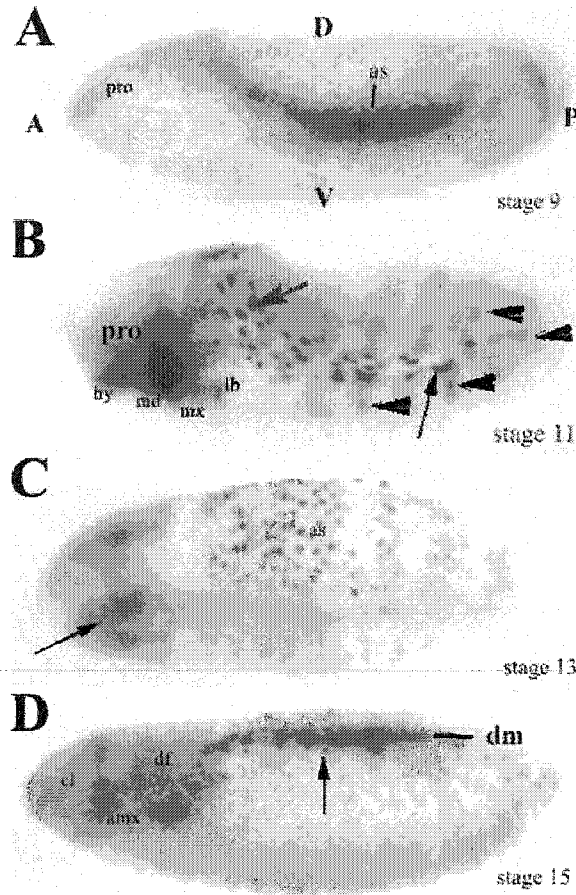
Based on the lethal embryonic phenotype and *lacZ* expression pattern, *A64* is required for embryonic dorsal patterning. The correlation between cells that express *A64 lacZ* and those cells whose behavior is regulated by *dpp* signaling, implies that *A64* may mediate *dpp* signaling. Therefore, the putative gene uncovered by the *A64 PZ* insertion may represent a novel component of the *dpp* signaling pathway. This putative gene may function directly within the *dpp* signaling cascade, or alternatively through a second signaling cascade that may indirectly modulate *dpp* signaling. This is of great interest, since very little is known about the modulation of the *dpp* signaling pathway. Since *A64* may represent a gene yet to be identified in the *dpp* pathway, I decided to molecularly characterize the *A64 P{lacZ ry+}* insertion mutant and attempt to identify the gene it represents.

III-2. Genetic analysis of the *A64* insertion.

III-2i. Segregation analysis of the *A64* insertion.

The *P{lacZ, ry+}* *A64* insertion was originally balanced with the *T(2;3)CyO-TM6, Ubx ry* chromosome. To determine the chromosome on which the insertion was located, a segregation analysis was carried out. **Figure 26** describes the crossing scheme used to map the *A64* lethality. Results of the crosses appear in **Table 9**. When *A64* was outcrossed to *Sco/CyO* or *Ly/TM3,Sb* balancer stocks, non-balancer F2 progeny were observed only in the first case. When crossed to *Ly/TM3, Sb*, all the F2

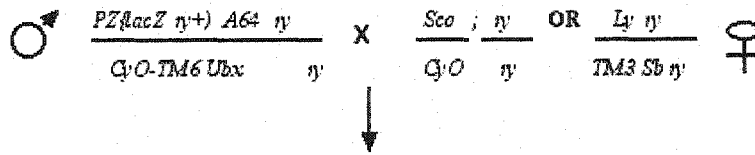
Figure 25. *LacZ* expression pattern of the *A64* PZ insertion during embryonic development.



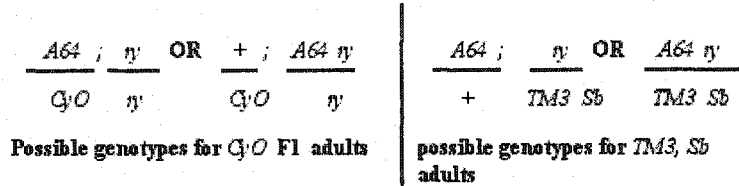
A64 PZ-insertion line stained for *lacZ* expression in *A64 lacZ*⁺ embryos. (A) Stage 9 embryo at germband extension shows *lacZ* expression in the amnioserosa (as) with light expression in the anterior or dorsal procephelon (pro). (B) At stage 11, high levels of *lacZ* expression remains in the amnioserosa (red arrow) and extends to the anterior head segments in the procephelon (pro), hypopharyngeal lobe (hy), mandible (md), maxilla (mx), and labium (lb), which mark the rudimentary first and third intercalary head segments. Light expression is also detected in dorsal ectodermal ridge cells (black arrow), and in patches of cells (possibly the pericardial cells) that extend from the dorsal ridge in the dorsal mesoderm (black arrowheads). (C) At stage 13, by the end of germband retraction, *lacZ* expression is maintained in some cells of the amnioserosa (as) and in the anterior head segments (black arrow). (D) At stage 15, dorsal closure is complete and *lacZ* expression is localized to the ectodermal dorsal ridge cells (black arrow) along the dorsal midline (dm), and in a few remaining amnioserosa cells. Expression is also maintained in the primordial head structures at the dorsal fold (df), the antennomaxillary complex (amx), and the clypeolabrum (cl). In all figures, anterior is to the left, and dorsal is up.

Figure 26. Segregation analysis of the lethal phenotype of A64.

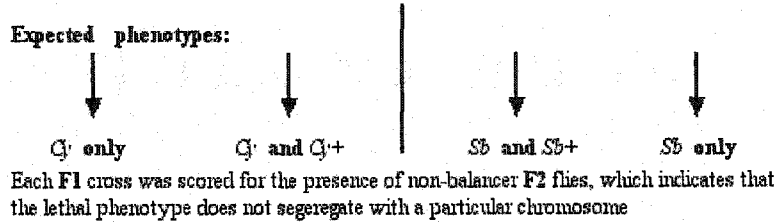
(1). Cross at 25°C



(2). Selected *CyO* or *Sb*, *Ubx+* F1 males and females:



(3). Male and female progeny from F1 were crossed:



The crossing scheme used to determine with which chromosome the lethal phenotype of *A64 PZ* segregates. (1) *A64 PZ* males were outcrossed with *Sco/CyO* or *Ly/TM3 Sb rosy+* balancer female lines. (2) *Inter se* crosses between *CyO* F1 sibling males and females that were *rosy+* were carried out. A similar cross was repeated with *TM3 rosy+* F1 male and female sibs. (3) The progeny from the F1 crosses were analyzed for the presence of non-balancer F2 flies, which indicates that the lethal phenotype does not segregate with the corresponding chromosome.

Table 9.
Segregation analysis of the *A64PZ* lethal phenotype

Parents	F2 Progeny		
	Total adults	Balancer	non-Balancer
$\frac{A64}{CyO-TM6} \times \frac{Sco}{CyO}$	456	362 <i>Cy</i>	94 <i>Cy+</i>
$\frac{A64}{CyO-TM6} \times \frac{Ly}{TM3, Sb}$	502	502 <i>Sb</i>	0 <i>Sb+</i>

Results of the segregation analysis from crosses in Figure 26. *A64 PZ* outcrossed to *Sco/CyO* resulted in F2 adults that did not carry the *CyO* balancer, whereas those outcrossed to *Ly/TM3 Sb* only gave adults that carried the *TM3 Sb* balancer.

adults carried the *TM3,Sb* balancer. This indicates that the lethal phenotype of *A64* segregates with the third chromosome.

III-2ii. Physical Mapping of the *A64 P{lacZ ry+}* insertion using polytene chromosomes.

To determine the cytological location of the *A64* insertion, polytene chromosome squash preparations were made from larvae heterozygous for the *A64 P{lacZ,ry+}* insertion, as shown in **Figure 27A**. The polytene chromosomes were then incubated with a Digoxigenin-labeled full-length *P{lacZ, ry+}* DNA probe to locate the insertion element. The probe hybridized to a band on the left arm of the third chromosome at cytological location 65D-E as shown in **Figure 27B**. No other sites of hybridization were detected. This result correlated the location of the *P{lacZ ry+}* insertion and the segregation of the lethality with the third chromosome. However, this does not prove that lethality in *A64* is due to the *P{lacZ ry+}* insertion.

III-2iii. Reversion of the *A64* embryonic lethal phenotype by excision of the *P{lacZ ry+}* insertion.

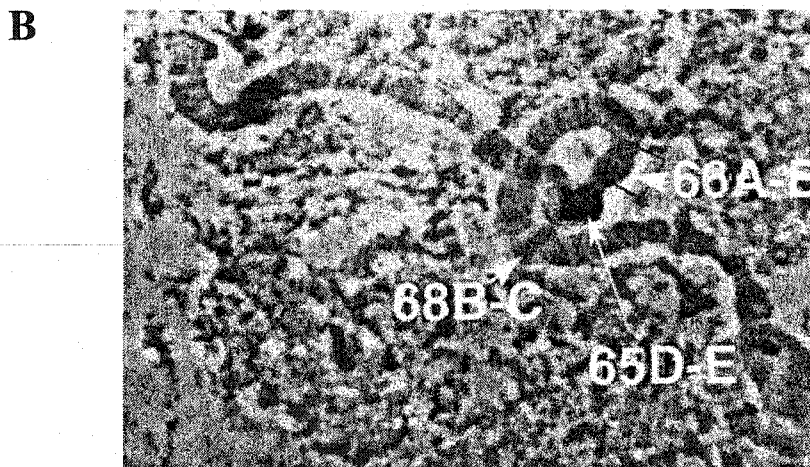
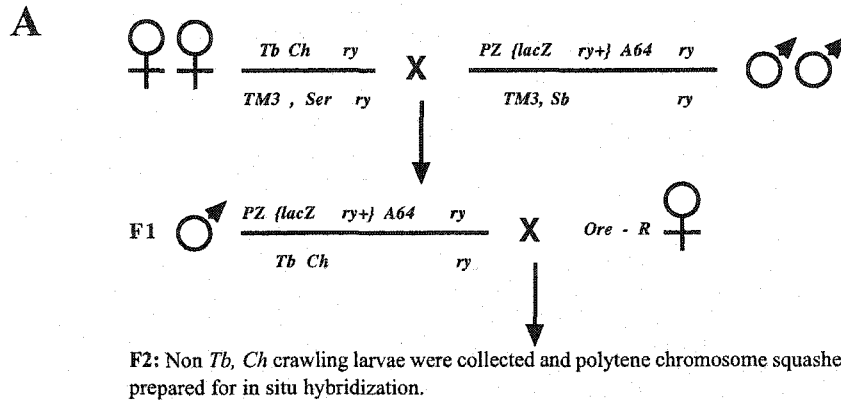
To determine whether the *A64* embryonic lethal phenotype is due to the *P{lacZ ry+}* insertion at 65D-E, an attempt was made to generate excisions of the *A64 PZ* insertion by mobilizing the P-element with a transposase source, as shown in **Figure 28A**. *P{lacZ ry+}* excisions were selected by scoring for the loss of the *ry+* marker in adult F2 males. Out of 40 chromosomes that were screened as putative excisions, 30 resulted in homozygous viable stocks (see **Figure 28B**). Presumably, these viable excision stocks were the result of the precise excision of the *P{lacZ, ry+}* element from its location on the third chromosome. It is deduced from these results that the lethality attributed to *A64* is the result of the *P{lacZ, ry+}* insertion. The remaining ten *ry* excisions resulted in embryonic lethal phenotypes all of which showed a weak *dpp*-like mutant effect, similar to the *A64* insertion line. When these lethal were crossed back to the *A64* insertion line, all failed to complement, thus demonstrating that the lethality of the *ry* derivatives and the *A64 P{lacZ ry+}* insert are caused by lesions in the same gene. Loss of the *P{lacZ ry+}* element was confirmed by looking for the presence of the *P{lacZ ry+}* element in polytene chromosome squash preparations of ten viable and ten lethal excision lines. None of the squash preparations showed labeling at 65D-E, after hybridization with the Digoxigenin-labeled full length *P{lacZ ry+}* DNA probe.

III-2iv. Genetic mapping and complementation analysis of *A64*.

Complementation analysis was conducted using overlapping deficiencies, P-element insertions and point mutations which span the cytological region between 64A1 and 66B10. This helped to refine the genetic location map of the *A64 P{lacZ, ry+}* insert within the cytological interval of 65 (see **Table 10**).

Crosses of *A64/TM3,Sb* with fly lines that carry the deficiency *Df(3L)w5.4/TM3,Sb* or

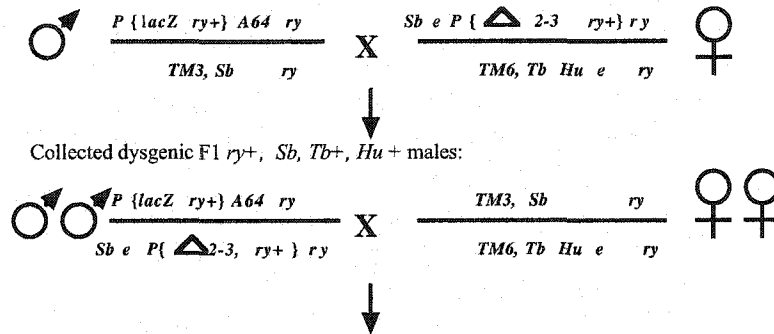
Figure 27. Cytological mapping of the PZ insert in the A64 line using polytene chromosome squashes.



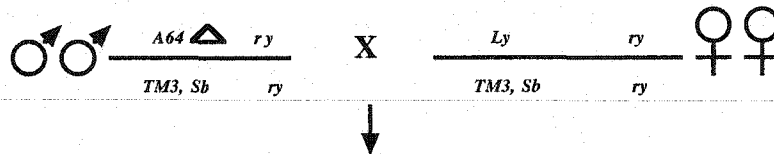
(A). The crossing scheme used to identify larvae that carried the chromosome with the *A64 PZ* insertion for polytene *in situ* analysis of the *P*-element insert. *A64 PZ/ TM3 Sb* males were crossed to *Tb Ch/ TM3 Sb* females. The mutants, *Tb* (*Tubby*) and *Ch* (*Chubby*), are dominant as larval stage markers that give rise to “fat” and “stout” larvae. F1 *Tb Ch* larvae that also contained the *A64 PZ* insert were then selected, allowed to eclose, and the adults were then crossed to *Oregon R* (*Ore-R*) females. (B). A polytene preparation of *PZ A64/+* larvae, probed with a Digoxigenin labeled *PZ* DNA probe. The probe hybridized to the cytological location, 65 D-E, indicated by the long white arrow. The cytological locations of 66A-B and 68B-C indicated by the white arrow heads were used as land marks on the polytene chromosomes to help map the *PZ* probe to its appropriate site. The *P*-element is localized to the cytological location 65 D-E on the left arm of the third chromosome (3L). The dark band at 65D-E corresponds to the blue stain produced by the Digoxigenin labeled probe. The other dark bands are a consequence of the counter stain that was used to stain the polytene chromosomes. Identification of the cytological location of the *PZ* insertion was determined by using the standard morphological map of polytene chromosomes provided in Lindsley and Zimm (1992).

Figure 28. Generation of revertants of the *A64* PZ-lethal phenotype

A. Introduction of P{ \triangle 2-3} transposase source into *A64* PZ line :



Saved *A64 ry* / *TM3 Sb ry*, F2 progeny males that have *rosy* (*ry*) eye colour and crossed individually to *Ly* / *TM3, Sb* females and stocks established from *Sb* progeny.



To check whether *ry* derivative chromosomes are caused by imprecise or precise excision of the PZ-element, each individual was subsequently checked for the presence of *Sb+* adult (precise) versus *Sb* (imprecise) adult flies.

B.

Total number of stocks scored from lines established from single <i>ry</i> F2 males.	# of viable <i>Sb+</i> (precise excisions)	# of lethal <i>Sb</i> (imprecise excisions)
40	30	10

(A). The crossing scheme used to generate *A64* PZ *ry*- excision lines to give viable revertant phenotypes. (B). Shows the number of viable (precise excision) versus lethal (imprecise excision) *A64* PZ *ry* revertants. It is inferred that imprecise excision is the result of the deletion of genomic sequences adjacent to the PZ insertion site upon the mobilization of the P-element due to improper DNA repair. *rosy* (*ry*), *Third Multiple chromosome balancer 3* (*TM3*), *Stubble* (*Sb*), *ebony* (*eb*), *Tubby* (*Tb*), *Humeral* (*Hu*), *Third Multiple chromosome balance 6* (*TM6*), *Lyra* (*Ly*).

Table 10.

Complementation Analysis of the *A64* PZ lethal insertion

Mutation	Cytological Location	Complementation with <i>A64</i> for lethal phenotype
DELETIONS		
Df(3L)CH39		(64A1-2; 65B5) YES
Df(3L)ZN47		(64C1-10; 65C1-5) YES
Df(3L)XA596		(64D1-E13; 65C1) YES
Df(3L)Vn		(64C12-D1; 65D2) YES
Df(3L)v65n		(64E1-13; 65C1-D6) YES
Df(3L)w5.4		(65A; 66A) NO
Df(3L)CH12		(65A7-9; 65C2) YES
Df(3L)XBB70		(65D1; 65D3) NO
Df(3L)Rm5.2		(65E1-12; 66B1-2) YES
Df(3L)pbl-xl		(65F3; 66B10) YES
P-ELEMENT INSERTION		
l(3)O8310) P(lacZ)P1731	65D4-5	NO
EMS INDUCED MUTATION		
C88 (pale)	65D1-3	YES
J83 (pale)	65D1-3	YES
ES2 (drifter)	65D2-3	YES
J82 (drifter)	65D2-3	YES
C76 (drifter)	65D2-3	YES
A31	65D4-66A	NO
N71	65D4-66A	NO
SG9	65D4-66A	NO
A99	65D4-66A	YES
X-RAY INDUCED MUTATION		
XAJ36	65D4; 66A	NO

Genetic mapping of the *A64* PZ-lethal insertion mutant by complementation crosses with various deficiency, EMS and X-ray induced lethal mutant lines that span the region of 64A to 66C.

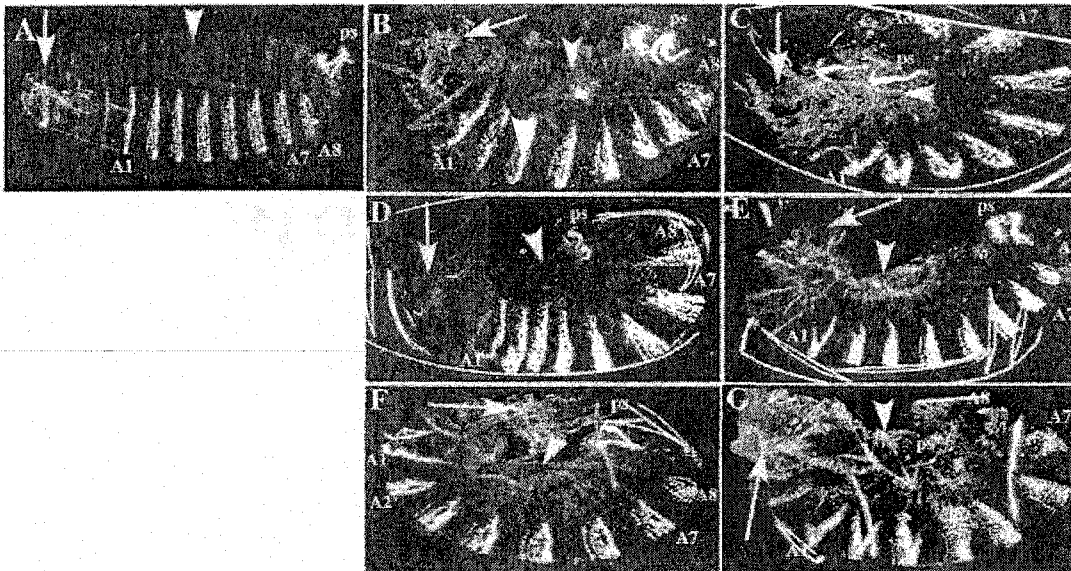
Df(3L)XBB70/TM3Sb, resulted in dead embryos. The crosses with the remaining deletions resulted in non-balancer adults, where the deletion over *A64 PZ* survived. Since *A64* complemented both *Df(3L)Vn* (64C12-65D2) and *Df(3L)Rm.5.2* (65E1-66B1), but not *Df(3L)XBB70* (65D1-65D3) or *Df(3L)w5.4* (65A-66A), the *P{lacZ ry+}* lethal insertion in *A64* must be located between 65D2 and 65E1. Several EMS and X-ray induced mutations that had been mapped within the 65D interval were crossed to *A64* in complementation tests to further refine this cytological map. The mutations *pale* and *drifter*, which are within 65D1-3, complemented *A64*. Thus, *A64* was not an allele of either of these genes. However, *A64 PZ* failed to complement four lethal mutations previously mapped to this region, *SG9*, *A31*, *N71*, and *XAJ36*, suggesting that the *P{lacZ ry+}* lethal insertion must be located between 65D4 and 65E. The *PZ* insertion *l(3)08310*^{*P1731*}, which maps to 65D4-5, also failed to complement *A64*. Therefore, six additional alleles of the gene affected by *A64* were identified, *P1731* (Bloomington stock center, Spradling et al., 1995), *Df(3L)w5.4*, *A31*, *N71*, *XAJ36* (generated in a previously reported screen by Anderson et al., 1995), and *SG9* (Shearn and Garen, 1974).

III-2v. Genetic analysis of *A64* alleles.

The *P1731* mutant *l(3)08310* has been characterized in several previous studies (Binari et al., 1997; Hacker et al., 1997; Haerry et al., 1997). These revealed a maternal-effect phenotype in non-rescued embryos from *P1731* homozygous germline, females, similar to the *wingless* loss-of-function phenotype in *wg* mutant embryos. It was shown that *P1731* disrupts a gene referred to as *sugarless* (*sgl*), which is required maternally for *wg* function in the embryo. The *sgl* gene encodes the *Drosophila* homolog of uridine diphosphate glucose dehydrogenase (Binari, et al., 1997; Hacker et al., 1997; Haerry et al., 1997) (see Discussion). The maternal-effect phenotype of *sgl*^{*P1731*} was initially identified in a screen of PZ-lethals for maternal-effect mutations (Perrimon et al., 1996), where it gave a segment polarity phenotype in the embryo. Based on the genetic complementation analysis it was concluded that the *A64* lethal mutant represented a new allele of *sgl*, which this study refers to as *sgl*^{*A64*}. Perrimon et al. (1996) reported that the zygotic lethal phase for *sgl*^{*P1731*} is observed during the second larval instar stage. In the present study, it is found that *sgl*^{*A64*} and its alleles *sgl*^{*P1731*}, *sgl*^{*A31*} and *sgl*^{*N71*} also present a zygotic lethal phase during late embryogenesis. In these lines, in which each mutant is balanced over a *TM6*, *Tb*, *Ch* balancer, the majority of the lethality occurred prior to hatching. For example, only 8% of fertilized embryos hatched to give non-*Tubby* homozygous *sgl*^{*A64*} mutant larvae, which then died by third larval instar.

In further experiments, the *TM6*, *TbCh* balancer was removed by out-crossing to *Ore-R* wild-type flies in order to control for any embryonic lethality in embryos homozygous for the balancer. *Tb*⁺, *Ch*⁺ F1 flies from this cross were mated and embryos collected. In the case of *sgl*^{*P1731*} (see Table 11B), 21% of the dead embryos showed the U-shaped cuticle defect phenotype (Figure 29C). This suggests that *P1731* may be a multiphasic embryonic and larval lethal mutation, with the lethal phase possibly influenced by genetic background or culture conditions. As shown in Table 11, similar experiments using the other alleles of *sgl* identified in this study, also resulted in dead embryos with the U-

Figure 29. Cuticle phenotype of embryos homozygous for *sgl* alleles



Cuticle phenotypes from an (A) unhatched wild-type embryo (+/+), (B) *sgl^{A64}/sgl^{A64}* and (C) *sgl^{P1731}/sgl^{P1731}* mutant embryos, embryos that are homozygous for the EMS mutant alleles of *sgl* (D) *sgl^{A31}/sgl^{A31}*, (E) *sgl^{N71}/sgl^{N71}* (F) *sgl^{A64}/Df(3L)w5.4*, and (G) *sgl^{P1731}/Df(3L)w5.4* hemizygous embryos. All mutant embryos show common phenotypic traits, which include incomplete germband retraction indicated by the dorsal positioning of the posterior spiracles (ps) and the posterior ventral denticle belts of abdominal segments 7 (A7) and 8 (A8), along with loss of anterior head segments (white arrow) and a dorsal open phenotype (arrowhead). (A1- first abdominal segment, A8 (eighth abdominal) segment, ps (posterior spiracle). In all figures, anterior is to the left, and dorsal is up.

Table 11.

Percentage of *sgl* mutant embryos that failed to hatch, that showed a U-shape phenotype

Crosses	# of fertilized embryos screened	# of embryos that failed to hatch (%)	# of unhatched embryos with U-shaped phenotypes (%)
A. <i>A64/+ X A64/+</i>	333	63 (19%)	57 (17%, c.i.= 14.0; 20.0)
B. <i>P1731/+ X P1731/+</i>	314	72 (23%)	65 (21%, c.i.= 17.8; 24.2)
C. <i>A64/+ X Df(3L)w5.4/+</i>	291	61 (21%)	58 (20%, c.i.= 16.8; 23.2)
D. <i>N71/+ X N71/+</i>	282	31 (11%)	31 (11%, c.i.= 8.5; 14.5)
E. <i>A31/+ X A31/+</i>	343	50 (14%)	44 (13%, c.i.= 10.4; 15.6)
F. <i>P1731/+ X Df(3L)w5.4/+</i>	310	74 (24%)	72 (23%, c.i.= 19.7; 26.3)
G. <i>A64/+ X P1731/+</i>	303	60 (20%)	54 (18%, c.i.= 15.0; 21.0)

To test if the differences in the frequencies of dead embryos observed with U-shaped and dorsal defects between different *sgl* mutant alleles were significant, a confidence interval (c.i.) statistical analysis was carried out (Moore and McCabe, 1993). The total number of embryos (*n*) scored for each cross, was screened for the number of dead embryos (*m*) (embryos that did not hatch) with dorsal cuticle and gastrulation defects. The frequency (*p*) of dead embryos with dorsal patterning defects in the progeny was then calculated ($p=m/n$). To determine the confidence interval (c.i.) for the true mean of the population as estimated by the proportion of successes (expressed as a percentage) in the sample of embryos that were scored for each cross the following equation used was:

$$c.i. = p \pm z \sqrt{\frac{p(1-p)}{n}}$$

where *p* is the percentage of positive scores (dead embryos with dorsal defects) in the sample embryos from each cross and *n* is the number of embryos that were scored (600) for each sample. The critical value *z* was set at 1.960 so that there was a 95% confidence level that the true population mean lies between the expressed values (Moore and McCabe, 1993). The confidence interval for the true population mean is provided for each cross.

shaped, dorsal-open phenotype. Seventeen percent of fertilized *sgl*^{A64} embryos died, resulting in a U-shaped phenotype (Table 11A, Figure 29B). The remaining dead embryos showed no noticeable patterning defect. Lower numbers of dead embryos were obtained for homozygous mutants of *sgl*^{A31} (13%) and *sgl*^{N71} (11%), suggesting that these mutants may represent hypomorphic alleles.

As reported above, homozygous lethal mutant alleles of *sgl* result in dead embryos that present a *dpp*-like zygotic phenotype. To determine if loss of dorsal cuticle and failure of germband retraction, is a loss-of-function effect, *sgl*^{A64} and *sgl*^{P1731} were examined in combination with the deficiency *Df(3L)w5.4* (see Figure 29F and G respectively). *sgl*^{P1731} and *sgl*^{A64}, in combination with *Df(3L)w5.4*, result in a higher percentage of dead embryos, with a dorsal-open and incomplete germband retraction. Therefore, the *Df(3L)w5.4* deficiency enhanced the *sgl* mutant embryonic lethal phenotype, suggesting that *sgl*^{P1731} and *sgl*^{A64} mutant phenotype was due to a loss-of-function effect. For example, 20% of dead embryos that are *sgl*^{A64}/*Df(3L)w5.4* (Table 11C), had dorsal cuticle and head defects, and were U-shaped, compared with 23% in *sgl*^{P1731}/*Df(3L)w5.4* embryos (Table 11F). These results also suggest that *sgl*^{P1731} and *sgl*^{A64} represent alleles that cause an incomplete loss of wild-type function. Thus, they may be classified as recessive hypomorphs as opposed to null mutants.

It was noted that when embryos are homozygous or hemizygous over *Df(3L)w5.4*, for *sgl*^{P1731}, this results in a higher frequency of dead embryos than that seen with homozygous mutations of *sgl*^{A64}, *sgl*^{A31} and *sgl*^{N71}. To examine the strength of each mutant allele, the penetrance and expressivity was determined based on the extent of pattern defects in dead embryos from each cross. Cuticles were prepared from fertilized embryos that failed to hatch, and the strength of the *dpp*-like mutant phenotype was scored. Embryos homozygous for *sgl*^{P1731} result in lethal embryos with the most extreme dorsal defects, suggesting that *sgl*^{P1731} may be the strongest loss-of-function allele. A comparison between typical *sgl*^{A64} (Figure 29B) and *sgl*^{P1731} (Figure 29C) homozygous mutant embryos shows that *sgl*^{P1731} embryos fail to retract at all after germband extension. This was indicated by the dorsal position of the posterior spiracles (ps) and eighth abdominal segment (A8) (compare panel A with panels B and C, Figure 29). In addition, head segments are completely abolished, with a loss of dorsal cuticle (see white arrow, compare panel A and C in Figure 29). If one compares the positions of the posterior spiracle (ps) and abdominal segment 8 (A8) between panels A, B and C in Figure 23, *sgl*^{A64} homozygous mutant embryos are almost fully retracted with only a small hole in the dorsal side of the embryo (see arrowhead in panel B, Figure 29). In addition, some of the head segments remain intact (white arrow, Figure 29B). When comparing the number of dead embryos observed for *sgl*^{A64} and *sgl*^{P1731}, *sgl*^{P1731} mutant embryos resulted in 4% more dead embryos (compare cross A and B, Table 11). Embryos homozygous for *sgl*^{A31} (Figure 29D) and *sgl*^{N71} (Figure 29E) show similar phenotypic defects to that of *sgl*^{A64}. However, the number of dead embryos observed for *sgl*^{N71} (Table 11 cross D) and *sgl*^{A31} is significantly lower than that of *sgl*^{P1731}, but not *sgl*^{A64} (Table 11, compare c.i. values of cross B with cross E). Again, these results suggest that *sgl*^{P1731} might represent the strongest loss-of-function allele whereas *sgl*^{A64}, *sgl*^{A31} and *sgl*^{N71} are weaker hypomorphic alleles.

To determine further the comparative strength of each *sgl* allele, embryos hemizygous for each *sgl* allele over *Df(3L)w5.4* were examined. Combinations of the *sgl* alleles with the deficiency typically resulted in dorsal-open, U-shaped embryos with loss of anterior head structures. In each case, the morphological criteria used to determine the severity of the mutant phenotype were to examine (i) the extent to which the embryo had retracted during germband retraction, (ii) the dorsal positioning of the posterior spiracle (ps) and (iii) the posterior ventral abdominal denticle belts. In normal wild-type embryos, following the completion of germband retraction and dorsal closure, the posterior spiracles are located at the dorsal-posterior-most position in the larvae (ps, **Figure 29A**). The abdominal denticle belts (A1 to A8) are all located ventrally after differentiation of the embryo (see **Figure 29A**). In the *sgl* mutants, germband retraction is incomplete as indicated by the dorsal positioning of the posterior spiracles and the ventral denticle belts of the abdominal segments A8 and A7. Embryos of the genotype *sgl^{P1731}/Df(3L)w5.4* (**Figure 29G**) typically gave a more severe mutant phenotype than *sgl^{A64}/Df(3L)w5.4* (**Figure 29F**), and resulted in a higher percentage of dead embryos. In *sgl^{P1731}/Df(3L)w5.4* mutant embryos the posterior spiracles are found dorsally, almost near the middle of the embryo, followed by ventral denticle belts from abdominal segments A8 to A7 as one progresses toward the posterior end of the embryo. The ventral denticle belt of A7 in *sgl^{P1731}/Df(3L)w5.4* is found at the dorsal posterior end of the embryo where the posterior spiracle is normally positioned (compare panels A with G in **Figure 29**). In *sgl^{A64}/Df(3L)w5.4* mutant embryos, the posterior spiracles are found on the dorsal side of the embryo, however they are located closer to the posterior end of the larva (**Figure 29F**). The ventral denticle belt of abdominal segment 8 is located at the dorsal posterior-most end of the embryo where the posterior spiracles are found, indicating that *sgl^{A64}/Df(3L)w5.4* embryos undergo more germband retraction than those of *sgl^{P1731}/Df(3L)w5.4*. Neither *sgl^{A31}* or *sgl^{N71}*, over the deficiency *Df(3L)w5.4* resulted in embryos that underwent a greater degree of germband retraction compared to that of *sgl^{P1731}* and *sgl^{A64}* over the *Df(3L)w5.4*. In addition, the number of dead embryos detected never exceeded 15% of fertilized embryos, for both *sgl^{A31}/Df(3L)w5.4* (dead embryos 15%) and *sgl^{N71}/Df(3L)w5.4* (dead embryos 12%). These results suggest that *sgl^{A31}* and *sgl^{N71}* may represent weaker loss-of-function alleles than *sgl^{A64}* and *sgl^{P1731}*. The *sgl^{P1731}* recessive allele represents the strongest loss-of-function allele sampled, as the difference in the number of dead embryos in *sgl^{P1731}/sgl^{P1731}* homozygous embryos when compared with *sgl^{P1731}/Df(3L)w5.4* hemizygous embryos was not statistically significant.

III-3. Molecular analysis of the *A64* PZ-lethal insertion line.

III-3i. Cloning of flanking DNA by P-element rescue.

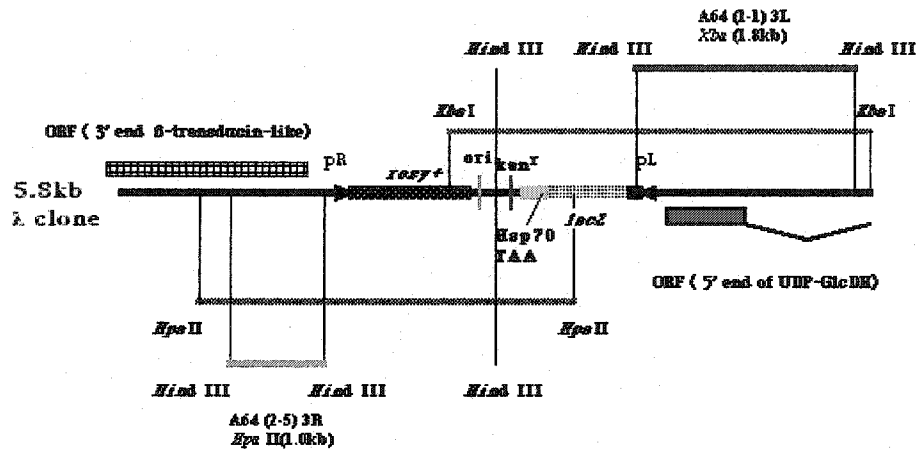
Genomic DNA flanking the *P{lacZ ry+ }A64* insertion site was isolated by P-element rescue (see **Figure 21**). Genomic DNA isolated from *A64/TM3, Sb* flies was digested with *Xba*I or *Hpa*II. Digested fragments were re-ligated and used to transform *E.coli* PMC103 host cells and transformants were selected on Kanamycin containing agar plates. Eight transformants from the *Xba*I digest and five from the *Hpa*II digest were isolated. Plasmids containing the ORI site in the P-element, along with

flanking genomic DNA, recovered from the transformants were designated *A64(1-1)3L/XbaI* and *A64(2-5)3R/HpaII*. The flanking genomic DNA was isolated by doing a *HindIII* digest on the rescued plasmid DNA. When *A64(1-1)3L/XbaI* was digested with *HindIII*, a fragment of approximately 1.8 kb was released, and a *HindIII* digestion of *A64(2-5)3R/HpaII* released a 1.0 kb fragment (see **Figure 30**).

The *HindIII* fragments from both *A64(2-5)3R/HpaII* and *A64(1-1)3L/XbaI* were subcloned into BluescriptKS+. Sequencing of both sense and antisense strands was carried out by the Amgen Institute (Toronto, Canada). **Appendix IV** shows the nucleotide sequence of the *A64(1-1)3L/XbaI* genomic clone. At the time a similarity search using the BLAST algorithm (Altschul et al., 1990) showed that the *A64(1-1)3L* genomic flanking DNA contained the 5' end of an open reading frame which was homologous to the bovine uridine diphosphate glucose dehydrogenase gene. A 5' initiation codon (ATG) was identified at position 297 which corresponds to a translation start site followed by an open reading frame (ORF) that extend 835 nucleotides downstream to position 1132. This 835bp stretch of DNA which encodes a putative protein homologous to bovine UDP-glucose dehydrogenase, is followed by a region of 214 nucleotides (from position 1133bp to 1347bp), which shows no significant similarity to any known sequence. In addition, a potential 5' consensus splice site following the 1132bp position, and corresponding to the end of the open reading frame, was identified. This suggests that the 214bp region may represent the beginning of an intron. The translated 5' amino acid sequence from *Drosophila* was compared to that of bovine UDP-glucose dehydrogenase and showed 85% similarity to the N-terminal end of the bovine amino acid sequence. Further analysis of the sequence upstream of the 5' translation start site, starting from position 297bp, showed that the 3' end of the P-element terminal repeat was also present in the 1.8 kb *HindIII* fragment. This allowed the mapping of the precise site of the insertion and its orientation in *A64* (see **Figure 30**). This was determined by comparing the nucleotide sequence of the *A64(1-1)3L* 1.8kb rescued fragment, with a 5.8kb lambda genomic clone isolated from *Drosophila* (A. Manoukian, Ontario Cancer Institute, unpublished results), which contained part of the 5' end of the *Drosophila* UDP-GlcDH gene and its upstream untranslated and promoter sequences. Based on this sequence comparison, the $P\{lacZ\ ry^+\}$ element is inserted in the 5' untranslated region of the UDP-GlcDH gene, 150 bp upstream of the ATG translation start site in the orientation shown in **Figure 30**.

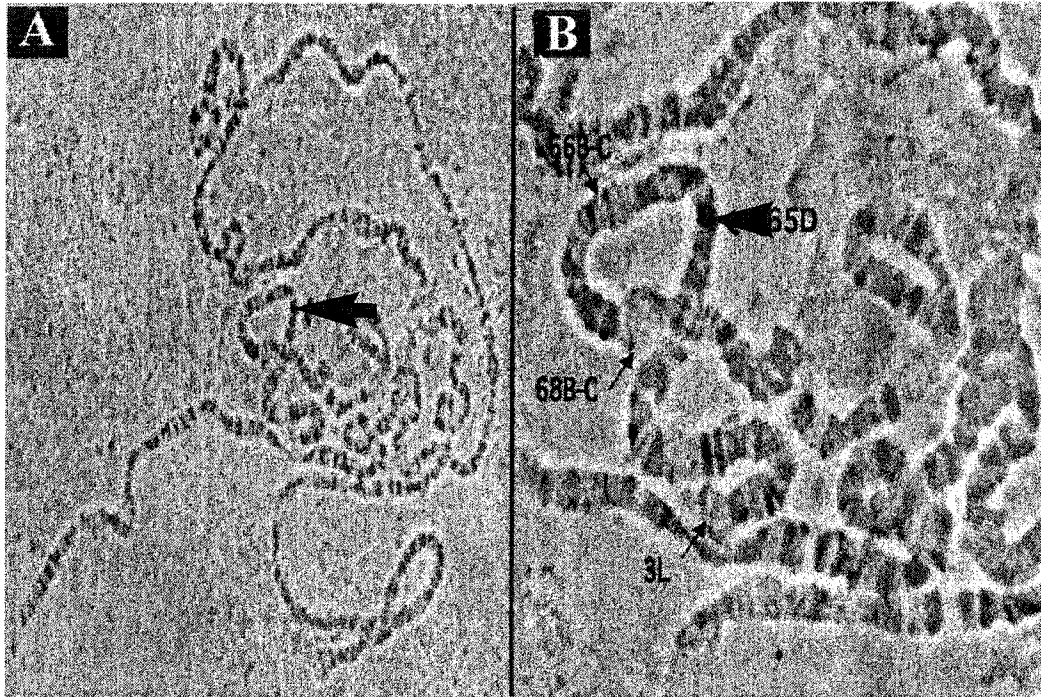
To determine if the genomic fragment that was sequenced maps to the same cytological location as the *PZ* insertion in *A64*, polytene chromosome preparations were probed with the 1.8 kb *A64(1-1)3L* genomic *HindIII* fragment. The 1.8kb fragment was labeled with digoxigenin and used to probe polytene chromosome squashes prepared from wild-type (*Ore-R*) larvae. The 1.8kb fragment hybridized at position 65, on the left arm of the 3rd chromosome. This is consistent with the site of the $P\{lacZ\ ry^+\}$ insertion in *A64* (**Figure 31A**). Closer examination showed that the 1.8kb fragment hybridized to 65D on the polytene map, corresponding with the cytological location of *P1731*, which was mapped to 65D4 (**Figure 31B**). These results suggest that the *A64 P{lacZ ry+}* lethal mutation identifies the *Drosophila* UDP-glucose dehydrogenase (UDP-GlcDH) gene. This is consistent with concurrent studies that showed that the *P1731* mutation is due to a P-element insertion in the *Drosophila* UDP-GlcDH

Figure 30. Schematic alignment of the *A64(1-1)* (3R) genomic rescued fragment with the 5.8 kb *lambda* genomic clone at 65D.



The *A64(1-1)3R* 1.8 kbp (red line) rescued genomic fragment overlaps with the 5' end of the *Drosophila* UDP-GlcDH gene. The diagram shows that the P-element is inserted in the upstream 5' untranslated region of UDP-GlcDH. The *A64(2-5)3R* 1.0 kbp (green line) rescued genomic fragment overlaps with the 3' end of an open reading (ORF) that shows similarity to a β -transducin protein of *Arabidopsis*. There is currently no known mutation of the β -transducin-like gene in flies (*Drosophila* β -transducin-like gene CG10064, Berkeley Genome Project, Flybase 2001). β -transducin is normally expressed only in retinal cells, and therefore, in this case it is unlikely that the *PZ* insertion is reflecting β -transducin expression or affecting β -transducin function in the embryo.

Figure 31. *In situ* hybridization of Digoxigenin-labeled A64(1-1)3L genomic DNA flanking sequence onto *Ore-R* polytene chromosome squashes.



Polytene chromosomes probed with the Digoxigenin-labeled 1.8 kbp rescued genomic DNA fragment A64(1-1)3L. The blue stain is visualized at (A) 20X objective (arrow) and (B) 40X objective (arrow head). A prominent signal is detected at chromosomal position 65D based on the standard polytene chromosomal map in Lindsley and Zimm (1993). 3L marks the tip of the left arm of the 3rd chromosome. The arrowhead at 65D indicates the dark band that corresponds to the blue stain produced by the Digoxigenin labeled probe. The other dark bands are a consequence of the counter stain that was used to stain the polytene chromosomes.

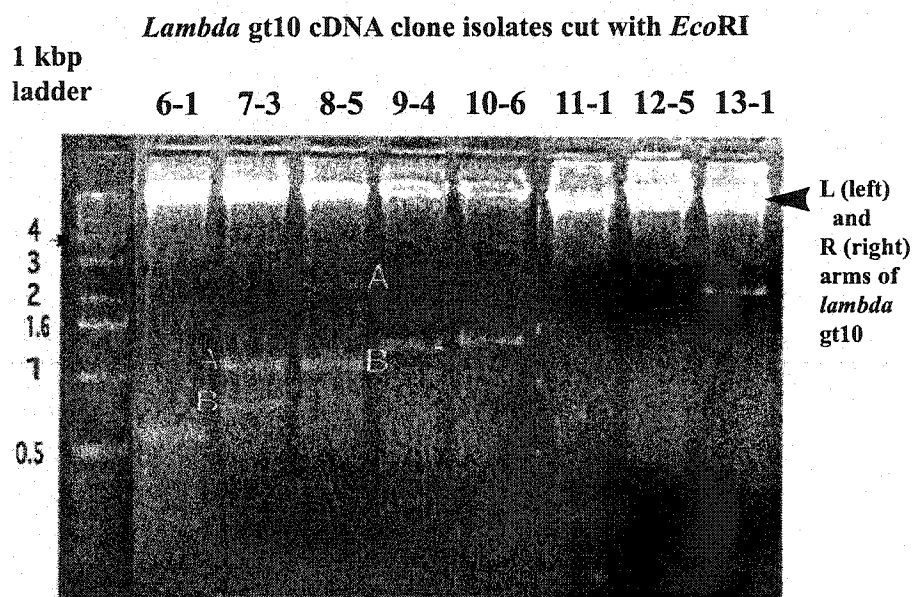
gene (Binari et al., 1997; Hacker et al., 1997), along with the genetic complementation analysis which indicated that *P1731* was allelic to *A64*.

III-3ii. Isolation of *Drosophila* UDP-GlcDH cDNAs

The *Hind*III *A64* (1-1)3L 1.8kb genomic fragment which contains the 5' end of the UDP-GlcDH gene was used to probe two *Drosophila lambda gt10* cDNA libraries, made from embryos 3-12 hr after egg lay (AEL) and 12-24 hr AEL (Huyh et al., 1985). An embryonic library was selected based on the *lacZ* staining of *A64* embryos (see **Figure 25**) which suggested that the gene identified in this study may be transcribed strongly during the early stages of embryogenesis. A total of 100,000 plaques were screened, from which 30 positives were isolated. Secondary and tertiary screens were carried out to obtain pure single-plaque isolates. Eighteen of the 30 initial positives were not picked up in the secondary and tertiary screens, suggesting that they may have been false positives or they were lost during the rescreening process. Four out of the remaining 12 did not lyse the host bacteria (Q358) during an initial small scale phage purification step. The eight final positives were brought through a large-scale phage purification step, followed by DNA isolation and then digested with *Eco*RI, in order to release the cloned cDNA insert from the phage arms (**Figure 32**). Six of eight isolates, 6-1, 7-3, 8-5, 9-4, 10-6, and 13-1 contained a cDNA insert that could be released with *Eco*RI. Two clones, 11-1 and 12-5, which did not release a fragment, could be the result of clones that had lost at least one *Eco*RI site upon cloning, thus preventing digestion and release of the clone. Clones 7-3 and 8-5 showed an additional internal *Eco*RI site resulting in two fragments, 7-3A, 7-3B and 8-5A, 8-5B (**Figure 32**). To confirm that the *Hind*III *A64*(1-1) probe hybridized with the clones, a Southern blot was performed on *Eco*RI-digested samples using each clone (not shown). The blot detected bands that corresponded to the cDNA insert in each clone with the exception of fragment 8-5A. This suggests that clone 8-5 may represent a chimera that may have been produced during the various amplifications of the library over time. This means that part of this clone may consist of sequence containing the UDP-GlcDH gene that was recognized by the probe (8-5B), whereas the part of the clone (8-5A) contains DNA from another region. In the case of clones 11-1 and 12-5, the band corresponded to uncut high molecular weight DNA band. This may represent clones that lost at least one of the *Eco*RI sites flanking the insert.

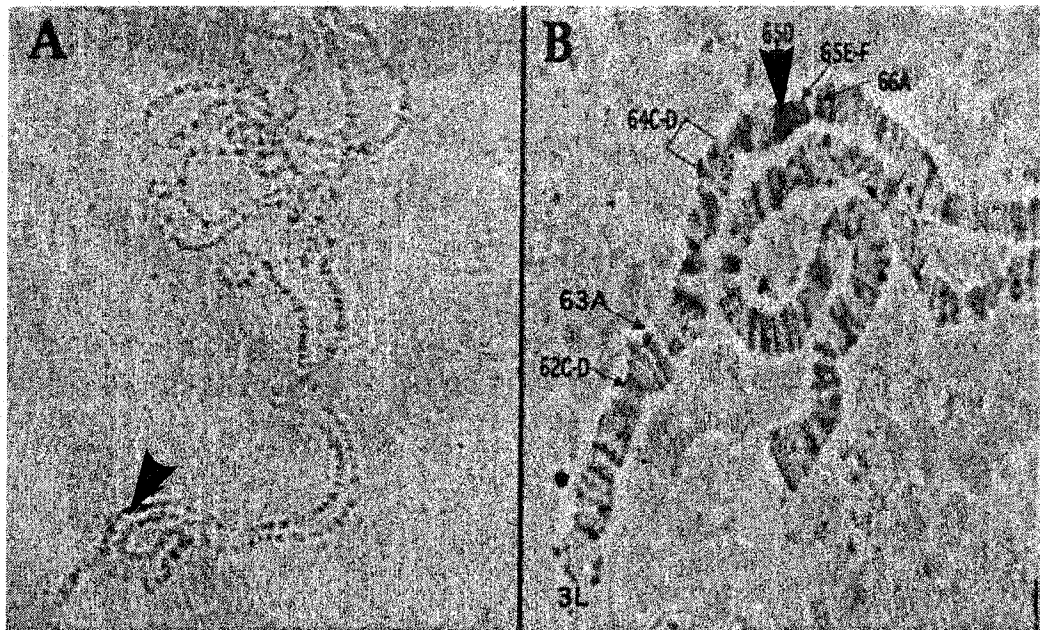
The *Eco*RI fragment from each clone (excluding clones 11-1 and 12-5) was gel purified and used to make a digoxigenin-labeled DNA probe for polytene chromosome *in situ* mapping. Polytene chromosomes prepared from *Ore-R* (wild-type) larvae were probed with each cDNA fragment. The cDNA clones, 6-1, 7-3A, 7-3B and 8-5B hybridized to cytological location 65D, which is consistent with that of the *PZ* insertion and the *A64*(1-1)3R rescued genomic flanking sequence. The 9-4, 10-6 and 13-1 cDNA clones hybridized to the cytological location 65D, as well as to other positions on the polytene chromosomes. This may be due to contamination from other cDNA sequences which resulted in chimeric clones or repetitive DNA (see **Table 12**).

Figure 32. *Lambda* gt10 cDNA clones isolated from a *Drosophila* embryonic cDNA library (Huynh et al., 1985).



Lambda-gt10 cDNA clone isolates 6-1 through 13-1 were digested with *Eco*RI. The resulting fragments were separated on a 0.5% agarose gel. The top bands (black arrowhead) represent the left and right arms of *lambda* gt10. In some isolates, two bands were detected for the cDNA insert (e.g., 7-3A, 7-3B, 8-5A, 8-5B), indicating the presence of an internal *Eco*RI site. 11-1 and 12-5 show no insert and represent clones that were not cut with *Eco*RI. The small black arrow indicates a 4 kb band in the 1 kbp DNA ladder.

Figure 33. Cytological mapping of the 7-3A cDNA clone to *Ore-R* polytene chromosomes.



The Digoxigenin labeled 7-3A cDNA clone maps to the left arm of the third chromosome (3L). (A) A unique band is detected at 20X objective near the tip of 3L (black arrowhead). (B) Upon close examination at 40X objective in the same preparation, the unique band is mapped to the cytological location 65D (black arrowhead). Cytological locations (62C-D, 63A, 64C-D, 65D, 65E-F and 66A) are determined according to the standard polytene chromosomal map in Lindsley and Zimm (1993). The arrowhead at 65D indicates the dark band that corresponds to the blue stain produced by the Digoxigenin labeled probe. The other dark bands are a consequence of the counter stain that was used to stain the polytene chromosomes.

Table 12.

Cytological positions of cDNA clones on *Oregon-R* polytene chromosomes.

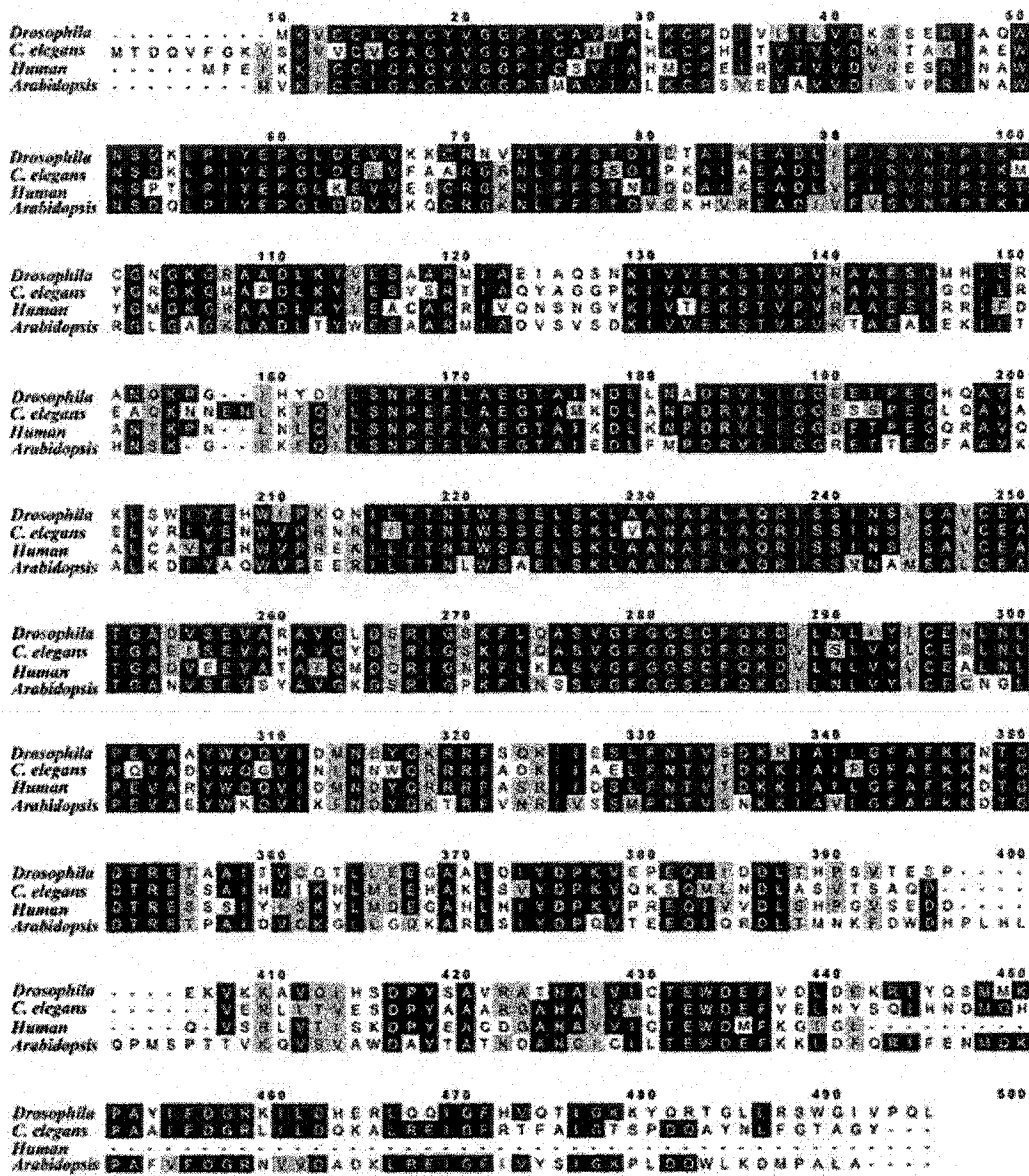
The cytological location of cDNA clones hybridized to wild-type *OreR* polytene chromosomes was determined by the standard polytene chromosomal map in Lindsley and Zimm (1993). Digoxigenin labeled cDNA clones 6-1, 7-3A, 7-3B and 8-5B were map to a single site at position 65D on the left arm of the 3rd chromosome. The remaining clones either mapped to a different location (e.g., clone 8-5A) or to various sites that also included the location at 65D (e.g., clones 9-4, 10-6, 13-1).

cDNA clone	Cytological location
6-1	65D
7-3A	65D
7-3B	65D
8-5A	65F
8-5B	65D
9-4	55A, 65D, 68B, 77A
10-6	37B, 65D
13-1	45A, 65D, 85C

cDNA clone fragments 7-3A and 7-3B when combined, represented the longest cDNA isolate that mapped to 65D. **Figure 33** displays a signal at 65D where polytene chromosomes were hybridized with the 7-3A Digoxigenin labeled DNA probe. Clones 7-3A (1100bp) and 7-3B (785bp) were subcloned into the *EcoRI* site in the BluescriptKS+ vector for sequencing. The cDNA was sequenced by the Department of Biological Sciences Sequencing facility at the University of Alberta. Sequence comparison analysis was performed using a BLAST search of the available sequence database (Altschul et al., 1990). The BLAST results show that 7-3A and 7-3B encode the *Drosophila* homolog of uridine diphosphate glucose dehydrogenase (UDP-GlcDH). This corresponded with the sequence of the *A64(1-1)3L* rescued genomic flanking sequence. The similarity search of the available databases at the time, using the BLAST algorithm (Altschul et al., 1990), showed that the initial 410bp of the 7-3A sequence encodes a 5' untranslated region. The remaining 690bp encodes the first 230 amino acids of the N-terminal portion of the UDP-GlcDH protein (Dougherty and van de Rijn, 1993; Hemple et al., 1994). The first 465bp of the 7-3B cDNA clone encoded the next 155 amino acids making up the C-terminal half of the UDP-GlcDH protein. The remaining 320bp showed no discernable similarity, at the amino acid level, to any notable protein sequence. When the amino acid sequence translated from 7-3A and 7-3B was compared with the complete *Drosophila* UDP-GlcDH 474 amino acid sequence (Binari et al., personal communication), 89 amino acids from the C-terminal end were missing. Therefore, the 7-3 clone represented an incomplete cDNA sequence, containing the partial C terminal end of UDP-GlcDH, in addition to extraneous pieces of DNA that may have been incorporated during the several amplification events of the cDNA library. The deduced full amino acid sequence shown in **Figure 34**, (kindly provided by Binari et al., personal communication), was used to produce a multiple sequence alignment (see **Figure 34**) with the amino acid sequences of *Arabidopsis*, *C. elegans* and human homologs obtained from the available databases (provided by NCBI, www.ncbi.nlm.nih.gov). Pair wise alignments using the BLAST algorithm (Altschul et al., 1997), with the *Drosophila* (Acc. # O02373) amino acid sequence showed that the greatest similarity occurred with *C. elegans* (Acc. # Q19905) UDP-GlcDH, with an overall sequence identity of 62% indicated by the black shaded boxes and an additional similarity of 14% as indicated by the grey shaded boxes. This was followed by *Arabidopsis* (Acc. # NP186750) that had a sequence identity of 61% and similarity of 14%, and then human (Acc. # O60701), that had a identity of 61% and similarity of 12% (Clustal W (v1.4) pairwise alignment parameters: Matrix-Blosum 30, Open gap penalty - 10.0, and extended gap penalty - 0.1). This suggests the clone that was isolated encoded the *Drosophila* homolog of UDP-GlcDH. The high identity observed between the UDP-GlcDH homologs from different metazoans showed that UDP-GlcDH protein sequence was not highly divergent, suggesting that UDP-GlcDH function may have remained conserved through evolution.

While this work was in progress, two groups identified *P1731* from the Spradling PZ-lethal lines in a germline clone screen for maternal-effects, as a regulator of the *wg* signaling pathway in the embryo. This was due to a mutation of the *Drosophila* homolog of UDP-GlcDH, which they independently called *kiwi* (Binari et al., 1997) and *sugarless* (Hacker et al., 1997). A third group showed that an allele of this gene, *SG9*, behaves as an enhancer of the *dishevelled* disc mutant *dsh^w* from the

Figure 34. Comparison of deduced amino acid sequence of various UDP-GlcDH proteins.



Multiple alignment of UDP-glucose dehydrogenase amino acid sequences using the ClustalW (v1.4) (Multiple alignment parameters: Matrix-Blossum series, Open gap penalty-10.0, Extended gap penalty-0.1). Deduced amino acid sequence of *Drosophila melanogaster* UDP-glucose dehydrogenase (Acc. # O02373) and alignment with *Arabidopsis* (Acc. # NP186750), *C. elegans* (Acc. # Q19905), and human (Acc. # O60701) homologs. Residues identical between more than half of the homologs are indicated by black shaded boxes. Similarities among the homologs are indicated by gray boxes. Parameters for amino acid sequence similarities: hydrophobic (non-polar R groups: A, I, L, M, F, P, W, V) vs hydrophilic (polar but uncharged R groups: N, C, Q, G, S, T, Y), and charged (positively charged R groups: R, H, K; or negatively charged R groups: D, E) vs uncharged (neutral). Gaps in the sequence introduced to maximize the alignment are represented with “ - ”.

wingless signaling pathway, and as a suppressor of the wing phenotype due to an activated form of the *dpp* receptor *thickveins* (*thv*) (Haerry et al., 1997). The *P1731* mutation is now referred to by the name *sugarless* (Hacker et al., 1997; Flybase 2001). The genetic evidence herein for allelism of *A64* and *P1731*, and sequence analysis of the *A64* genomic flanking sequence and cDNAs, shows that *A64* is an allele of the *sugarless* gene.

III-3iii. Rescue of the *A64* zygotic embryonic lethal phenotype by *Drosophila* UDP-glucose dehydrogenase cDNA expression.

To confirm the hypothesis that the *A64* embryonic lethal phenotype was due to the loss of UDP-GlcDH activity, I attempted to rescue the lethal phenotype of *A64* by expression of the *Drosophila* UDP-GlcDH cDNA using the *Gal4-UAS* system in homozygous *A64* embryos.

A transgenic fly line containing a viable insertion of a UAS-*sgl* full-length cDNA construct (R. Sasisekharan, MIT, R. Binari and B. Staveley, OCI, unpublished), was crossed to *Df(3L)w5.4/TM3 Sb e* to establish a *UAS-sgl/UAS-sgl; Df(3L)w5.4/TM3, Sb* stock. Ectopic expression of UDP-GlcDH was induced during embryogenesis by crossing *UASsgl/UASsgl; Df(3L)w5.4/TM3, Sb* females to an *armadillo-Gal4* transgenic stock in which *sgl^{A64}* or *sgl^{P1731}* had also been introduced: *armGal4/armGal4; sgl^{A64}/TM3, Sb* and *armGal4/armGal4; sgl^{P1731}/TM3, Sb* (See Table 13). *ArmGal4* was chosen because it will drive the ectopic expression of UAS-*sgl* ubiquitously from as early as the syncytial blastoderm stage in embryos.

Table 13 shows the results of this cross along with the control crosses. In crosses 1 and 2, the embryonic lethal phenotype of embryos hemizygous for either *A64* or *P1731* over *Df(3L)w5.4* was repressed by ectopic expression of the *Drosophila* UDP-GlcDH construct. This suggests that ectopic expression of the full length UDP-GlcDH cDNA clone was able to rescue the *sgl* loss-of-function lethal mutants of *sgl^{A64}/Df(3L)w5.4/TM3* and *sgl^{P1731}/Df(3L)w5.4* hemizygous embryos. Over half of the embryos (82% {164/200} for *sgl^{A64}* and 61% {154/250} for *sgl^{P1731}*) that were expected to die, based on the results in Table 11, hatched and progressed into the larva stage. Of these larvae that hatched, over half eclosed and gave adults (60% {99/164} for *sgl^{A64}* and 59% {92/154} for *P1731*). In the control crosses 3 and 4, we observe that approximately 1/4 of the embryos that were screened did not hatch and died, as expected according to Mendelian ratios from the cross. In addition, no *Sb+* adult flies were observed. Thus, in the absence of either the *armGal4* driver or the *UASsgl* construct, all *sgl^{A64} / Df(3L)w5.4* hemizygous embryos died. In control cross 5, I expected to see no dead embryos, but did in fact see 21 dead embryos. Cuticle preparations of these embryos showed no embryonic pattern defects, which may suggest that the ectopic expression of *sgl* in a wild-type background might be slightly toxic or affect the internal development of the embryo. The effects of higher levels of ectopic expression of UDP-GlcDH in the embryo using a stronger *Gal4* driver will be examined later.

Experimental crosses 1 and 2 (summarized in Table 13) in which ectopic UDP-GlcDH expres-

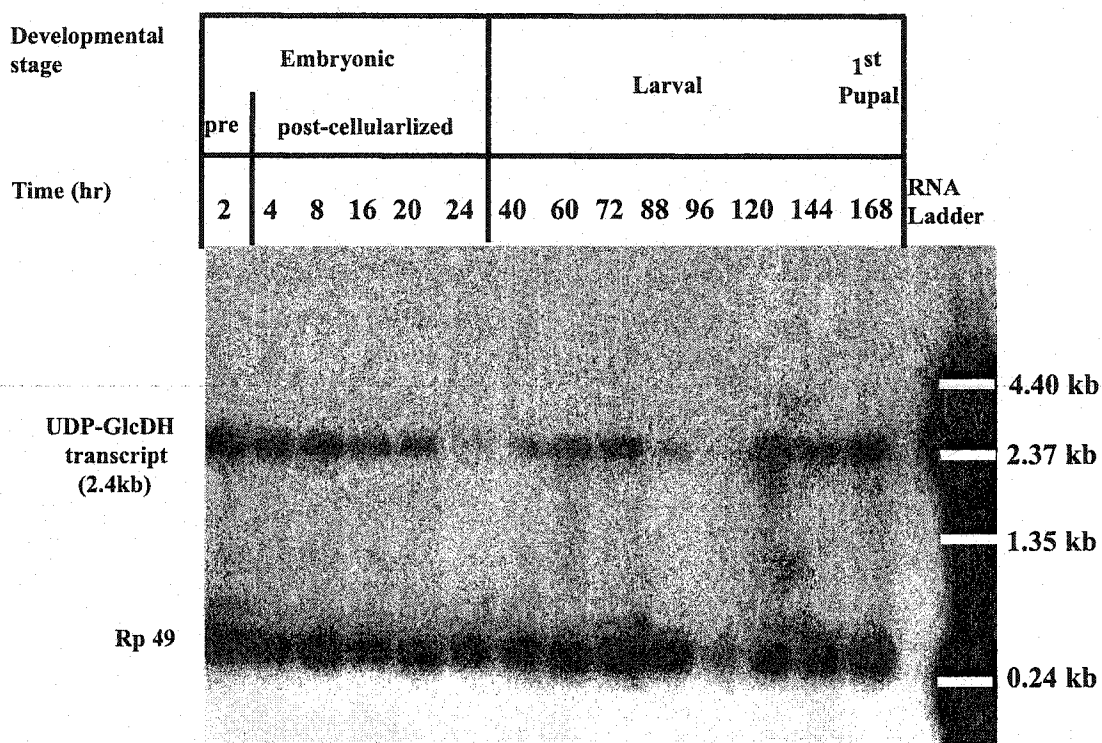
sion is driven by *armGal-UASsgl*, result in adult flies that did not carry the *TM3,Sb* balancer. This indicates that ubiquitous expression of UDP-GlcDH was able to rescue some of the lethality caused by the hemizygous *sgl^{A64}/Df(3L)w5.4* and *sgl^{P1731}/Df(3L)w5.4* mutations to adulthood. For example, if one looks at cross 1, only 86 of the expected 200 fertilized hemizygous embryos died, that is 8% from the total number of embryos that were treated (1000). This was significantly lower than the lethality of 24% and 21% expected for embryos hemizygous for *sgl^{P1731}/Df(3L)w5.4* and *sgl^{A64}/Df(3L)w5.4* (see **Table 13**), if the UDP-GlcDH cDNA did not rescue the lethal phenotype. Thus, the remaining *sgl^{A64}/Df(3L)w5.4* hemizygous mutant embryos seem to have survived past the embryonic lethal phase, 99 of which reached adulthood as *Sb+*. The rest may have died at larval and pupal stages—indicating that some of the *sgl^{A64}/Df(3L)w5.4* embryos were rescued only to larval or pupal stages. The rescue by expression of *sgl* cDNA shows that the *A64* lethal phenotype was caused by a loss of UDP-GlcDH function due to the *PZ* insertion.

III-3iv. Expression pattern of UDP-GlcDH in *Drosophila* embryos and imaginal discs.

The wild-type developmental expression profile of UDP-GlcDH mRNA was determined by means of a Northern blot. A ³²P-labeled 7-3A cDNA probe detected a single transcript of approximately 2.4kb (**Figure 35**). A putative maternal transcript was detected prior to cellularization (0-2 hr AEL), along with abundant expression following cellularization throughout embryogenesis (2-24 hr AEL). UDP-GlcDH expression was also seen during each larval stage (24-144 hr AEL) and into pupation (P1). Based on a visual inspection of the X-ray film, the highest levels of UDP-GlcDH transcript expression are observed in syncytical (pre-cellularized, 0-2 hr AEL) and early blastoderm (4 to 8 hr AEL) embryo. The level of transcript expression seems to drop off at end of embryogenesis (24 hr AEL). Transcript levels then seem to increase during the larval third instar (40 to 72 hr AEL), dropping off again at 88 hr AEL. Levels of transcript could not be determined at 96 hr, due to underloading of the gel. Transcript expression was also observed during pupal stages. Preliminary evidence may suggest that UDP-GlcDH transcript expression may be temporally regulated during development.

To determine the spatial distribution of UDP-GlcDH mRNA in the embryo, whole-mount *in situ* hybridization was performed (**Figure 36**). The UDP-GlcDH transcript was detected with a Dig-labeled 7-3A cDNA probe in *Ore-R* (wild-type) whole-mount embryos. UDP-GlcDH transcripts are present uniformly throughout the embryo prior to cellularization (not shown), and subsequently become localized to the presumptive amnioserosa beginning at stage 9 (**black arrow Figure 36A**). By stage 11, UDP-GlcDH transcript expression still remains in the amnioserosa (**see black arrow, Figure 36B**), as low expression begins to appear in pericardial cells (mesoderm) underlying dorsal ectoderm (**see black arrowheads, Figure 36B**) and cephalic head segments (**red arrow, Figure 36B**). This pattern of expression at stage 11 in the embryo was consistent with the *lacZ* expression pattern observed in *PZ A64* (**see Figure 25B**). Expression in the amnioserosa is maintained by stage 13 (**arrow Figure 36C**) and persists up to stage 15 (not shown) in the dorsal ridge cells of the embryo until completion of dorsal closure. The changes in the expression patterns showed that UDP-GlcDH may also be spatially

Figure 35. Developmental Northern blot showing the expression profile of UDP-GlcDH mRNA in *Drosophila melanogaster*.



The UDP-GlcDH transcript on the Northern blot corresponds approximately to a 2.4 kb RNA band detected using the 7-3A(A64) P³² labeled cDNA probe. The level of expression of ribosomal RNA 49 (Rp49) was used as a control to measure the relative amounts of RNA loaded in each lane. The Rp49 transcript was detected by a Rp49 cDNA P³² labeled probe. Both probes were used simultaneously in a cocktail during the hybridization process of the filter. The numbers 2 to 168 (going left to right) represent the time at which mRNA extractions were performed in hr following egg lay. RNA Ladder is the lane that contains the 0.24-9.5 kb RNA size ladder. Due to overloading of the RNA ladder, white lines are used to mark the location and the corresponding sizes of the RNA bands on the film.

Figure 36.
Expression of the UDP-GlcDH transcript in *Drosophila* embryos.

(A) The UDP-GlcDH transcript accumulates in the amnioserosa by stage 9 (germband extension) embryos (see black arrow). (B) In stage 11 embryos, (beginning of germband retraction) UDP-GlcDH transcript expression persists in the amnioserosa (black arrow). In addition, expression starts to accumulate in groups of cells in underlying mesodermal germ layer which may represent the pericardial cells (black arrowheads). Low-level expression is also observed in the anterior head segments (red arrow). (C) By stage 13 (end of germband retraction) UDP-GlcDH expression is lost in the pericardial cells as expression levels of UDP-GlcDH in the amnioserosa (black arrow) is reduced. In all figures, anterior is to the left, and dorsal is up.

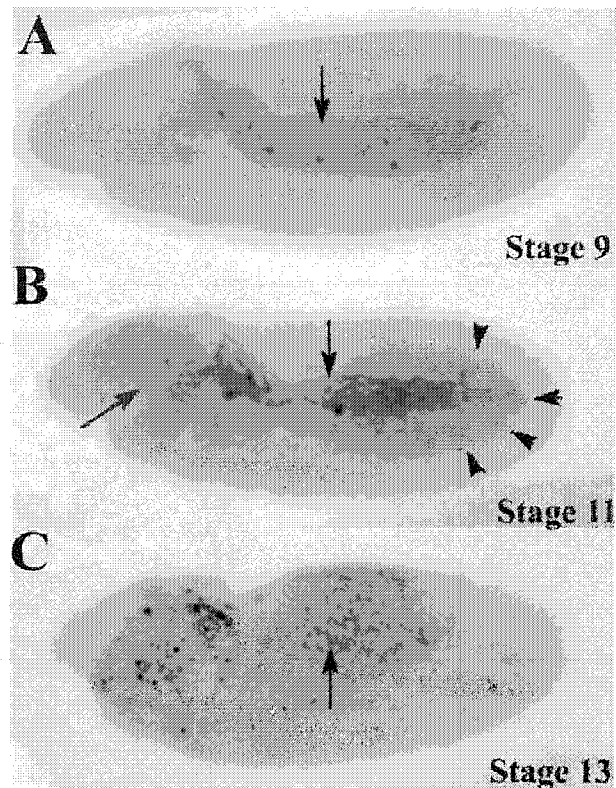
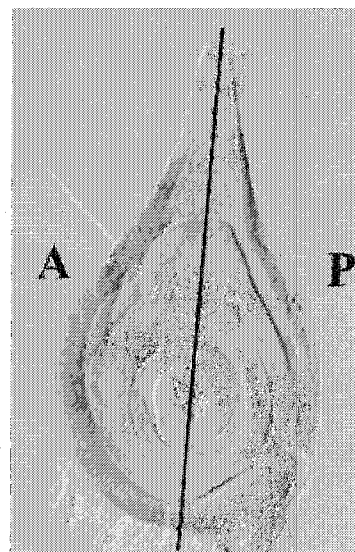


Figure 37.
Expression of UDP-GlcDH transcripts in the imaginal leg disc.

UDP-GlcDH transcript expression detected by a Digoxigenin labeled UDP-GlcDH cDNA probe from *Drosophila* in second thoracic leg discs in third instar larvae. Expression in the second thoracic leg disc is uniform. Expression in earlier larval stages of disc development was also uniform (not shown). Anterior is to the left and dorsal is up. The black line represents the approximate anterior/posterior compartment boundary. Anterior (A), posterior (P).



regulated. The spatial expression of the UDP-GlcDH transcript in an embryo appears to correlate with tissues that are responsible for dorsal patterning and gastrulation. This observation is consistent with the observed head and dorsal tissue defects that show missing head segments and dorsal cuticle in cuticle preparations of *sgl* mutant embryos (see **Figure 24** and **Figure 29**).

In situ hybridization of the same probe to imaginal discs, showed uniform expression of UDP-GlcDH transcript occurs throughout the second and third larval instar. **Figure 37** shows the staining of an early third instar second leg disc. The presence of UDP-GlcDH expression in imaginal discs is consistent with its possible role in normal imaginal disc patterning, implied by the changes in expression that were observed during pattern regulation in regenerating leg discs.

III-4. Developmental effects of the UDP-GlcDH gene in *Drosophila* embryos.

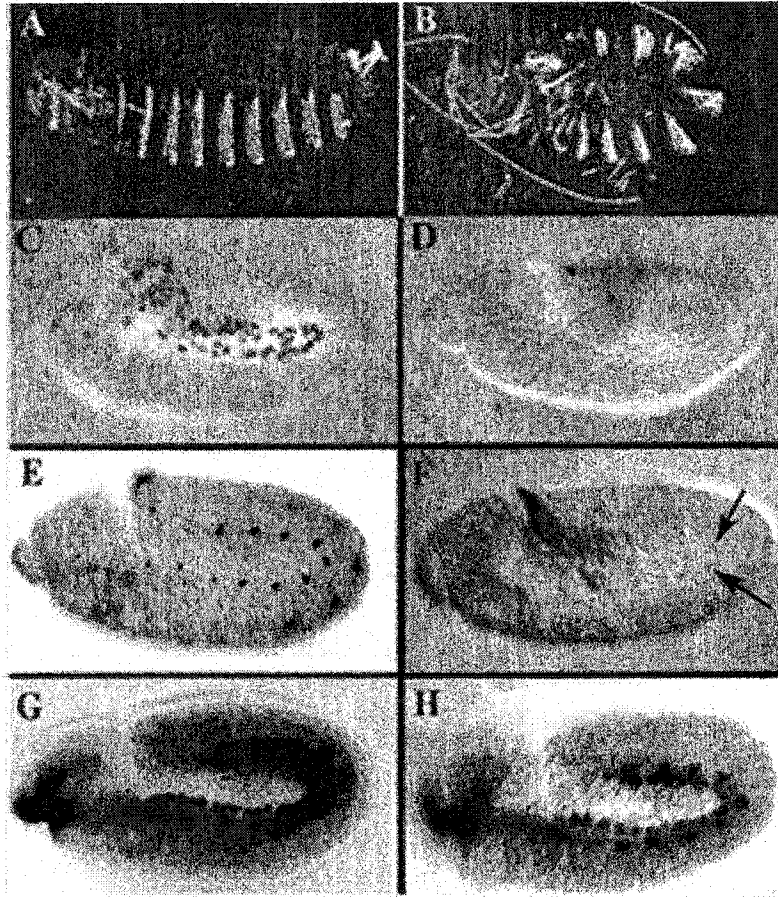
III-4i. *Drosophila* UDP-GlcDH zygotic mutations result in loss of dorsal-specific gene expression.

As shown earlier, embryos mutant for the UDP-GlcDH gene result in incomplete germband retraction and significant loss of dorsal cuticle. This phenotype is similar to the zygotic mutant phenotypes of the signaling gene *dpp* and its receptors, *punt* and *thv*. **Figure 38B** shows an embryo homozygous for *sgl*^{P1731}. In order to establish a role for UDP-GlcDH in *dpp* signaling, it is crucial to determine if the *dpp*-like ventralized phenotype in UDP-GlcDH mutant embryos is, indeed, due to effects on *dpp* signaling. If this is the case, the expression of immediate downstream target genes of *dpp* should be affected. Therefore, possible effects on *Kruppel* (KR), *even-skipped* (EVE) and *tinman* (TIN) protein expression in stage 11-12 *sgl*^{P1731} homozygous embryos were examined.

sgl^{P1731}/*TM3,Sb* flies were outcrossed to *Ore-R* wild flies, and non-*Sb* F1 *sgl*^{P1731}/+ sibs were crossed. Batches of embryos from this cross were collected over 2 hr intervals, and allowed to develop for another 8 hr up to embryonic stage 11-12. Stage 11-12 embryos represent the time point at which induction of *dpp*-regulated gene expression is initiated in the dorsal ecto- and mesodermal cell layers. This stage is marked by the activation of *eve* in pericardial cells, and *tin* in the mesoderm and near the dorsal ridge cells of the ectoderm. In addition, KR expression can be found at this stage in the amnioserosa, the dorsal most region of the embryo.

Embryos were stained with antibodies to detect KR, EVE and TIN proteins. **Figure 38C, E** and **G** show the expression of KR, EVE and TIN in *Ore-R* (wild-type) stage 11-12 control embryos respectively. In about one-quarter of the embryos from the experimental cross, EVE (**Figure 38F**) and TIN (**Figure 38H**) expression was significantly reduced, but was not completely lost during stages 11-12. This suggested that *dpp* signaling is attenuated but not completely lost. In the case of KR, one would typically observe a complete loss of expression in the amnioserosa by stage 11-12 as seen in **Figure 38D**, or in some cases only a few cells would show some reduced expression of KR. This is consistent with observations that typically higher levels of *dpp* activity are required for KR expression

Figure 38. Loss of UDP-GlcDH blocks *dpp* signaling.



Zygotic effects of a mutation in UDP-GlcDH on dorsal patterning and expression of *dpp* target genes involved in ectodermal and mesodermal patterning. All embryos are oriented with anterior to the left and dorsal up. Cuticle preparations of wild-type (A) and *sgl*^{P1731} homozygous (B) embryos. Homozygous *sgl*^{P1731} embryos are U-shaped with head defects and loss of dorsal cuticle. (C) Wild-type and (D) *sgl*^{P1731}/*sgl*^{P1731} stage 10 embryos stained with an antibody to the *Kruppel* protein which is normally expressed in the amnioserosa under the control of *dpp* signaling. In *sgl*^{P1731}/*sgl*^{P1731} embryos (D), *Kruppel* protein expression is lost. Stage 11 wild-type (E) and *sgl*^{P1731} (F) embryos stained with an antibody against *evenskipped* (EVE) protein. (E) Normally EVE expression is localized in the pericardial cells in the mesoderm. (F) In *sgl*^{P1731}/*sgl*^{P1731} embryos, EVE protein expression fades (see black arrow), suggesting that the *dpp* signal from the overlying ectoderm germ layer is being compromised. (G) and (H) are stage 11 embryos stained with antibody against *tinman* protein (TIN). In wild-type embryos (G), TIN expression is observed in the dorsal ectodermal ridge and the underlying dorsal mesodermal cells that give rise to the visceral mesoderm. (H) In *sgl*^{P1731}/*sgl*^{P1731} embryos, TIN expression is not completely abolished, but ectodermal expression has faded or is lost in some cells. In the mesoderm, the band of TIN expressing cells is also interrupted.

in the amnioserosa (the dorsal-most cells). One would then expect that the amnioserosa, and therefore KR expression would be the most sensitive to attenuations in *dpp* signaling.

Loss of KR expression in the amnioserosa of the *sgl^{P1731}* mutant indicates that the dorsal-most cell fate specified by *dpp* signaling in the embryo is affected. The effect on EVE expression in the segmental clusters of pericardial cells, on either side of the amnioserosa (Frasch et al., 1987) also indicates a patterning defect in the dorsal mesoderm, possibly due to the loss of *dpp* signaling. The effect on TIN expression in the underlying dorsal mesoderm is especially important, as *tin* is thought to be exclusively under the control of *dpp* signaling. The DPP signal in this case acts as a paracrine signal from the dorsal ectoderm, which is required for the proper specification of the underlying dorsal visceral mesoderm (Staehling-Hampton et al., 1994; Frasch, 1995). Failure to express the critical patterning genes in the dorsal amnioserosa, mesoderm, and ectoderm, is consistent with the later dorsal cuticle and gastrulation defects observed in UDP-GlcDH mutants.

Therefore, it appears that UDP GlcDH zygotic mutant embryos exhibit a loss of dorsal cell fates as a result of the *sgl^{P1731}* mutation affecting *dpp* signaling. The different responses observed with these various markers are consistent with dosage-sensitive effects observed with the *dpp* signaling pathway. These results imply that UDP-GlcDH is required for *dpp* signaling for the specification of dorsal cell fates in the embryo.

III-4ii. Genetic interactions between UDP-GlcDH and *dpp* signaling pathway genes.

As described earlier, mutant alleles of *sgl* affect dorsal patterning in the embryo. The phenotype of these mutant alleles typically show embryos with incomplete germband retraction, disruption of head involution, and loss of dorsal cuticle (see **Figure 29B, C, D and E**). The strongest mutant phenotypic effects are shown by the *sgl^{P1731}* allele and include a disruption of germband retraction, resulting in severe U-shaped embryos, a failure to undergo dorsal closure, resulting in a prominent hole on the dorsal side of the embryo and loss of head segments (**Figure 29C**). As was concluded earlier, patterning defects in *sgl* mutant embryos result from an attenuation of the *dpp* signaling pathway.

Patterning of the dorsal region of the embryo requires a gradient of DPP activity (see Introduction). This process should, therefore, be inherently sensitive to dosage-induced changes of *dpp* signaling activity. Trans-heterozygous genetic interactions which enhance the mutant phenotype of weak *dpp* alleles have been observed using mutations in other genes that mediate *dpp* signaling. This includes genes such as *schnurri* (*shn*) (Arora et al., 1995), *thickveins* (*tkv*) (Affolter, et al., 1994), *screw* (*scw*) (Arora et al., 1994; Finelli, et al., 1995) and *tolloid* (*tld*) (Shimell et al., 1991).

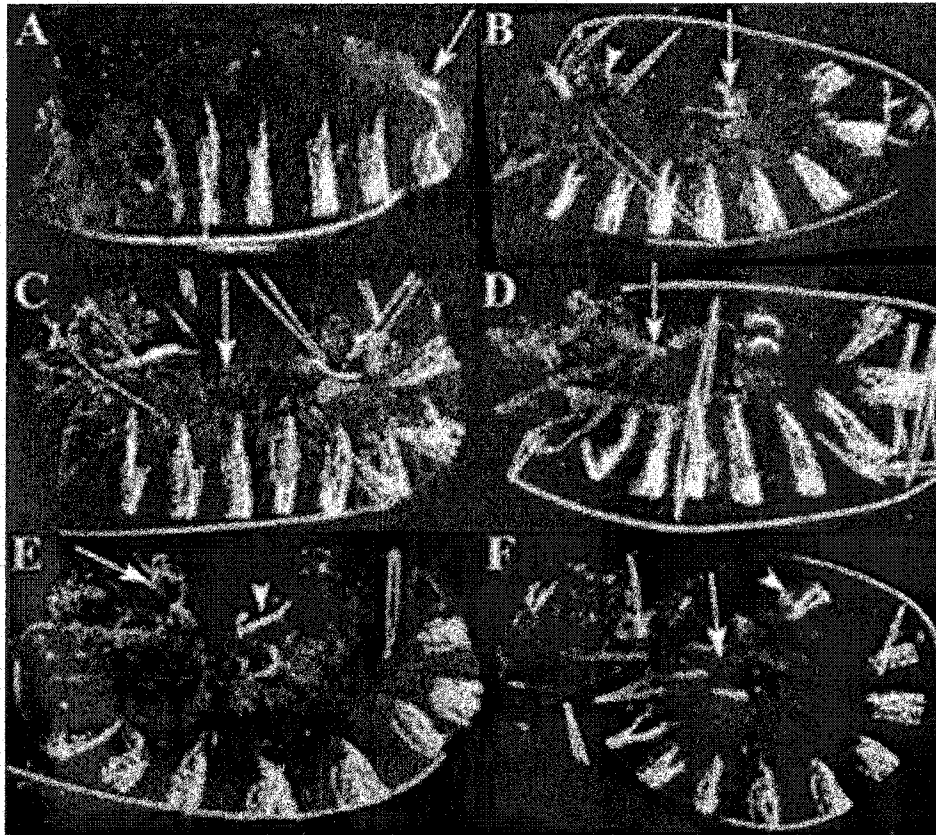
Based on the genetic evidence so far, I hypothesized that UDP-GlcDH may act as a modulator of the *dpp* signaling pathway. To determine if *dpp* signal transduction is dependent on UDP-GlcDH function, I decided to test for dosage-dependent genetic interactions of trans-heterozygous combina-

tions between a *sgl* mutant allele and loss-of-function mutant alleles of genes in the *dpp* signaling pathway (Figure 39, Table 14). Heterozygous *sgl*^{P1731}/+ or *sgl*^{A64}/+ virgin females were crossed to males that were heterozygous for a *dpp* pathway mutant. Assuming random and non-biased segregation of the chromosomes, approximately 25% of the embryos from these crosses will be heterozygous for two mutations at different locations that are in trans to one another: these are trans-heterozygous embryos. The *sgl* heterozygous embryos are normally viable resulting in only 0.8% and 1.1% embryonic lethality for *sgl*^{A64} and *sgl*^{P1731} respectively (Table 14). Trans-heterozygous embryos are also missing one wild-type copy of a *dpp* pathway gene. Therefore, since the mothers from these crosses are *sgl*^{P1731}/+ or *sgl*^{A64}/+ heterozygotes, the *sgl* heterozygous embryos from this cross are carrying only half the normal copy number of both zygotic and maternal UDP-GlcDH gene copy. Based on copy number, one assumption that is made is that the *sgl* heterozygote from these crosses may lack half the normal amount of both zygotic and maternal UDP-GlcDH expression. If the gene product of *sgl* has a function in *dpp* signaling, it is possible that loss of half of both the zygotically- and maternally-derived *sgl* expression, when combined with half of the normal copy number of *dpp* or its receptors, could result in a significant increase in embryonic lethality (Table 14). Cuticle phenotypes of unhatched first instar larvae (see Figure 39) were analyzed for dorsal pattern defects to determine the extent of each genetic interaction with the *dpp* signaling pathway.

The *dpp*^{hr27} allele is a haplo-insufficient loss-of-function lethal mutant (Arora and Nusslein-Volhard, 1992; Wharton et al., 1993). Embryos homozygous for *dpp*^{hr27} are lethal and present a moderate ventralized cuticle phenotype that includes head involution, terminal defects that include internalization of the seventh and eighth abdominal segments, and almost no dorsal hairs. These phenotypes reflect the loss of dorsal fates (Arora and Nusslein-Volhard, 1992). Defective movements of the germband are due to loss of the amnioserosa and loss of dorsal and dorsal-lateral fates in the ectoderm, and subsequent expansion of ventrolateral cell fates. From a cross involving *dpp*^{hr27}/+ heterozygous mutant parents, approximately 29% of fertilized embryos died. All of the dead embryos showed the characteristic dorsal defects usually observed in *dpp*^{hr27} homozygous mutant embryos (Figure 39A).

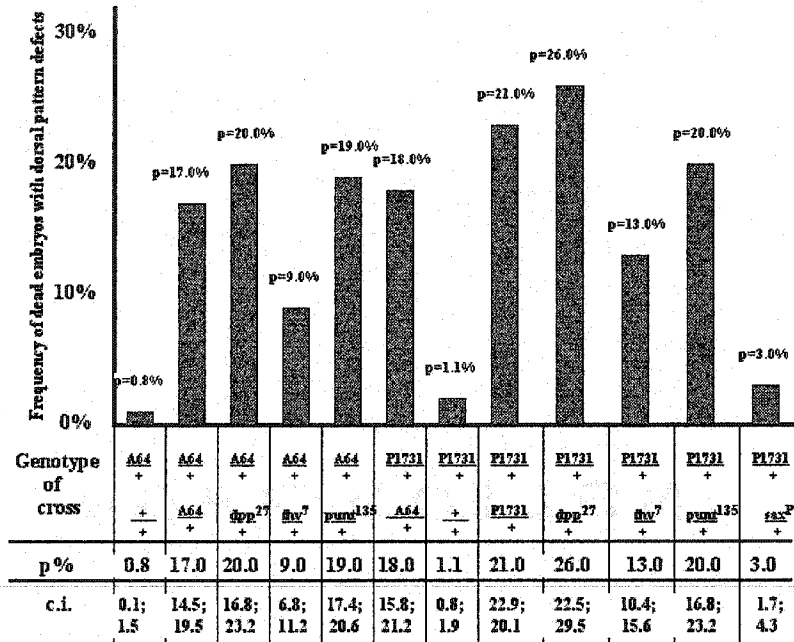
Crosses between *dpp*^{hr27}/+ (male) and *sgl*^{P1731}/+ (female) heterozygous parents, result in one quarter of the embryos dieing (see Table 14). The dead embryos display a strong U-shape, dorsal-open embryonic cuticle phenotype with head segment defects (Figure 39B). These defects are similar to *sgl*^{P1731} homozygous embryos and partial loss-of-function *dpp* mutants. This trans-heterozygous dominant phenotype is observed in approximately 26% of the embryos that were scored (Table 14). The trans-heterozygous combination of *dpp*^{hr27} with *sgl*^{A64}, a weaker allele of UDP-GlcDH, results in fewer (20%) dead embryos (Table 14). However, the dead embryos show a similar cuticle phenotype to that exhibited by *dpp*^{hr27}/+, *sgl*^{P1731}/+ embryos. In a control cross between *dpp*^{hr27}/+ and *Ore-R*, only 5% of the embryos died. Cuticle preparations of these embryos show slight dorsal pattern defects. Control crosses between *sgl*^{P1731}/+ or *sgl*^{A64}/+ adults and *Ore-R* (+/+) flies result in dead embryos with even weaker dorsal defects (e.g. posterior tail up) at a frequency of 1.1% and 0.8% respectively (Table 14).

Figure 39. Genetic interactions among *sgl^{P1731}*, *dpp*, *thv* and *punt* mutants.



(A) Unhatched *dpp²⁷/dpp²⁷* embryos are weakly ventralized showing head involution and tail-up defects. In most cases, the tail (posterior spiracles) is displaced into the embryo (arrow). (B) A trans-heterozygous *dpp²⁷/+; sgl^{P1731}/+* embryo shows a U-shaped defect with loss of head and cephalic structures (arrowhead), loss of dorsal epidermal cuticle, and dorsal displacement of the posterior spiracles (arrow), due to defects in gastrulation. (C) A *punt¹³⁵/punt¹³⁵* embryo typically results in a U-shaped dorsal-open phenotype (arrow). (D) A *punt¹³⁵/+; sgl^{P1731}/+*, trans-heterozygous embryo shows a similar U-shaped dorsal-open phenotype (arrow), in which the dorsal cuticle is reduced. (E) A *thv⁷/thv⁷* embryo showing a dorsal-open phenotype, with dorsally displaced posterior spiracles (arrowhead) and lack of dorsal anterior head segments (arrow). (F) A *thv⁷/+; sgl^{P1731}/+* embryo also shows similar dorsal open defects (arrow), resulting in a severe U-shaped phenotype, a dorsally displaced tail (arrowhead), and head-segment defects. Embryo orientation is anterior to the left and dorsal is up.

Table 14. Results of trans-heterozygous genetic interactions among *sgl* and *dpp* pathway mutant alleles.



Frequency of dead embryos with dorsal cuticle patterning defects observed in crosses involving heterozygous mutant parents of *sgl* and *dpp* pathway mutant alleles show dominant negative genetic interactions. The bar graph is a diagrammatic representation of the dorsal defective mutant phenotypes observed in dead embryos in control ($A64/+ \times +/+$) and trans-heterozygous (e.g., $A64/+ \times dpp^{27}/+$) crosses. To test if the dominant negative interactions among *sgl* and *dpp* pathway mutant alleles were significant, I used the confidence interval (c.i.) statistical analysis (Moore and McCabe, 1993). The total number of embryos ($n = 600$ plated embryos) of each cross (indicated below the bar diagram) was screened for the number of dead embryos (m) (embryos that did not hatch) with cuticle defects which included the involution of head segments, loss of dorsal cuticle, disruption of germband retraction and internalization of the posterior spiracles. The frequency of dead embryos with dorsal patterning defects ($p = m/n$) in the progeny was then calculated. The frequency of dead embryos with dorsal defects for $dpp^{27}/+$, $punt^{135}/+$, $thv^7/+$ and $sax^P/+$ heterozygous mutants males crossed to wildtype *OregonR* ($+/+$) females were 5% (ci: 3.6; 6.4), 1.2% (ci: 0.4; 2.0); 0.9% (ci: 0.1; 1.7) and 0.7% (ci: 0.1; 1.3) respectively (not shown in bar graph). The confidence interval (c.i.) for true mean of the population of each sample was determined as described in Table 11, is shown below the bar graph.

Patterning defects resembling those observed in *sgl* homozygous mutant embryos are also observed in embryos that are homozygous for mutations with the *punt* and *thv* receptors. Zygotic loss-of-function mutations of *punt*¹³⁵ (Figure 39C) and *thv*⁷ (Figure 39E) homozygous embryos fail to undergo dorsal closure, show a reduction in the dorsal cuticle, and result in retardation of germband retraction (Brummel et al., 1994; Nellen et al., 1994a,b; Penton and Hoffmann, 1994; Letsou et al., 1995). Again, the similar phenotypes observed between the *sgl*^{P1731} mutation, and these receptor mutants, further suggest that UDP-GlcDH interacts with *dpp*, and might represent a new component of the *dpp* signaling pathway.

To ascertain if mutations in these *dpp* receptors also genetically interact with UDP-GlcDH mutations, heterozygous combinations of *sgl*^{P1731} and *sgl*^{A64} with *punt*¹³⁵ and *thv*⁷ were made by crossing *punt*^{135/+} (chromosome III) and *thv*^{7/+} (chromosome II) males to *sgl*^{P1731/+} and *sgl*^{A64/+} females (Table 14). These heterozygous combinations resulted in dominant embryonic lethal interactions. In the case of *thv*^{7/+}; *sgl*^{P1731/+} embryos, 13% of the embryos that were scored died and showed dorsal pattern defects (Table 14). These trans-heterozygous embryos typically present loss of dorsal cuticle and anterior head segments, along with incomplete germband retraction (Figure 39F). *sgl*^{P1731/punt}¹³⁵ heterozygous embryos produce an even higher percentage of embryonic lethality, that resulted in approximately 20% of the embryos showing dorsal defects (Table 14). Again, cuticle preparations of these embryos display a dorsal-open phenotype (Figure 39D) typical of *punt*¹³⁵ homozygous embryos, along with loss of head structures and incomplete germband retraction. Heterozygous combinations with the *sgl*^{A64} mutant allele also gave dead embryos, with phenotypes similar to those observed for *sgl*^{P1731}. However, the number of dead embryos that showed dorsal defects is reduced (Table 14). Embryos heterozygous for either *punt*^{135/+} or *thv*^{7/+} alone resulted in dead embryos that showed dorsal defects at a frequency of only 1.2% and 0.9% respectively.

I used the confidence interval (c.i.) analysis (see bottom of Table 11) to determine the significance of the difference in the number of dead embryos with dorsal defects that were observed in trans-heterozygous crosses of *sgl* and *dpp* pathway mutants when compared to dead embryos in control crosses. Control crosses involved matings between *sgl* or *dpp* pathway mutant heterozygous mothers to wild-type Oregon-R (+/+) males. Using this statistical analysis, the lethality that was observed in the trans-heterozygous crosses between *sgl* and *dpp* pathway mutant alleles was shown to be significantly different from the percent lethality observed in each of the control crosses (see Table 14 and legend below). If the values for the confidence intervals from two different samples overlap, then the difference between the population means is not significant. However, if the confidence intervals do not overlap then it can be stated with 95% confidence that the difference between the population means is significant. A summary of the confidence interval from each sample of embryos for comparison is presented at the bottom of Table 14. Comparisons were made between experimental and control crosses.

Based on this analysis, it was concluded that the percent lethality observed for *dpp*^{hr27/+}, *punt*^{135/+} or *thv*^{7/+} heterozygous embryos was significantly enhanced by removing one wild-type

copy of the UDP-GlcDH gene (compare 95% c.i. values of control crosses with the trans-heterozygous crosses). This suggests that the activity of *dpp* is reduced below the threshold necessary for normal *dpp* function in the dorsal-most cells that require the highest level of *dpp* activity. UDP-GlcDH may therefore be a gene required for the proper transmission of the *dpp* signal. One interesting observation was that *sgl*^{P1731} in heterozygous combination with *punt*¹³⁵ (a *dpp* typeII receptor) resulted in a significantly stronger loss-of-function genetic interaction than observed with the *tkv*⁷ (a type I receptor) mutant (see Table 14). However, heterozygous combinations of *sgl*^{P1731} and the mutant *sax*^P (a second type I *dpp* receptor) did not result in a significant dominant negative interaction (Table 14). The removal of one wild-type copy of UDP-GlcDH gene in *sax*^{P/+} heterozygous embryos did not result in a significant increase in embryonic lethality with dorsal patterning defects.

These experiments demonstrate that UDP GlcDH and *dpp* pathway genes may interact during embryo development. Removal of one copy of UDP-GlcDH during early stage embryogenesis appears to dominantly block *dpp* signaling once the *dpp* signaling pathway has already been partially compromised by removing one copy of *dpp* or its receptors *thv* or *punt*. Mutants of UDP-GlcDH appear to be able to limit the function of *dpp* signaling to its target cells. The dominant negative interactions observed with *dpp*²⁷, *thv*⁷ and *punt*¹³⁵ suggest that UDP-GlcDH may play a direct role in mediating the interaction between the DPP ligand and its receptors. Such dominant negative interactions are reminiscent of those observed between *dpp* mutants and receptor mutants of *thv* and *punt* (Brummel et al., 1994; Nellen et al., 1994a,b; Penton and Hoffmann, 1994; Letsou et al., 1995). This dominant interaction between UDP-GlcDH mutations and the *dpp* receptors is consistent with results described by Haerry et al. (1997), who showed the suppression of the activated *thickveins* mutation by the UDP-GlcDH mutant allele *suppenkasper* (*sgl*^{SG9}).

In a reciprocal cross, where *sgl*^{P1731/+} males were crossed to females heterozygous for *dpp*^{27/+}, *thv*^{7/+} or *punt*^{135/+}, the frequency of dead embryos with dorsal cuticle defects was significantly reduced compared to the opposite crosses performed in Table 14. For example, *sgl*^{P1731/+} males crossed to *dpp*^{27/+} females resulted in dead embryos with dorsal mutant phenotype at a frequency of 12% (c.i.: 10.0, 14.0), whereas, *sgl*^{P1731/+} females when crossed to *dpp*^{27/+} males resulted in dead embryos with dorsal defects at a frequency of 26% (c.i.: 22.5; 29.5) (see Table 14). Control crosses that include *dpp*^{27/+} females crossed to +/+ males, or *dpp*^{27/+} males crossed to +/+ females, produced dead embryos that showed dorsal defects occurring at a frequency of 5% (c.i.: 3.3, 6.7) and 1.2% (c.i.: 0.8, 1.6) respectively. A similar reduction in the frequency of lethal phenotypes was observed with crosses that involved the *dpp* receptor mutants for *punt*¹³⁵ and *thv*⁷ (not shown). These preliminary tests suggest that the *sgl* mutants may have maternal-effects. Therefore, the maternal contribution of *sgl* may be critical for maximal *dpp* signaling, with respect to the initial dorsal-ventral patterning events in the embryo events following cellularization.

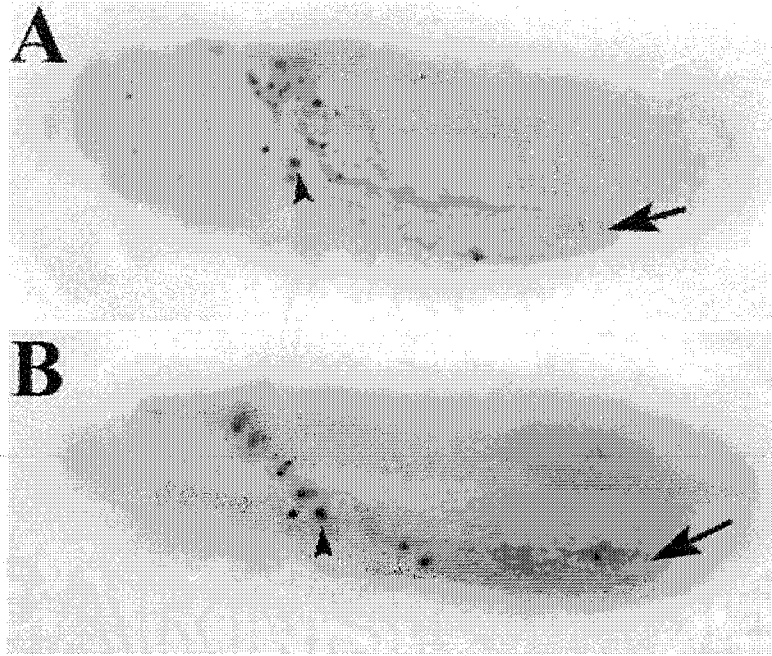
III-4iii. Regulation of *dpp* expression by UDP-GlcDH.

One possible explanation for the *dpp*-like phenotype, described for *sgl* mutants, could be that UDP-GlcDH is a downstream target gene of *dpp* signaling, which therefore would regulate UDP-GlcDH transcription. One could expect that a mutation in a target gene would prevent the proper read-out of the signal transduction by a cell, resulting in a *dpp*-like loss-of-function phenotype. This was tested by looking at UDP-GlcDH transcript accumulation in stage 11 *dpp^{hr27}* homozygous mutant embryos. The expression of UDP-GlcDH transcript in the amnioserosa shows no significant change in *dpp^{hr27}* homozygous mutant embryos (**Figure 40B**) relative to the expression in wild-type embryos (**Figure 40A**). Therefore, *dpp* does not appear to regulate UDP-GlcDH transcription. In the case of the *dpp^{hr27}* mutation, the dorsal/ventral patterning defects in the ectoderm and mesoderm do not result from loss of UDP-GlcDH transcription.

This leaves two other possible roles for UDP-GlcDH. UDP-GlcDH may be required for either expression of DPP protein, or transduction of the DPP signal. Disruption of either of these processes could be consistent with the mutant phenotype and genetic interactions that are observed. To test whether UDP-GlcDH affects *dpp* expression, the distribution of *dpp* transcripts in UDP-GlcDH mutant embryos was examined. *sgl^{P1731}/TM3,Sb* females were outcrossed to *Ore-R* males, the F1 *Sb+ sgl^{P1731}/+* sibs were then crossed, F2 embryos collected for 2 hr and allowed to develop for 8 hr until stage 11 of embryogenesis. These embryos were then stained with a DNA Digoxigenin-labeled full length *dpp* cDNA probe to look for presence of the *dpp* transcript. Assuming random and non-biased segregation of the chromosomes, approximately 25% of the embryos from this cross will be homozygous for the *sgl^{P1731}* mutations. The *dpp* transcript is normally expressed on the dorsal side of the embryo in ectodermal cells, during germband extension around stage 11 (Gelbart et al., 1985, see **Figure 41B**). In these wild-type embryos, expression is restricted to the ectodermal cells along the dorsal ridge abutting the amnioserosa (black arrow) and the lateral pits (white arrowheads) in the ectoderm. Expression is also localized to the hypopharyngeal lobe, the mandible and the maxilla head segments (black arrowheads). In *sgl^{P1731}* mutant embryos (stage 11), *dpp* transcript expression is unaffected (**Figure 41D**). This suggests that UDP-GlcDH is not primarily involved in transcriptional activation of *dpp* at a stage that would explain the embryonic lethal phenotype. This is relevant because ectodermal expression of *dpp* at around stage 10 is required for the specification of the underlying visceral mesoderm where *dpp* targets such as *evenskipped* and *tinman* are expressed (Frasch, 1995). Since *dpp* transcription levels remain unaffected in *sgl^{P1731}* embryos prior to stage 11, even though *sgl^{P1731}* affects the expression of EVE and TIN protein as shown earlier, the embryonic defects cannot be attributed to the loss of *dpp* transcripts.

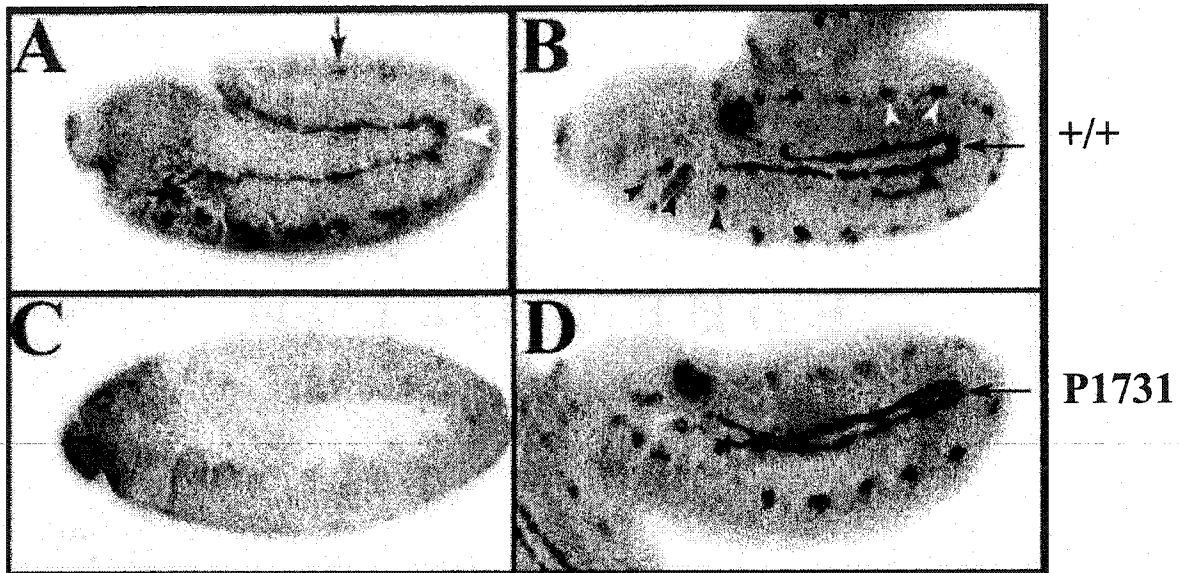
One alternative explanation may be that regulation of *dpp* signaling occurs at the level of the DPP protein expression or stability. UDP-GlcDH activity is involved in the production of glycosaminoglycans (GAGs) such as heparan sulfate and heparin. Heparin and heparan sulfate residues associated with proteoglycans have been implicated in the regulation of growth factor activity (see

Figure 40. Expression of the UDP-GlcDH transcript in WT and *dpp*²⁷ mutant embryos.



(A) Wild-type (+/+) stage 10 embryo stained for UDP-GlcDH transcript expression using a Digoxigenin UDP-GlcDH cDNA labeled probe. UDP-GlcDH transcript expression is detected in the amnioserosa (arrow). (B) shows *dpp*²⁷/*dpp*²⁷ mutant embryos, which result in dorsal defects in the embryo. These embryos were stained for UDP-GlcDH transcript expression and show no discernable changes in expression in the amnioserosa (arrow). UDP-GlcDH signal in *dpp*²⁷ mutants (B) appears comparable with that observed in wild-type embryos (A). Control (+/+) embryos and experimentals (*dpp*²⁷/*dpp*²⁷) were stained in parallel and stopped at the same time, to ensure that there was no bias in the intensity of the staining while the signal is being developed. The dark spots non-specific staining of amnioserosal cells that have undergone cell death (arrowhead). Lateral views of stage 10 embryos are shown. In both figures, anterior is to the left, and dorsal is up.

Figure 41. Expression of *dpp* in WT and *sgl^{P1731}* mutant embryos



Stage 11 embryos were stained for DPP protein (A, C) or *dpp* transcript (B, D) expression. (A, B) are wild-type and (C, D) are *sgl^{P1731}/sgl^{P1731}* embryos. (A) There is a high level of protein expression observed in cells along the dorsal ridge, abutting the amnioserosa (white arrowhead). Lower levels of DPP are also found in the head segments and lateral pits (black arrow) in each segment. In (B), *dpp* transcript is detected using a Digoxigenin labeled *dpp* cDNA probe. Expression is localized to the dorsal ridge cells (black arrow) and to the lateral pits (white arrowheads) of the embryo. Transcript expression is also localized to head segments (black arrowheads) starting from the most anterior, the hypopharyngeal lobe, the mandible and the maxilla. (C) Most of the DPP expression is lost from the dorsal ectodermal ridge and lateral pits. (D) *Dpp* transcript is localized along the dorsal ridge and remains unaffected in *sgl^{P1731}* mutant embryos (black arrow). The expression of *dpp* transcript in these embryos was not noticeably different from that of wild type embryos in (B). In all figures, anterior is to the left, and dorsal is up.

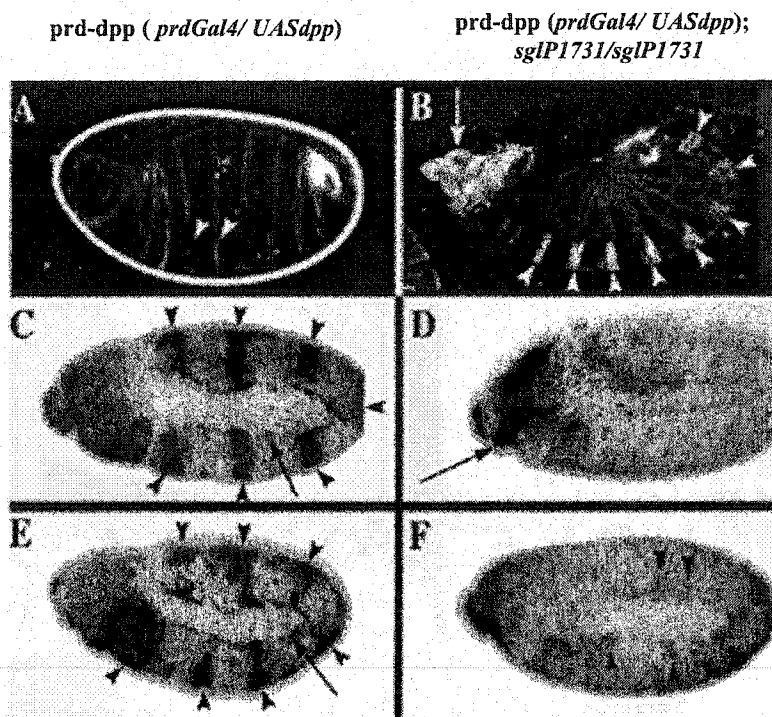
Introduction). The level of this regulation has been shown to occur at several levels, one which includes regulating protein expression by affecting translation or stability of the protein (reviewed in Jackson et al., 1991; Kjellen and Lindahl, 1991; Bernfield et al., 1999). DPP is normally expressed in cells along the dorsal ectodermal ridge at stage 11 (Figure 41A). When DPP expression is examined in *sgl^{P1731}* homozygous stage 11 embryos, approximately 19% of the embryos that were collected (from *sgl^{P1731}/+* heterozygous parents) and stained showed a reduction or complete loss of DPP protein expression in dorsal ridge cells (Figure 41C). This suggests that UDP-GlcDH function may modulate *dpp* signaling post-transcriptionally, regulating the levels of DPP protein, possibly by affecting its translation or stability once it is secreted. In *sgl^{P1731}* homozygous embryos DPP signaling activity would then be compromised, resulting in its inability to activate dorsal ectodermal and mesodermal patterning genes (see Figure 38). These results suggested that UDP-GlcDH may function downstream of *dpp* transcription.

III-4iv. Epistasis analysis of UDP-GlcDH and *dpp* mutations.

The results above can perhaps be most simply explained by a defect in *dpp* signaling efficiency resulting from a loss of UDP-GlcDH function. To test more directly if this is caused by an upstream or downstream affect of *sgl* mutations on *dpp* function, effects of overexpression of *dpp* in combination with embryos that were mutant for *sgl^{P1731}* were examined. This was accomplished by expressing *dpp* ectopically using the *GAL4-UAS* system (Brand and Perrimon, 1993) in embryos homozygous for *sgl^{P1731}*. *PrdGal4/prdGal4* flies were crossed with flies from a *UASdpp/UASdpp* homozygous stock. Embryos were collected for 2 hr and then allowed to develop for 30 hr. Approximately (78%) of the embryos died. Cuticle preparations of unhatched embryos revealed dorsalization of lateral and ventral cell fates caused by ectopic DPP expression. Ventral denticle belts were replaced by thin rows of dorsal hairs (see white arrowheads Figure 42A). A sample of these embryos was fixed at stage 11 of embryogenesis and stained using an antibody to DPP. In approximately half of the embryos that stained, DPP expression was detected in cells along the dorsal ectodermal ridge, representing the endogenous wild-type expression (see arrow Figure 42C), as well as in ectopic stripes in alternate segments (see arrowheads Figure 42C). However, the transformation of ventral to dorsal fate was not restricted to the alternate segments in which DPP was expressed. The fate of lateral and ventral cells in adjacent segments was also affected. This may be due to diffusion and a long range of influence of DPP protein. Dorsalization of the lateral and ventral cell fates was also shown by the ectopic activation of the DPP nuclear target, *tinman*. A sample of *prdGal4, UASdpp* embryos at stage 11, when stained with antibody to TIN protein, showed that TIN was expressed in broad *paired*-like stripes in the same lateral and ventral cells corresponding to ectopic DPP expression, in approximately half of the embryos that stained (see arrowheads Figure 42E). This shows that dorsalization of ventral cells is due to the ectopic activation of the *dpp* pathway.

When *prdGal4/prdGal4; sgl^{P1731}/+* males were crossed to *UASdpp/UASdpp; sgl^{P1731}/+* females (Figure 42B), over half (72%) (375/500) of the embryos died prior to hatching. Cuticle prepa-

Figure 42. Suppression of ectopic effects of *dpp* by the *sgl^{P1731}* mutation.



Ectopic expression of DPP in embryos from the *prdGAL4/UASdpp* (*prd-dpp*) line (A,C,E), and *prd-dpp; sgl^{P1731}/sgl^{P1731}* crosses (B,D,F). Cuticle preparations of (A) *prd-dpp* and (B) putative *prd-dpp; sgl^{P1731}/sgl^{P1731}* mutant embryos. (A) *Prd-dpp* in embryos results in severely dorsalized phenotypes indicated by the loss of denticle belts in the ventral cuticle of the embryo. The ventral denticle belts seem to be replaced by dorsal hairs (see white arrow heads) (B) A cuticle preparation of dead embryos from the *prd-dpp; sgl^{P1731}/sgl^{P1731}* cross show that the gain-of-function effect of ectopic *dpp* expression by *prd-dpp* is suppressed, resulting in a *sgl^{P1731}/sgl^{P1731}* homozygous mutant phenotype. In these embryos the ventral cuticle is restored, as is indicated by the presence of the ventral denticle belts (white arrowheads). However, these show head segment (white arrow), dorsal cuticle, and germband retraction defects typically observed in *sgl^{P1731}/sgl^{P1731}* homozygous mutant embryos. (C-D) show stage 11 embryos from the same crosses stained with an antibody to DPP. (C) In a *prd-dpp* embryos DPP is expressed in pair-rule stripe patterns (see black arrowheads). Endogenous expression is also observed in cells along the dorsal ectodermal ridge (see black arrow) and the head segments. (D) In some embryos from the *prd-dpp; sgl^{P1731}/sgl^{P1731}* cross, the DPP paired stripes and endogenous DPP expression patterns are not present except for DPP expression in the head (see black arrow). (E-F) Stage 11 embryos from the same crosses stained with an antibody to TIN. (E) In the *prd-dpp* embryos TIN protein is expressed in a pattern similar to that of DPP, showing that cells are responding to the ectopic *dpp* signal (arrowheads). Endogenous TIN expression was weak along the dorsal ectodermal ridge (arrow). (F) In embryos from the *prd-dpp; sgl^{P1731}/sgl^{P1731}* cross, TIN expression is almost completely absent in some embryos. Very low expression remains in cells close to the dorsal ridge in the ectoderm (see arrowheads).

rations of these unhatched embryos gave two different patterning defects. Approximately 73% (275/375) of the dead embryos showed a dorsalized phenotype as observed in *prdGal4,UASdpp* embryos as described above (Figure 42A). Of the remaining dead embryos, approximately 14% (52/375) resulted in the *sgl*-like (UDP-GlcDH loss-of-function) mutant phenotype (Figure 42B). Assuming random and non-biased segregation of the chromosomes, the fraction of dead embryos showing the *sgl*-like mutant phenotype is consistent with the dead embryos being homozygous for *sgl*^{P1731}. The remaining 13% of the dead embryos showed no apparent cuticle defects. However it is not known if lethality in these embryos is due to the embryos being *prdGal4/UASdpp*; *sgl*^{P1731}/*sgl*^{P1731} or *prdGal4/UASdpp*; +/+, in which case the expressivity of the ventralized or dorsalized phenotypes is not noticeable in this assay. Thus, the effects of ectopic DPP expression seem to be suppressed by the *sgl*^{P1731} homozygous mutation. This implies that this gene functions downstream of *dpp*, consistent with the above results showing that UDP-GlcDH does not directly affect *dpp* transcription.

A sample of stage 11 embryos from the cross in Figure 42B, that were fixed and stained with an antibody to DPP, gave a number of embryos that showed a loss of the normal dorsal ectodermal expression along with ectopic striped expression of DPP (Figure 42D). The loss of DPP expression is likely due to the loss of UDP-GlcDH function caused by the fact that these embryos were also homozygous for the *sgl*^{P1731} mutation. Expression in the head segments is reduced but not completely lost. This is consistent with results shown in embryos that were solely homozygous for *sgl*^{P1731} mutation (Figure 42B), suggesting that, in the absence of UDP-GlcDH function, the levels of both endogenous and ectopic DPP may be compromised, thereby affecting the signaling efficiency of the *dpp* pathway. When a sample of embryos in Figure 42B was stained using antibody to TIN, the expression of TIN was almost completely lost (see arrowheads Figure 42F). This showed that these embryos were deficient in *dpp* signaling, possibly as a result of loss of DPP caused by a loss of UDP-GlcDH function. In conjunction with the results in Figures 40 and 41, UDP-GlcDH function seems to modulate *dpp* signaling at the level of DPP. Could UDP-GlcDH enzyme somehow affect DPP activity by regulating its translation in the endoplasmic reticulum, or affecting its modification through Golgi prior to its secretion from the cell, thus making the DPP more susceptible to degradation? Is this effect on DPP function direct or indirect, in other words, does UDP-GlcDH enzyme affect DPP function by affecting the synthesis and function of a second factor required for regulating DPP translation or modifications?

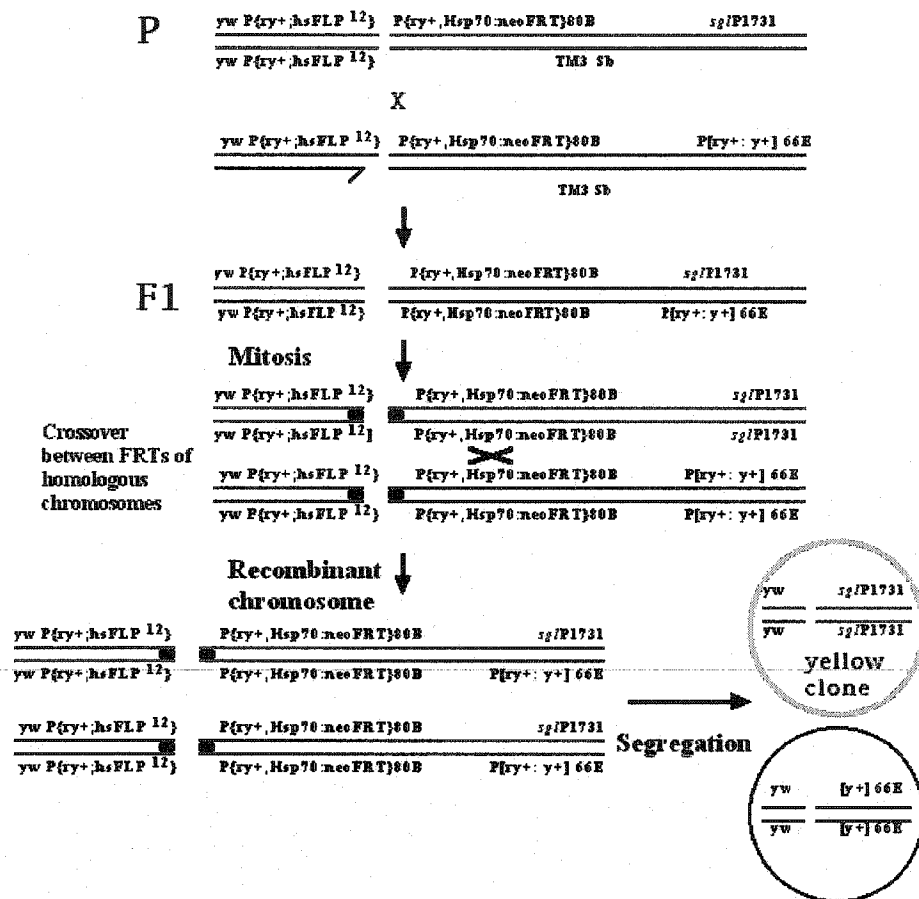
III-4v. Mosaic analysis of UDP-GlcDH function

To help further understand the role of UDP-GlcDH, a mosaic analysis using *sgl* mutants of UDP-GlcDH was carried out in imaginal discs. This helps to determine at what level in the cell UDP-GlcDH function is required. Based on the results from the mosaic analysis of somatic clones in adults, one can determine if UDP-GlcDH function is cell autonomous (function is required in the cell) or cell non-autonomous (function is required outside of the cell, possibly affecting the behavior of adjacent cells). Somatic clones of *sgl*^{P1731} were generated in imaginal discs using the hsFLP/FRT recombina-

tion system (Xu and Rubin, 1993). The *sgl^{P1731}* allele of UDP-GlcDH was chosen because it is a strong loss-of-function mutation. Since *sgl^{P1731}* is an embryonic lethal mutation, it was necessary to induce homozygous somatic mutant clones in larval stages. If a mutant clone of UDP-GlcDH affects cell fates in the imaginal discs, re-specification of cell fates would be observed as changes in the pattern of adult structures derived from imaginal discs. These changes would be expected to correlate with the presence of phenotypically marked *yellow* (*y*-) mutant clones. The *yellow* mutant is a visible viable mutant that is used to mark somatic clones in the adult cuticle. If UDP-GlcDH function acts either at the cell surface or within a cell to help activate transduction of a signal such as *dpp* or *wg*, deletion or changes in the pattern of normal cuticular structures would only be localized within the loss-of-function *sgl^{P1731}* marked clones (autonomous effect). In a cell non-autonomous effect, the *sgl^{P1731}* marked clones would consist of affected (mutant phenotype) and non-affected (wild-type phenotype) *sgl^{P1731}* mutant cells, that are marked with *yellow*. With this type of non-autonomous clonal effect the cells at the edge of the *sgl* mutant clone might be rescued by adjacent wild-type cells, which are *sgl⁺*. The result would be yellow cells that show no phenotypic effects of their *sgl* mutation. In this case, cells that express UDP-GlcDH would compensate for the loss of UDP-GlcDH in adjacent *sgl* mutant cells. This behavior in *sgl* clones would suggest that the gene encodes a secreted factor or is responsible for the production of a second factor, whose function is required outside of the cell.

I constructed recombinant lines which were used to mark somatic clones homozygous for *sgl^{P1731}*. These lines carried a transgene which contained a cassette consisting of a heat shock protein 70 promoter linked to a Flipase gene (*hsFLP*) on the X chromosome, a Flipase recombine target site (FRT) cassette, a series of markers on the left arm of the third chromosome (Xu and Rubin, 1993), and the *sgl^{P1731}* mutant. See **Figure 43** for a description of the crossing scheme used to generate somatic *sgl^{P1731}* mutant clones marked with the *yellow* (*y*) mutant gene. As shown in **Figure 43**, this was accomplished by crossing *y w hsFLPase12/y w hsFLPase12; FRT80B, sgl^{P1731}/TM3, Sb* females with *y w hsFLPase12; FRT80B, y⁺66E/TM3, Sb* males. F1 larvae were heat-shocked at late first (36 hr after egg lay) and early second (60 hr after egg lay) instar, to induce the expression of the *hsFLPase* and produce large mitotic clones of *sgl^{P1731}*. The F1 *y⁺, Sb⁺* adult legs and wings were scored for the presence of yellow marked clones in addition to any morphological defects. Results are shown in **Figure 44** and **Table 15**. From a total of 795 wings that were scored from three separate experiments (see **Table 15**), I observed 189 that contained *yellow* clones visible along the wing margin (arrows, **Figure 44B**). Forty-three of those wings that contained *yellow* clones had morphological defects, the most common consisted of deletions along the wing margin (arrow **Figure 44A**). In **Figure 44A** we see a loss of anterior wing margin as a result of a *sgl^{P1731}* mutant clone. Loss of wing margin tissue was found in both anterior and posterior wing compartments. However, the majority of wings that contained *yellow sgl^{P1731}* clones show no morphological abnormalities (see **Figure 44B**). This suggested that the region of the yellow clones that were mutant for *sgl^{P1731}*, but that appeared normal, was rescued by neighboring non-*yellow* (non-mutant *sgl⁺*) cells, suggesting that UDP-GlcDH function is non cell-autonomous.

Figure 43. Somatic clonal analysis of *sgl^{P1731}* in the imaginal leg disc.



FLP/FRT system

y : recessive yellow mutant

y+ : wild type yellow gene

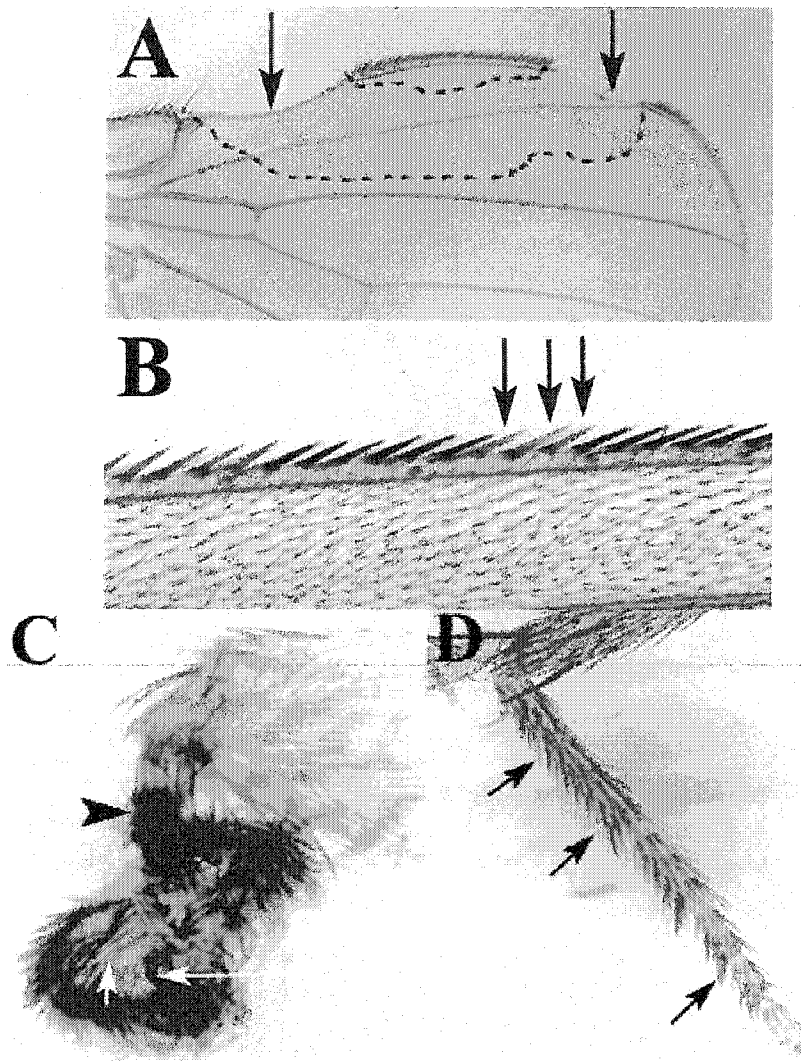
FRT : FLP recombinase target site

FLP : flip recombinase enzyme

sgl^{P1731} : lethal gene of interest

Schematic representation of the events leading to the generation of somatic mutant clones using the FLP recombinase (FLP) and its target site (FRT). The figure shows the crossing scheme used for generating *y* (*yellow*), *sgl^{P1731}* mutant somatic clones in adult flies. Somatic clones are induced during mitosis in imaginal disc cells. P1 flies were allowed to lay eggs for 24 hr at 25°C, and were then removed from the vial. F1 larvae were heat-shocked at 36 hr (AEL) and 60 hr (AEL) for 1 hr at 37°C to activate the expression of the FLP recombinase. After FLP generates a crossing-over event between the FRT sites, which are proximal to the *y+* wild-type allele and the lethal locus *sgl^{P1731}*, mitotic segregation of the chromatids either produces cells that carry two copies of the *y+* (*yellow* wild-type gene) and two copies of the wild-type gene of *sgl* (*wild-type* clone) or results in cells that are homozygous mutant for *sgl^{P1731}*, generating *yellow* cells in adult tissue (*mutant* clone) (see Figure 44).

Figure 44. Effects of *sgl^{P1731}* somatic clones in legs and wings.



(A) Large clones of *sgl^{P1731}* induced during early second larval instar result in loss of wing margin as observed by the notches in the wing blade (black arrows). The black dash line demarcates the position of the yellow clone. (B) Dorsal wing margin (40X objective) showing effects of *sgl^{P1731}* clones generated during 3rd larval instar, these result in small patches of yellow clones of yellow bristles (arrows) interspersed with normal bristles. The yellow bristles in the clone appear light in a black and white photo. No patterning defects are observed in these small clones. (C) Severe morphological defects result from large clones of *sgl^{P1731}* in an adult leg induced during the early stages of second larval instar. The long white arrow marks the distal claw structure. The short black arrow points to a yellow bristle. The white arrowhead points to necrotic tissue. (D) Smaller clones of *sgl^{P1731}* in the leg result in patches of yellow bristles (black arrows) and are not associated with any morphological defects.

Table 15.
Mosaic analysis of *sgl^{P1731}* somatic clones in the adult wing and leg.

Expt.	Total # of adults scored	# legs scored	# of wings with y marked clones	# of legs with y marked clones	# of abnormal wings with y marked clones	# of abnormal legs with y marked clones
		# wings scored				
1.	200	1020	—	114	—	15
		180	71	—	14	—
2.	166	811	—	119	—	11
		300	62	—	13	—
3.	175	990	—	111	—	7
		315	56	—	16	—
Total	541	2821	—	344	—	33
		795	189	—	43	—

Table 15 depicts the frequency of yellow marked clones associated with morphologically normal or abnormal adult wings and legs. The high number of yellow marked clones that are homozygous for *sgl^{P1731}*, observed in legs or wings that show no obvious morphological phenotypic defects, suggests that UDP-GlcDH function in the tissue is cell non-autonomous (see text).

Twelve percent (344 of 2821, see **Table 15**) of the legs that were scored had *yellow* marked clones. Only 33 of these 344 legs showed any morphological defects. In each of these cases, the leg was severely deformed and only certain bristles types (e.g. the apical bristle) or structures like the claw could be discerned with any confidence (long arrow, **Figure 44C**). In **Figure 44C**, structures that are distal to the femur are lost or have gross defects; the bristles and a distal claw have formed, yet the segmental structure is lost, resulting in a spherical mass of tissue. A large group of *yellow* bristles that would normally mark the presence of a mutant clone could not be distinguished in these legs. More often, a few *yellow* bristles are observed that are isolated among normal-looking bristles. One possibility is that most *sgl*^{P1731} mutant cells in the clone die. As observed in wings, 90% of legs that were scored (311 of 344) showed *yellow* clones without any morphological defects (**Figure 44D**). Typically, the small *yellow sgl*^{P1731} clones, denoted by *yellow* bristles (see arrows) are observed in a leg; and they are surrounded by normal bristles. These clones show no abnormal phenotype, suggesting that the wild-type cells that surround them are able to rescue the *sgl*^{P1731} mutant cells. However, in the larger mutant clones in the leg, only the peripheral cells are rescued, as the rest of the mutant clone may cause gross phenotypic defects in the leg, such as those observed in **Figure 44C**. Dark necrotic regions that are observed along with the abnormal morphological phenotype (arrowhead, **Figure 44C**) may be due to dead cells in the clone, caused by the *sgl*^{P1731} mutant.

To show that the abnormalities associated with the *yellow* clones in the wing and leg are due to the *sgl*^{P1731} homozygous mutation, *yellow* marked clones were induced in wild-type (*sgl*^{+/sgl}⁺) imaginal discs. For the generation of these adult somatic clones in the wing and leg, the same cross was repeated in the absence of the *sgl*^{P1731} mutation (see **Figure 43**). Larvae from this cross were heat-shocked at first and early second instar as before. Adults of the target class with *yellow* clones in both the wing and leg were observed but showed no abnormalities, except for bent legs and blisters in the wing at frequencies of 0.8% and 1.1 %, respectively, in the adult target class. This supports the conclusion that abnormalities associated with *yellow* clones in the target class containing *sgl*^{P1731} mutation are due to loss of UDP-GlcDH function in those cells.

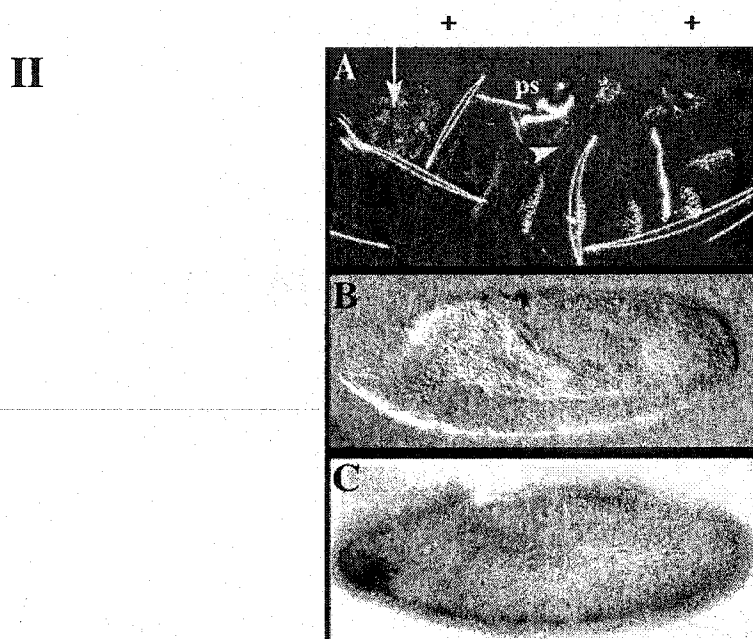
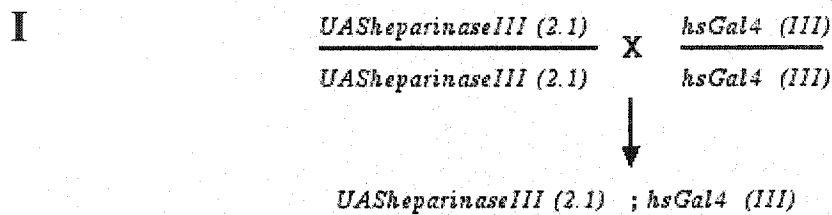
Somatic clones of mutations in genes such as *dpp* typically behave cell non-autonomously in mosaics. That is, somatic clones that are homozygous for mutations in *dpp* can form structures that look morphologically normal. This is because signaling from wild-type cells surrounding the clone can rescue the mutant cells. However, this is not true for mutations in genes encoding the *dpp* receptors, or for other intracellular components of its signal transduction pathways in the target cells. Clones that are homozygous for mutations in these genes (e.g., *thv*, *punt*, *mad*, *medea*, *schnurri*) act cell autonomously, so that morphological defects coincide with the mutant marked cells. Mutant clones of *sgl*^{P1731} behave much like those of *dpp*. Thus, the non-cell-autonomous behavior of *sgl*^{P1731} suggests that UDP-GlcDH function is required outside of the cell. This non-cell-autonomous behavior of UDP-GlcDH, along with the effects of DPP expression in *sgl* mutant embryos, would place UDP-GlcDH function upstream of the *dpp* receptors *thv* and *punt*.

UDP-GlcDH activity is localized in the cytoplasm of the cell. The non-cell-autonomous behavior of UDP-GlcDH suggests that its functional readout is required outside of the cell (extracellularly). This raises the question of how UDP-GlcDH carries out its cell-non-autonomous effects. As stated earlier, UDP-GlcDH is involved in the production of glucuronic acid, a saccharide that is a component of complex polysaccharides called glycosaminoglycans (GAGs). The majority of GAGs produced by a cell are localized to the ECM, usually associated with the extracellular domains of various proteoglycans found on the surface of the cell or in the ECM (see Introduction for details). Heparan sulfate is a biosynthetic product of UDP-GlcDH and represents the majority of GAGs associated with the ECM. Therefore, a loss of UDP-GlcDH function in the cell would result in the loss of heparan sulfate GAG production, and a depletion of heparan sulfate GAGs in the ECM. It was shown that the *wg*-like loss-of-function phenotype as seen in germline clones of *sgl*^{P1731} was due to a depletion of heparan sulfate in embryos (Binari et al., 1997; Hacker et al., 1997). Hacker et al. (1997) looked at the production of heparan sulfate GAGs in germline clones of *sgl*^{P1731}. They showed that in extracts from *sgl*^{P1731} germline clones heparan sulfate GAGs were absent. Binari et al. (1997) showed in a direct test, in which heparinase III degradative enzyme was injected into precellularized embryos, that the *wg*-like phenotype was caused by a direct loss in heparan sulfate GAGs in the embryo. Only embryos injected with heparinase III (also called heparanase), an enzyme specific for heparan sulfate GAG degradation, resulted in *sgl* germline clone phenotype. Injection of other degradative enzymes such as heparinase I (specific for heparin sulfate) and chondroitinase ABC (specific for chondroitin 4-sulfate, chondroitin 6-sulfate and dermatan sulfate) did not mimic the *sgl* germline clone phenotype. This implicated heparan sulfate, an ECM component, as a crucial moiety required in mediating *wg* signaling during embryonic patterning. Therefore, the non-cell-autonomous behavior of UDP-GlcDH mutant clones is consistent with the hypothesis that heparan sulfate is the component of the ECM through which UDP-GlcDH may regulate function of growth factors such as DPP and WG.

III-4vi. Ectopic expression of heparinase III in cellularized embryos.

To see if the effects of UDP-GlcDH on DPP function might be mediated indirectly through the action of heparan sulfate GAGs in the ECM, I looked at the effects of over expression of heparinase III using the *hsGAL4/UAS* expression system in embryos (Figure 45). As previously shown by Binari et al. (1997), injection of active heparinase III [cloned from *Flavobacterium heparium* (Hopwood, 1989; Sasisekharan et al., 1993; Ernst et al., 1996) and expressed and purified from serum of S2 (*Drosophila* Schneider) cells] into *Drosophila* pre-cellularized blastoderm embryos, depleted heparan sulfate GAGs in the embryo. This resulted in a *wg*-like mutant phenotype as observed in *sgl* germline clones. Thus, heparan sulfate moieties were identified as crucial GAGs in mediating the *wg* signal. A *hsp70-Gal4* line was crossed with a line carrying the *UAS-heparinase III* transgene (provided by the Manoukian lab, University of Toronto, Ontario Cancer Institute, see Figure 45-I) that contained the 5' signal sequence that would allow for its secretion out of the cell. Heparinase III enzyme was ectopically expressed in cellularized stage 5 embryos, between 2 to 3 hr after egg deposition. Ectopic expression of heparinase III in these embryos resulted in 68% embryonic lethality prior to hatching (Table 16).

Figure 45. Expression of heparinase III degradative enzyme inhibits *dpp* signaling in the embryo.



(I). Crossing scheme used to generate embryos that express heparinase III degradative enzyme. Embryos were collected from 0-1 hr at 25°C, allowed to develop for 1 hr at 25°C, and heat shocked for 10 min at 37°C. Half of the embryos were aged for another 6 hr at 25°C, then fixed and stained for *Kruppel* (KR) and *tinman* (TIN) expression respectively. The remaining embryos were allowed to develop for another 20 hr at 25°C to analyze the cuticle phenotype. **II.** Ectopic expression of heparinase III using *hsGal4/UAShepIII* in wild-type embryos. **(A)** The cuticle from an embryo where heparinase III was expressed. Upon differentiation of these embryos, cuticles show head involution defects (white arrow), incomplete germband retraction resulting in the dorsally displaced posterior spiracles (**ps**) and loss of dorsal cuticle pattern (white arrowhead). **(B)** In stage 11 *hsGal4/UAShepIII* embryos stained for *Kruppel* protein expression, KR expression in the amnioserosa is lost. **(C)** Similar embryos stained for *tinman* protein expression show a loss of TIN expression in the dorsal ectoderm and mesoderm. TIN expression in the head is unaffected. All panels in **(II)** show a lateral view of embryos, with anterior to the left and dorsal up. The frequency of dead embryos observed with a dorsal defective U-shaped phenotype is shown in Table 16.

Table 16.
Frequency of lethal phenotype in heparinase III treated embryos.

Crosses	% Dead U-shaped embryos
<i>hsGal4 (III)</i> <u><i>hsGal4 (III)</i></u>	0 (n=500)
<i>UAShep 2.1 (II)</i> <u><i>UAShep 2.1 (II)</i></u>	0 (n=500)
<i>hsGal4 (III);</i> <i>UAShep 2.1 (II)</i> non-heat treated	0 (n=500)
<i>hsGal4 (III);</i> <i>UAShep 2.1 (II)</i> heat treated	68 (n=500)

Heat treatments of *UAShep2.1/UAShep 2.1*, *hsGal4/hsGal4* embryos resulted in dead embryos with a U-shaped dorsal defective cuticle pattern. The controls *UAShep 2.1/ UAShep 2.1*, *hsGal4/hsGal4* (non-heat treated), *hsGal4/hsGal4* (heat treated), and *UAShep 2.1/ UAShep 2.1* (heat treated) resulted in no dead embryos with U-shaped dorsal defects. n is the number of embryos that were scored from each cross.

Cuticles from these embryos showed a severe U-shape phenotype, loss of dorsal cuticle fates and anterior head structures, similar to the zygotic lethal phenotype observed in embryos homozygous for *sgl* mutant alleles (Figure 45-IIA). Control embryos showed no such effects (Table 16). To analyze if *dpp* signaling was affected, the expression of both KR and TIN in stage 11 embryos was examined. Loss of expression was observed for both KR (Figure 45 II-B), and TIN (Figure 45 IIC) protein in embryos that expressed the heparinase III enzyme. This shows that *dpp* signaling is severely compromised in heparinase III treated embryos. The ability to phenocopy the *dpp* mutant phenotype of *sgl* by over expressing the heparinase III enzyme in the embryo, suggests that heparan sulfate GAGs may be crucial moieties required to modulate DPP signaling.

III-4vii. Ectopic expression of UDP-GlcDH results in dorsalized embryos.

If loss of UDP-GlcDH function results in loss of *dpp* signaling, one would predict that overexpression of UDP-GlcDH might result in enhancement of *dpp* signaling. Reichsman et al. (1996), has shown in *Drosophila* Schneider (S2) cell line that loss of heparan sulfate GAGs in WG-responsive cells reduced *wg* signaling. Addition of exogenous heparin or heparan sulfate to these cells was able to restore WG activity. Binari et al. (1997) later showed that injection of heparan sulfate into pre-cellularized embryos in *Drosophila* results in the conversion of ventral denticle into naked cuticle, mimicking the ectopic effects of *wg* signaling and a gain-of-function of WG activity. These two studies suggest that heparan sulfate GAGs are able to directly up-regulate WG activity and possibly ectopically activate *wg* signaling.

Gain-of-function mutations that cause ectopic activation of the *dpp* signaling pathway in an embryo result in dorsalized cuticle phenotypes. Ectopic expression of UDP-GlcDH was carried out using a *hsp70-UDP-GlcDH* (full *Drosophila*) cDNA transgene (Binari and Staveley, Manoukian lab, unpublished) to drive the expression of UDP-GlcDH throughout the embryo at any stage. This resulted in an increase in heparan sulfate GAG expression (Manoukian lab, unpublished).

Ectopic expression of UDP-GlcDH was induced between 2 and 3 hr (in cellularized blastoderm embryos) following egg deposition (stage 5), for 12 to 15 min at 37°C. Close to half of the embryos failed to hatch (Table 17). About 3/4 of the dead embryos showed a significant narrowing or a complete loss in ventral denticle belts that were replaced by dorsal hairs (see Figure 46A), which extended into lateral and ventral regions of the embryo. This suggests that ventral cells adopted dorsal cell fates. However, transformation into dorsal cell fate was incomplete. The naked cuticle could also be interpreted as the result of an increase in *wingless* signaling. This could explain the observed defects in the head segments and naked cuticle, but would not explain the presence of ectopic dorsal hairs and the internal displacement of the posterior spiracles.

To determine if ectopic expression of UDP-GlcDH results in the ectopic activation of the *dpp* signalling pathway in more ventral cells, the expression of TIN in a sample of the same heat treated

Figure 46. Effects of ectopic expression of UDP-GlcDH in the embryo.

Ectopic expression of UDP-GlcDH activates the *dpp* signaling cascade. (A) Cuticle of an embryo in which UDP-GlcDH was ectopically expressed by a heat-shock *sgl* transgene (*hs-sgl*) at 2 hr into embryogenesis. This results in the loss of ventral denticle pattern which is replaced with dorsal lateral cuticle and anterior head deletions (white arrow-head). The white arrows point to some of the remaining ventral denticles (Orientation: a ventral view with anterior to the left.). (B) Stage 11-12 non-*hs-sgl* embryo stained for expression of TIN. Normal TIN expression is visible along the dorsal ectodermal ridge, the underlying dorsal mesoderm and the anterior head segment in the clypeolabrum, optic lobe and mandible. (C) In a heat shocked *hs-sgl* stage 11-12 embryo, TIN expression expands into ventral lateral and ventral mesodermal regions of the embryo. (D) DPP expression show no effects on the normal expression pattern of DPP, in heat treated *hs-sgl* transgenic stage 11-12 embryos. Compare panel (D) in this figure with the wild-type expression pattern in Figure 41A. Panels (B) to (D) show a lateral view of embryos, with anterior to the left and dorsal up.

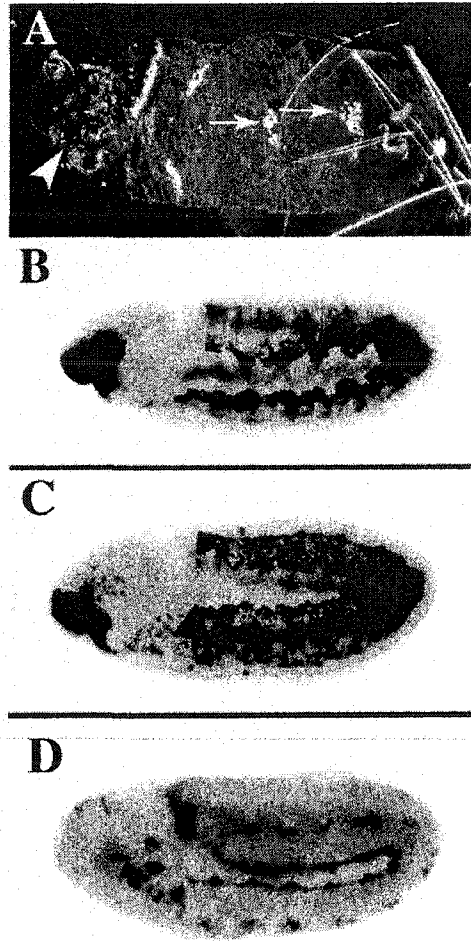


Table 17. Number of lethal and dorsalized phenotypes generated by ectopic expression of UDP-GlcDH (*sgl* cDNA) during embryogenesis.

Number of dorsalized phenotypes induced upon the ectopic expression of *sgl* cDNA transgene during embryogenesis. Control embryos that carried the *sgl* full-length cDNA, but were not heat shocked (non-HS) showed no observable phenotypic effects. Over half of the embryos that were heat shocked prior to cellularization died. Of the dead embryos, 70% showed a dorsalized cuticle phenotype.

Treatment	# of embryos	Cuticle phenotype	
		# dead embryos	#dorsalized embryos
<i>hs sgl</i> non-HS	500	23	0
<i>hs sgl</i> HS	500	235	168

embryos was also monitored. *Hsp70-UDP-GlcDH* embryos were collected for 2 hr and then heat shocked at 37°C for 12-15 min. The embryos were then allowed to develop for another 6 hr until stage 11, and stained for TIN expression. Normally, TIN protein is localized to cells in the dorsal ectoderm along the dorsal ridge and the underlying mesoderm (Figure 46B). After ectopic activation of UDP-GlcDH, TIN protein expression expands ventrally into ventral lateral and ventral cells (Figure 46C). These results show that the loss of ventral lateral and ventral cell fates by ectopic expression of UDP-GlcDH is due to ectopic activation of downstream targets of the *dpp* signaling pathway that are normally expressed in dorsal tissue. However, when stained using an antibody to DPP a normal pattern of expression was observed in these embryos. No ectopic expression of DPP was detected in lateral or ventral cells of the embryo (Figure 46D, compare to 41D). Therefore, the overexpression of UDP-GlcDH enzyme, which may cause an increase in heparan sulfate GAG expression, is able to ectopically activate the *dpp* signaling pathway without ectopically increasing DPP expression.

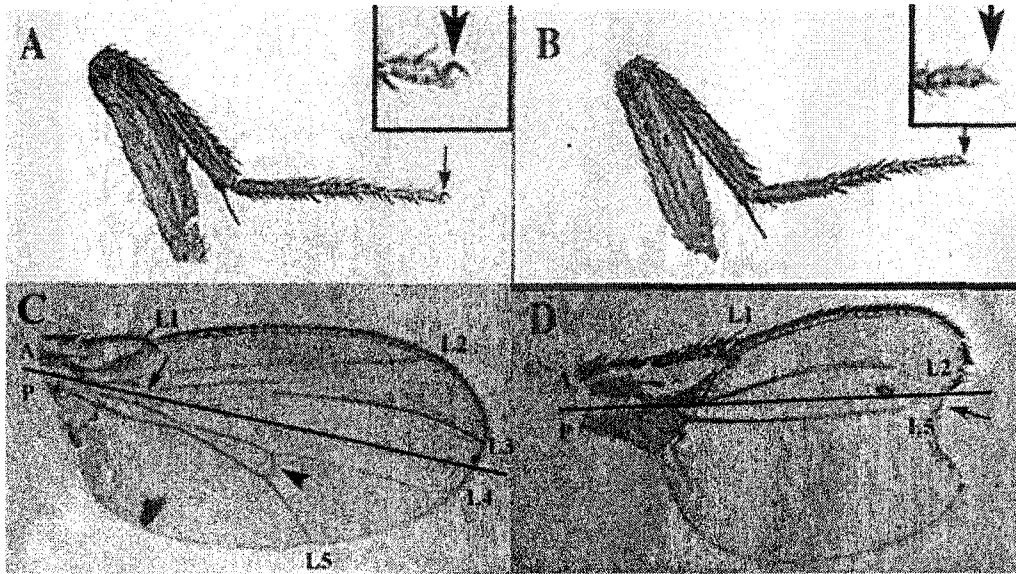
III-5. Role of UDP-GlcDH function in imaginal disc pattern formation.

The detection of UDP-GlcDH in the imaginal disc regeneration screen for novel patterning genes suggested a role that had not been previously suspected for this gene. Therefore, we decided to investigate what function UDP-GlcDH has in imaginal disc pattern formation. Based on the results presented above on its role in regulating *dpp* signaling during embryogenesis, the initial analysis looked at effects of *sgl* on *dpp* disc specific mutants. Genetic evidence has shown that *dpp* signalling is required for imaginal disc pattern formation and development. The disc-defective class of mutations in *dpp* results in variable loss of distal leg and wing structures (Gelbart, 1989). *Dpp* is expressed in a stripe of cells in the anterior compartment that runs adjacent to the anterior/posterior compartment boundary. It has been shown that *dpp* activity can influence A-P patterning of a wing disc and the dorsal compartment of leg discs (Zecca et al., 1995, Nellen et al., 1996; Lecuit et al., 1996). Furthermore, *dpp* can affect the process of patterning the proximal-distal axis (Lecuit and Cohen, 1997). Therefore, I examined whether UDP-GlcDH regulation of *dpp* signaling extended to imaginal disc patterning.

III-5i. Regulation of *dpp* signaling by UDP-GlcDH during imaginal disc patterning.

Evidence to support a role for UDP-GlcDH function in *dpp* signaling was sought by testing the ability of the *sgl*^{P1731} mutant to enhance the adult phenotypes of *dpp* mutations (see Figure 47). To do this, I tested whether the removal of one copy of UDP-GlcDH can enhance the *dpp* phenotypes of weak disc-specific *dpp* mutant alleles in adult legs or wings. Basler and Burke (1996) showed that the *dpp* allelic combinations *dpp*^{d5}/*dpp*^{d6} and *dpp*^{d5}/*dpp*^{hr4} result in minor defects in adult leg and wing anatomy, respectively. For example, 5% of *dpp*^{d5}/*dpp*^{hr4} adult wings showed a loss of the anterior crossvein (arrow Figure 47C). In about 2% of *dpp*^{d5}/*dpp*^{d6} adult legs one observes loss of claws in the leg; however, in most cases the legs are normal (Figure 47A). Basler and Burke (1996) also showed that the removal of one copy of the *sax* or *thv* receptor gene could dominantly enhance the adult phenotype in the *dpp*^{d5}/*dpp*^{hr4} flies, causing a substantial loss of medial wing tissue. In

Figure 47. Genetic interactions between *sgl^{P1731}* mutation and *dpp* disc mutant alleles in the wing and leg



The *sgl^{P1731}* mutant allele dominantly enhances the loss-of-function phenotypes generated by weak *dpp* disc mutant alleles in adult fly wings and legs. (A) and (C) show the weak phenotypes generated by weak hypomorphic disc mutant alleles of *dpp*. (B) and (D) show that losing one wild-type copy the UDP-GlcDH gene can dominantly enhance the phenotypes of weak *dpp* loss-of-function disc mutants. (A) The heterozygous combination of *dpp^{d5}/dpp^{d6}* exhibits no phenotypic effect in the adult leg. The black arrow marks the position of the distal claw on a leg. For a close-up see inset in top right-hand corner. (B) Trans-heterozygous combinations of *dpp^{d5}/dpp^{d6}*; *sgl^{P1731}/+* adults show loss of the claw in the adult leg (see black arrow). For a close-up see inset in top right-hand corner. (C) The heterozygous combination of *dpp^{hr4}/dpp^{d5}* resulted in a very weak phenotypic effect (e.g., loss of the proximal cross vein in the anterior compartment). The arrow marks the position where the proximal cross vein would be normally found. The black arrowhead points to the posterior cross vein, which was not affected in the adult wings. L1 to L5 refer to longitudinal veins of the adult wing. The black line demarcates the putative anterior/posterior boundary, based on fate mapping, that divides the wing into the anterior (A) and posterior (P) compartments. (D) The mutant combination of *dpp^{hr4}/dpp^{d5}*; *sgl^{P1731}/+* shows loss of medial wing structure in the wing blade adjacent to the anterior/posterior compartment boundary. The phenotypic effects that were observed between L2 and L5 in the wing blade, includes the loss of L3 and L4 wing veins, the proximal and posterior cross veins as well as loss of the intervening wing tissue. In addition, loss of the distal wing margin was observed (see black arrow). This phenotype depicted in panel (D) is characteristic of severe *dpp* disc mutant effects.

Table 18.

Frequency of dominant negative genetic interaction between *sgl^{P1731}* and *dpp* loss-of-function disc mutants in wings and legs of adult flies.

Crosses	# of F1 Adults scored	# of F1 adults with leg defects	# of F1 adults with wing defects
$\frac{dpp\ d5}{CyO} \times \frac{dpp\ d6}{CyO}$	354	7 (2%) (c.i.: 1.3; 2.7)	1
$\frac{dpp\ d6}{CyO} \times \frac{dpp\ hr4}{CyO}$	405	2	20 # (5%) (c.i.: 3.9; 6.1)
$\frac{dpp\ d5}{CyO} \frac{sgl^{P1731}}{TM3} \times \frac{dpp\ d6}{CyO} \frac{Ki}{TM3}$	377	63* (17%) (c.i.: 15.1; 18.9)	6
$\frac{dpp\ d6}{CyO} \frac{sgl^{P1731}}{TM3} \times \frac{dpp\ hr4}{CyO} \frac{Ki}{TM3}$	396	5	79* (20%) (c.i.: 18.0; 22.0)

One copy of *sgl^{P1731}* introduced into a trans-heterozygous combination of weak *dpp* disc mutants, *dpp^{d5}/dpp^{d6}* and *dpp^{hr4}/dpp^{d6}* led to a significant dominant enhancement of the *dpp* mutant phenotype in legs and wings of the adult. Both the frequency (table above) and severity (see **Figure 47 B and D**) of the *dpp* loss-of-function phenotype were significantly enhanced in adults. To test if the dominant interactions between *sgl* and partial loss-of-function *dpp* disc mutant alleles are significant, I used the confidence interval (c.i.) statistical analysis as described in **Table 11** (Moore and McCabe, 1993).

* : includes *Cy+*, *Sb*, *Ki+* and *Cy+*, *Sb+*, *Ki* adults in the F1 progeny.

: includes adults that showed weak loss of wing margin in addition to the expected loss of the anterior crossvein.

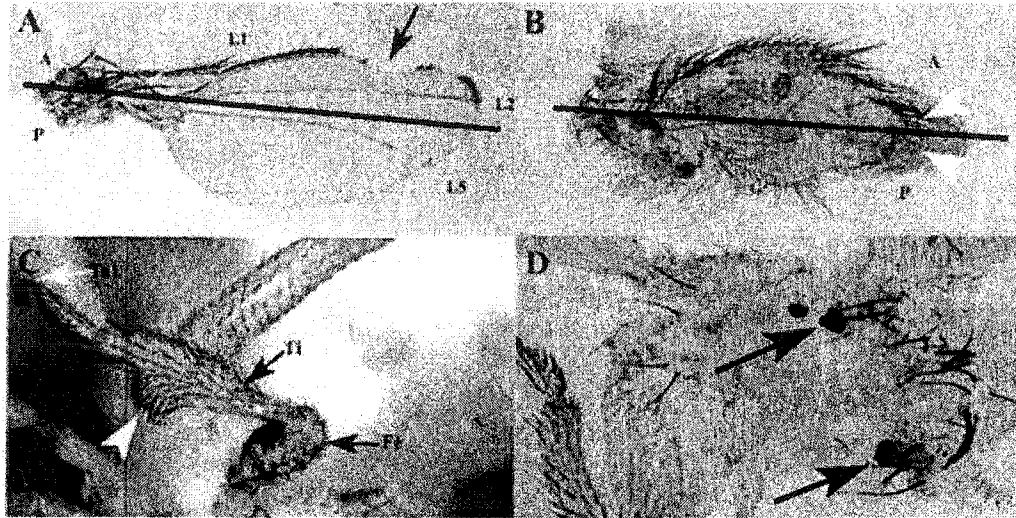
dpp^{d5}/dpp^{d6} flies, loss of one copy of *sax* or *thv* resulted in loss of distal claw and truncations in the fifth tarsal segment. They showed that receptor mutants of the *dpp* pathway can act as dominant enhancers of *dpp* disc loss-of-function mutants. Thus, these weak *dpp* mutant phenotypes can be enhanced by a reduction in the dosage of other components of the *dpp* signaling pathway.

In a similar experiment, one copy of UDP-GlcDH was removed by crossing *dpp^{d5}/CyO*; *sgl^{P1731}/TM3,Sb* males with *dpp^{hr4}/CyO*; *Ki/TM3,Sb* females. The presence of one copy of the *sgl^{P1731}* mutant allele resulted in a dominant effect that enhanced a weak *dpp* loss-of-function wing mutant phenotype. Approximately 20% of adults that eclosed (genotype *dpp^{hr4}/dpp^{d5}*, *sgl^{P1731}/TM3,Sb* or *Ki*) (see Table 18, Figure 47D) showed a loss of medial wing structures between the longitudinal wing veins L2 and L5. This included L3 and L4 wing veins, along with the intervein regions (L2-L3, L3-L4 and L4-L5) and the anterior and posterior cross veins, all tissues that require normally higher levels of *dpp* activity for their proper determination and patterning. In addition, a loss of the distal wing margin was observed. This phenotype is a characteristic of *wingless* disc mutations, however *wg* does not specifically affect the distal wing margin. The distal margin effect might be enhanced by loss of *dpp* function, which in conjunction with *wg* is also required for distal patterning. Removing one copy of UDP-GlcDH from *dpp^{d6}/dpp^{d5}* flies, by crossing *dpp^{d5}/CyO*; *sgl^{P1731}/TM3,Sb* males with *dpp^{d6}/CyO*; *Ki/TM3,Sb*, resulted in the enhanced *dpp* mutant phenotype of the adult leg. Approximately 17% of the adult progeny showed loss of a claw, suggesting that one copy of *sgl^{P1731}* acted as a dominant enhancer of the *dpp^{d6}/dpp^{d5}* loss-of-function mutant phenotype (compare arrows in Figure 47A and Figure 47B). These wing and leg structures correspond with regions that require the maximal levels of DPP activity for their formation during imaginal disc patterning. Proximal regions of the leg and more posterior and anterior regions of a wing that require lower DPP activity remain unaffected. These results suggest that DPP activity may be regulated by UDP-GlcDH in the imaginal tissues.

III-5ii. Ectopic expression of heparinase III in imaginal discs causes adult patterning defects.

Ectopic expression of heparinase III, a degradative enzyme specific for heparan sulfate GAGs, during different embryonic stages in *Drosophila* resulted in *wg*-like (Binari et al., 1997) and *dpp*-like (this study) mutant patterning defects in the embryo. When heparinase III was ectopically expressed during the second larval instar, it resulted in patterning defects in adults which resembled phenotypes resulting from a loss in *dpp* signaling (Figure 48). The phenotypes were generated by using a *hsp70-Gal4* transgene to drive the general expression of *UAS-heparinase III* in imaginal discs at specific stages during larval development. Homozygous *Hsp70-Gal4* (on chromosome III) males were crossed with homozygous *UASheparinaseIII* (chromosome II) females. Embryos were collected for 12 hr at 25°C, and allowed to develop until mid-second instar (60 hr AEL). Larvae were then heat shocked at 37°C for 1 hr followed by a second 1 hr heat shock the following day. Second instar larvae were chosen since heat treatments during first instar were lethal and resulted in dead larvae by the third instar stage. Heat shock at second instar resulted in patterning abnormalities in 40% of the adults.

Figure 48. Morphological abnormalities induced by heparinase III expression in imaginal discs.



Ectopic expression of heparinase III degradative enzyme results in *sgl* and *dpp* mutant-like defects in the adult leg and wing. (A) Ectopic heparinase III expression can cause loss of the L3 and L4 veins, proximal and posterior cross veins, intervening regions of the wing blade between L2 and L5 and the notches in the anterior wing margin (black arrow). (B) In some severe cases a loss of both the distal anterior and posterior wing margin (white arrowheads) along with the entire wing blade was observed, resulting in a vestigial-like wing. (C) In the second thoracic leg, defects varied from loss of distal leg segments such as the claw and T4 to T5 (white arrow), to outgrowths such as those observed in the tibia (Ti) (white arrowhead). (D) In rare cases, a complete deletion of the leg can be observed (see black arrows). Anterior compartment (A), posterior compartment (P), longitudinal veins 1, 2 and 5 (L1, L2, L5), first tarsal leg segment (Ta1), tibia (Ti), femur (Fe). For comparison, a wild type like wing is shown in Figure 47C; for a wild-type second thoracic leg see Figure 49A. The black line marks the approximate position of the A/P boundary in panels A and B.

Table 19. Frequency of defects observed with heparinase III treatment of imaginal discs.

The number of leg and wing defects caused by the ectopic expression of heparinase III in imaginal discs. Heparinase III expression was induced during the second larval instar, using *hsGal4* to drive ectopic expression of heparinase III under the regulation of the *UAS* promoter.

Genotype	# of legs scored	# of leg with defects	# of wing with defects
	# of wings scored		
<i>hsGal4; UAShep III</i> heat shock	1009	201	-
	510	-	89
<i>hsGal4; UAShep III</i> no heat shock	459	5	-
	179	-	8
<i>hsGal4</i> heat shock	499	0	-
	189	-	0
<i>UAShep III</i> heat shock	502	0	-
	200	-	0

Heat shocks at third instar only resulted in weak eye defects, with a small loss of ommatidia (not shown) in 5% of adults.

This treatment caused several phenotypic effects in the adults, most of which showed morphological defects that included the deletion of leg segments (19% of legs) and wing margin (18% of the adult wings) (Table 19). In Figure 48C, distal tarsal leg segments (Claw, T1 to T4) are missing (see white arrow). In some rare cases the opposite effects are observed. In Figure 48C (white arrow-head) an outgrowth in the ventral compartment is observed near the proximal end of the tibia. Defects in adult wings (Figure 48A) typically included the loss of longitudinal veins L3 and L4 and medial intervein tissue on both sides of the A/P compartment boundary. In some cases this was accompanied with deletions in the wing margin (arrow Figure 48A). Approximately 8% of the adults, demonstrated a complete loss of all leg segments (Figure 48D). In these flies, I observed necrotic tissue in the thorax in place of the leg (arrow, Figure 48D). To determine if this tissue was leg disc that had failed to elongate during pupariation, the tissue was dissected and examined under the microscope. The tissue appeared to be a lump of differentiated cuticle, with some bristles, but without any distinguishing leg features. In the case of the wings, severe effects included loss of wing blade as well as reduction in distal anterior and posterior wing margin resulting in a vestigial like wing (Figure 48B).

The leg and wing discs affected by heparinase III ectopic expression mimic phenotypes that result from *dpp* and *wg* loss-of-function disc mutants, suggesting that heparinase III treatment during disc development may abrogate DPP and WG function required for proper patterning of leg and wing tissue. More significantly, ectopic expression of heparinase III in imaginal discs phenocopies effects caused by somatic clones in *sgl^{P1731}* mutants, and the dominant negative enhancer effects of *sgl^{P1731}* on partial loss-of-function *dpp* disc mutants (compare Figure 47D to Figure 48A). *Dpp* activity is crucial for furrow progression in the patterning of ommatidia in an imaginal eye disc (Treisman and Rubin, 1995). Loss of *dpp* function in an eye disc inhibits furrow progression, thus causing loss of ommatidia. Overexpression of heparinase III in larvae gives rise to adults with fewer ommatidia, similar to the phenotype caused by the inhibition of furrow progression by *dpp*-disc mutations (Treisman and Rubin, 1995). Results in Figure 41 and 42 suggest UDP-GlcDH is required for imaginal disc patterning by regulating *dpp* signaling. Heparinase III treatment of *Drosophila* Schneider cell lines and embryos resulted in the inhibition of the *wingless* signaling pathway, as a result of heparan sulfate degradation (Riechman et al., 1996; Binari et al., 1997; Hearry et al., 1997). This suggests that regulation of *dpp* signaling by UDP-GlcDH in the imaginal disc may work through heparan sulfate GAGs modulation of DPP activity levels.

III-5iii. Ectopic expression of UDP-GlcDH in imaginal discs.

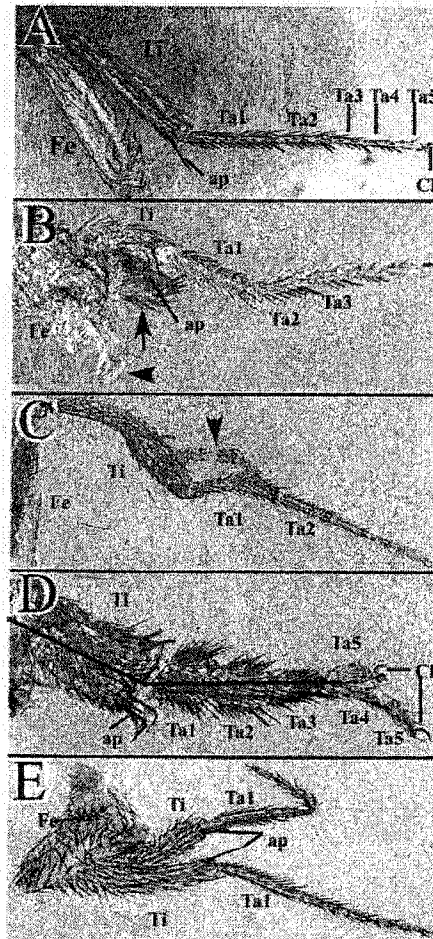
In a variety of both vertebrate and invertebrate developmental systems, it has been demonstrated that groups of cells have the ability to influence the developmental programme of neighboring cells. These groups of cells are referred to as "organizers." Several factors have been identified in

Drosophila that possess organizer-like activity, and can lead to distal duplications in adult legs and wings. One such gene is *dpp*, which in conjunction with *wg*, may specify the position of the distal organizer in imaginal leg and wing discs (see Introduction).

If UDP-GlcDH can indirectly modulate DPP and WG activity through heparan sulfate biosynthesis, ectopic expression of UDP-GlcDH might also result in the ectopic activity of DPP or WG. One possible outcome could be duplication of leg and wing structures. To test this, I expressed UDP-GlcDH in imaginal disc cells using a *Hsp70-Gal4* line to drive the ectopic expression of a *UAS-UDP-GlcDH* *Drosophila* full-length cDNA construct during different stages of larval development. This leads to a significant increase in the level of heparan sulfate GAG as detected in imaginal disc tissue using monoclonal antibodies to heparan sulfate (unpublished data from Dr. Manoukian's lab, University of Toronto).

Homozygous *Hsp70-Gal4/Hsp70-Gal4* (3rd chromosome) males were crossed to *UAS-UDPGlcDH(2.1)/UAS-UDPGlcDH(2.1)* (on the 3rd chromosome) females. Eggs were collected for 6 hr at 25°C. At second larval instar (50 hr AEL), larvae were heat shocked at 37°C for 1 hr followed by a second heat shock 12 hr later for 1 hr. Using this treatment leg duplications in adults were observed, whereas a single heat treatment at this stage was ineffective (see **Figure 49**). Similar heat treatments at first instar resulted in larval death at the third instar stage, whereas heat treatments during the third larval instar resulted in minor effects such as bent legs or blisters in the wing. As shown in **Figure 49**, the effects were variable, with limb bifurcation occurring at various proximal-distal positions along the leg (see **Figures 49B, C, and D**) in 6-8% of the adults examined. The percentage is the frequency of duplications observed in legs of adult flies that were scored out of 3150 heat-treated individuals. Proximal outgrowths from the femur included anterior and posterior ventral pattern elements (**Figure 49B**). This is very similar to effects observed after ectopic expression of WG (Lecuit and Cohen, 1997). In addition, medial outgrowths were found originating from the tibia that rejoined distally in the tarsal segments, creating an O-ring structure (**Figure 49C**). Distal bifurcation, as seen in **Figure 49D**, included duplications of claw and fifth tarsal segments (Ta5). In some cases, bifurcations were associated with mirror-image duplications of the anterior leg compartment (**Figure 49D**). In **Figure 49D**, it can be seen that the femur, tibia and tarsal segments 1-3 have undergone a thickening of their anterior dorsal and ventral compartments. This is similar to the effects of ectopic *hh* expression (Basler and Struhl, 1994), which leads to ectopic activation of both *wg* and *dpp* in the ventral-anterior and dorsal-anterior sub-compartments (see Introduction). Bifurcations which led to complete leg duplicates were rarely observed (**Figure 49E**). In these cases, the structures included within the duplicate branch contained pattern elements belonging to all compartments; that is, the duplicate appeared to be circumferentially and distally complete. Bifurcations were observed to originate from either the dorsal or ventral (as shown in **Figure 49E**) compartments of the leg. Therefore, increased levels of UDP-GlcDH expression suggest that this may likely lead to elevated activities of *dpp* or *wg* signaling in imaginal discs.

Figure 49. Morphological defects in adult legs induced by the ectopic expression of UDP-GlcDH in imaginal discs.



Pleiotropic morphological patterning effects in leg appendages caused by the ectopic expression of the *UAS* UDP-GlcDH transgene in imaginal leg discs. (A) Wild-type, second thoracic leg, showing the femur (Fe), tibia (Ti), tarsal segments 1 to 5 (Ta1 to Ta5), distal claw (Cl) and apical bristle (ap). (B) Shows proximal outgrowths in the femur (Fe) and tibia (Ti). In this case, there is an over-growth of the femur (arrowhead) and the start of a duplication of the tibia (arrow), which is indicated by the differentiation of a second apical bristle (ap). (C) In some cases, medial duplication occurred, resulting in a ring-like structure. The duplication (arrowhead) begins at the distal part of the tibia (Ti) and rejoins at the distal end of the first tarsal segment (Ti). (D) Shows expansion of the anterior compartment of the tibia (Ti), and tarsal segments 1 to 3 (Ta1 to Ta3). This is indicated by a thickening of the anterior ventral compartment [note a duplication of the apical bristle (ap)] and anterior dorsal compartment. It also shows the bifurcation of the distal fifth tarsal segment (Ta5) and the claw (Cl). The black line marks the putative dorsal-ventral compartment boundary. (E) In rare cases, a complete duplication of the second thoracic leg is observed. The distal bifurcation initiates from the proximo-ventral region of the tibia (Ti).

III-6. UDP-GlcDH organizer-like function required during pattern regulation in regenerating imaginal leg discs in *Drosophila*.

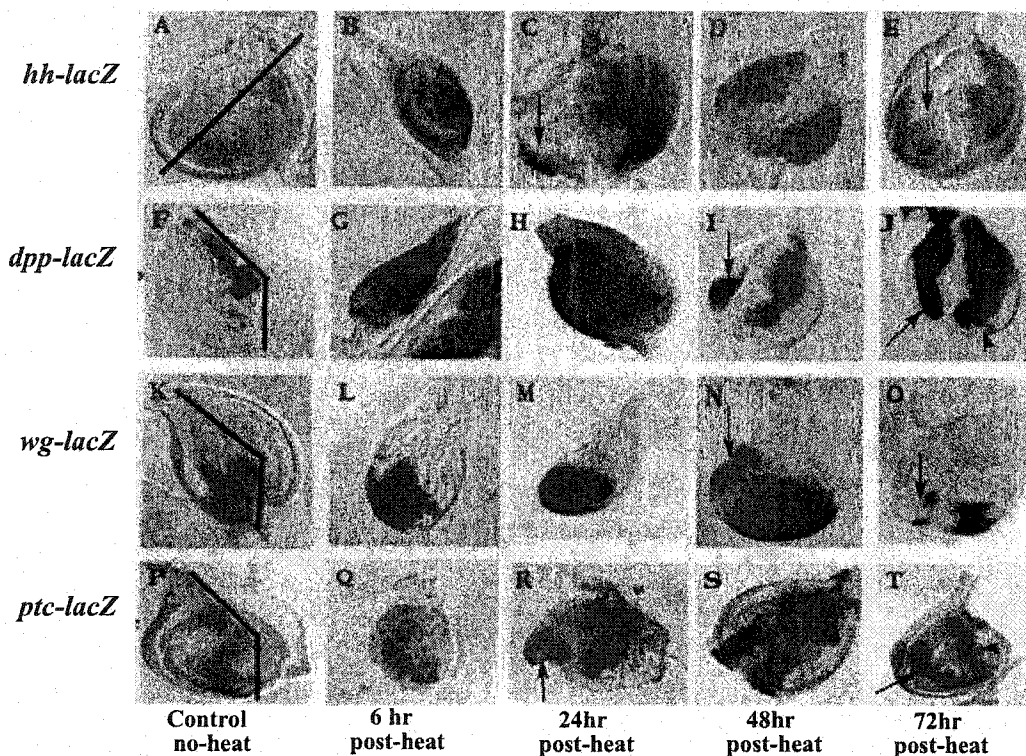
III-6i. Misexpression of *hh*, *ptc*, *wg* and *dpp* in duplicating imaginal discs.

The isolation of *A64* in the regeneration screen (Brook et al., 1993), followed by its identification as an allele of *sugarless* (this study), shows that UDP-GlcDH is ectopically activated following cell death-induced regeneration in imaginal leg discs. Recent ectopic expression studies have implicated various signaling molecules in the formation of axial duplications. These genes include *en* (the selector gene for posterior compartment identity) *hh*, *wg*, *dpp* and *ptc*, all of which are involved in signaling across a compartment boundary that defines the distal organizer in imaginal leg discs (see Introduction). If these genes are required for distal organizer activity, their expression patterns would be expected to change appropriately when discs undergo duplications following cell death induced pattern regulation in the *su(f)¹²* mutant after heat-treatment. Therefore, the temperature-sensitive cell-lethal mutation *su(f)¹²* was used to conveniently initiate pattern regulation, and simultaneously monitored the response of *hh*, *wg*, *dpp* and *ptc* expression using the *lacZ* reporter.

Homozygous *su(f)¹²* females were crossed with males from various lines which contained a *lacZ* reporter construct whose expression was under the regulation of *en* (not shown), *hh*, *dpp*, *wg* and *ptc* upstream promoter sequences. To induce duplications in imaginal leg discs, progeny from the cross were allowed to develop until mid-second instar larvae (60 hr AEL). The larvae were then shifted to 29°C (restrictive temperature) for 48 hr, and then returned to 18°C. The expression of these genes in the resulting duplicating imaginal leg discs was then monitored by assaying the expression of β -galactosidase activity at various stages after the heat treatment. Beginning at 6 hr following heat treatment, and at daily intervals thereafter, samples of male larvae were dissected, fixed and stained to monitor the pattern of *lacZ* expression in the duplicating leg discs. Females were fixed and stained in parallel as a control. Results of this experiment are shown in **Figure 50**. Normal expressions patterns of *hh*-, *dpp*-, *wg*-, and *ptc-lacZ* in second thoracic leg discs are shown in **Figure 50A,F,K and P**, respectively, from control female larvae.

At 6 hr following heat treatment, the discs showed a necrotic appearance and had only a single circular fold defining the proximal-distal axis. *Hh* (**Figure 50B**) and *en* (not shown in this figure) were ectopically activated throughout the anterior compartment, as well as in the posterior compartment where they are normally expressed. Expression of *dpp*, normally found only along the A/P compartment boundary, also appeared strongly throughout the disc epithelium immediately after heat treatment (**Figure 50G**). *Wg* (**Figure 50L**) expression had spread into the anterior ventral quadrant, while *ptc* (**Figure 50Q**) expression was broadened and showed patchy expression in the anterior lateral region of the disc, suggesting that the normal A/P compartmental restriction of gene expression had broken down.

Figure 50. Misexpression of segment polarity genes during pattern regulation of imaginal leg discs induced in the *su(f)¹²* temperature sensitive mutant.



Detection of *lacZ* expression using X-Gal staining of enhancer-trap lines of segment polarity genes (*hh*, *dpp*, *wg* and *ptc*), in second thoracic leg discs during pattern regulation in *su(f)¹²* temperature sensitive mutants. Wild-type expression pattern of (A) *hh-lacZ*, (F) *dpp-lacZ*, (K) *wg-lacZ* and (P) *ptc-lacZ* in non-heat treated *su(f)¹²* in second thoracic leg discs in control female larvae. The black line in (A), (F), (K), and (P) approximates the presumptive anterior/posterior compartment boundary. Ectopic expression patterns of (B) *hh-lacZ*, (G) *dpp-lacZ*, (L) *wg-lacZ* and (Q) *ptc-lacZ* in second thoracic leg discs at 6 hr following heat treated *su(f)¹²* in male larvae. *Lac-Z* expression of (C) *hh*, (H) *dpp* (M) *wg* and (R) *ptc* at 24 hr after heat treatment. At this time small out-growths in the imaginal leg discs begin to emerge (C and R, see arrow). Expression of (D) *hh-lacZ*, (I) *dpp-lacZ*, (N) *wg-lacZ* and (S) *ptc-lacZ* at 48 hr after heat treatment. An ectopic patch of expression from enhancer trap lines is observed. The expression patterns overlap or coincide in cells along the edge of the leg disc, which corresponds to the medial-lateral region of the anterior compartment (I and N, see arrow). Mirror image expression patterns are observed at 72 hr after heat-treatment, for (E) *hh-lacZ*, (J) *dpp-lacZ*, (O) *wg-lacZ* and (T) *ptc-lacZ*. The arrow in panel (O) marks the ectopic expression of *wg-lacZ* in the duplicate. These mirror image expression patterns correspond to the mirror image duplication of the proximal-distal axis of the second thoracic leg disc, which is indicated by the formation of a distal endknob (E, see arrow). The arrowhead in panels (J) and (T) indicate the position of the original stripe of expression of *dpp-lacZ* and *ptc-lacZ* respectively. The arrow in panels (J) and (T) mark the stripe of expression of *dpp-lacZ* and *ptc-lacZ* along the secondary A/P boundary of the duplicate. In all panels the imaginal leg discs are oriented with anterior to the left and dorsal up.

By 24 hr, normal *hh-lacZ* expression remains in the posterior compartment as ectopic expression dissipates in the anterior compartment, with the exception of some expression in medial lateral cells of the anterior compartment (arrow, **Figure 50C**). *Ptc-lacZ* expression at the A/P boundary remains broadened relative to untreated controls; however a discrete ectopic stripe is also observed in some discs in medial lateral cells of the anterior compartment (along the presumptive D/V boundary) of a leg disc (arrow, **Figure 50R**). This was an indication that a new A/P-like boundary may have formed which, would be a requirement for distal-proximal axis formation in a leg imaginal disc, based on Meinhardt's (1983) boundary model. *Wg-lacZ* expression extended dorsally to fill the entire anterior-ventral compartment (**Figure 50M**). There was no sign of ectopic *wg-lacZ* expression in the posterior compartment. Conversely, *dpp-lacZ* expression extended ventrally in the anterior-dorsal quadrant of a leg disc (**Figure 50H**). The zones of *wg* and *dpp* expression appear to meet along the D/V boundary, corresponding with the expression of the ectopic *ptc-lacZ* stripe (**Figure 50R**).

By 48 hr, *dpp-lacZ* (**Figure 50I**) and *wg-lacZ* (**Figure 50N**) expression were often localized in two discrete zones, with *dpp-lacZ* in a line along the original A/P compartment boundary and *wg-lacZ* in a wedge-like stripe along the ventral A/P compartment boundary. At the second site we see that both *dpp-lacZ* (arrow, **Figure 50I**) and *wg-lacZ* (arrow, **Figure 50N**) expression are located in a smaller ectopic patch near the anterior lateral edge of the disc. Anterior-ventral *wg* and dorsal-anterior *dpp* expressions disappear between 24 and 48 hr, except where these two zones of expression meet at the D/V boundary. In conjunction with the extended ectopic stripe of *ptc-lacZ* expression in the same region, this ectopic expression of *dpp*, *wg* and *ptc* in what may be adjacent regions, might be the first indication of the formation of an ectopic P/D axis associated with a duplication event in a leg. The formation of a second P/D axis, is further supported by the ectopic expression of *hh-lacZ* in cells along the edge of the anterior compartment, in a mirror-image pattern (**Figure 50D**) to its normal *lacZ* expression pattern in the posterior compartment. This ectopic expression of *hh* seems to overlap, or is adjacent, to ectopic expressions of *dpp*, *wg* and *ptc*, implying that a second posterior compartment fate is determined as a prelude to the formation of a secondary leg axis.

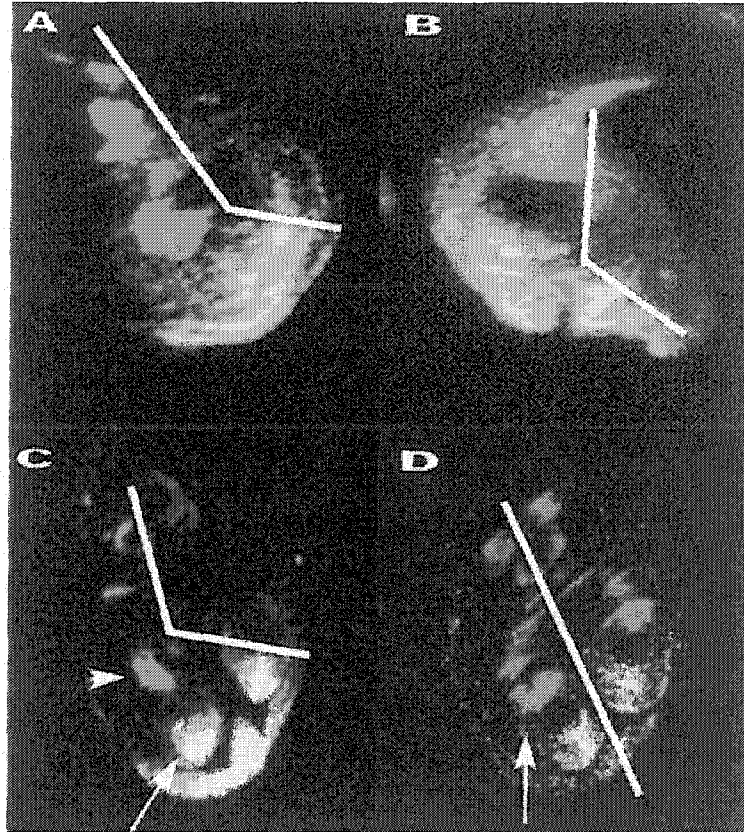
By 72 hr, a new epithelial fold is sometimes found, clearly showing the formation of a duplicate in the leg disc, indicated by a second distal endknob (arrow, **Figure 50E**). The duplicate is associated with the mirror-image ectopic expression patterns of *hh*-, *dpp*-, *wg*- and *ptc-lacZ*. Ectopic *wg-lacZ* expression is seen as a second small wedge-like pattern in the ventral half of the duplicating leg disc (arrow, **Figure 50O**). *Hh-lacZ* expression is maintained in the posterior compartment as it expands in its ectopic site at the anterior margin, in cells that are adjacent to those that express ectopic *wg-lacZ*, possibly due to the fact that the duplicate is growing (**Figure 50E**). By this stage, the mirror image ectopic expression pattern of *hh-lacZ* is a good indication that a second posterior compartment has formed. The formation of a new posterior compartment by 72 hr is indicated by both *dpp-lacZ* and *ptc-lacZ* expression. Both *dpp-lacZ* (**Figure 50J**) and *ptc-lacZ* (**Figure 50T**) expression are observed in a stripe of cells in the anterior compartment, that run adjacent to the original A/P boundary (see arrowhead in **Figure 50J** for *dpp-lacZ* and in **Figure 50T** for *ptc-lacZ*) and the new A/P boundary (for

dpp-lacZ see arrow in **Figure 50J**; for *ptc-lacZ* see arrow in **Figure 50T**). These results show that by 72 hr the imaginal leg disc has undergone pattern respecification that re-establishes the normal A/P boundary and anterior/posterior compartment gene expression patterns, along with the formation of a new secondary A/P boundary and P/D axis. The new A/P boundary intersects at the site of the secondary distal extremity as indicated by the new concentric folds and a second distal endknob. Formation of ectopic anterior patches of *wg*, *dpp*, *hh*, and *ptc* expression are associated with, but precede the formation of the ectopic proximodistal axis, as indicated by later formation of a second set of concentric epithelial folds and a distal endknob in this region. These results establish a correlation between the specification of a new secondary axis during leg duplication and the ectopic expression of various genes that have been shown to possess distal organizing abilities in imaginal discs.

A current model to account for the formation of a distal organizer in imaginal discs requires that *dpp* and *wg* must be expressed in adjacent cells in order to initiate the formation of a proximal-distal axis (reviewed, Campbell and Tomlinson, 1995). Therefore the expression of *wg* and *dpp* was examined using confocal immunofluorescence microscopy in duplicating imaginal leg discs in *su(f)¹²* mutant larvae as described above. The results show that *wg* and *dpp* ectopic expression are expressed not only in adjacent cells (as would predicted by the Meinhardt model), but they also overlap, in cells at the medial-lateral edge of the anterior compartment where the ectopic distal extremity later arises as described in Girton and Russell (1980 and 1981) (see **Figure 51**).

Figure 51A shows the expression of WG (green) and *dpp*- β -Galactosidase (*dpp*- β -Gal, red) expression in a normal leg disc. *Dpp* β -Gal expression is localized to a stripe of cells along the A/P boundary in the anterior compartment. WG expression is localized to the ventral compartment of the leg. The yellow stain in the ventral compartment marks the expression where WG and *dpp* β -Gal overlap. Low levels of *dpp* expression are normally found in the ventral compartment of the leg disc along the A/P boundary. However, the functional significance of this expression has not yet been determined. In the ventral compartment, *wg* acts to suppress *dpp* function (Brook and Cohen, 1996; Theisen et al., 1996; Jiang and Struhl, 1996; Penton and Hoffmann, 1996). Perhaps, in this case, normally high levels of *wg* could suppress any effects of *dpp* function. Approximately 24 hr after heat treatment of *su(f)¹²* mutants, one sees the misexpression of WG and *dpp* β -Gal in cells of the anterior-ventral and anterior-dorsal subcompartments (**Figure 51B**). By this time expression of WG and *dpp*- β -Gal overlaps significantly. At 48 hr, WG and *dpp*- β -Gal ectopic expression is restricted to cells near the medial-lateral periphery of the leg disc in the anterior compartment (**Figure 51C** see arrow), as the expanded expression of WG and *dpp*- β -Gal is throughout most of the anterior compartment. The ectopic site include cells that express WG and *dpp*- β -Gal, along with cells that show overlap of expression. In addition, the original *dpp*- β -Gal stripe of expression has begun to re-establish itself (see white arrowhead in **Figure 51C**). The formation of a new secondary A/P boundary, as indicated by the expression of a second stripe of *dpp*- β -Gal and a wedge of WG (see white arrow in **Figure 51D**), seems to coincided with the earlier conjoined ectopic expression of WG and *dpp*- β -Gal, as observed in **Figure 51C**. Thus, the ectopic patch of WG and *dpp* expression (as seen in **Figure 50** panels I and N,

Figure 51. Overlapping ectopic expression of *wg* and *dpp* during pattern regulation of imaginal leg discs in a *su(f)¹²* mutant.



Expression of *wg* [monitored by the expression of wingless protein (WG) green] and *dpp-lacZ* (monitored by the expression of the β -galactosidase protein; red) associated with the *su(f)¹²* mutant in second thoracic leg discs. Yellow stain represents the regions of imaginal disc where the expression of *wg* and *dpp* overlap. Orientation of the leg discs; anterior to left and dorsal up. The white line marks the approximate anterior/posterior compartment boundary. (A) Expression of WG and *dpp-lacZ* in a non-heat treated *su(f)¹²* control leg disc. *Dpp-lacZ* (red) is expressed in a stripe in cells of the anterior compartment adjacent to the A/P compartment boundary. WG expression is localized to cells of the ventral compartment. Ectopic expression of *wg* and *dpp* during pattern regulation in the leg disc, induced in *su(f)¹²* mutant at (B) 24 hr, (C) 48 hr and (D) 72 hr after heat treatment. In panel (B) both *dpp* and *wg* become ectopically expressed in the anterior-dorsal and anterior-ventral subcompartments respectively, of the leg disc. The white arrow in panel (C) marks the ectopic patch of WG and *dpp-lacZ* expression that overlap in the medial-lateral region of the anterior compartment of the leg disc. The white arrowhead marks the normal expression of *dpp*. The white arrow in panel (D) marks the duplicated axis in the leg disc and the mirror image staining pattern of *dpp-lacZ* (red) and WG (green) in the duplicate.

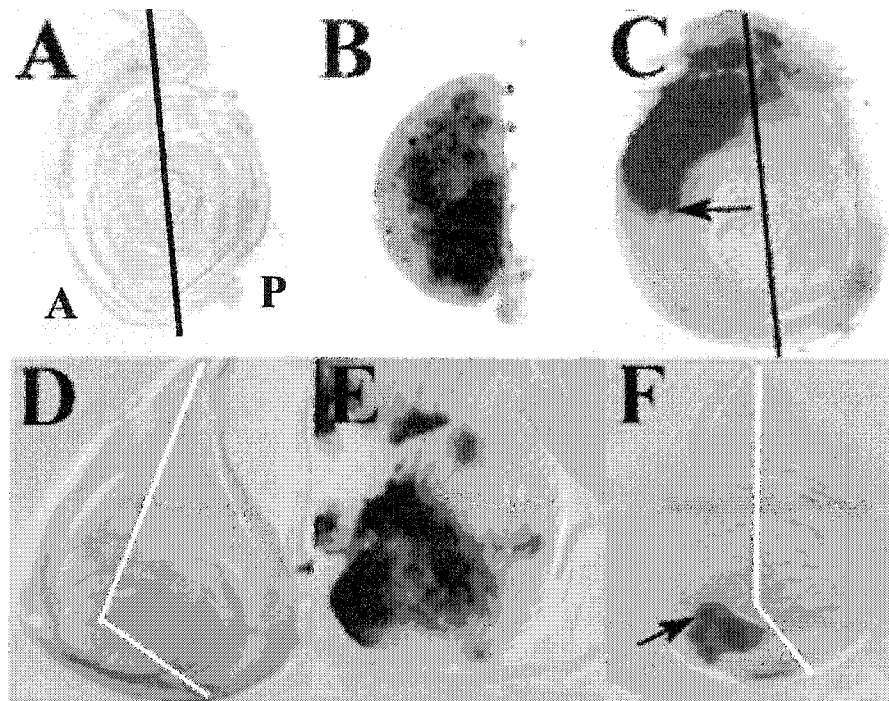
and in **Figure 51C**) seems to coincide with region of the new distal organizer, that is responsible for secondary axis formation during duplication. The expression data seems to agree with Meindhardt's hypothesis which states that adjacent expression of *dpp* and *wg* is required to establish a new compartment boundary. However, evidence showing that both *wg* and *dpp* function is required in order to form a duplicate during regeneration is thus far only based on the correlative expression studies.

The changes seen in the *wg*, *dpp* and *hh* expression patterns in duplicating discs are consistent with their normal roles in distal organizer function in imaginal leg discs, suggesting that these genes may be involved in ectopic axis initiation and repatterning during leg duplications in the *su(f)¹²* mutant. The regeneration screen identified the UDP-GlcDH gene as another possible participant in this process. The results described in prior sections of this study and by other published work, suggest that UDP-GlcDH plays a role in *dpp* signaling during normal imaginal disc development. It was also shown that ectopic UDP-GlcDH expression can cause pattern duplications in adult legs, suggesting that it may have a role as a distal organizer during normal leg development (see **Figure 49**). Therefore, it was of interest to determine if UDP-GlcDH may have some role in the formation of the duplicate during pattern regulation in regenerating imaginal leg discs.

III-6ii. UDP-GlcDH transcript and heparan sulfate GAGs are ectopically expressed during pattern regulation of imaginal leg discs in *su(f)¹²* mutant larvae.

To determine if the ectopic expression of UDP-GlcDH during regeneration coincides with that of *wg*, *dpp* or *hh*, I investigated the expression patterns of both the UDP-GlcDH transcript and heparan sulfate GAGs in duplicating imaginal leg discs in heat treated *su(f)¹²* mutant larvae (see **Figure 52**). *In situ* hybridizations were performed at various times after heat treatment, using a Digoxigenin-labeled *Drosophila* UDP-GlcDH cDNA probe. In non-heat treated *su(f)¹²* mutant controls, UDP-GlcDH transcript is observed in a uniform pattern in the imaginal leg disc (**Figure 52A**). At 6 hr following heat treatment, UDP-GlcDH was expressed throughout the leg disc (**Figure 52B**). This pattern was typical of 56/200 (25%) of the leg discs that were examined. The remaining leg discs showed no detectable ectopic expression of the transcript. By 24 hr the uniform expression was lost and it became restricted to various regions of the anterior compartment. The pattern of expression varied between different second thoracic leg discs. **Figure 52C** shows UDP-GlcDH transcript restricted predominantly to the anterior-dorsal quadrant of imaginal leg discs, extending up to the presumptive medial-lateral boundary of the anterior compartment (see arrow in **Figure 52C**). This pattern was found in approximately 45 of the 300 (15%) leg discs that were examined. In 36 of the 300 (12%) leg discs, UDP-GlcDH transcript expression was observed throughout the anterior-ventral compartment. A smaller number (15 out of 300) of legs discs showed UDP-GlcDH transcript expression throughout most of the anterior compartment. The remaining leg discs showed weak uniform expression that did not vary from the non-heat treated leg discs (not shown). When the expression of heparan sulfate GAGs was analyzed using a monoclonal antibody during pattern duplication in the heat treated *su(f)¹²* discs expression was more restricted than that of UDP-GlcDH transcript. In non-heat treated *su(f)¹²* con-

Figure 52. UDP-GlcDH transcript and heparan sulfate GAG misexpression during pattern regulation in leg discs in the *su(f)¹²* mutant.



Ectopic expression of UDP-GlcDH and heparan sulfate during pattern regulation in imaginal leg discs. The dark line in (C) and white line in (D) and (F) mark the approximate anterior/posterior compartment boundary. Anterior (A), Posterior (P), Dorsal (D), Ventral (V). (A) UDP-GlcDH transcript expression in non-heat treated *su(f)¹²* second thoracic leg disc. (B) Ectopic expression of the UDP-GlcDH transcript observed throughout the second thoracic leg discs at 6 hr following heat treatment in *su(f)¹²* mutant. By 24 hr after heat treatment UDP-GlcDH transcript shows variable patterns of expression throughout the anterior compartment of the leg disc. (C) UDP-GlcDH transcript expression that is localized to the anterior-dorsal compartment, extending to the medial-lateral region (see arrow). Expression extends up to the presumptive medial-lateral border (see black arrow). The UDP-GlcDH transcript was detected using a UDP-GlcDH Digoxigenin-labeled cDNA probe. (D) Heparan sulfate GAG expression (monitored by a heparan sulfate specific monoclonal antibody) in non-heat treated *su(f)¹²* mutant second thoracic leg disc. (E) Expression of heparan sulfate during pattern regulation in a second thoracic leg disc, at 6 hr and (F) 48 hr following heat treatment in a *su(f)¹²* mutant. (E) At 6 hr elevated heparan sulfate expression is observed mostly throughout the anterior compartment. (F) By 48 hr elevated levels of heparan sulfate are detected only in a patch of cells in the presumptive medial-lateral region of the anterior compartment marked by the black arrow. The arrows in both panels (C) and (F) mark the approximate medial-lateral region of the anterior compartment in both leg discs. Because of growth and cell division induced in *su(f)¹²* heat treated discs, the morphology of imaginal discs become distorted, resulting in the dorsal or ventral shift (see arrow F) of the anterior medial lateral regions of the leg disc. In all panels, the anterior compartment is to the left, and the dorsal compartment is up.

trols, second thoracic leg discs showed uniform expression of heparan sulfate (**Figure 52D**). At 6 hr following heat-treatment, increased expression of HS was seen only throughout the anterior compartment of imaginal leg discs (**Figure 52E**), unlike that observed for the UDP-GlcDH transcript. By 48 hr, elevated levels of heparan sulfate expression is restricted to a region of cells in the anterior medial-lateral region of the leg disc (arrow **Figure 52F**). Due to the extensive growth and cell division that occurs around the anterior medial-lateral region upon duplication, distortions are commonly observed in the morphology of the leg disc in the anterior compartment, which may explain the ventral displacement of the patch of HS expression. Even though UDP-GlcDH transcript shows variable expression in the anterior compartment, elevated HS expression seem to be maintained in only in the medial-lateral region, the region that corresponds with the putative position of the second distal organizer. This is similar to the expression patterns seen for *wg* and *dpp* (compare to **Figure 50I** and **50N**). Therefore, there seems to be a strong correlation between the expressions of *wg*, *dpp*, and heparan sulfate in later stages during pattern duplication in *su(f)¹²* mutants, corresponding to the period when the second A/P boundary and presumptive distal organizer is established. However, based only on the expression study, the question of whether HS is functionally required for distal organizer function during regeneration remains to be answered. To help answer this question, I looked at the effects of heparinase III expression on pattern regulation in *su(f)¹²* mutants during heat treatment.

III-6iii. UDP-GlcDH is required for distal organizer function in imaginal leg discs.

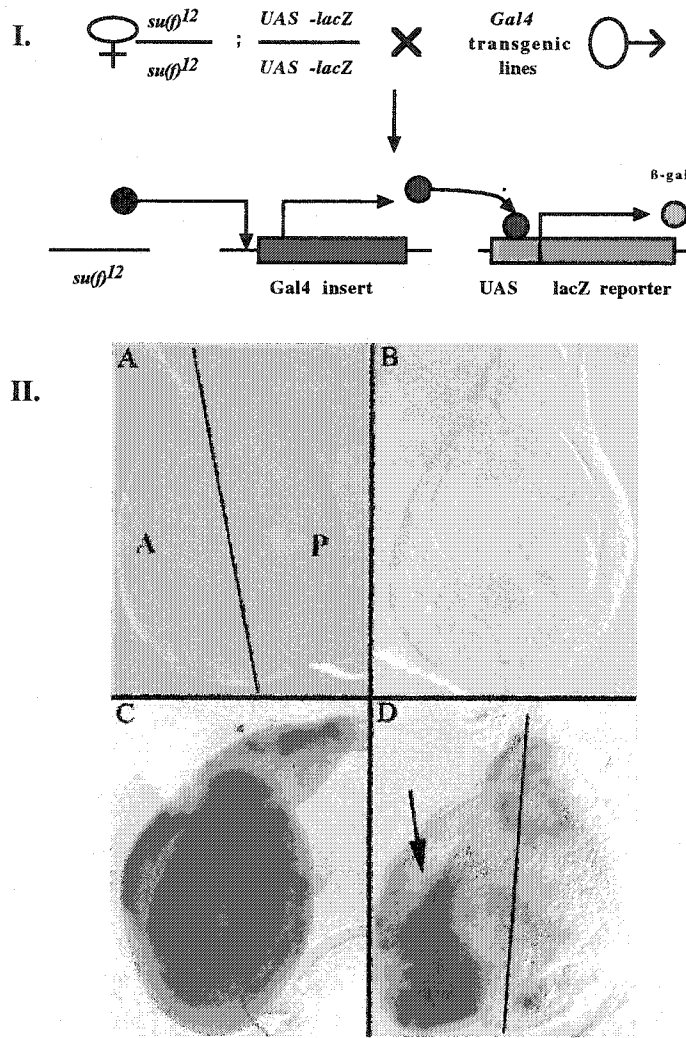
To determine if UDP-GlcDH function is required during pattern regulation and formation of the distal organizer region in duplicating leg discs, I wanted to look at the effects of *sgl* mutants only in cells that define the secondary distal organizer (regeneration blastema) during duplication in *su(f)¹²* larvae. However, because of the non-cell-autonomous property of *sgl* mutant in somatic clones, phenotypic effects could only be seen when large clones were generated. In the case of regeneration in *su(f)¹²* mutants, the number of cells that make up the regeneration blastema initially involves only a small number of cells (see Girton and Russell, 1980). Clones generated using the *sgl* mutant in this case were ineffective because of the cell non-autonomous property of the *sgl* mutant. To circumvent this problem, I induce the expression of the heparinase III enzyme using a *UAS-heparinase III* construct in the regeneration blastema, only during regeneration and duplication events induced in the heat treatment of *su(f)¹²* mutant larvae. The mosaic study of the *sgl* mutant, the genetic interactions of the *sgl* mutant and *dpp* disc mutant alleles and *UAS-heparinase III* treatment, all suggest that ectopic expression of heparinase III mimics the effects of the *sgl* mutant in discs.

Spatial and temporal control of *UAS-heparinase III* was achieved by using *GAL4* lines isolated in a screen using the *su(f)¹²* mutation, that are only expressed during duplication-induced during pattern regulation (see **Figure 53-I**). Using a *UAS-lacZ* reporter construct, approximately 100 random *Gal4* insertion lines were screened (see **Table 4**) for specific ectopic activation of *Gal4* during pattern regulation in imaginal leg discs induced in *su(f)¹²* mutant larvae using the same conditions as in the regeneration screen (Brook et al., 1993; Russell et al., 1998). By looking at *UAS-lacZ* expression 48 hr

after heat treatment, I was able to determine which of the *Gal4* lines were activated in specific regions of a leg disc, at a particular period during pattern regulation (**Figure 53-II**). Two *Gal4* lines were isolated that were of particular interest. *C5-Gal4* showed activation that coincided with cells of a regeneration blastema, or secondary distal organizer, which localized to the medial lateral region in the anterior compartment. This restricted expression was observed as early as 24 hr following heat treatment, just prior to any visible indication of an outgrowth (**Figure 53-IID**). The *C52-Gal4* line showed activation throughout imaginal leg tissue (**Figure 53-IIC**). Again, further expression analysis showed that activation of *C52-Gal4* expression was observed as early as 12 hr following heat treatment, prior to any visible outgrowth (duplicate) occurring in a leg disc. However, unlike *C5-Gal4* which remains localized to the outgrowth in a leg disc (see arrow in **Figure 53-IID**), *C52-Gal4* shows general expression in the leg disc during pattern regulation. The *C5* and *C52 Gal 4* lines were used to direct heparinase III expression. It was hypothesized that any observed effect after expression of the heparinase III enzyme would be due to a reduction or loss of heparan sulfate GAGs by cells, mimicking the loss of UDP-GlcDH function in *sgl* mutants.

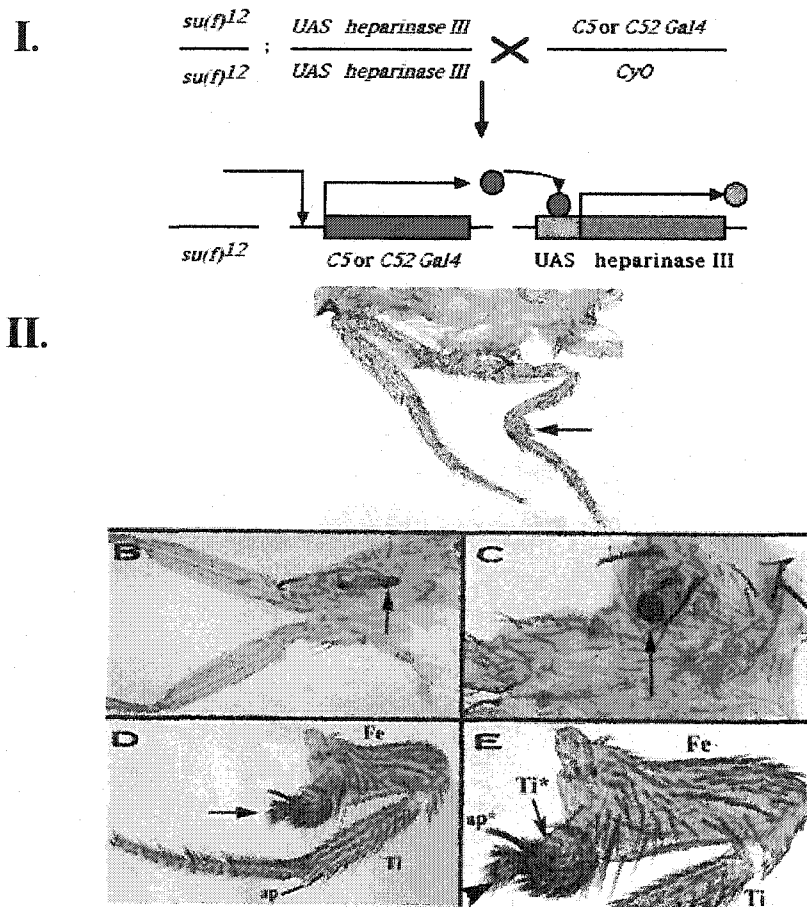
Therefore, I used the *C52-Gal4* driver to express heparinase III, to determine whether UDP-GlcDH function is required during regeneration for distal organizer function, I first attempted to express heparinase III during the early stages of regeneration, soon after the induction of cell-death, by using the *C52-Gal4* driver. In this case, the expression of heparinase III enzyme in the initial stages of pattern regeneration resulted the complete loss of distal limb structures in adults (**Figure 54-II B&C**). When heparinase III was expressed prior to any visible morphological effects (due to cell growth and proliferation), not only was pattern duplication inhibited, but the regeneration of the original primary limb was also hindered. This was observed in 17% of adults. This number coincides closely with the frequency of leg duplications (20%) obtained after the same heat treatment of *su(f)¹²* mutant larvae in the absence of heparinase III expression (**Figure 54-IIA**). Thus, almost all duplication events were completely inhibited when heparinase III was expressed throughout the regenerating leg disc. However, some legs remained unaffected. This may be due to variation in the amount of enzyme expressed, and may also reflect the developmental stage of each disc when heat treatment is performed. Perhaps legs that were affected were able to recover because not all of the heparan sulfate was degraded by the heparinase III enzyme. This may be because the enzyme is not being efficiently secreted into the ECM. There was no apparent logic as to which legs were affected. In order to see if there are any graded effects based on amount of heparinase III enzyme expressed, the strength of the *Gal4* driver would have to be varied. In this case it would be unrealistic to expect to isolate *Gal4* lines that are expressed in similar patterns but vary in the amount of their expression upon *su(f)¹²* heat treatment. Controls in which *su(f)¹²* larvae were heat-treated with only the *C52 Gal4* or *UAS-heparinase III* construct present resulted in 18% and 19.5% leg duplication frequency, respectively. This was similar to *su(f)¹²* heat-treated controls. This suggests that the reduction of heparan sulfate at a critical stage early in regeneration prevents discs from recovering their pattern after cell death-induced damage during heat treatment. When the *C5 Gal4* line was used to drive expression of heparinase III exclusively in cells associated with a regeneration blastema in *su(f)¹²* heat treated larvae, only duplicate limb forma-

Figure 53. Identification of *Gal4* lines that are activated during pattern regulation of imaginal leg discs in the *su(f)¹²* mutant.



I. Crossing scheme used to identify *Gal4* lines that are misexpressed during pattern regulation in imaginal leg discs in *su(f)¹²* mutant flies. A *su(f)¹²/su(f)¹²; UAS-lacZ/UAS-lacZ* reporter construct line is established and crossed with various *Gal4* lines. *Gal4* misexpression is then detected following heat treatment, by a *UAS-lacZ* reporter gene in a *su(f)¹²* mutant background during pattern regulation. **II.** *Gal4* lines that are ectopically misexpressed during pattern regulation in a second thoracic leg disc. (A) *C52-Gal4* and (B) *C5-Gal4* expression in non-heat treated *su(f)¹²* larvae. (C) *C52-Gal4* and (D) *C5-Gal4* expression in the second thoracic leg discs in *su(f)¹²* larvae, 24 hr and 48 hr after heat treatment respectively. The black arrow in panel (D) marks the expression of *C5-Gal4* reported by the *UAS-lacZ* construct, in the duplicating region of the leg disc. The black line in panel A and D marks the approximate position of the A/P boundary. In all panels of (II), anterior is to the left, and dorsal is up.

Figure 54. Adult defects induced by the expression of heparinase III degradative enzyme in imaginal leg discs during pattern regulation in the *su(f)¹²* mutant.



I. Crossing scheme used to express heparinase III degradative enzyme during patterning regulation in *su(f)¹²* mutants in imaginal leg discs. **II.** (A) Duplication of the second thoracic leg (arrow) in adult flies, induced during pattern regulation in *su(f)¹²/su(f)¹²; UAS heparinase III/UAS heparinase III* mutants heat treated at second larval instar. (B) Defects induced in the second thoracic leg in adult flies during pattern regulation, following heat treatment of *su(f)¹²; C52-Gal4/UAS heparinase III* second instar larvae (20X objective). A duplication is never observed and the second thoracic leg is lost and is replaced by a necrotic mass of tissue (see arrow in B and C). (C) *su(f)¹²; C52-Gal4/UAS heparinase III* in (B) at 40X objective. (D-E) Panel (D) shows defects induced in the second thoracic leg in adult flies during pattern regulation, following heat treatment of *su(f)¹²; C5-Gal4/UAS heparinase III* second instar larvae (20X objective). In these adult flies no phenotypic effects were observed in the original second thoracic leg. However, duplication in these flies is incomplete or severely truncated (arrow). In panel (E) (at 40X objective) the outgrowth occurs from the proximal end of the femur (Fe). The partial duplication includes the tibia, see panel (E) [Ti*, arrow] and a bleb adjacent to the apical bristle in the duplicate [panel (E), arrowhead]. The apical bristle (ap*) is marked for the distal tibia (Ti) [see panel (E)]. In panel (D) the apical bristle of the original leg (ap) is indicated.

tion was inhibited in adults. In 79% of the duplications adults showed second legs that either had distal segments that were truncated, or the complete duplicate was missing (**Figure 54 D and E**). The duplicates were scored for the presence of claw, tarsal segments, tibia and femur. The original leg remained unaffected. **Figure 54D** (arrow) shows a duplication initiated at the base of the femur. The growth seems to contain a portion of the distal tibia (see arrow Ti*, **Figure 54E**) indicated by the presence of an apical bristle (ap*), and a tissue mass (arrowhead, **Figure 54E**), which might be a rudimentary first tarsal segment (Ta1). In some cases, the duplicate is nothing more than a necrotic lump of tissue at the base of the femur where many duplicates normally appear (not shown). This extreme phenotype was seen in 4% of the legs. Only 3% of the duplications were complete and contained the claw, all five tarsal segments, a tibia and a femur. Control experiments using either *UAS heparinase III* or a *C5-Gal4* line in combination with *su(f)¹²* showed no effect on the frequency of leg duplications.

It is inferred that loss or reduction in heparan sulfate GAGs, due to the expression of heparinase III, inhibits various cellular processes during pattern regulation (*i.e.* cell-cell signalling, adhesion and movement) in a leg disc, preventing formation of, or proper function of, the distal organizer. Thus, heparan sulfate may be needed to modulate these cellular events in repatterning of the proximal-distal axis of a leg disc. These results are consistent with the idea that UDP-GlcDH functions through heparan sulfate GAGs and may be necessary for distal organizer function in imaginal discs required in pattern formation. The heparan sulfate GAGs may help mediate growth and cell proliferation, by regulating *dpp* activity, in a spatially and temporally restricted manner to allow proper cell patterning.

IV. DISCUSSION

IV-1. Isolating novel genes involved in pattern formation.

Using the enhancer-trap technology in conjunction with the conditional cell-lethal mutation *su(f)¹²* to induce regeneration in imaginal leg discs (Russell, 1974), screens were performed to search for *PZ* insertion lines that showed altered *lacZ* expression patterns during regeneration (Brook et al., 1993; Russell et al., 1998). Various patterns of altered expression of *lacZ* were found. These included: i) ectopic expression, during regeneration, of reporters not normally expressed in discs; ii) ectopic misexpression of *lacZ* in reporters that normally show restricted expression in a disc; and iii) loss of *lacZ* expression, in reporters that are normally expressed in imaginal discs (Brook et al., 1993; Russell et al., 1998). These results suggested the existence of a program involving positive and negative regulation of different genes during pattern regulation.

It was assumed that *lacZ* misexpression detected in the *su(f)¹²* mutant following a 24 hr heat treatment, coincided with the initial steps in pattern regulation that are important for the re-specification of a new leg pattern. These events followed cell death (Clark and Russell, 1977), but preceded the re-initiation of cell division and re-establishment of compartment restrictions (cell fates) during regeneration of the leg disc (Girton and Russell, 1981). Intercellular signals are known to provide the positional cues normally responsible for pattern formation in various *Drosophila* tissues. Three signals have critical roles in patterning the embryo and imaginal discs; they are encoded by the *hh*, *dpp*, and *wg* genes (see Introduction). Either loss-of-function mutations of these genes, or local ectopic misexpression in imaginal discs can cause a long-range re-organization of disc pattern (see Introduction, Struhl and Basler, 1993; Basler and Struhl, 1994; Tabata and Kornberg, 1994; Diaz-Benjumea et al., 1994; Capdevilla and Guerrero, 1994; Felsenfeld and Kennison, 1995; Pan and Rubin, 1995; Lepage et al., 1995). This study, along with that of Brook (1993), showed that the *wg*, *dpp* and *hh* genes are deregulated and misexpressed in the *su(f)¹²* mutant during regeneration in imaginal discs, implying that they may also play important roles in pattern respecification in the imaginal leg disc during regeneration.

This complex regulation of gene expression during the initiation of a novel axis in the leg during pattern respecification may partly involve the program of gene regulation that occurs during normal pattern formation in the embryo and imaginal discs. Therefore, my hope was that this approach would allow me to identify novel genes that mediate the formal rules of a general positional information system in imaginal discs. If genes required early in the development of the embryo or imaginal discs (such as *wg*, *hh* and *dpp*) are also re-utilized during regeneration, patterning mutants of this class would die early in development. Thus these genes would go undetected in a mutagenesis screen for regeneration in adult flies. The enhancer-trap screen helps us to by-pass this problem. However, there have been several examples in which the zygotic function of a gene in the embryo may also be required for a similar genetic program in imaginal disc patterning. Therefore, mutant effects in the

embryo can provide useful information on the developmental function of the genes identified in the enhancer-trap screen. For this reason I focused on enhancer-trap lines (scored as positive in the regeneration screen) that also caused an embryonic lethal phenotype when homozygous.

A number of the *PZ*-lethal enhancer-trap lines identified in the regeneration screen produced embryonic lethal mutations that resulted in specific morphological effects on embryonic pattern formation; consistent with the zygotic requirement for these genes during embryogenesis (see Table 5; Russell et al., 1998; Perrimon et al., 1996). By using the zygotic embryonic-lethal phenotype as an assay for identifying the possible developmental function of a gene, several lines were identified that may represent either novel genes or genes with previously unrecognizable functions required for the regulation of pattern formation. Some *PZ* lines identified in the screen represent insertions in genes that have already been characterized (see Table 6). For example, *schnurri* (*P1836*, *shn*) (Arora et al., 1995; Grieder et al., 1995), a gene involved in the *dpp* signal-transduction pathway, encodes a putative zinc finger transcription regulator factor. Zygotic mutations in *shn* have been shown to affect several events that require *dpp* signaling in the embryo, such as the establishment of dorsal identity, as well as gut morphogenesis and imaginal disc development. Another example included, *shortsighted* (*shs*) (*P936*) (Treisman et al., 1995) which is the *Drosophila* homolog of the murine *TSC-22* gene. This gene encodes a typical leucine zipper transcription factor that is induced in response to TGF-beta signaling in vertebrates. Mutations in *shs* cause a delay in photoreceptor differentiation in *Drosophila*, suggesting that *shs* may be required for the transmission of the *dpp* signal. *P1484* is an allele of the *Drosophila* homolog of the human *EB1* gene. EB1 protein is localized to microtubules of the mitotic apparatus during cell division, suggesting a role in microtubule polymerization and spindle function. EB1 protein has also been shown to bind to the carboxyterminus of the APC protein of the *WNT/Wingless* signaling pathway (Su et al., 1995). Loss of this domain is associated with the majority of familial and sporadic forms of colon carcinoma in humans. By its association with the mitotic apparatus, EB1 may play a physiological role in connecting APC (i.e., the *Wnt/Wingless* pathway) to cell division, thus coordinating the control of normal growth and differentiation.

There were many other *PZ*-lethal lines that showed specific embryonic patterning defects but for which no gene has yet been correlated with the P-element insertion. These insertions may affect genes the functions of which are co-opted from the embryo by the imaginal discs during regeneration; these genes may also be required during normal patterning of the imaginal discs. *Bona fide* components of the *wg* and *dpp*-signaling pathways, which are known to be required in both embryonic and imaginal disc pattern formation, may also be recruited in regeneration, possibly reiterating the early patterning steps in the imaginal disc primordia. This is consistent with earlier findings which showed that both *wg* and *dpp* activities are necessary for the initial determination and patterning of the imaginal disc primordia when they are recruited as progenitor cells from the ectoderm of the embryo shortly after the establishment of the parasegmental boundary (Cohen, 1990). Therefore, if regeneration in imaginal discs makes use of parts of the embryonic genetic program, then those *PZ*-lethal lines with zygotic mutant effects on embryonic patterning that resemble mutations of known genetic pathways

(such as *wingless* or *decapentaplegic*) may potentially identify genes involved in these pathways.

A second group of *PZ* lethals, in which the lethal phase was at either the larval or pupal stage (Table 5), also showed misexpression of *lacZ* during regeneration. In these lines (e.g., *P1491*, *P1529*, *P1586*, *P1688*, and *P1705*) *lacZ* expression is not normally observed in control discs, but is activated during regeneration. Perhaps these lines represent genes that are remnants from an ancestral program in the fly, in which at one time the progenitor of the fly was able to regenerate its limbs. However, during its evolution to its current state, the fly may have lost this ability to regenerate. In this case, the lethal effects of the *PZ* insertion could be the result of a mutation to either a vital function in some larval tissue, or to a function required during morphogenesis in the pupae. Thus, a wound healing response from these *PZ* enhancer-trap lines in the imaginal discs may in some cases represent genes that initiate part of an ancient genetic program for regeneration in the progenitor. For example, these genes may either coordinate the cell movements required to form the wound heal in the disc or regulate the recruitment of downstream genes like *wg* and *dpp* that are required to mediate early steps in pattern regulation during regeneration.

IV-2. Isolation of the *Drosophila* homolog of UDP-glucose dehydrogenase.

P(lacZ ry+)A64, was ectopically misexpressed during regeneration in imaginal discs, and was selected for further analysis based on its lethal embryonic phenotype which resulted in dorsal defects in the embryos resembling mutants in the *dpp*-signaling pathway. The *PZ A64* mutation was able to enhance the embryonic loss-of-function mutant phenotypes of the *dpp* ligand and its receptors, suggesting that *A64* represented a mutation in a gene that is able to modulate *dpp* signaling. The *A64* locus was cloned by plasmid rescue of the *PZ* insertion and shown to encode the *Drosophila* homolog of UDP-glucose dehydrogenase. Other mutant alleles of UDP-GlcDH were isolated in several concurrent independent studies. *Kiwi* (*kiwi*^{*P1731*}, Binari et al., 1997) and *sugarless* (*sgl*^{*P1731*}, Hacker et al., 1997) were isolated due to their maternal-effect on *wg* signaling in the embryo. Another allele, *suppenkasper* (*skn*^{*P8310*}, Haerry et al., 1997), was isolated as an enhancer of the *dishevelled* (*dsh*^{*M20*}) mutant of the *wg* signaling pathway and as a suppressor of an activated *thickveins* (*thvA*) mutant of the *dpp* signaling pathway.

The UDP-GlcDH enzyme, located in the cytosol of cells, is required for the conversion of UDP-glucose to UDP-glucuronic acid. In vertebrates, UDP-glucuronic acid serves many functions. In the liver, UDP-glucuronate helps detoxify non-polar molecules by converting them into more easily secreted polar derivatives (Tephyl and Burchell, 1990). UDP-glucuronate is also converted into L-ascorbic acid (vitamin C) (Lehninger et al., 1993). However, it is unlikely that either of these two pathways can account for the *A64* zygotic mutant phenotype in the *Drosophila* embryo. UDP-glucuronate is further utilized in the biosynthesis of glycosaminoglycans (GAGs) such as hyaluronic acid, chondroitin sulfate, heparin, and heparan sulfate (Ernest et al., 1995). GAGs are modified chains of sugar residues that are covalently linked to various proteoglycans, which are either found associated on

the surface of cells or secreted into the ECM. Heparan sulfate is similar to heparin except for a lower degree of sulfation and a higher percentage of glucuronate residues. The results herein suggest that the most crucial role for UDP-glucuronic acid during *Drosophila* development is to permit the synthesis of GAGs the role of which is to mediate signaling of the *dpp* pathway in regulating dorsal-ventral patterning in embryonic tissue.

IV-2i. Loss of UDP-glucose dehydrogenase inhibits *dpp* signaling in the embryo.

The shape of the *Drosophila* egg shell already shows dorsal-ventral asymmetry at the time it is oviposited. Following cellularization, different cell types within the embryo along the dorsal-ventral axis become distinguishable as determined by changes in cell shape and pattern of cell division during gastrulation and germband elongation. These cells eventually give rise to four distinct cellular regions (see **Figure 15**). Cells at the ventral midline become muscle and other mesodermal derivatives. Ventrolateral cells give rise to the ventral epidermis and the ventral nerve cord. Dorsolateral cells give rise to dorsal epidermis, and cells of the dorsal midline form the extraembryonic amnioserosa (Chasan and Anderson, 1993). Mutations that disrupt the embryonic dorsal-ventral pattern fall into one of three classes that affect these specific cellular regions as described in the introduction (section I-8i). These mutations are: (1) maternal-effect mutations that perturb the polarity of the embryo and surrounding egg shell; (2) maternal-effect mutations that produce embryonic defects within a wild-type egg shell, and (3) zygotic mutations that affect embryonic pattern within more limited regions of the dorsal-ventral axis.

Based on the results in this study up to now, the phenotypic effects described for *sgl* mutants suggest that UDP-GlcDH function falls into the third category of dorsal-ventral patterning mutations. The current data demonstrate that: (1) UDP-GlcDH function can increase the sensitivity of cells to DPP protein, thus enhancing DPP activity; (2) UDP-GlcDH is required for maximal *dpp* signaling; and (3) UDP-GlcDH functions downstream of DPP signaling, possibly modulating DPP stability or binding to its receptor, thus affecting the cellular response to the DPP activity gradient.

Sgl zygotic mutants typically show loss of dorsal and dorso-lateral cell fates, causing defects in gastrulation and dorsal closure. Loss of the dorsal and dorsal-lateral epidermal pattern are usually considered to be partial loss-of-function effects of *dpp* signaling. Typically, a complete loss of DPP activity, results in a total loss of dorsal and dorsal lateral cell fates, which are replaced with ventral cell fates. In these embryos, the ventral denticle belts form a complete ring around the circumference of the embryo upon differentiation (Irish and Gelbart, 1987; Ferguson and Anderson, 1992a; Wharton et al., 1993). These severe phenotypes are usually characteristic of *dpp* null alleles, dominant negative mutants of *thv*, or null alleles of the maternal-effect gene *cactus*. Weak dorsoventral mutant effects are usually characteristic of either zygotic hypomorphic mutant alleles of *dpp*-pathway genes, which include *dpp* and the receptors, *thv*, *punt* and *sax*, or of loss-of-function mutants of *tolloid*, and *screw* which act as positive modulators of DPP activity. These modulators are required to pattern the dorsal

(amnioserosa) and dorso-lateral (dorsal epidermis) most aspects of the embryo. Therefore, zygotic mutations in UDP-GlcDH (*sgl*^{A64} and *sgl*^{P1731}) result in phenotypes in the embryo that are similar to those caused by partial loss-of-function alleles of *dpp* or by zygotic *dpp*-pathway genes (*thv*, *punt*) and typical of the mutants of *tolloid* and *screw*.

The zygotic phenotype in *sgl* mutant embryos was confirmed to be due to a loss in *dpp* signaling, as demonstrated by the loss of expression of *dpp* nuclear target genes. *Dpp* expression in the dorsal half of the embryo normally induces the transcription of downstream target genes like *Kr* in the amnioserosa and *tin* and *eve* in the dorsal mesoderm and pericardial cells (Azpiazu and Frasch, 1993; Frasch et al., 1987). *Sgl* homozygous embryos showed a loss or reduction in KR expression, as well as TIN and EVE expression by stage 10-11 of embryogenesis. Thus, dorsal defects due to loss of UDP-GlcDH function result from loss of expression of specific *dpp* target genes required for dorsal ectodermal and mesodermal patterning (Azpiazu et al., 1996), that strongly implicating UDP-GlcDH in modulating *dpp* signaling. The loss of EVE and TIN expression in the pericardial cells suggests that UDP-GlcDH function is specifically required for determination of the heart precursor cells, which is dependent on a DPP signal from the overlying dorsal ectoderm. In a recent paper by Walsh and Stainier (2001), UDP-GlcDH function was implicated in proper cardiac valve formation in zebrafish, suggests that UDP-GlcDH may play a general role in heart development in several species.

The dominant enhancement of *dpp* loss-of-function alleles by *sgl* mutants further supported the role of UDP-GlcDH as modulator for *dpp* signaling. Trans-heterozygous combinations of *sgl*^{P1731} with various *dpp*-pathway mutations showed loss of the amnioserosa and dorsal ectoderm pattern resulting in gastrulation and dorsal-closure defects. The appearance was similar to that of the phenotypes seen in embryos hemizygous for *sgl* alleles over the deficiency *Df(3L)w5.4* which encompasses the UDP-GlcDH locus, and in embryos heterozygous for the haplo-insufficient allele *dpp*^{H46}. Enhancing the dorsal defects of *dpp* mutants by removing one copy of UDP-GlcDH reflects its role in regulating the dosage-sensitive activity of *dpp* signaling in this region (Irish and Gelbart, 1987). Loss of KR expression in the amnioserosa of these trans-heterozygous embryos (not shown), the normal expression of which requires the highest levels of DPP activity, supports this proposed the role of *sgl* as a positive modulator of *dpp* signaling.

Further support for the positive modulator role of UDP-GlcDH was demonstrated by the ectopic expression of UDP-GlcDH in blastoderm embryos. These embryos mimicked a *dpp* gain-of-function phenotype. The resulting cuticle showed a dorsalization of ventrolateral and ventral embryonic epidermis, as opposed to the ventralized phenotypes caused in *sgl* zygotic loss-of-function mutant embryos. Normally no detectable *dpp* expression is observed in ventral cells of the blastoderm embryo that give rise to the mesoderm and neuroectoderm germ layers, because *dpp* expression is normally suppressed in these cells. In addition, any DPP activity resulting from the diffusion of DPP from the dorsal side of the embryo would be inhibited by high levels of SOG in the ventral ectoderm. As expected, the ventral epidermal fates of these cells remain unaffected in *dpp* and *sgl* zygotic mutations.

However, when *dpp* is ectopically expressed in these ventral cells of the blastoderm embryo, the ventral program can be suppressed and these cells instead adopted dorsal cell fates (Ferguson and Anderson, 1992a; Wharton et al., 1993). This study showed that ectopic UDP-GlcDH expression in the blastoderm embryo was sufficient to cause the ectopic activation of the *dpp* signal cascade and transformation of ventral cell fates to those of dorsal. This was reflected later in the ectopic expression of TIN in the underlying ventral mesoderm. This was not caused by either the ectopic activation of *dpp* transcription or elevated translation of DPP in the corresponding ventral region of the embryo (see **Figure 46**). One possible explanation could be that if UDP-GlcDH acts as a positive modulator of DPP activity, higher expression levels of UDP-GlcDH will make the lower concentrations of DPP that have diffused further from dorsal side of the embryo more potent in ventral cells. This result suggests that ectopic activation of the *dpp*-signaling pathway can apparently occur in the absence of detectable levels of DPP expression. This dosage-sensitive modulation of DPP activity by UDP-GlcDH is characteristic of the interactions observed with some other modulators of DPP for example, SCW and TLD which act to augment DPP activity and SOG (a negative modulator) which inhibits it; the expression of these modulators is also spatially regulated.

Concurrent studies presented evidence that maternal germ-line clones mutant for *sgl*^{P1731} result in cuticle phenotypes of the embryo that were indistinguishable from the *wg*-like mutant phenotype in the embryo (Binari et al., 1997, Hacker et al., 1997). This suggested that the full maternal contribution of UDP-GlcDH is critical for *wg* signaling during embryogenesis. With the exception of gastrulation defects caused by a zygotic mutant effect observed in embryos homozygous for *sgl*^{P1731} (Binari et al., 1997), *dpp*-like mutant phenotypes were never reported in these studies. Initially, the *dpp*-like phenotypes observed in *sgl*^{A64} and *sgl*^{P1731} zygotic mutants for the most part, affected the later functions of *dpp* signaling during embryogenesis, such as dorsal mesoderm patterning, gastrulation and dorsal closure. However, as described above, a closer examination of the phenotypes from embryos homozygous for various *sgl* mutant alleles showed dorsal-patterning defects that were consistent with effects on earlier *dpp* function required for dorsal epidermal patterning in the blastoderm embryo. These defects included the loss of the dorsal extraembryonic tissue (e.g., the amnioserosa) which leads to dorsal open phenotypes and loss of the dorsal lateral epidermal pattern. Loss of KRUPPEL protein expression in the amnioserosa in homozygous *sgl* mutant embryos suggested that early *dpp* signaling may have been compromised. In addition, the ectopic effects of UDP-GlcDH misexpression are consistent with the effects of *dpp* signaling on dorsal epidermal patterning of the blastoderm embryo.

In embryos derived from parents that were heterozygous for the *sgl* mutation, the *wg*-like cuticle phenotype was never observed. In this case, it seems that UDP-GlcDH expression contributed by the heterozygous mother is enough to allow for proper *wg* signaling in the embryo. In fact dosage effect alleles of *wg* pathway genes have never been observed, suggesting that the *wg* signaling pathway is not dosage sensitive. Conversely, germ-line clones (GLC) of *sgl*^{P1731} never gave *dpp*-like mutant phenotypes in the embryo, but rather gave only strong *wg*-like mutant phenotypes when crossed to

fathers heterozygous for the *sgl* mutation (Binari et al., 1997). However, when GLC females of *sgl*^{P1731} were crossed to males that were wild-type (+/+), this resulted in partial rescue of the *wg*-like phenotype. In addition, a very small number of these embryos showed gastrulation defects and loss of dorsal pattern that were similar to those observed in the zygotic *sgl* mutant phenotype. Therefore, the GLC phenotype of UDP-GlcDH mutations may reflect an early crucial role for UDP-GlcDH function - one that is required for *wg* signaling during A-P segmental determination in the embryo upon cellularization. Since *wg*-like mutant phenotypes have not been observed in the zygotic effects of *sgl* mutations in the embryo, this suggests that the maternal contribution of UDP-GlcDH is sufficient for *wg* signaling in the embryo. The *dpp*-like zygotic phenotype in *sgl* mutant embryos suggests that the maternal UDP-GlcDH contribution may not be able to compensate for the loss of zygotic UDP-GlcDH with respect to *dpp* function. The failure to observe the *dpp*-mutant phenotypes in GLCs of *sgl*^{P1731} may be the result of the *wg*-signaling requirement for UDP-GlcDH being epistatic to that for *dpp* signaling during embryo patterning.

However, it was observed that the cross of females heterozygous for *sgl*^{P1731/+} with males heterozygous for one of the three *dpp* pathway mutants (*thv*⁷, *punt*¹³⁵ or *dpp*²⁷) resulted in a higher frequency of dead embryos with dorsal epidermal pattern defects than did crosses between heterozygous *sgl*^{P1731/+} males and *dpp*-pathway mutant females. This implied that the *sgl* mutant had a maternal-effect on *dpp* signaling. Mothers containing only one normal copy of wild-type UDP-GlcDH (*sgl*+/+) seem to have effects on the DPP activity that are limited to the dorsal-most region of the embryo; these effects are characteristic of certain genes (e.g., *tolloid*, *sog*, *screw*, *sax*, *thv*, and *punt*) that are required for the early regulation of DPP signaling in the blastoderm embryo. Maternal effect mutant alleles have been described for activated genes in the *dpp*-signaling pathway, including *dpp* itself, *thv* and *sax* (Brummel et al., 1994; Nellen et al., 1994a and b; Penton and Hoffman, 1994; Xie et al., 1994; Letsou et al., 1995; Ruberte et al., 1995). These authors showed that *dpp* signaling can be compromised when one functional copy of these genes are simply removed in the mother in combination with other mutants that regulate *dpp* signaling. The regions most affected in these embryos by slight changes in *dpp* signaling, were regions that require the maximal levels of DPP activity, (e.g., the amnioserosa and the dorsal ectoderm). Therefore, the maternal component of UDP-GlcDH function may have a role in regulating the *dpp*-signaling cascade.

The maternal-effect of *sgl* mutants never resulted in embryos that showed egg-shell asymmetry defects. This latter observation suggested that UDP-GlcDH function was not required for the early events in D-V polarity during oogenesis. However, the possibility of an earlier function for UDP-GlcDH - one that affects the maternal - signal pathway (i.e. dorsal group genes and *cactus*) involved in dorsal-ventral pattern specification in the syncytial embryo cannot yet be excluded.

IV-2ii. Role of UDP-GlcDH in *dpp* signaling during *Drosophila* embryo development.

Based on the genetic analysis which suggests that UDP-GlcDH functions directly downstream

from *dpp* but upstream from receptor function to augment *dpp* signaling, three possible models that are consistent with the present paradigm of *dpp* signaling can be used to describe UDP-GlcDH function. First, UDP-GlcDH function may help mediate the activation of *dpp* receptors by promoting DPP binding and PUNT and THV receptor clustering. Second, UDP-GlcDH function may be required to directly potentiate DPP activity by regulating DPP ligand processing and stability. Third, UDP-GlcDH may enhance DPP signaling primarily by enhancing SCREW activity, a second TGF β -like ligand, that is required to maximize the DPP/THV signaling cascade through SCREW's receptor, SAX, to specify dorsal most epidermal cell fates.

The first model is supported by the observation that mutations in *sgl* can dominantly enhance *dpp*-receptor loss-of-function mutants of *thv* and *punt* in trans-heterozygous combination in the embryo. The loss-of-function phenotypes in embryos that were heterozygous for *thv* or *punt* mutant alleles were each dominantly enhanced when one copy of UDP-GlcDH was removed, suggesting that UDP-GlcDH could be interacting directly with the receptors. Genetic epistasis analysis showed that the ectopic effects of DPP expression in the embryo, which normally causes dorsalization of wild-type embryos, could be suppressed in *sgl*-mutant embryos. Haerry et al. (1997) showed that the *sgl*^{P8310} mutation was able to suppress the activated form of the *thv* receptor. This result initially suggested that UDP-GlcDH may act downstream from the *dpp*-receptor complex. On the other hand when I ectopically expressed UDP-GlcDH in embryos that were homozygous for *thv*⁷ or *punt*¹³⁵ mutant alleles, in neither case was the mutant phenotype suppressed (Scanga and Manoukian, unpublished). These results are consistent with UDP-GlcDH function required downstream of DPP activity but upstream of THV and PUNT receptor function. The hypothesis most consistent with these data is that UDP-GlcDH may act with the receptors to modulate receptor-complex activation by DPP.

Even if *sgl* mutant embryos, possess functional DPP protein, receptor activation could be inhibited because loss of UDP-GlcDH function may prevent the PUNT receptor from complexing and activating THV. In this case the model in this case could involve UDP-GlcDH interacting directly or indirectly through some other factor with the receptors PUNT and THV, to help promote receptor clustering upon DPP binding. One question would be whether UDP-GlcDH promotion of the PUNT/THV receptor complex is dependent on DPP binding. In this scenario, UDP-GlcDH could help DPP bind more efficiently to its receptors, thus enhancing the interactions between PUNT and THV, or it may promote PUNT-THV interaction independent of DPP binding. Ectopic UDP-GlcDH expression is able to partially rescue dorsal cell fates and suppress the ventralizing effects in *dpp*^{H46/+} haplo-insufficient mutant embryos (Scanga and Manoukian, unpublished). However, when we ectopically expressed UDP-GlcDH in embryos that were homozygous for the haplo-insufficient null allele *dpp*^{H46} (which leads to a completely ventralized embryo), we were not able to rescue any of the dorsal pattern. This suggests that in embryos that completely lack DPP function, increasing the levels of UDP-GlcDH expression were not sufficient to activate PUNT/THV receptor function. Partial rescue of the weak phenotype in *dpp*^{H46/+} mutant embryos, suggests that UDP-GlcDH requires the presence of functional DPP in order to promote PUNT/THV receptor clustering. Therefore, as proposed by the second model,

UDP-GlcDH could either function, to help to stabilize and initiate DPP dimerization that is required for DPP ligand binding, or it could be directly regulating binding of the DPP dimer (active ligand) to the PUNT and THV receptors, which results in their clustering and activation.

To help test this hypothesis, the effects of UDP-GlcDH loss- and gain-of-function mutations on *dpp* transcript and DPP expression were tested. Embryos homozygous for the *sgl*^{P1731} loss-of-function mutant resulted in the reduction in, and in some cases, a complete loss of DPP expression in the dorsal hypodermis by stage 11. However, *dpp* transcript expression remained unaffected. Conversely, no detectable effects on UDP-GlcDH transcript expression in *dpp*²⁷ homozygous embryos was observed in the amnioserosa. In addition, the regulation of UDP-GlcDH transcript expression did not appear to require DPP activity. When dorsalization of the embryo by ectopic expression of *dpp* was suppressed in mutant embryos homozygous for *sgl*^{P1731}, DPP expression was either significantly reduced or completely lost, from both ectopic and endogenous sites (see **Figure 42**). In turn, increased expression of UDP-GlcDH, which caused ectopic activation of *dpp* signaling in the ventral region of the embryo, and resulted in dorsalization of the embryo epidermis, seemed to have no effects on DPP translation or transcription. In these embryos, DPP expression patterns apparently remained unaltered, because no ectopic DPP was detected in the ventral region of the embryo. These results suggest that UDP-GlcDH may modulate DPP activity by regulating the stability of DPP protein and, in turn, the effective biological levels of DPP for its receptors at the cell surface.

Regulation of DPP stability could occur during the processing of the DPP precursor form prior to its secretion from the cell. UDP-GlcDH enzyme function is cytoplasmically localized (Lindahl et al., 1998). Here, UDP-GlcDH enzyme could be responsible for the synthesis of (a) factor(s) that may be directly responsible for modifications of DPP during its synthesis in the ER or its migration through the Golgi apparatus. Such modifications could function to protect DPP from non-specific protease degradation in the extracellular matrix. In turn, specific modifications may allow for the regulated degradation and clearing of DPP from the ECM and cell surface during *dpp* signaling, once the *dpp* signal transduction pathway is activated in the receiving cells, attenuating DPP signaling. Lack of these modifications may cause unregulated turnover and premature degradation of the DPP ligand by specific proteases; these processes may possibly lead to reduced *dpp*-signaling activity. One could expect, that an increase in modifications that result in a more stable form of the DPP protein as a result of increased UDP-GlcDH activity, would also reduce or inhibit the proper turnover of DPP protein, thus causing DPP to accumulate in an embryo. However, this role for UDP-GlcDH is hard to reconcile with results that show that when UDP-GlcDH is ectopically activated *in vivo*, no accumulation or elevation of ectopic DPP is observed, even though there is evidence that the *dpp* signaling pathway is ectopically activated in ventral cells of the embryo. A more sensitive assay using a Western blot to compare wild-type embryos with those that have ectopic UDP-GlcDH expression should be carried out. It is possible that an increase in DPP protein occurs that is high enough to ectopically activate the receptors at the surface of ventral cells, but too low to be detected by the current wholemount staining technique.

Assuming that DPP expression is not affected by the expression levels of UDP-GlcDH, another model could have UDP-GlcDH indirectly regulating DPP stability and activity via another secreted factor. This factor may directly interact with DPP and modulate its effective biological activity at the cell surface. The function of this ECM factor would, in turn, be directly regulated by UDP-GlcDH activity in the cell, such that a decrease or increase in UDP-GlcDH expression (or activity) may result in concomitant increase or decrease in the expression (or activity) of the ECM factor. DPP activity normally is thought to be spatially regulated by a post-translational mechanism, involving TLD and SOG, that enhances DPP activity on the dorsal side and repress DPP activity on the ventral side of the embryo. One possibility is that the ECM factor could enhance TLD inactivation and subsequent degradation of SOG, thus alleviating SOG inhibition of DPP activity. TLD degradation of SOG allows the release of DPP preprotein, which is then cleaved to form an active DPP ligand. Active DPP ligand can then diffuse and bind to its receptors. TLD is not directly involved in the cleavage of DPP preprotein, because loss of TLD activity is suppressed by increasing *dpp* dosage. Thus, the ECM factor could act as a colocalizing factor that allows TLD to bind with the SOG/DPP inhibitory complex, and promote TLD targeted degradation of SOG. In addition, the ECM factor could also remain associated with the DPP preprotein to promote its cleavage, and the subsequent release of activated DPP ligand. To test if UDP-GlcDH acts directly in the cleavage of the DPP preprotein, one could test if the loss of TLD activity is suppressed by increasing the expression of UDP-GlcDH. In a converse experiment, one could test if ectopic TLD activity can be suppressed by *sgl* mutants. The observation that ectopic DPP expression can be suppressed by the *sgl* mutation, is suggestive that UDP-GlcDH may affect DPP preprotein cleavage. However, DPP expression was also lost in these embryos, consistent with the hypothesis that UDP-GlcDH may instead regulate DPP stability.

Two earlier studies have suggested that SOG inhibition of DPP signaling is indirect, acting to primarily block SCW signaling (Neul and Ferguson, 1998; Nguyen et al., 1998). They showed that spatially restricted activation of SCW by TLD results in the activation of the SAX receptor which enhances DPP/THV signaling in the embryo (Neul and Ferguson, 1998). The authors concluded that maximal DPP function requires synergistic signaling from the second BMP-like ligand, SCW, which acts through the SAX receptor (Arora et al., 1994). The mechanism(s) by which TOLLOID/SOG mediates non cell-autonomous elevation of DPP signaling through SCW, or by which the SCW/SAX signal is integrated into the DPP/THV signaling pathway are presently unknown. The question then arises whether UDP-GlcDH function affects DPP/THV signal by modulating the SCW/SAX signal and its integration with the DPP/THV signaling cascade.

Support for a role of UDP-GlcDH of mediating SCW/SAX signaling was initially suggested by the observation that mutant alleles of *sgl* resulted in phenotypes that were similar to those caused by loss-of-function mutant alleles of *scw*, *sax*, and *tld* (Ferguson and Anderson, 1992; Arora et al., 1994). This suggests that the function of SCW, SAX, and TLD can be attenuated with a loss in UDP-GlcDH function. Null alleles of *saxophone* typically result in loss of the dorsal-most pattern element, the *amnioserosa* (Nellen et al., 1994a). Trans-heterozygous analysis of *sgl*⁺ and *sax*⁺ mutant embryos

showed no dominant interactions that resulted in a loss-of-function *dpp*-like phenotype in the embryo. However, dead larvae were observed by the second larval instar stage. One reason could be that the maternal contributions from one wild-type copy of *sax* or UDP-GlcDH is sufficient to rescue their zygotic deficiency in the embryo. This suggests that there may be different requirements for the *thv* and *sax* receptors in relation to UDP-GlcDH function, further supporting the hypothesis that *thv* and *sax* have independent functions during development. Because of the dosage effects associated with the *dpp* signaling pathway, another way to test whether *sax* requires UDP-GlcDH function would be to cross viable females that are heterozygous for both *sax* and *sgl* mutations with males that are heterozygous for either *sgl* or *sax* mutant alleles, and then check whether the lethal phase can be shifted to the embryo or earlier stages of first instar larvae.

When it was shown that expression of UDP-GlcDH was able to partially rescue the loss-of-function phenotypes in *dpp^{H46}/+* heterozygous embryos, the initial explanation was that increasing UDP-GlcDH expression was able to elevate residual DPP activity. However, another explanation could be that ectopic UDP-GlcDH function enhances the SCW/SAX signaling pathway which would increase the synergistic interaction with the residual DPP activity. Therefore, if one did a similar experiment in a *scw* or *sax* mutant background, one would expect that ectopic UDP-GlcDH expression would be able to rescue the partial loss-of-function mutant of *dpp*. Conversely, whether or not ectopic expression of UDP-GlcDH can rescue *scw* embryonic mutant alleles must also be established.

To test whether the modulation of SCW activity (by the combined action of SOG and TLD) requires UDP-GlcDH function, one could look to see whether ectopic expression of SOG is suppressed or enhanced in the presence of the *sgl* mutant. Injections of *sog* RNA can normally block the dorsalizing activity of SCW mRNA injected into *scw* mutant embryos, but cannot do so when *dpp* RNA is also injected (Neul and Ferguson, 1998; Nguyen et al., 1998). One could investigate the effects of a loss-of-function *sgl* mutant (with a decreased amount of UDP-GlcDH) and of a gain-of-function mutant (with an increased amount of UDP-GlcDH) in a similar experiment. For example, if UDP-GlcDH activity is a positive regulator of TLD inactivation of SOG, loss of UDP-GlcDH activity in *scw* mutants that are injected with *sog* and *scw* RNA should enhance the ectopic effects of SOG, thus blocking the dorsalizing activity of injected *scw* mRNA. On the other hand, increased UDP-GlcDH expression should inhibit the effects of injected *sog* RNA on injected SCW activity. Also, genetic analysis between loss-of-function mutant alleles of *scw* or *tolloid* and *sgl* has yet to be done. These, and other experiments should further help clarify the role of UDP-GlcDH in the SCW/SAX signaling pathway and the nature of this interaction.

Therefore, based on the current genetic evidence, UDP-GlcDH may act to enhance DPP function at three levels: (1) by indirectly regulating DPP activity by regulating its processing with respect to TLD/SOG interaction in the ECM, (2) by promoting the stability of active DPP ligand or (3) by regulating DPP binding to its receptor complex. By helping to regulate DPP protein processing and stability, UDP-GlcDH may modulate the effective biological concentration of DPP in a spatially restricted

manner in the ECM, allowing for a proper cellular response by promoting the efficient formation of the DPP ligand-receptor complex. The question then remains, how does the UDP-GlcDH enzyme, which is localized in the cytosol, execute its function outside the cell?

IV-3. The role of heparan sulfate proteoglycans in DPP signaling in *Drosophila* embryos.

In this study, UDP-GlcDH has been characterized as an enhancer of DPP signaling. Mosaic analysis of somatic clones of *sgl* mutants suggested that UDP-GlcDH function behaves as a cell non-autonomous regulator of the *dpp*-signaling pathway. The cell non-autonomous function of *sgl* mutants suggests that UDP-GlcDH activity, which is normally localized in the cytosol of the cell, in fact has regulatory effects outside the cell. Two models were proposed to explain how UDP-GlcDH may regulate DPP activity: (1) UDP-GlcDH may help to modify DPP ligand prior to its secretion from the cell, or (2) UDP-GlcDH may regulate the expression or activity of a second factor that is localized to the ECM, that in turn can directly affect DPP activity or stability.

UDP-GlcDH enzyme is required in the biosynthesis of glycosaminoglycans (GAGs), residues that are covalently attached to the extracellular domains of proteoglycans found on the surface cells and in the ECM. Proteoglycans are involved in various extracellular processes, one of which involves the regulation of growth factor activity. This regulation is usually specified by the type of GAG residues associated with the core protein. Mutations that affect the synthesis and biochemical properties of the GAG residues have been shown to have profound effects on proteoglycan function and growth factor activity (see Introduction). Therefore, some initial experiments were formed in this study to address the possibility of the second model. The preliminary data presented in this study so far has implied that the phenotypes resulting from UDP-GlcDH loss and gain-of-function mutant effects may be the due to effects on heparan sulfate GAG biosynthesis, which in turn may affect the regulative role of specific proteoglycans on DPP signaling in the ECM.

IV-3i. Heparan sulfate GAGs and their possible role in *dpp* signaling in *Drosophila* embryos.

In *Drosophila*, the maternal effects of *sgl* mutation on *wg* signaling was shown are due to a block in the synthesis of heparan sulfate GAGs (Binari et al., 1997; Haerry et al., 1997). In the experiment in which heparinase III enzyme was injected into syncytial blastoderm embryos, the authors were able to directly correlate the loss of HS GAGs with a block in *wg* signaling in the embryo (Binari et al., 1997). In *Drosophila* tissue culture cells, *wg* signaling was, upon incubation with heparinase III enzyme, inhibited by removing HSGAGs from the surface of cells receiving the WG signal (Reichsman and Cumberledge, 1996). Protein extracts from maternal and zygotic *sgl* mutant embryos lack several proteoglycans that are recognized by an antibody against heparan sulfate (Haerry et al., 1997). In addition the authors showed that the high-molecular-weight bands of the heparan sulfate-containing protein syndecan are shifted to a lower-molecular-weight band in *sgl* mutant embryos. They

demonstrated that this was not due to protein degradation, and therefore concluded that it was due to a block in the synthesis of GAG chains. In these studies, the addition of excess exogenous heparan sulfate restored *wg* signaling in embryos and cells that were depleted in heparan sulfate residues. This suggested that heparan sulfate is the crucial moiety in *wg* signaling. Based on this evidence, the zygotic *sgl dpp*-like mutant phenotype most probably results from a similar block in the synthesis of the heparan sulfate GAGs (Figure 18), consistent with the second model.

In *Drosophila*, the two major families of cell-surface proteoglycans that contain heparan sulfate GAG residues are syndecans (Spring et al., 1994) and glypicans (Nakato et al., 1995) (see Figure 18). Syndecans are transmembrane HS-proteoglycans that function as co-receptors in FGF signaling in mammals (David, 1993). The expression pattern of *Drosophila* syndecan in the central nervous system coincides with the expression of the FGF receptor (Spring et al., 1994). However, no mutant phenotype for syndecan has of yet been observed. The *dally* gene, which encodes a glypican homolog in *Drosophila*, was initially isolated as a mutant that affected control of cell division and morphogenesis in the eye, wing and antenna (Nakato et al., 1995). Jackson et al. (1997) showed that *dally* is required for normal *dpp* signaling during imaginal disc development. Mutations in *dally* can reduce cellular responses to DPP, whereas ectopic expression of *dally* can enhance the tissue response to DPP. In the latter case, this led to enhanced duplications of the wing disc. This suggests that *dally* may act by modulating the signaling strength of DPP at the cell surface. Jackson et al. (1997) proposed that *dally* may function as a co-receptor, interacting with DPP and promoting ligand-receptor complex formation at the cell surface. In this study, it was shown that mutants of *sgl* were able to enhance weak loss-of-function disc mutants of *dpp*, both in the leg and wing, consistent with the effects observed with *dally* mutant effects. The phenotypes in the wing resembled the effects observed in *dally* mutants on *dpp* signaling. Therefore, this implies that the heparan sulfate residues in DALLY were critical for *dally* regulation of *dpp* signaling. Recently, Tsuda et al. (1999) implicated *dally* as a regulator of *wg* signaling during *Drosophila* embryogenesis. Ectopic expression of *dally* in the embryo produces expansion of naked cuticle along the anteroposterior axis and a loss of most of the ventral denticles. This is consistent with an increase in WG activity and the effects of GLC mutants of *sgl* in the embryo.

One study has suggested that heparan sulfate proteoglycans may also play a role in specifying early dorsal-ventral polarity in the syncytial embryo, even though no evidence was found that showed that *sgl* mutants had any effects on dorsal-ventral pattern at this stage. *Pipe*, a dorsal group gene, is required to specify the *dorsal* protein (DL) gradient which establishes the initial dorsal-ventral pattern in the syncytial embryo. *Pipe* RNA is only expressed in the ventral follicle cells, such that the position of *pipe* expression is sufficient to define the dorsal-ventral polarity of the embryo. Sen et al. (1998) demonstrated that the expression of *pipe* in what would normally be dorsal follicle cells reversed the dorsal-ventral polarity of the embryo. The authors also showed that the *pipe* encodes a heparan sulfate 2-O-sulphotransferase, an enzyme that is known to modify the glycosaminoglycan (GAG) side chains of proteoglycans in the Golgi (Sen et al., 1998; see Figure 14 and Figure 18). Based on its homology to a heparan sulfotransferase, it was assumed that PIPE activity is localized within the Golgi apparatus

of the ventral follicle cells. It is speculated that, along with *windbeutel* (Konsolaki and Schubach, 1998), which appears to encode a protein localized to the ER and Golgi, PIPE may act to modify a proteoglycan that is secreted by the ventral follicle cells to orient the dorsal-ventral axis of the embryo.

Loss of *pipe* function results in no activation of EASTER, the protease required to activate SPATZLE, resulting in the transformation of ventral cells into dorsal cell fates (Morisato and Anderson, 1994; Misra et al., 1998). Therefore, in the absence of PIPE, dorsal-ventral signaling is completely blocked. NUDEL a membrane associated serine protease proteoglycan (Hong and Hashimoto, 1995), is speculated to be a substrate for PIPE. It contains a conserved amino acid sequence that could be sites for GAG addition. NUDEL is exported by the ventral follicle cells into the peri-vitelline space on the ventral side of the oocyte. It was unclear whether NUDEL is associated with the vitelline membrane that surrounds the oocyte before fertilization, or if it is anchored to the ventral side of the oocyte, during oogenesis. LeMosy et al. (1998), showed that NUDEL is localized to the plasma membrane of the egg and then the embryo, providing an ideal source for the morphogen gradient. Therefore, based on the mutant phenotype of *pipe*, sulfation of the GAG residues possibly associated with the NUDEL protein is essential for NUDEL activity. Upon fertilization, NUDEL activates a complex on the ventral side of the embryo consisting of two proteases, EASTER (Chasan and Anderson, 1989) and SNAKE (Smith et al., 1995), possibly by helping to remove a protease inhibitory factor and by regulating the targeted cleavage of EASTER and SNAKE. This protease cascade in turn acts as a ventral extracellular cue which triggers the proteolytic processing and activation of the SPATZLE ligand (Morisato and Anderson, 1994; Schneider et al., 1994), directing the presentation of the processed SPATZLE ligand to its receptor TOLL, located on the outer surface of the cell membrane of the embryo (Gerttula et al., 1988; Hashimoto et al., 1988). The graded activation of TOLL in turn induces the translocation of DORSAL from the cytoplasm to the nucleus in a ventral-to-dorsal nuclear gradient in the embryo (Anderson et al., 1985; Anderson and Hecht, 1993), reflecting the ventral-dorsal graded distribution of activated SPATZLE in the perivitelline space. Thus, events that are described downstream of *pipe* suggest that the modified proteoglycan must act by controlling the proteolytic activation of the ligand SPATZLE. In the model, the initiation of dorsal-ventral polarity may require the PIPE-dependent sulfation of HS GAGs of a proteoglycan, possible NUDEL, which in turn helps to localize a ventral protein complex on the plasma membrane of the embryo initiating the sequence of proteolytic events to produce activated SPATZLE ligand.

Sugarless (see **Figure 18**) mutations, when analyzed for their maternal-effect phenotype in germline clones (Binari et al., 1997; Hacker et al., 1997; Haerry et al, 1997), surprisingly showed no effects that were consistent with disruption of the maternal dorsal-ventral patterning that involves the SPATZLE/TOLL signaling pathway. One possible explanation is that there may be another UDP-GlcDH-like gene that is specifically required for production of the heparan sulfate GAG residues for the proteoglycan(s) that regulate the early maternal SPATZLE/TOLL signaling pathway. However, one must remember that the mutant *wg*-like phenotypes observed in the embryos were due to germline clone effects of *sgl*^{P1731}, whereas *pipe* function is determined by the somatic follicle cells that sur-

round the oocyte in the egg chamber. Therefore, another explanation would be that UDP-GlcDH function is still provided by the same set of follicle cells, even if the germline cells are mutant (e.g., the nurse cells or oocyte). In this case, one should look at the effects of *sgl* mutant clones in the follicle cells. In another experiment, one could generate mothers that are heterozygous mutant for both *pipe* and *sgl*. In this case, *pipe*⁺, *sgl*⁺ mothers would be crossed to fathers that are heterozygous for *sgl*⁺ to determine whether mutants of *sgl* can dominantly enhance mutants of *pipe*. By injecting heparinase III enzyme into the perivitelline space of embryos, one can also test directly whether heparan sulfate GAGs are required in SPATZLE/TOLL activation. In this case, one would predict that the degradation of heparan sulfate would result in the disruption in the proteolytic activation of EASTER and SPATZLE ligand, mimicking the *pipe* mutant phenotype.

In this study, it was shown that ectopic expression of heparinase III following cellularization of the syncytial embryo resulted in loss of the dorsal cuticle pattern and generation of U-shaped embryos, which is much like the phenotype observed in zygotic loss-of-function mutants for *sgl* and *dpp* pathway genes. It was inferred from these results that the dorsal defects caused by the ectopic expression of heparinase III in the embryos was the result of heparan sulfate degradation, that caused the block in *dpp* signaling. Heparinase III can degrade both heparin and heparan sulfate into di- and tetrasaccharides (Nakajima et al., 1983; Ototani et al., 1981; Godavarti and Davis, 1996). However, heparan sulfate is favored over heparin as the possible GAG moiety responsible for the phenotype because heparin is largely intracellular, whereas heparan sulfate is extracellular. This would then suggest that heparan sulfate GAG residues, which are most likely associated with specific membrane or ECM-associated proteoglycans may play a role in mediating DPP activity in the embryo. The block in *dpp* signaling was confirmed by the loss of *tinman* and *Kruppel* expression in the embryo.

This indicated that the similar phenotype observed in *sgl* mutant embryos may be explained by defects in heparan sulfate biosynthesis. However, only 68% of the embryos that expressed heparinase III resulted in a lethal phenotype. This observation could be explained by two caveats: (1) It has not been determined whether the heparinase III enzyme is secreted by the cells in the embryo. Even though the heparinase III construct carries a N-terminal signal sequence, and expression of this construct in *Drosophila* Schneider cells in culture results in heparinase III activity in the serum, *in vivo* confirmation of heparinase III activity in the embryo remains to be determined. the existence of *in vivo* activity can possibly be determined possibly by looking for the effects of extracts from embryos that ectopically expressed heparinase III on the migration (on polyacrylamide gels) of various heparan sulfate proteoglycans, for example, syndecan or DALLY, two common membrane-bound HSPGs, or perlecan, an ECM-associated HSPG. If the heparinase III is properly secreted from the cell, one would expect that degradation of the heparan sulfate residues found on these proteoglycans would cause the latter to migrate further down the polyacrylamide gel, when compared to controls (see Haerry et al., 1997). As the HS GAGs are being removed, one would expect the sharpening of bands created by shifts in the the migration of HSPGs (due to a reduction in molecular weight), as the HS GAGs are removed in embryos that ectopically expressed heparinase III. (2) Assuming that heparinase III

enzyme is secreted by the cell, the heparinase III only enzyme degrades heparin and heparan sulfate GAG residues. Therefore, other GAG residues such as chondroitin sulfate or dermatin sulfate (Appendix II) may still be present. Even though the heparan sulfate molecules may be degraded, the presence of other GAG residues that remain may allow for some residual function of the proteoglycans that may be involved in regulating DPP activity. Therefore, it is inferred from these experiments that the phenotype that resulted from ectopially expressed heparinase III was due to degradation of the heparan sulfate moieties in the ECM. This implied that the UDP-GlcDH may regulate the production of HS GAGs that are specifically required for *dpp* signaling.

Binari et al. (1997) showed that injection of excess heparan sulfate into syncytial embryos prior to cellularization resulted in a naked cuticle phenotype similar to that observed when WG is ectopically expressed in embryos (Macdonald and Struhl, 1988). Later, Tsuda et al. (1999) showed that ectopic expression of DALLY (a heparan sulfate proteoglycan) in the embryo produces expansion of naked cuticle and loss of most of the denticles, which is consistent with an increase in ectopic WG activity. The use of polyclonal antibodies to heparan sulfate shows that when UDP-GlcDH was expressed ectopically at cellularization in blastoderm embryos, levels of heparan sulfate increased by stage 10-11, (Manoukian lab, unpublished). This resulted in dorsalization of the embryo similar to that seen in embryos in which *dpp* signaling was ectopically activated (see **Figures 42 and 46**). This implied then that elevated expression of heparan sulfate may enhance DPP activity throughout the embryo. There was no evidence to show that *dpp* transcript or protein expression had increased as a result of ectopic UDP-GlcDH expression, in the embryo. However, loss of heparan sulfate GAGs in embryos, whether due to heparinase III treatment or *sgl* mutants resulted in a loss of DPP expression.

One possible explanation for these effects may be that higher levels of heparan sulfate localized to the cell surface help to stabilize the DPP in the ECM, in turn making the cells more responsive (sensitive) to the lower levels of endogenous DPP. Also, higher levels of HS GAGs at the cell surface may enhance the sequestering of active DPP to the cell surface so it can bind more effectively with its receptors. In effect, this would lower the threshold of response of the ventral cells to DPP, in turn leading to the activation of its receptors and their downstream signal-transduction cascade. Another possible explanation could be that higher levels of heparan sulfate may enhance TLD activity, leading to the degradation of SOG, which is normally found at high levels in the ventral part of the embryo. This in turn would allow for the release and activation of the DPP ligand. Excessive levels of heparan sulfate in this case, could, promote TLD-specific interactions with the SOG/DPP complex, cleaving SOG and releasing the DPP ligand. The subsequent proteolytic activation of the DPP preprotein could also be enhanced by high levels of heparan sulfate. Therefore, one may speculate that the cumulative effects of these steps could allow for enough DPP ligand to be targeted to its receptors in the ventral cells to cause a biological response.

The ectopic phenotypic effects caused by increasing the level of UDP-GlcDH expression suggest that the UDP-GlcDH enzyme represents the limiting factor in heparan sulfate biosynthesis that

affects *dpp* signaling. If UDP-GlcDH function is rate limiting, one would expect that an increase in the expression of other enzymes involved in the biosynthesis of heparan sulfate GAGs would not cause phenotypic effects similar to those of ectopically expressed UDP-GlcDH. Therefore, these results suggest that there may be other isoforms of the UDP-GlcDH enzyme that are required for the biosynthesis of HS residues that specifically affect the activity of other growth factor molecules. To date, a search of the sequence data base from the Berkeley *Drosophila* genome project (2001) has not yielded other UDP-GlcDH like sequences. Thus far, increasing the expression of other enzymes in the biosynthetic pathway has been shown to specifically affect the activity of other signaling molecules. Over-expression of TTV (a HS co-polymerase enzyme) in *Drosophila* results in only a *hh* loss-of-function phenotype (Bellaïche et al., 1998; The et al., 1999). In the case of HS regulation of HH protein, TTV may be acting as the limiting factor for the *hh* signaling. Therefore, another enzyme in the biosynthetic pathway may act as the limiting factor for another signaling pathway, consistent with UDP-GlcDH being the limiting factor for the DPP signaling pathway.

Studies in mice have shown that specific isoforms of these HS copolymerases, for example, the sulphotransferases (see **Figure 18**), may be responsible for the discrete sulfate modification patterns of heparan sulfate GAGs (Bullock et al., 1998; Forsberg et al., 1999; Humphries et al., 1999). Specific modified forms of heparan sulfate GAGs were shown to regulate the specific activity of different growth factors, underscoring the discrete action of different modified forms of HSGAGs. The spatial and temporal regulation of expression of these modifying enzymes seems to regulate the temporal and spatial activity of growth factors during development, as reflected in the tissue specific effects of mutants of the isoforms. Modification of HSGAGs, for example, deacetylation followed by sulfation, modulates the growth factor binding-specificity of HS GAGs. The modifications of functional groups along HSGAG chains provides a chemical specificity for interactions with growth factors such as FGF (Rapraeger et al., 1991) and TGF β (Lopez-Cassalis et al., 1993). In *Drosophila* the gene *sulfateless* (*sfl*) (see **Figure 18**), encodes the homolog of heparin, as well as of heparan sulfate N-deacetylase/N-sulphotransferase, an enzyme that to modifies heparan sulfate, replacing the acetyl groups with a sulfur group. *Sfl* was shown to be essential for *wg* signaling but has no effects on *dpp* signaling (Lin and Perrimone, 1999). Lin et al. (1999) showed that germline clones of *sfl* resulted in a *wg*-like embryonic phenotype. Therefore, the loss of specific sulfate groups can affect GAG or PG function in a tissue, by lowering or eliminating the affinity of the GAGs for a specific growth factor, such as WG. This demonstrates that the specific sulfate groups found in HSGAG residues are critical for promoting only *wg* signaling. In fact genes that encode various other enzymes that are involved in the production and modification of heparan sulfate GAGs in *Drosophila* have been isolated and shown to specifically affect only certain signaling pathways (**Figure 18**). This suggests that these genes may represent different isoforms of the enzymes that are required for the production of specific HSGAGs that are responsible for the regulation of a specific signal transduction pathway. A summary of the genes and their effects is shown in **Figure 18**.

As mentioned earlier, one caveat to the model that has been proposed is the possibility that the

phenotypes observed when UDP-GlcDH expression is decreased or increased are not due to the direct attenuation or enhancement of the DPP signal by heparan sulfate. In *sgl* mutant embryos or in embryos in which heparinase III was ectopically expressed, transcript expression of DPP remained unaltered; however, DPP protein expression was reduced or completely lost. Conversely, when UDP-GlcDH was ectopically expressed in the embryo, expression of both *dpp* transcript and protein was not altered. Based on the direct interaction model for heparan sulfate and DPP protein, it was proposed that the presence of heparan sulfate contributed to the stability of endogenous levels of DPP in the ECM. However, changes in the level of *dpp* expression have been shown to have effects that attenuate or enhance *dpp* signaling, without producing any observable change in its transcript or protein expression. Therefore, it is possible that increases or decreases in heparan sulfate expression can affect DPP signaling by regulating the transcription or translation levels of *dpp* in the embryo, enough to cause *dpp*-like loss- or gain-of-function phenotypes. In this case, the current *in vivo* methods of detection may not be sensitive enough to resolve any slight differences in transcript or active protein levels.

Human cell-culture studies demonstrate several examples in which GAGs were shown to regulate transcript and protein levels in cells (reviewed in Jackson et al., 1991). During hepatocyte-cell differentiation in the liver, GAGs were shown to increase the secretion of transferrin, haptoglobin, albumin, alpha1-inhibitor, alpha1-antitrypsin, and hemopexin. GAGs were also shown to regulate levels of cytosolic aldolase expression and cause increases in the cytoskeletal gene expression of mRNA for β -actin, β -tubulin, cytokeratins, alpha-actin, and desmoplakin (Schuetz et al., 1988; Ben-Zelev et al., 1988). The ECM components that regulate these genes have been linked to the proper maintenance of cell morphology. HS-GAGs were also shown to specifically up-regulate the synthesis of whey acidic protein, transferrin, and β -casein in mammary epithelial cells during pregnancy and lactation (Bissell and Hall, 1987; Chen and Bissell, 1987 and 1989). Mechanisms for the regulation of transcription or translation remain to be determined; however, one proposed model suggests that HSPG(s) could modulate a signal transduction cascade to indirectly regulate the expression levels of these genes in response to changes in the extracellular environment around a cell (Chopra et al., 1989; reviewed in Jackson et al., 1991). A second model suggests a direct physiological role for intracellular HS-GAGs; in this model, the HSPG is internalized by the cell through a facilitated mechanism, and the GAG moieties are degraded and delivered to the nucleus. In the nucleus, the HS-GAG molecules interact with specific transcription factors to regulate gene expression (Ishihara et al., reviewed in Jackson et al., 1991).

To address this caveat, quantitative analysis of the *dpp* transcript or protein expression must be undertaken under conditions in which UDP-GlcDH activity is either decreased, as in *sgl* embryos or heparinase III treated embryos, or increased, as in embryos that ectopically express UDP-GlcDH. To assess changes in *dpp* transcript levels, quantitative Northern, 5' RT-PCR, or RNase protection can be used to determine relative *dpp* transcript expression. Using quantitative Western analysis would allow comparison of the levels of DPP preprotein prior to its cleavage activation with levels of active secreted DPP ligand, thus revealing whether DPP translation is attenuated or enhanced. In this case antibodies that discriminate between preprotein and cleaved active form must be used.

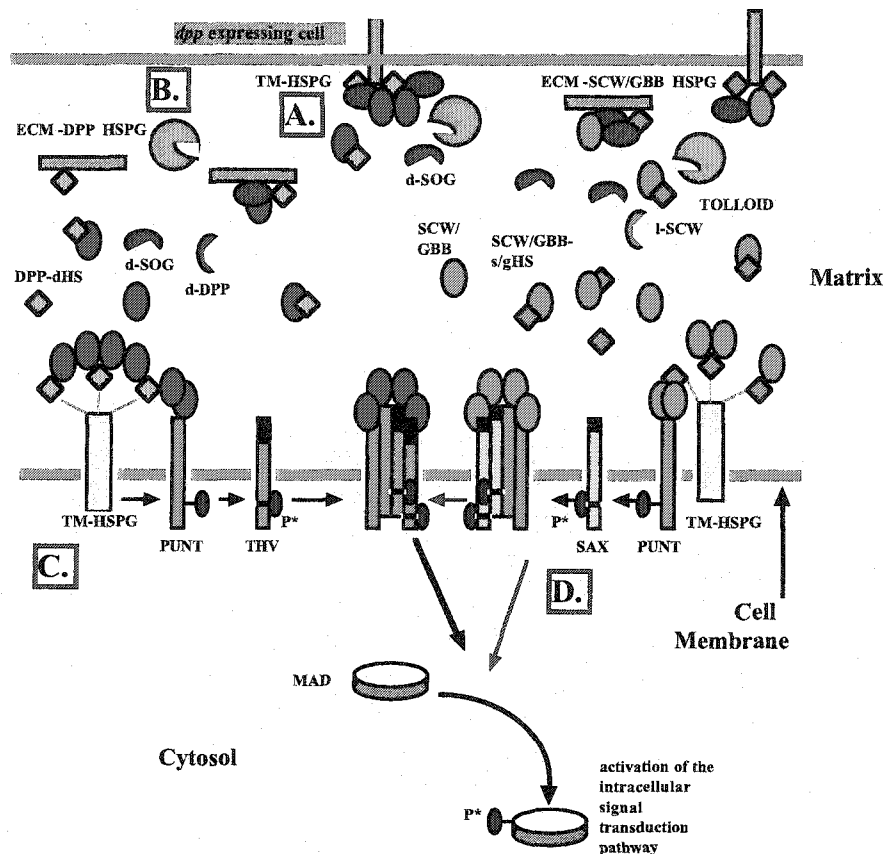
The results presented thus far suggest that heparan sulfate GAGs may be the critical moieties required to stabilize DPP in the ECM, and enhance DPP signaling during embryo development in *Drosophila*. The results underscore the important role that the cellular environment plays in growth factor signaling. The lack of biochemical evidence thus far makes it unclear which particular mechanism is involved in this regulation. It has shown that the *in vivo* regulation of heparan sulfate GAG turnover in a cell by hydrolytic cleavage with endogenous lyases or hydrolases may play a role in modulating the biological function of heparan sulfate GAGs in binding proteins (Ernst et al., 1995). Previous studies involving heparan sulfate and WG regulation suggest that WG directly interacts with heparan sulfate. One could expect that a similar scenario could also apply to DPP. Reichsman et al. (1996) showed that heparan sulfate can directly modulate extracellular localization of WG and promote its signal transduction in *Drosophila* cell cultures. They demonstrated that WG signaling was restored in UDP-GlcDH mutant cell lines when heparan sulfate was added to the cell culture. Another experiment (Wesley and Manoukian, unpublished), showed that *in vivo* immunoprecipitation (IP) analysis of *Drosophila* embryo extracts using either a WG or a heparan sulfate antibody resulted in the isolation of a complex that contained WG and a heparan sulfate containing factor. They showed that in a similar IP in *sgl*-mutant embryos, a complex of low molecular mass was pulled down only when WG antibody was used. This complex could not be detected on a Western blot with heparan sulfate antibodies, however, direct interactions between HS-GAGs and DPP have not yet been tested for. If it turns out that direct interactions between HSGAGs and DPP do occur, then regulation of the levels of heparan sulfate GAG synthesis and turnover in the ECM would be critical in its role in regulating the threshold response of a cell to the DPP and other growth factor signals. However, since loss of UDP-GlcDH does not result in a complete loss of DPP activity, it is possible that, in addition to heparan sulfate GAGs, other components yet to be identified in the extracellular matrix are involved in transducing the DPP signal. These unidentified factors may compensate for the absence of heparan sulfate caused by *sgl* mutants.

IV-3iii. Models for heparan sulfate GAG modulation of *dpp* signaling in *Drosophila* embryos.

In light of the preliminary evidence presented above, I propose that UDP-GlcDH regulation of *dpp* signaling is carried out by the regulation of heparan sulfate GAG biosynthesis. Based on the models proposed for UDP-GlcDH regulation of *dpp* signaling in section IV-2ii of the discussion, I speculate that heparan sulfate GAGs and their proteoglycans are involved in modulating various aspects of DPP signaling in the embryo. Modulation by specific HSGAGs residues associated with either membrane or ECM forms of heparan sulfate proteoglycans (HSPGs), may occur directly at either the level of DPP ligand processing and stabilization or at receptor binding and activation (**Figure 55**). Enhancement may also occur indirectly by specific HSGAGs that regulate the synergistic SCW/SAX signaling pathway.

The modulation of DPP activity is a key aspect of *dpp* signaling during dorsal-ventral axis specification in the embryo. For example, activation of SAX by SCW enhances DPP/THV activity to

Figure 55. Models for the *dpp* signaling cascade involving HSPG regulation.



A schematic diagram showing possible roles of transmembrane- and ECM- associated HSPG(s), in regulating *dpp* signaling. **Figure 55** depicts four possible models that are consistent with the evidence discussed herein. (A) The first model suggests that a transmembrane HSPG (TM-HSPG) found on the surface of *dpp* expressing cells exists in a complex with the DPP and SOG inhibitor protein. HS residues help to sequester diffusible TOLLOID to the complex at the cell surface, where TOLLOID then degrades SOG (d-SOG) and releases active DPP ligand into the ECM. (B) In the second model diffusible DPP once released from *dpp* expressing cells is complexed with SOG inhibitor and an extracellular matrix associated HSPG (ECM-HSPG), localizing the DPP ligand. Diffusible TOLLOID is then sequestered by the ECM-HSPG, to degrade SOG (d-SOG) and release active DPP near the cells that will receive the signal. (C) In a third model, a TM-HSPG on the surface of cells receiving the DPP signal, acts as a low affinity co-receptor, to sequester diffusible DPP ligand from the ECM to the surface of the cell, where it then helps to promote DPP dimerization and binding to its receptors PUNT and THV. This then promotes PUNT and THV receptor clustering, which activates THV and the downstream intracellular signal transduction pathway. (D) A fourth possible model could be one in which HSPG(s) are required, in a similar fashion, to regulate the second TGF β signaling pathway in *Drosophila*. In this case, HSPG(s) modulate SCW and GBB to promote signaling through a second receptor complex, SAX and PUNT, which in turn is required to synergistically enhance the *dpp* signaling pathway. These models do not preclude the possibility that the HSPG(s) described here may also perform a second role, one of limiting or promoting DPP ligand diffusion through the ECM.

determine the dorsal-most cell fates (e.g., amnioserosa) (Arora et al., 1994; Neul and Ferguson, 1998; Nguyen et al., 1998). However, it is not clear how the combined activities of these two ligands are integrated to specify positional information. In contrast, SOG, an extracellular protein (Marques et al., 1997), inhibits DPP activity possibly by direct protein-protein interactions with DPP (Francois et al., 1994; Holley et al., 1995; Piccolo et al., 1996). Loss of *sog* results in *dpp*-dependent expansion of dorsal cell fates, whereas ectopic dorsal expression of *sog* leads to a partial ventralization of the embryo (Ferguson and Anderson, 1992b; Francois et al., 1994; Holley et al., 1995; Biehs et al., 1996). In turn, *tolloid* (*tld*), a secreted zinc metalloprotease related to BMP1, is expressed in the dorsal half of the embryo (Shimell et al., 1991; Mullins, 1994), and acts a positive regulator of DPP activity by degrading SOG, thus suppressing the inhibition of DPP (Marques et al., 1997). In addition, SOG also antagonizes SCW, by blocking its activity and thus limiting its ability to augment DPP signaling in a graded manner along the dorsal-ventral axis (Neul and Ferguson, 1998; Nguyen et al., 1998). These observations have led to a model in which a ventral-to-dorsal gradient of SOG results in the production of a reciprocal dorsal-to-ventral gradient of DPP activity (Marques et al., 1997).

In one model, HSPGs may physically interact with DPP or SCW via the HSPGs' HS residues that are specific for only DPP or SCW binding. In this case, for temporal and spatial regulation of DPP activity to occur, HSPGs would have to be expressed in a specific spatially and temporally manner in the embryo such that once DPP or SCW is released upon SOG cleavage, the HSPGs can help to sequester the active ligand to the cell surface, thus enhancing ligand binding to its receptors. Therefore, HSPGs would act as co-receptors for DPP and SCW signaling (Figure 55C and D). Another possibility could be that the heparan sulfate GAGs may, at the same time, help promote receptor clustering of PUNT and THV at the cell surface upon DPP binding. The HSPGs at the cell surface could maintain low-affinity interactions with PUNT and THV, keeping them in close proximity to each other. At the same time the HSPGs could also contribute to increasing the local concentration of active DPP ligand at the surface of cells. This would then allow for the rapid binding of DPP, clustering of its receptors, followed by activation of the signaling cascade in the receiving cell. Therefore, for example, high levels of heparan sulfate may, in the presence of low levels of DPP, act to concentrate DPP to the surface of cells, allowing it to reach the necessary threshold level for ligand-receptor oligomerization. Biochemical evidence from studies in vertebrates proposed a similar mechanism for HSPG regulation of FGF receptor activation. Lin et al. (1999) provided genetic evidence that, in *Drosophila* of a similar mechanism, showing that specific modified forms of HSGAGs maybe essential for FGF signaling. They demonstrated that embryos mutant for *heartless* or *breathless*, which encode two *Drosophila* FGF receptors (Beiman et al., 1996; Gisselbrecht et al., 1996; Klambt et al., 1992), have zygotic phenotypes similar to those of embryos that lack UDP-GlcDH (*sgl*) and N-deacetylase/N-sulphotransferase (*sfl*). They showed that the *sfl* mutant enhances the mutant phenotypes of these two FGF receptors in the embryo. Since the clustering of FGF receptors is a key process in the transduction of the FGF signal, HSGAGs may somehow be involved in regulating this process indirectly through its involvement in the production of heparan sulfate. In fact, both *breathless*- and *heartless*-dependent MAPK activation is significantly reduced in embryos that fail to synthesize heparan sulfate in *sfl* mutant embryos. In

vertebrates, heparan sulfate is not believed to be required for receptor binding of the growth factor, but instead it enables the formation of a high affinity complex that potentiates receptor signaling at low growth factor concentrations (Nugent and Edelman, 1992; Roghani et al., 1994). The FGF receptors have been shown to bind to a specific pentasaccharide sequence in heparan sulfate (Maccarana et al., 1993; Guimond et al., 1993). Low-level activity results from bringing the two kinase domains of the FGF tyrosine kinase receptors into close proximity, thus allowing the phosphorylation of one of the receptor kinases by the other (Klemm et al., 1998). In the presence of FGF ligand, activity is maximized, suggesting that heparan sulfate is used to enhance FGF signaling. Therefore, a similar mechanism could be used to explain heparan sulfate regulation of *dpp* signaling.

The data could also be explained by a second model, in which HS-GAGs play a more direct role in establishing the DPP/SCW activity gradients (see **Figure 55A**). One of the best-defined biochemical functions of HSPGs is their interaction with serine proteases and growth factors, both of which are central in the extracellular events that lead to activation of the ligand, and its downstream receptor. An example of this would be the activation of SPATZLE and its receptor TOLL (see **Figure 14**). In another example, the anticoagulant activity of heparin is based on specific binding to both the serine protease thrombin and the serpin inhibitor of thrombin, antithrombin III (see **Figure 17**). Heparan sulfate GAGs synthesized by mast cells and basophils activate antithrombin III, a protease inhibitor, providing a precedent for GAG-mediated control of extracellular enzyme activity (Finelli et al., 1995; Shimell et al., 1991, reviewed in Hornebeck et al., 1994). In the model proposed here, localized HS-GAGs found associated with either ECM- or membrane- bound HSPG, could localize DPP preprotein, in a complex that would include SOG, at the surface of the *dpp*-expressing cell. In addition, the HSPG complex can, in turn, help to co-localize TLD to this complex and promote TLD cleavage of SOG in dorsal regions of the embryo, thus releasing the DPP ligand. Therefore, in this case, HS-GAG function allows for the localization and efficient binding of TOLLOID to SOG, inducing the cleavage and release of the DPP preprotein from its inhibitory complex.

In another model, a specific ECM-HSPG could be involved in the processing step of the DPP preprotein into an active ligand (**Figure 55B**). The same, or different, ECM- or membrane- bound HSPG could then promote the proteolytic cleavage of the DPP preprotein into an activated DPP ligand. The HS-GAG would act as an initiation signal for a specific DPP proteolytic processing enzyme. Therefore, the expression of this specific HS-GAG would have to be both spatially and temporally regulated, tying it in with the proper regulation of DPP activation in dorsal cells of the embryo. In a similar scenario, HS-GAGs in the ECM could also remain associated with the activated DPP ligand by acting as a chaperone through DPP's migration across the ECM to its receptor on a cell surface. This interaction could protect DPP from natural proteases that would result in its premature degradation and turnover. In this case HS-GAGs may act to maintain the effective biological concentration of active DPP in the ECM. The HS-GAGs may also help to regulate DPP diffusion to its receptors in the neighboring cells. Therefore, any loss of HS-GAG expression in the ECM would leave free DPP ligand unprotected from degradation once DPP is released from SOG. Lastly, the HS-GAGs could be

required at the level of SCW regulation of DPP signaling. To help promote maximum DPP activity for the determination of the dorsal-most cell fates in the embryo, HSGAGs may be involved in mediating the integration of SCW signal with the *dpp* signaling cascade.

Although SOG has been primarily characterized as an inhibitor of DPP and SCW signaling, closer analysis has also suggested that it exerts a long-range positive, cell non-autonomous effect on DPP and SCW activity; this activity which is essential for the specification of dorsal-most cell fates (amnioserosa) (Zusman et al., 1988; Ashe and Levine, 1999), requires extracellular SOG diffusion and TLD function (Ashe and Levine, 1999). The mechanism by which SOG mediates cell non-autonomous elevation of DPP and SCW signaling remains unknown. One hypothesis proposed by the authors is that SOG may facilitate the diffusion of DPP and SCW toward the dorsal-most side of the embryo, whereupon TLD would cleave SOG to liberate active DPP and SCW ligand and thereby increase the dorsal DPP ligand concentration (Holley et al., 1996). Alternatively, while full-length SOG inhibits DPP/SCW signaling, a TLD-mediated cleavage product of SOG may elevate DPP/SCW signaling, either directly or as an independent signal (Marques et al., 1997). In this model, the SOG/DPP complex may be formed and stabilized by a ECM-associated HSPG that helps to target the complex to the dorsal-most side of the embryo. Therefore, in *sgl* mutants, targeting of the SOG/DPP complex is abrogated, resulting in the loss of the extra-embryonic tissue (amnioserosa) in the embryo blastoderm.

Each of the models proposed here can be used to explain the observations that show loss of *dpp* signaling and the fading of DPP in embryos as a result of the *sgl* mutant or heparinase III treatments. By increasing or decreasing the levels of heparan sulfate in the extracellular matrix (in different regions of a tissue), one may enhance or attenuate these various processes, resulting in the promotion or suppression of *dpp* signaling respectively. However, at this point, there is no direct biochemical evidence to support existence of the interactions proposed by any one of the models. Thus, the specific level at which HS and HSPGs regulate the DPP signal remains to be determined. Biochemical studies of HS GAG-protein binding would allow determination of which proteins (e.g., DPP itself or one of its receptors in the signaling cascade) may interact directly with the HS moieties. If such interactions occur, then which specific HS moieties are involved in the binding? Identification of the type of HSPG involved in the interaction would also be critical. An IP (immunoprecipitation) approach in which antibodies to proteins suspected to be interacting with HSPGs could be used to pull down, from embryonic extracts, any factors that may complex with a protein of interest. The components from the complex could then be separated and identified biochemically. An approach using genetic screens could help isolate specific components involved in the regulation of expression of heparan sulfate moieties that specifically affect *dpp* signaling. A genetic suppressor or enhancer screen of the *sgl* mutation in the embryo may help isolate other mutations that result in dorsal-ventral patterning defects in the embryo. In turn, one could then ectopically express heparan sulfate in these mutant lines by injecting heparan sulfate into the perivitelline space of the syncytial blastoderm embryo to see whether the phenotype can be suppressed or enhanced. Simply expressing ectopic UDP-GlcDH would not work. Even though, as suggested in this study, UDP-GlcDH activity is rate limiting, the mutant phenotypes of any

downstream mutations that affect either the modification of the HS chains, or the expression of the protein core of the proteoglycan would not be altered by the ectopic expression of UDP-GlcDH, which would only increase the production of the HS chains that had yet to be modified.

IV-4. The role of heparan sulfate GAGs in regulating DPP morphogen in imaginal discs in *Drosophila*.

The context-dependent requirement for HS or HSPG(s) in the normal function of a morphogen may be important. DPP-dependent activities defined in two different developmental contexts, one in the embryo and the other in the imaginal discs, may reflect distinct differences in the way of which gradients of the DPP morphogen are created and maintained and/or the way in which receptors are activated. As described earlier, in the blastoderm embryo, *dpp* and *scw* are expressed over a broad area in which they are required for patterning. The gradient of DPP activity is formed rapidly through post-translational mechanisms. The principal mechanism used to generate positional information in the embryo, is a cell non-autonomous, spatially restricted modulation of DPP and SCW signaling by SOG and TLD. The rapid inhibition of SOG by TLD may preclude morphogen diffusion from a localized source, particularly as the DPP and SCW receptors are all provided to the embryos from the maternal genome during oogenesis and thus unlike the imaginal discs, cannot be subjected to feedback regulation. In contrast, DPP in the wing disc is secreted from a localized source, and behaves as a morphogen gradient that is established by the diffusion of DPP protein across a field of cells over a long distance. This is believed to provide a gradient of spatial information (which is defined by the local concentration of the DPP) that specifies positional information and, ultimately the behavior of the responding cells (Nellen et al., 1996; Lecuit et al., 1996; Zecca et al., 1996).

IV-4i. ECM molecules that regulate WG and HH diffusion in imaginal discs: possible models for the DPP morphogen gradient.

The factor(s) involved in creating a concentration gradient in a cellularized environment with the appropriate range, slope and spatial restrictions are not well understood as the possible mechanisms remain speculative. One assumption would be, if these factor(s) can physically interact with the morphogen, then temporal and spatial regulation of such (a) factor(s) in the ECM or on the cell surface would be critical for the formation of the gradient. Also, one would have to determine whether these factors are involved in the passive or active diffusion of the morphogen through the ECM, or whether they are part of an active endocytic-exocytic regulated process in which the morphogen travels from cell to cell. Several possible molecules could be used by the cell to regulate diffusion of a morphogen molecule. These could include lipids, cholesterol moieties, membrane receptors, and ECM- and membrane- associated HSPGs, to name a few. Recent studies in *Drosophila* have shed some light on possible factors and mechanisms involved in establishing a morphogen gradient.

Zecca et al. (1996) have shown that WG behaves as a morphogen gradient in wing imaginal

discs. In these discs, *wg* is transcribed in a 4- to 5-cell-wide stripe straddling the dorsal/ventral (D/V) boundary in the wing pouch (Baker, 1988; Williams et al., 1993; Couso et al., 1994). *Distalless* (*Dll*) expression, a direct nuclear target, is regulated by WG, in a concentration-dependent manner, some 20 cells away from the site of WG synthesis at the D/V boundary (Zecca et al., 1996, Neumann et al., 1997).

Cadigan et al. (1998) suggested the WG receptor *Dfrizzled-2* (*Dfz2*) (Bhanot et al., 1996), as one potential factor involved in shaping the WG gradient. The current model describes the WG gradient as being biphasic, with an initial steeply decreasing slope followed by a more gradually decreasing slope (Cadigan et al., 1998). Cadigan et al. (1998) showed that high levels of *Dfz2* receptors bind and stabilize WG, allowing it to reach cells far from its stripe of synthesis. In this case *Dfz2* acts as a positive regulatory factor in modulating the WG gradient. *Dfz2* is, therefore, an important factor for the establishment of the gradual decreasing slope of the morphogen gradient. However, the identity of the factor(s) that cause the initial slow rate of diffusion and/or rapid turnover of WG in the gradient is still in question? Recent evidence seems to point to HS-GAGs as being one of these factors.

Haerry et al. (1997) showed that the depletion of HS-GAG production in *sgl* mutant embryos has effects on the range of WG activity in the embryo. In wild-type embryos, *en*, (which is under the control of WG) is expressed in stripes that are two cells wide in each parasegment. The authors observed that in *sgl*-mutant embryos, the initial expression of EN protein expanded the stripe of expression to more than two cells wide. One possible explanation offered was that WG was able to diffuse further from source cells in *sgl*-mutant embryos than in wild-type embryos. These authors speculated that the HS-GAG chains in the ECM may be required to help concentrate WG, perhaps by restricting its diffusion, in addition to modulating the reception of the WG signal. In fact, WG itself was shown to migrate further in *sgl*-mutant GLC embryos, causing the expansion of EN expression and expansion of naked cuticle upon differentiation (Scanga and Manoukian, unpublished). However, the levels of WG are eventually reduced in *sgl*-mutants, thus attenuating the *wg* signal and causing EN expression to fade, finally resulting in the *wg*-like mutant phenotype in the embryo. When imaginal wing discs were incubated in culture with heparinase III enzyme, WG protein was observed to travel further into the wing pouch. This correlated with the expansion of *Dll* expression to the edge of the wing pouch (Scanga and Manoukian, unpublished). Neither the HSPG nor the type of HSGAG molecule involved in this process has been identified. Therefore, in conjunction with the results presented by Cadigan et al. (1998), the data suggest that the WG gradient seems to form by regulated diffusion, in which the receptor and HSPG(s) may act to constrain WG migration in the ECM.

In a recent paper by Greco et al. (2001), the authors implicate HS-GAGs in a novel cell biological mechanism that disperses the WG morphogen via membrane fragments over long distances through the imaginal disc epithelium. Membrane exovesicles called argosomes, are derived from basolateral membranes in imaginal discs. These argosomes travel through adjacent tissue in which they are found predominantly in endosomes. The authors showed that WG colocalized with argosomes derived from

wg-producing cells, providing a vehicle for the spread of WG. They further showed that HSPG(s) are required for the localization of WG to these argosomes on the membrane surface of the producing and receiving cells. Therefore, the data suggest that WG diffusion may involve more than one mechanism, and that HSPG(s) may be required as a general factor in these different processes.

Another recent study reported the identification of another *Drosophila glypican* gene, *dally-like* (*dly*) (see **Figure 18**), an HSPG that is involved in WG signaling (Kharen and Baumgartner; 2000; Baeg et al., 2001). The authors showed that over-expression of *dly* resulted in a *wg*-like phenotype in the adult wings; this phenotype exhibited the notching of the wing margin and loss of sensory bristles. Over-expression of DLY, was followed by an increased accumulation of extracellular WG protein in the ECM. The phenotype was the result of excessive DLY protein sequestering WG along the D/V compartment boundary (the putative wing margin), *wg* is expressed in cells that straddle the boundary, thus preventing it from accessing and activating its receptor, *Dfz2*. *Sulfateless* (*sfl*), a N-deacetylase/N-sulphotransferase, is involved in GAG modification; in *sfl* mutants, the GAG chains are not synthesized properly and the modified form of DLY protein is significantly reduced. WG expression is not altered in *sfl*-mutant clones, indicating that *sfl*-mutant cells normally transcribe *wg* and secrete WG. Outside the *sfl*-mutant cells expressing *wg*, extracellular WG is dramatically decreased. However, an abnormally high accumulation of extracellular WG was detected on *sfl* mutant cells located adjacent to wild-type cells, suggesting that HSPGs act locally in a cell non-autonomous manner. Taken together, the evidence suggested that DLY HSPGs are involved in restricting extracellular WG accumulation and diffusion.

Tout velu (*ttv*), a gene that affects heparan sulfate biosynthesis in *Drosophila*, was identified based on the inability of HH protein to diffuse across a field of cells in the imaginal disc (Bellaiche et al., 1998). The *tout velu* gene encodes the *Drosophila* homolog of EXT1 (**Figure 18**) (Toyoda et al., 2000), a heparan sulfate-specific co-polymerase. Mutations in these genes have been associated with reductions in the levels of heparan sulfate (Lind et al., 1998; McCormick et al., 1998). EXT1 mutations are associated with exostoses, which are cartilaginous tumors of the growth plate in bone tissue (McCormick et al., 1998; Kitagawa et al., 1999). Using genetic mosaics in imaginal discs, Bellaiche et al. (1998) showed that *ttv* function does not abrogate the ability of cells to respond to HH, although this ability is reduced; rather, it alters the distribution of HH, preventing its diffusion from HH-synthesizing cells. The fact that the *ttv* mutant affected HH function in the disc, but not that of other morphogens such as DPP or WG, shows that specific heparan sulfate residues exist that are produced by this co-polymerase for an HSPG(s) responsible for regulating the diffusion of HH across the disc epithelium. This also shows that the specific HSPG(s) synthesized by *ttv* perform a function opposite to that of DLY. Further studies suggested that membrane-targeted cholesterol-modified HH protein requires heparan sulfate proteoglycans either to be trapped by receiving cells or to move from cell to cell (The et al., 1999). The converse seems to be true for the PTC protein, a multiple-pass transmembrane protein, which has been implicated in HH reception when complexed with serpentine transmembrane protein SMO (Ingham et al., 1991; Chen and Struhl, 1996), the receptor essential for the transduction of

the HH signal (Hooper, 1994; van den Heuvel and Ingham, 1996). The studies showed that PTC receptor limits the range of HH diffusion from the posterior compartment into the anterior compartment. They provide evidence that the up-regulation of PTC expression induced by HH (Hooper and Scott, 1989; Tabata and Kornberg, 1994) serves to sequester any free HH by creating a barrier to its further movement. This reflects a novel self-limiting mechanism by which HH restricts its own range of action. A second mechanism by which HH movement is impeded is by the cholesterol moiety, which is covalently bound to the C-terminus of the N-terminal portion (Porter et al., 1996) of the HH protein once it undergoes autoproteolytic cleavage (Lee et al., 1994; Porter et al., 1995). The lipid modification acts as an anchor, tethering activated HH to the membrane surface of the *hh*-expressing cells. *Dispatch* (*Disp*), a gene that encodes a 12-pass transmembrane protein, is required in posterior compartment cells to release cholesterol-modified HH from the membrane surface of producing cells. In the absence of *Disp*, HH is retained by the posterior cells; however, its diffusion into the anterior compartment is inhibited, resulting in a loss of HH signaling. An interesting observation is that PTC contains a sterol-sensing domain (Osborne and Rosenfeld, 1998), which raises the possibility that PTC can interact directly with the cholesterol moiety of HH, thus sequestering HH and restricting its mobility (Beachy et al., 1997). Looking at HH and WG signaling, a complex picture begins to emerge, that shows that receptors, lipid moieties, and HSPG(s) may all be involved in an integrated negative and positive regulation of morphogen movement through the ECM.

A similar picture is starting to emerge for regards to the regulation of DPP gradient morphogen. From tissue-culture experiments, Gurdon and colleagues had proposed from earlier tissue cultures experiments that activin, a TGF β homolog in vertebrates, forms a concentration gradient by passive diffusion (reviewed in McDowell et al., 1997). The current model proposed is that DPP diffuses from its site of expression in a stripe of anterior cells adjacent to the A/P compartment boundary; this protein, behaving as a morphogen, confers positional information that specifies anterior/posterior pattern in discs (Lecuit et al., 1996; Nellen et al., 1996). However in the case of DPP in *Drosophila* imaginal discs, some evidence suggests more of a regulated diffusion process in which DPP is constrained as the protein spreads, rather than just spreading by passive diffusion (O'Connor, 1998; Lecuit and Cohen, 1998). By looking at clones in wing discs that produced DPP at different rates, these two groups looked at the effects that the formation of the DPP gradient had on target-gene expression. Activation of *omb* and *spalt*, two targets of *dpp* signaling in the wing, requires different levels of DPP activity. Since *omb* is activated at lower levels of DPP than is *spalt*, one would expect, in this experiment a passive diffusion model in which the area of activation of *omb* should always be greater than that of *spalt*, irrespective of the rate of DPP production from the clones. The aforementioned authors showed that in clones producing low levels of DPP, *omb* was activated before *spalt*. However, in clones producing high levels of DPP, both *omb* and *spalt* activation occurred in the same cells before DPP could spread. Eventually, *omb* expression expanded into cells further from the clone, but *spalt* expression remained localized in cells adjacent to the clone. The rate of production of DPP seems to control the sequence of *omb* and *spalt* activation. Perhaps more importantly, an unidentified factor/process seems to initially limit the movement of DPP in tissue exposed to high levels of this protein.

Another study showed that the *dpp* receptor THV may, in addition to binding to DPP in order to activate the signaling cascade, also contribute to constraining the movement of DPP in the ECM, thus causing the slow initial phase of DPP-gradient formation (Nguyen et al., 1998; Haerry et al., 1998). Haerry et al. (1998) suggested that DPP must down-regulate the expression of its receptor to permit its own diffusion. In the wing disc, for example, THV is normally expressed at high levels in the periphery of the wing pouch but only weakly in the medial regions of the disc, resulting in the dosage-dependent activation of *spalt* and *omb*. High levels of DPP near the center activate both of these genes, whereas *omb* alone is activated at the periphery of the wing pouch, where levels of DPP and THV expression are lower (Grimm and Pflugfelder, 1996; Nellen et al., 1996). It was postulated that these high levels of THV at the lateral margins of wing discs may restrict DPP diffusion and provide boundaries for its area of action (O'Connor et al., 1998). Lecuit and Cohen (1998) showed that clones over-expressing *thv* sensitized cells to low levels of DPP and induced target-gene expression in cells in which DPP levels are normally insufficient to do so. This showed that high levels of receptor could increase the sensitivity of cells to low levels of DPP. However, broad over-expression of THV led to a reduction in the area of expression of *omb*, and *sal* and in the size of the wing. Furthermore, O'Connor et al., (1998) showed that ectopic over-expression in the wing pouch of a dominant negative form of *thv* that can bind the ligand but not transmit the signal also resulted in smaller wings and a reduction of the area in which *omb* was expressed. These observations suggested that high levels of THV can limit the ability of DPP to diffuse in the wing disc (Nguyen et al., 1998; Haerry et al., 1998; Lecuit and Cohen, 1998). These groups postulated that DPP activity spreads slowly over the wing disc, up-regulating the expression of its target genes, as THV in turn limits the effective range of DPP. Thus, the DPP-dependent down-regulation of *thv* expression is essential for proper DPP gradient formation and may be the kinetically limiting factor in DPP diffusion across the developing wing disc.

Recent reports suggest that cellular processes that involve endocytosis (Gonzalez-Gaitan and Jackle, 1999; Entchev et al., 2000) and the formation of cytoneme formation (Ramirez-Weber and Kornberg, 1999) may shape the DPP gradient, thus implicating cellular trafficking of DPP as an important means of regulating DPP diffusion. Gonzalez-Gaitan and Jackle (1999) showed that *dpp* signaling is reduced in endocytosis-defective *Drosophila* wing discs. Further studies showed that the long-range movement of DPP involves not only DPP receptor function but also Dynamin function and the rate of endocytic trafficking and degradation (Entchev et al., 2000). Entchev et al. (2000) proposed a model in which the gradient is formed by intracellular trafficking that is initiated by receptor-mediated endocytosis of the DPP ligand in receiving cells, the gradient's slope is determined by the balance between endocytic recycling and endocytic degradation of this ligand. An alternative mechanism was proposed that was based on the observation that described lateral cells of the wing imaginal disc projecting long slender processes called cytonemes. These cytonemes are oriented in a nearly parallel fashion towards the DPP-signaling center in the central region of the disc (Ramirez-Weber and Kornberg, 1999). Whereas no specific function has yet been ascribed to cytonemes, the authors suggest a mechanism by which target cells in the lateral regions of the disc could sense DPP directly at its site of production, without the need for extracellular DPP diffusion. The graded effects of DPP signaling across the disc

could then derive intracellularly from the spatial or temporal decay of the DPP signal as it is transduced from the cytoneme tip to the cell body. As yet, long-range DPP signaling via cytonemes is not easily reconciled with the observed requirement for THV receptor down regulation within the central region of the wing disc (Haerry et al., 1998; Lecuit and Cohen, 1998). If all disc cells use cytonemes to sense DPP at its source, then the experimental elevation of THV receptor levels throughout the disc should effect an increase, rather than the observed decrease, in DPP signaling (Haerry et al., 1998; Lecuit and Cohen, 1998). Teleman and Cohen (2000) support the hypothesis that the DPP gradient forms by the diffusion of DPP through the extracellular matrix. They showed that DPP forms an unstable extracellular gradient that spreads rapidly in the wing disc. Rapid turnover of secreted DPP as it diffuses through the ECM supports the earlier endocytic cellular trafficking model proposed by Entchev et al. (2000). However, the activity gradient visualized by the rapid activation of MAD differs in shape from the DPP ligand gradient. The evidence suggests that the DPP activity gradient may be shaped at the level of receptor activation. The processes described so far are not necessarily mutually exclusive. Therefore, establishing the DPP gradient in the ECM could involve more than one mechanism; multiple mechanisms would integrate to regulate extracellular diffusion, interaction with the cell membrane, and turnover of the secreted DPP protein.

This integration of mechanisms would have to occur outside the cell, either on the membrane surface and/or in the ECM. This implies that other factors (in the ECM or associated with the cell membrane) that may come into contact with DPP could regulate the shape of its gradient. In several vertebrate cell culture studies, it has been shown that the ECM provides a physical and chemical connection between cells of a tissue. With respect to signal transduction, the ECM is thought to provide the scaffolding for the tethering of diffusible ligands (such as secreted growth factors, proteases, and membrane receptors) that somehow regulates their migration and activity (Folkman et al., 1989; Ingber and Folkman, 1989; D'Amore, 1990; Sporn and Roberts, 1990; Vlodavsky et al., 1991a, b). For example, bone induction and differentiation by the BMPs are governed by components of the ECM (reviewed in Chen et al., 1991). Various macromolecules that make up the ECM, such as type IV collagen, heparin, heparan sulfate proteoglycans, fibronectin, and hydroxyapatite, have been shown to act synergistically with BMP extracts, providing optimal osteogenic activity during bone development (Sampath and Reddi, 1981; Luyten et al., 1989; Ozkaynak et al., 1990; Wozney, 1998; Wozney and Rosen, 1998). The binding of BMPs in the presence of heparin and heparan sulfate is in some cases sufficient for osteogenesis (Paralkar et al., 1990; Hemmati-Brivanlou et al., 1994). It was proposed that BMPs are sequestered by proteoglycans or other ECM-associated molecules; the secreted growth factors are converted into an insoluble matrix-bound form, thus allowing BMP to act locally in inducing osteogenesis (Paralkar et al., 1990). This suggested that the inductive signals from secreted growth factors like BMP require the proper extracellular molecular environment for proper localization and activity, that includes the presence of heparin or heparan sulfate proteoglycans. It is believed that such ECM molecules would act as the scaffolding required for the regulated diffusion and delivery of the secreted growth factor to its proper receptors (Paralkar et al., 1990). For example, in certain primates, an ectopic source of hydroxyapatite in the form of a disc implant alone was osteoinductive (Ripamonti,

1996; Ripamonti et al., 1996). One observation was that endogenous BMPs in circulation progressively bound to the implanted hydroxyapatite disc, which then becomes highly osteoinductive. This showed not only that specific ECM factors act as modulators of BMP activity, but that they can also regulate the diffusion of these BMPs.

In another study, different structural forms of hydroxyapatite implants were studied for their osteogenic capabilities (Marouf et al., 1990). Prior to implantation, both disc and bead forms of hydroxyapatite were treated with BMPs. The disc form was consistently osteoinductive, whereas the bead form was inactive, despite the fact that the chemical composition of the two hydroxyapatite configurations was identical. This demonstrated that the structural context for effectively presenting BMPs is also important in determining the efficiency of bone induction (Ripamonti et al., 1996). Further studies showed that other ECM molecules such as collagen and fibronectin a glycoprotein, which have properties similar to those of hydroxyapatite, had similar effects on BMP activity (McPherson et al., 1992). This suggests that a combination of ECM factors may be required to modulate TGF β /BMP function.

If a combination of certain ECM factors can tether a specific ligand to regulate its migration and create reservoirs in which the levels and specific activity of the ligand can be regulated, then regulating the expression pattern of these ECM factors could affect the distribution pattern and activity of a secreted morphogen. Based on some initial evidence in this study, I propose that one such factor(s) may involve HSPG(s).

IV-4ii. Heparan sulfate GAGs may regulate the distribution of DPP in the ECM of imaginal discs.

Based on genetic analysis, this study showed that weak *dpp* disc mutant phenotypes were enhanced when only one copy of the UDP-GlcDH gene was removed. This resulted in the loss of the most distal leg structure (claw), the distal wing margin and the anterior/posterior medial regions of the wing blade that are adjacent to the A/P compartment boundary. Thus, when the level of DPP signaling is reduced by the removal of one functional copy of *dpp*, the further loss of UDP-GlcDH causes a more-than-additive effect. This severe dominant negative enhancement of the *dpp* phenotype by UDP-GlcDH (*sgl*^{P1731}) mutations suggests that UDP-GlcDH is crucial in modulating the levels of DPP activity in a dosage-dependent manner. The distal segment of the leg (claw), the distal wing margin, and the medial region of the wing blade all require maximal DPP activity. These regions were shown to be the most sensitive to slight fluctuations in the level of *dpp* signaling, as is evident from the similar phenotypes observed in partial loss-of-function disc mutants of *dpp* (*disc-dpp*) in the imaginal discs. Haerry et al. (1998) had shown that the phenotype caused by an activated-THV receptor mutant in adult wings was suppressed when one copy of UDP-GlcDH gene was removed. The authors inferred that suppression was caused by a reduction in heparan sulfate levels. In this study, dominant enhancement of *dpp* disc mutants by *sgl* mutants may be caused by a similar reduction in HS levels, which

directly affects DPP activity, supporting the hypothesis that proposes that HS or HSPG(s) are required for maximal DPP signaling in the imaginal disc. The specification of the wing blade region closest to the anterior and posterior wing margin normally requires lower levels of DPP activity. The lateral regions of the wing disc, that were not affected by the loss of one copy of UDP-GlcDH, depend more on GBB signaling through SAX to specify their cell fates (Haerry et al., 1998; Khalsa et al., 1998). Therefore, reducing, but not completely abolishing the heparan sulfate levels may have less of a negative effect on GBB signaling in this region of the wing. However, regions adjacent to the A/P compartment boundary are more dependent on high levels of DPP activity and therefore, may be more sensitive to any attenuation of the signal by factors (e.g., HSGAGs) that behave as modulators.

Further support for the hypothesis that heparan sulfate may regulate the DPP signal by directly interacting with DPP or modulators of the *dpp* signaling pathway, was suggested by experiments involving *dally* (Nakato et al., 1995, Jackson et al. (1997)). Jackson et al. (1997) showed that *Dally* positively modulates *dpp* signaling strength in a graded fashion in imaginal discs. Ectopic *dally* expression enhanced *dpp* gain-of-function mutant phenotypes resulting in mirror-image wing duplications. Conversely, loss-of-function *dally* mutants were able to repress *dpp* gain-of-function mutants in the wing. In each case, the authors did not observe changes in *dpp* expression; however, target-gene expression was expanded or reduced concomitantly with an increase or decrease in *dally* expression respectively (Nakato et al., 1995). The results of these experiments are consistent with the positive modulator role of *dally* for *dpp* signaling. In fact, *dally*'s regulation of WG signaling in imaginal discs is specified by the former's heparan sulfate moieties, as is indicated by the loss of WG signaling in *sgl* mutants, in which heparan sulfate residues are absent (Tsuda et al., 1999). These authors also showed that loss-of-function mutants of *dally* in the embryos were enhanced by the *sgl*^{P1731} mutant in trans-heterozygous embryos. Similar dominant negative interactions were observed between *dally* and *sfl* mutants, which also showed reductions in heparan sulfate production, resulting in a *wg*-like mutant phenotype (Li and Perrimon, 1999). These experiments showed that the heparan sulfate moieties were responsible for the specific function of DALLY.

When heparinase III was ectopically expressed in imaginal discs, a range of patterning defects was observed, including the phenotype that was observed in the *disc-dpp* and *sgl* trans-heterozygous combination mutants (compare **Figure 47D** with **Figure 48A**). It was inferred from the expression of heparinase III that the phenotypes were caused by the inhibition of DPP signaling that resulted from heparan sulfate degradation in the ECM. To date, the evidence showing that heparinase III is active and localized to the ECM, and has a direct effect on heparan sulfate levels in the imaginal discs *in vivo*, has not been confirmed. However, in a preliminary experiment in which imaginal wing discs were cultured in the presence of active heparinase III enzyme *in vitro*, the expression of DPP target genes were shown to be affected. *Spalt-lacZ* expression was reduced or lost near the A/P boundary in the wing pouch, whereas less severe or no significant effects on *omb-lacZ* expression were observed (Scanga and Manoukian, unpublished). One could speculate that since activation of *sal* normally requires a high level of DPP activity, this may explain why *sal-lacZ* expression was inhibited. This showed that

heparinase III treatment of discs, which results in the reduction of heparan sulfate, had a direct effect on DPP signaling. Conversely, when levels of heparan sulfate were increased in imaginal discs, using the *hs-sgl* construct, distal axis bifurcation occurred in some legs, as did other partial duplication effects that were restricted to only certain segments of the leg.

The gradient of DPP activity is reflected in the concentration-dependent manner in which cells respond to DPP. Experimental evidence found herein and provided by others suggests that regulating levels of heparan sulfate GAGs in the ECM of imaginal discs may affect the cell patterning and morphology of adult tissues, due to its ability to directly attenuate (due to a loss of HS) or enhance (due to an increase in HS) the effective biological activity of DPP signaling (in the context of DPP's behavior as a morphogen gradient) on its receptor complex at the cell surface. This may be accomplished by specific HS residues found on proteoglycans that are expressed in a spatially and temporally regulated fashion, acting as co-receptors to modulate DPP binding. Therefore, by regulating the levels of HS residues on the surface of the cell, one can regulate the affinity of the co-receptor to its ligand, thereby enhancing or reducing the efficiency with which the ligand can find and bind to its receptor. On the other hand, regulating the levels of heparan sulfate could affect GBB signaling to its SAX receptor, thereby indirectly enhancing the DPP signal-transduction pathway. There is no evidence so far that would exclude this possibility. In either case, up-regulation or down-regulation of the DPP signal transduction pathway in imaginal discs normally leads to specific pattern duplications or truncation respectively in both the adult leg and wing, thereby reflecting the graded morphogenic activity of DPP (see Introduction). For example, duplications of discrete pattern elements of the leg are shown to be caused by either discrete changes in the levels of DPP ectopic expression or constitutive activation of the DPP receptors. When the expression of DPP transcript or protein was looked at *in vivo* in imaginal discs during ectopic expression UDP-GlcDH, no observable increase in DPP transcript or protein was observed (Scanga and Manoukian, unpublished). However, as was shown by Struhl and Basler (1993), only small amounts of morphogen can have profound organizing activity in the imaginal disc, resulting in axis duplications. Again, one possibility that cannot be discounted, may be that any increase or decrease in UDP-GlcDH expression may lead to an increase or decrease in transcription or translation of *dpp* respectively that cannot be detected *in vivo* by current staining methods. In either case, either increasing the activity of endogenous DPP protein in the gradient or increasing DPP expression may lead to the up-regulation of the *dpp* signal-transduction pathway, resulting in ectopic pattern duplications.

The occurrence of complete axis duplications in the legs of adult flies, upon ectopic expression of UDP-GlcDH, suggests that the over expression of HS-GAGs in cells of the imaginal disc seem to induce distal organizer-like activity. It has been shown that cells possessing distal organizer function in imaginal discs are defined by the coordinated interaction of adjacent cells expressing high levels of *wg* and *dpp* (Campbell et al., 1993; Campbell and Tomlinson, 1995). This suggests that both *wg* and *dpp* signaling may be coordinately activated at ectopic sites, at which time they are expressed in adjacent cells, thus creating a distal organizer, as a result of UDP-GlcDH over-expression. Based on the co-

receptor model for HSPG(s), one could hypothesize that an ectopic distal organizer can be created by high levels of heparan sulfate GAGs expressed on the surface of the cell, thus sequestering both DPP and WG from the ECM, localizing them to their respective receptors on the cell surface of adjacent cells and enhancing their signaling activities. Therefore, high levels of heparan sulfate GAG residues presented at the cell surface could increase a cell's sensitivity to low levels of DPP and WG ligand in the ECM, and increase the binding efficiency to their receptors. This would, in effect, cause an artificial decrease in the response threshold for a cell, stimulating the inappropriate ectopic activation of both DPP and WG signaling cascades. Thus, by varying the amount of heparan sulfate GAG residues in the ECM, one may modulate the effective threshold response of cells to DPP and WG ligand, which would in turn would stimulate an organizer-like activity in the cells.

However, a closer look at the pleiotropic phenotypes observed when heparinase III or UDP-GlcDH are ectopically expressed in imaginal discs suggests that a more complex interaction may be involved between the DPP ligand and HS or its HSPG(s), other than the HSPG behaving as a co-receptor or enhancer of DPP activity. For example, ectopic heparinase III expression in imaginal discs resulted not only in loss of leg segments or wing blade, but also in outgrowths, suggesting that ectopic organizer-like activity was also induced (see **Figure 48**). Based on these observations, one could hypothesize that HS and HSPG(s) may regulate the movement of DPP through the ECM to its site of action. Reducing the levels of HS residues could cause unregulated diffusion of DPP from its site of expression, possibly causing the inappropriate accumulation of DPP in different regions of the imaginal disc, and exposing cells to higher levels of DPP ligand than they normally see. Based on this explanation, the function of HSPG may then be required to restrict DPP diffusion in the ECM. Consistent with this, Jackson et al. (1997), showed that loss-of-function mutants of *dally* were able to suppress partial loss-of-function disc *dpp* mutant phenotypes in the wing. This suggested that *dally* behaves as a negative modulator of *dpp* signaling. This is consistent with either HS residues inhibiting DPP binding to its receptors, or with a requirement that HSPG(s) may also constrain DPP migration. However, the *dpp*-like disc mutant phenotypes induced by heparinase III treatments in the wing and leg discs do not exclude the possibility that HS residues may be required to promote DPP migration. Therefore, the question of whether HS residues promote or inhibit diffusion of DPP remains unresolved.

In experiments in which UDP-GlcDH was ectopically expressed in specific regions of the imaginal leg disc, loss of distal or proximal leg segments or size deformities such as the compression of leg segments were typically observed (Thomson, Russell, and Scanga, unpublished). This supports the hypothesis that HSPG(s) may act to limit DPP diffusion. For example, over-expression of heparan sulfate using *Dll-Gal4* resulted in distal leg deletions that were similar to effects observed in *dpp* loss-of-function disc mutants. Therefore, ectopic expression of heparan sulfate may, in some cases, act to block diffusion by either sequestering DPP ligand to the surface of DPP expressing cells or by trapping DPP in the ECM. This would cause, in effect, the lowering of DPP activity in the imaginal leg discs. Therefore, patterns that require high levels of DPP activity (e.g., the distal leg segments) would be most affected. Using a *dpp-Gal4* driver to ectopically express UDP-GlcDH resulted in phenotypes that

mimicked the over-expression effects of *wg* (Wilder and Perrimon, 1995) in imaginal leg discs (Thomson, Russell and Scanga unpublished). Over-expression of UDP-GlcDH in the *dpp*-expressing stripe of cells along the A/P boundary resulted in mirror-image duplications of ventral tissue, proximo-distal compression and lateral expansion of leg segments. In this case UDP-GlcDH expression overlaps the endogenous expression of *dpp* along the A/P compartment boundary in the anterior-dorsal quadrant. To explain the phenotypes, it is speculated that DPP secreted from these cells may be tethered by excess amounts of HS-GAG residues located either on the cell surface or in the surrounding ECM. This would then prevent DPP from diffusing to its target cells. Normally, *wg* expression is suppressed in the anterior-dorsal quadrant by the presence of DPP expression (Brook and Cohen, 1996; Basler and Struhl, 1996). If DPP diffusion away from the A/P boundary were restricted, WG activity would spread more dorsally, thus ectopically activating the *wg* signaling cascade and accounting for the observed ectopic *wg*-like phenotype in the anterior-dorsal quadrant of the leg. However, unlike the over-expression of *wg*, which also results in the loss of dorsal structures (Wilder and Perrimon, 1995), the over-expression of heparan sulfate in this case may continue to enhance DPP activity in the *dpp*-expressing cells themselves; thus, those structures remained present. WG in this case would not be able to convert these cells to ventral cell fates because DPP activity would still be present and inhibitory to WG activity. Baeg et al. (2001), showed a similar effect when they over-expressed Dally-like in the wing discs resulting in a *wg* loss-of-function phenotype. This suggested to the authors that DLY limits WG diffusion in the wing pouch from its expression at the wing margin, such that when DLY was over expressed it led to the accumulation of extracellular WG at the wing margin.

To further address the role of HS GAG(s) in DPP migration, additional experiments are currently under way. By varying the levels of heparinase III treatment using a heat inducible promoter, one can test the effect of varying the amount of HS residues in DPP signaling. One prediction would be that moderate reductions in HS may have diffusion effects, whereas completely abolishing HS residues would also abolish the co-receptor function of HSPG on the cell surface. We would expect that the latter treatment would abrogate *dpp* signaling, leading to loss-of-function phenotypes as in *dpp*-mutant discs. Thus, the two roles proposed for HSPG(s) may be separated, by controlling the amount of heparinase III treatment. In another experiment, generating large clones expressing heparinase III in anterior cells adjacent to DPP expression at the A/P boundary in the wing disc would tell us whether HS residues at the cell surface or in the ECM limit or promote DPP migration. Assuming that cells expressing heparinase III in the clone should be devoid of HS residues, one can, by looking at DPP expression, look at the effects of DPP diffusion through the heparinase III-expressing clones. If HS is required to promote DPP migration, one would predict that DPP would not be able to diffuse through the clone and thus would accumulate at the edge of the clone that is adjacent to the *dpp*-expressing cells. Conversely, if HS residues restrict DPP diffusion, then one might expect accumulation of DPP protein on the edge of the clone furthest from the cells expressing *dpp*. In this instance one would also expect to observe low levels of DPP through the clone. Therefore, small changes in heparan sulfate levels in the ECM may cause shifts in the diffusion pattern of a secreted growth factor like DPP, thus affecting a discrete areas of the disc.

It has recently been shown that *Dll* expression, which is normally localized to the wing margin, expands both ventrally and dorsally through the wing pouch when whole discs are incubated in culture with heparinase (Scanga and Manoukian, unpublished). This suggested that the cells in the wing pouch were exposed to increased levels of WG activity not normally found in that region. The wing pouch is regulated by a gradient of WG activity emanating from the wing margin. When we looked at WG expression in the wing pouch of discs cultured in the presence of heparinase III, extracellular WG expression had expanded, and WG had diffused further from the wing margin into the pouch. This correlated with the observed expansion of *Dll* expression from the margin. Cells further away from the margin were now exposed to a higher concentration of WG; thus the threshold for *Dll* activation in these cells was exceeded. Lowering the levels of heparan sulfate allows WG to diffuse further, causing an expansion of the WG gradient. Therefore, small changes in heparan sulfate levels in the ECM may only cause shifts in the diffusion patterns of a secreted growth factor like WG, thus affecting the spatial patterning of the tissue. Whether or not similar effects are associated with changes in the diffusion of the DPP protein is currently being studied (Scanga and Manoukian, unpublished).

By promoting the migration of DPP, ECM or membrane bound HSPG could act as a chaperone, helping DPP diffusion through the ECM. On the other hand, if HSPG(s) limits DPP diffusion, the HS residues would act as barriers to restrict DPP movement. A recent study by Paine-Saunders et al. (2002) shows that *noggin*, (a secreted peptide that has been shown to inhibit ventral fate and promote dorsal fate from the Spemann organizer during embryo development in *Xenopus*) binds strongly to heparan sulfate proteoglycans on the surface of cultured cells. *Noggin* protein (NOGGIN) promotes dorsal cell fate by binding to BMPs' and inhibiting their ventralizing function by preventing interactions with receptors on the cell surface (Zimmerman et al., 1996; Thomsen., 1997). NOGGIN is detected only on the surface of cells that express heparan sulfate. Heparan sulfate bound NOGGIN is shown to remain functional and can bind BMP2 and 4 at the plasma membrane (Paine-Saunders et al., 2002). BMPs normally act as ventralizing morphogens during dorsal-ventral axis specification in early *Xenopus* embryos (Jones et al., 1996; Dosch et al., 1997; Dale and Jones, 1999; Dale and Wardle, 1999). NOGGIN is assumed to diffuse from the dorsal lip of the Spemann organizer, establishing an inhibitory gradient that binds to BMP thus forming an ventralizing BMP activity gradient that mirrors that of NOGGIN (Jones and Smith, 1998; Dale and Jones, 1999; Dale and Wardle, 1999). Paine-Saunders et al. (2002) proposed that heparan sulfate proteoglycans *in vivo* can regulate the diffusion of NOGGIN, which in turn regulates the diffusion, and therefore the formation of gradients of BMP activity. This sort of model can explain the observation that shows that when ectopic UDP-GlcDH is expressed at high levels in certain regions of the imaginal disc, it can inhibit DPP activity. Conversely, when heparinase III is ectopically expressed in imaginal discs DPP activity can be enhanced, resulting in outgrowths. In this case, the function of a NOGGIN-like (Holley et al., 1996) inhibitor can be enhanced or inhibited when heparan sulfate levels at the cell surface are either increased by the ectopic expression of UDP-GlcDH, or decreased by the expression of heparinase III respectively. When its function is enhanced, a NOGGIN-like inhibitor will bind to DPP and inhibit its diffusion and activity; when inhibited, it is unable to bind to DPP, thus allowing DPP diffusion and possibly ectopic activity.

The outcome in both scenarios would be that the HSPG(s) are acting to restrict DPP ligand diffusion, which in turn would allow for frequent encounters with DPP's high-affinity receptors. Thus, by regulating the pattern of expression of extracellular or membrane-associated HSPG(s), the tissue may then be able to modulate the pattern and range of DPP diffusion; this modulation ultimately determines the shape of the DPP gradient. One trend that is observed is that morphogens may use specific HSPG(s) to carry out specific biological roles. For example DALLY is required to promote WG signaling, behaving possibly like a co-receptor, whereas DALLY-LIKE is required to limit the distribution of WG ligand in the imaginal disc. Therefore, future experiments must look at the identification and role of specific HSPG(s) that act in DPP signaling and gradient formation. Discrete HS residues associated with a specific proteoglycan (ECM- or membrane-tethered [MT]) may then be expressed in a regulated manner; this regulation determines their spatial and temporal expression pattern in imaginal discs. These HSPGs could then specifically regulate the pattern of DPP diffusion or local activity levels in the imaginal tissue, thus ultimately affecting positional information. Therefore, any changes in the levels and pattern of expression of the ECM or membrane associated HSPG molecules, could modify the gradients of positional information by altering the normal diffusion pattern of the morphogen.

IV-5. Role of the ECM during regeneration.

This study has also implicated UDP-GlcDH and HS-GAGs in the regeneration process of imaginal discs. Regeneration of appendages in some vertebrates (e.g., urodeles) begins with the local formation of a growth zone or blastema at the plane of amputation (wounding). The blastema in urodeles is a group of cells that can influence neighboring cell fates via cell-cell interactions that promote cell division and de-differentiation. These interactions are thought to involve either local inductive cell signals or the graded diffusion of (a) morphogen(s) (Bryant and Fraser, 1988; Bryant and Gardiner, 1992; Gardiner et al., 1992). Several studies have identified these signaling proteins as members of various families of secreted growth factors such as TGF β /BMPs (Viviano and Brockes, 1996); WNTs (Chang et al., 1994), and Sonic hedgehog (SHH) (Stark et al., 1998). These are the vertebrate homologs of DPP, WG and HH. Several interesting events that occur in the urodele blastema after wound healing and prior to growth-factor regulation underscore the importance of the ECM in the early stages of regeneration. Metalloproteases (MMP) are expressed in the mesenchyme upon limb amputation, resulting in the degradation of the ECM (Tang and Tu, 1994). It was thought that this may permit cells to escape from their matrix and migrate to form the blastema. In other studies, ECM degradation was thought to facilitate de-differentiation by disrupting cell contacts (Tang et al., 1997). This response to wounding was shown to be inhibited when the contact between cells were re-established (Miyazaki et al., 1996). The subsequent reconstitution of the ECM was important in the repatterning of the vertebrate limb, allowing the proper response of cells to soluble mediators such as TGF β and WNTS in the amputated limb of urodeles (Chen et al., 1991; Nace and Tassava, 1995).

Remodeling of the matrix in vertebrates has long been thought to be important for patterning,

since the matrix could limit or enhance differential gene expression and cell migration (Jackson et al., 1991). Increased expression of GAG chains were shown to regulate the activities of growth factors during wound repair in mice and humans. The expression of heparin, and heparan sulfate GAG-associated proteoglycans such as the syndecans, is increased after tissue injury (Gallo et al., 1996). A retarded wound-healing response was seen in syndecan-1-deficient mice, because angiogenesis and cell migration in the wound were poor. Normally, the factors released upon tissue injury (e.g., the antimicrobial peptides synducin and cathelicidin) cause the up-regulation of syndecans on the cell surface (Gallo et al., 1994). This is quickly followed by the regulated shedding (due to metalloprotease) into the wound fluid of the highly-sulfated heparan GAG chains found on syndecans-1 and -4, (Subramanian et al., 1997; Kato et al., 1998). These syndecan GAG chains inhibit proteases, heparan binding epidermal growth factor (HB-EGF), and fibroblast growth factor 2 (FGF2) signaling, which are collectively responsible for the migration and proliferation of keratinocytes in the wound (Kainulainen and Wang, 1998). This is consistent with studies that show that these soluble ectodomains inhibit cell proliferation (Mali et al., 1994; Forsten et al., 1997). Later, heparinases are expressed by neutrophils and macrophages, which digest the syndecan-1 and -2 GAG chains to produce heparan-like fragments that bind to FGF2 and stimulate its activity; this activity is required for proliferation of subdermal fibroblasts (Kato et al., 1998). Many ECM proteins that are expressed (e.g., fibrillar collagens, fibronectin, and tenascin) avidly bind the released heparan sulfate fragments and act as a reservoir as the new ECM is formed. Incorporation of these GAGs into the ECM allows proteases and growth factor activities to return to normal levels; this return to normal may be required for the regeneration of cell-differentiation pattern of the lost tissue. In a similar manner, heparan sulfate GAGs, along with other ECM components accumulated during regeneration, may provide a suitable ECM environment to regulate the activities of growth factors such as DPP and WG during re-patterning of the leg imaginal disc (Dealy et al., 1997). Therefore, the shedding of syndecan ectodomains maintains growth-factor and proteolytic balance at the wound site (Kato et al., 1998; Kainulainen et al., 1998).

In this study, it was found that the up-regulation of UDP-GlcDH expression in the regenerating imaginal leg disc is followed by the ectopic accumulation of heparan sulfate in the anterior compartment of the regenerating disc (see **Figure 52E and F**). This may be indicative of a remodeling of the ECM following the random cell death in *su(f)¹²*-mutant discs. Axis duplication of the leg in *su(f)¹²* mutants suggests that, at some point, stable ectopic activation of *wg* and *dpp* is achieved, which results in the stable formation of a distal organizer and in the global re-patterning of the imaginal leg disc. Heparan sulfate GAGs have been implicated as a key modulator of this process, underscoring the importance of the extracellular matrix in pattern regulation during regeneration. When I analyzed the expression of various genes (*en*, *hh*, *ptc*, *wg*, and *dpp*) (**Figure 50 and 51**) that are responsible for organizing spatial pattern in imaginal discs, I observed that changes in the expression pattern of these genes during pattern regulation of the leg in *su(f)¹²*-mutant flies somewhat correlated and overlapped with the changes in the expression pattern of UDP-GlcDH and heparan sulfate GAGs (see **Figure 52**). Ectopic expression of *en* is initially detected in the anterior compartment approximately 6-12 hr after

the heat treatment (AHT) used to induce cell death in *su(f)¹²*-mutant leg discs. The loss of the posterior-compartment restriction of *hh* expression also seems to occur simultaneously with the ectopic expression of *en*. It is possible that during the initial stages of regeneration, a breakdown in the ECM occurs that could result in the loss of cell-cell contacts that may be responsible for maintaining A/P compartmental restriction of *en* and *hh* expression. At this stage in regeneration, expression levels of UDP-GlcDH and heparan sulfate increased, possibly in response to an ECM remodeling cue. The breakdown in the compartment boundary and the ectopic misexpression of *hh* in the anterior compartment correlated with the expression of *ptc* in the anterior compartment. Normally, *ptc* expression is localized in a stripe of cells in the anterior compartment that abuts the A/P boundary and responds to HH protein secreted from the posterior compartment. The loss of cell-cell contacts may result in a deregulation of *en* expression in the anterior compartment and a simultaneous increase in the diffusion of HH into the anterior compartment.

At 24 hr AHT, ectopic expression of both *dpp* and *wg* was observed throughout the anterior compartment. This was consistent with the findings of Basler and Struhl (1994), which showed that general ectopic expression of *hh* in the leg disc resulted in misexpression of *dpp* and *wg* in the anterior compartment. This suggested that cells beyond those located near the A/P compartment boundary (where *dpp* and *wg* are normally activated by HH) are receiving higher-than-normal levels of HH. However, *wg* and *dpp* expression soon became restricted to the anterior-ventral and anterior-dorsal quadrants, suggesting that the dorsal/ventral difference in competence to respond to HH is still maintained. More interestingly, even though the A/P compartment restriction had broken down with respect to *hh* expression, it was maintained with respect to *dpp* and *wg* expression, suggesting that cells in the posterior compartment were still able to repress *dpp* and *wg* expression. By this time, the reconstitution of the ECM may have begun to take place, as is suggested by the up-regulated expression of UDP-GlcDH and heparan sulfate, particularly in the anterior-dorsal and anterior-ventral quadrants of the leg disc. Assuming that heparan sulfate GAGs are required as co-receptors for HH signaling (as was suggested by Perrimon and Duffy, 1998), cells may require a minimal level of heparan sulfate to respond to HH. This could account for the observed general ectopic activation of *dpp* and *wg* expression in the anterior compartment. However, the amount of heparan sulfate expression at this time may have been too low to restrict HH diffusion.

At more than 24 hr AHT, both UDP-GlcDH and heparan sulfate GAG expression levels began to level off, suggesting that the ECM was completing its recovery by this stage. At about the same time both *en* and *hh* ectopic expression in the anterior compartment faded, along with that of *wg* and *dpp*. *en* and *hh* expression became restricted to the posterior compartment, and *dpp* and *wg* expression was re-established along the A/P compartment boundary suggesting that the A/P compartmental restriction had been also established. This may be the result of the re-synthesis of the ECM and re-formation of cell-cell contacts in the tissue. However, in the leg discs, ectopic expression of *en* and *hh* was still detected in a patch of cells in the anterior compartment near the edge of the disc. By 48 hr, a stripe of *ptc* expression was observed in cells overlapping the expression of *en* and *hh* in the anterior compart-

ment. This suggested that a new ectopic A/P compartment boundary had formed. Furthermore, ectopic *wg* and *dpp* expression was also observed in the same region of the leg disc. The formation of a second end knob with a set of concentric folds in the leg disc and the mirror-image duplication patterns of expression of *en*, *hh*, *ptc*, *dpp* and *wg* seen later in discs, indicate that this ectopic pattern of expression preceded the formation of a duplicate P/D axis. I propose that this anterior ectopic expression, which represents a new secondary A/P boundary, may initiate the establishment of a new distal organizer that gives rise to the duplicate P/D axis in the leg. The morphology of duplicates in the leg suggests that they may originate from the region corresponding to the anterior medial extremity of the leg (Russell, Girton and Morgan, 1977), which is consistent with the site of ectopic expression of the genes described above. The localized misexpression of diffusible morphogens like DPP and WG at this ectopic site in the leg disc may, therefore, explain how these cells acquire organizing abilities and provide the proper patterning signals to neighboring cells to create the duplicate leg in the adult. This is consistent with the current compartment boundary model's describing imaginal disc patterning; in this model, the distal organizer is defined by the confrontation between the AP, AD, and AV compartments, which is determined by *en/hh*, *wg*, and *dpp* expression at the boundary. The adjacent expression of both *wg* and *dpp* expression at the distal organizer is required for distal outgrowth in the leg discs (see Introduction, reviewed by Campbell and Tomlinson, 1995; Brook et al., 1996). Heparan sulfate GAG expression, along with that of *dpp* and *wg*, in the cells in the medial-lateral region of the disc is also consistent with its possible role in regulating *dpp* and *wg* function as organizers.

Neither the compartment boundary model nor the distal organizer model completely explains how the new gene-expression pattern itself is generated during a duplication event. Heparan sulfate GAGs may be among the molecules involved in the initial events in the disc that lead to the ectopic expression of *hh*, *wg*, and *dpp* in the small group of cells that eventually provide the cues for pattern formation of the duplicate. The possible importance of this remodeling of the ECM is underscored by the observation that duplication and regeneration of the leg in adults was inhibited by a depletion of heparan sulfate (see **Figures 53** and **54**). Regeneration of the leg disc was suppressed by the expression of heparinase III in regenerating imaginal leg discs in heat-treated *su(f)¹²* mutants. In addition, when heparan sulfate was removed from the medial-lateral region of the leg disc that forms the duplicate, the formation of a secondary P/D axis was suppressed, resulting in a necrotic stump. These two results imply that heparan sulfate may be required to establish or regulate distal organizer activity for the original D/P and a duplicate in the leg disc. Furthermore, the expression of both UDP-GlcDH and heparan sulfate in *su(f)¹²*-mutant discs during regeneration supports a role for heparan sulfate in forming the distal organizer (**Figure 52**). The later expression of heparan sulfate is restricted to cells at the lateral edge of the anterior compartment, where it overlaps the expression of both *wg* and *dpp*. This occurs prior to any apparent morphological evidence of a duplication event in the leg discs. This pattern of misexpression of heparan sulfate is consistent with the effects of heparan sulfate depletion during regeneration and further supports the idea of its involvement in the events leading to distal-organizer formation. The ectopic activation of UDP-GlcDH at the 6-12 hr prior to heat treatment suggests that the ECM may be critical for an early step in re-patterning (such as the re-specification of cell fate and

compartmental restrictions). Heparan sulfate GAG expression, combined with that of *dpp* and *wg*, in the cells of this region of the disc is also consistent with HSGAGs possible role in regulating the function of *dpp* and *wg* as organizers.

BMP-2, the human homolog of *dpp*, plays a decisive role during bone regeneration and repair in animals (Wang et al., 1990; Torumi et al., 1991). Human BMP-2 can substitute for the *Drosophila* homolog during dorsal-ventral patterning of the *Drosophila* embryo, just as DPP can, in turn, induce ectopic bone formation in animals (Padgett et al., 1993; Sampath et al., 1993). BMP-2 protein is normally found attached to the bone matrix together with other BMPs (e.g., BMP-4, and BMP-6) (Israel et al., 1992). The binding of BMP-2 to abundant sites on the cell surface and the extracellular matrix is thought to be promoted by heparin-binding sites found in its N-terminal sequence (Koeing et al., 1994; Ruppert et al., 1996). Similar heparin-binding motifs were found to exist in the N-terminal region of *Xenopus laevis* BMP-2 and *Drosophila* DPP and GBB proteins (Plessow et al., 1991; Ruppert et al., 1996). The occurrence of heparin-binding sites in BMP-2 explains why the specific biological activity of BMP-2 is enhanced by heparin or heparan sulfate in embryonic limb-bud cells or during chondrogenesis in chick limb-bud mesenchymal cells (Roark and Greer, 1994; Ruppert et al., 1996).

With respect to *dpp* and regeneration in imaginal discs, these observations provide further support for the critical role that GAGs may play in regulating *dpp*/BMP activity in tissue regeneration. Like BMP-2, the HSGAGs expressed during imaginal disc regeneration may interact with the GAG binding sites of DPP, helping to localize and potentiate DPP activity to the wound heal and future regeneration blastema (organizer). However, there is no biochemical evidence showing direct interaction between DPP and heparin or heparan sulfate GAGs. In addition, the question of whether *dpp* function is required for regeneration in imaginal discs still remains to be answered. IP studies using antibodies against HS proteoglycans or HS GAGs are being carried out to determine whether DPP protein can be co-precipitated from *Drosophila* embryonic extracts (Gupta and Scanga, Manoukian lab). *Thv* and *punt* null mutants will be used to generate somatic clones during regeneration in specific regions of the leg disc, in *su(f)¹²* mutants. This will be accomplished by using the *Gal4/UAS* expression system to specifically generate mutant clones in the regenerating part of the disc (see **Figure 53**).

V. Summary

Vertebrate cell-culture studies provided the initial evidence for the involvement of an HSPG - specifically, betaglycan, an integral membrane-bound proteoglycan - in the regulation of the TGF β /BMP family of secreted growth factors (Lopez-Casillas and Cheifetz., 1991; Lopez-Casillas et al., 1993; Lopez-Casillas et al., 1994). Betaglycan, a type III receptor that acts as a non-signaling receptor accessory molecule, increases the efficiency of TGF β ligand binding to its type I and type II signaling receptors. In most cell lines, the GAG chains of betaglycan are a mix of heparan sulfate (HS) and chondroitin sulfate (Segarini and Seyedin, 1988). The GAG chains on betaglycan were, however found to be dispensable in binding TGF β . (Cheifetz and Massague, 1989; Lopez-Casillas et al., 1993; Lopez-Casillas et al., 1994). No such type III receptors have been reported for vertebrate BMPs. *Dally* was the first HSPG to be shown through genetic means, to regulate DPP/BMP signaling during development in imaginal discs (Jackson et al., 1996). *Dally* acts as a positive regulator of DPP, by enhancing DPP signaling, suggesting to the author that it may serve as a DPP co-receptor. However, it was not determined which active region - the protein core or the HS residues of *Dally* - affected *dpp* signaling. Haerry et al. (1997), to help further define the *dpp*-signaling pathway, designed a genetic enhancer and suppressor screen to identify novel components of the pathway. A constitutively active form of the DPP type I receptor, encoded by the gene *thickveins* (*thv*), was expressed ectopically in the wing discs resulting in a highly blistered phenotype. The authors identified a P-element mutant, *SG9*, from a previous imaginal disc screen (Shearn and Garen, 1974); *SG9* dominantly suppressed the wing blister phenotype of the activated THV (A-THV) mutant. The *SG9* mutant turned out to be an allele of *sugarless* (Binari et al., 1997; Haerry et al., 1997; Hacker et al., 1997), which encodes the gene for UDP-glucose dehydrogenase (UDP-GlcDH) in *Drosophila*. UDP-GlcDH is involved in the biosynthesis of heparan sulfate GAGs in the cell. The *SG9* allele of this mutation (which has reduced activity relative to the wild type) with reduced activity was shown to cause lethality during pupal stages. The pharate adults show all structures derived from the imaginal discs (e.g., legs, wing, eyes, and antenna) to be small or not fully developed. The authors concluded that the phenotype of the dead pupae and evidence from genetic interactions with *dpp* disc mutants supported the suggestion that HS is important for *dpp*-signaling in the wing disc. Although HS synthesis seems to be involved in the *dpp*-signaling pathway in imaginal discs, embryos without either maternally supplied or zygotically derived mRNAs encoding UDP-GlcDH showed no defects in dorsal-ventral patterning, a process that is critically dependent on DPP signaling (Binari et al., 1997; Haerry et al., 1997; Hacker et al., 1997). Binari et al. (1997), however, did report that the zygotic phenotype of the *sgl* allele *P1731* [1(3)08310] (Spradling et al., 1995) showed extensive loss of dorsal cuticle structures and perhaps of the amnioserosa. This zygotic phenotype is characteristic of partial loss-of-function alleles of *dpp* and its two known receptors *thv* and *punt*.

The study herein demonstrates that the zygotic contribution, and possibly the maternal contribution as well, is required for DPP signaling during dorsal-ventral patterning of the embryo. From an enhancer-trap regeneration screen in imaginal discs (Brook et al., 1993), I identified a P-element lethal

insertion line (*A64*) that produced dead embryos that showed dorsal cuticle and gastrulation defects. *A64* turned out to be another allele of *sugarless* (*sgl*). Developmental processes are often sensitive to the level of function in a signaling pathway. It has been shown that when DPP signaling is reduced below a certain threshold, a relatively modest change in function can produce drastic effects on developmental patterning in both the embryo and imaginal discs. I showed that adults heterozygous for a *dpp* partial loss-of-function mutant or a receptor loss-of-function mutant, when crossed to adults that were heterozygous for the *sgl* mutant alleles *A64* and *P1731*, result in embryos with dorsal defects. This showed that *sgl* mutants were able to dominantly enhance *dpp*-pathway mutants in the embryo. This type of genetic interaction, intergenic non-complementation, provides strong evidence that the two genes affect a common signaling pathway in the embryo. Similar genetic interactions were observed between *sgl* mutant alleles and *dpp* disc mutants, suggesting that the phenotypic effects observed with *dally* are also due to the absence of the HS residues. These results suggest that the HS residues are critical moieties that help modulate DPP signaling. From the heparinase III expression studies in the embryo and imaginal discs, which phenocopy the *dpp* loss-of-function phenotype, it was inferred that the HS residues in the ECM may directly affect DPP activity. Preliminary studies of the effects of the *sgl* mutant and heparinase III treatments in imaginal discs, opens the possibility that HS residues may also play a role in organizing the extracellular distribution of DPP. It has been shown, in other studies, that mutations in *sulfateless* (*sfl*; N-deacetylase/N-sulphotransferase; Lin and Perrimon, 1999) and *tout-velu* (*ttv*; transmembrane HS polymerase; Bellaiche et al., 1998), two enzymes that are involved in the modification of HS residues on HSPG(s), can specifically affect the extracellular distribution of WG and HH, respectively. The specific effects of these biosynthetic enzymes may be due to the presence of different isoforms of an enzyme that is responsible for producing specific modified forms of HS residues. These HS residues may in turn be responsible for the regulation of a specific morphogen. Thus, regulating the diversity of HS residues found on HSPG is critical for their specific functional roles (review Lindahl et al., 1998). Several studies in wound repair have implicated HSPG(s) in modulating growth factors, such as FGF and BMP during wound repair in mice and humans. *In vitro* cell-culture studies have established that BMPs can induce bone regeneration and that various ECM components are essential in the induction processes. This study provides the first *in vivo* genetic evidence for the requirement of HS residues during regeneration of imaginal discs. Ectopic expression of UDP-GlcDH was also shown to induce distal leg duplications. Along with the observations from the regeneration experiments, this suggests that cells expressing high levels of HS residues may possess properties of a distal organizer. Therefore, specific HS moieties expressed at high levels in a concentrated area may possess the ability to enhance the levels DPP and/or WG (two gene products that, when combined, define distal organizer function) in imaginal discs.

VI. References

- Abbott, L. C., Karpen, G. H., and Schubiger, G. (1981). Compartmental restrictions and blastema formation during pattern regulation in *Drosophila* imaginal leg discs. *Dev. Biol.* **87**, 64-75.
- Affolter, M., Nellen, D., Nussbaumer, U., and Basler, K. (1994). Multiple requirements for the receptor serine/threonine kinase *thickveins* reveal novel functions of TGF- β homologs during *Drosophila* embryogenesis. *Development* **120**, 3105-3117.
- Alevizopoulos, A., and Mermoud, N. (1997). Transforming growth factor- β : the breaking open of a black box. *BioEssays* **19**, 581-591.
- Alexander, C., Jacinto, A., and Ingham, P. W. (1996). Transcriptional activation of *hedgehog* target genes in *Drosophila* is mediated directly by the *cubitus interruptus* protein, a member of the Gli family of zinc finger DNA-binding proteins. *Genes Dev.* **10**, 2003-2013.
- Altschul, S. F., Gish, W., Miller, W., Myers, E. W., and Lipman, D. J. (1990). Basic local alignment search tool. *J. Mol. Biol.* **215**, 403-410.
- Altschul, S. F., Madden, T. L., Schaffer, A. A., Zhang, J., Zhang, Z., Miller, W., and Lipman, D. J. (1997). Gapped BLAST and PSI-BLAST: a new generation of protein database search programs. *Nucleic Acids Res.* **25**, 3389-3402.
- Anderson, K. V. (1987). Dorsal-ventral embryonic pattern genes of *Drosophila*. *Trends Genet.* **3**, 87-94.
- Anderson, K. V., Bokla, L., and Nusslein-Volhard, C. (1985). Establishment of dorsal-ventral polarity in the *Drosophila* embryo: the induction of polarity by the *Toll* gene product. *Cell* **42**, 791-798.
- Anderson, K. V., and Hecht, P. M. (1993). Genetic characterization of *tube* and *pelle* genes required for signaling between *Toll* and *dorsal* in the specification of the dorsal-ventral pattern of the *Drosophila* embryo. *Genetics* **135**, 405-417.
- Anderson, M. G., Perkins, G. L., Chittick, P., Shrigley, R. J., and Johnston, W.A. (1995). *drifter*, a *Drosophila* POU-domain transcription factor, is required for correct differentiation and migration of tracheal cells and midline glia. *Genes Dev.* **9**, 123-137.
- Anders, J. L., Defalcis, D., Noda, M., and Mssague, J. (1992). Binding of two growth factor families to separate domains of the proteoglycan Betaglycan. *J. Biol Chem.* **267**, 5927-5930.
- Arora, K., and Nusslein-Volhard, C. (1992). Altered mitotic domains reveal fate map changes in *Drosophila* embryos mutant for zygotic dorsoventral patterning genes. *Development* **114**, 1003-1024.
- Arora, K., Levine, M., and O'Connor, M. (1994). The *screw* gene encodes a ubiquitously expressed member of the TGF- β family required for specification of dorsal cell fates in the *Drosophila* embryo. *Genes Dev.* **8**, 2588-2601.
- Arora, K., Dai, H., Kazuko, S. G., Jamal, J., O'Connor, M. B., Letsou, A., and Warrior, R. (1995). The *Drosophila schnurri* gene acts in the Dpp/TGF- β signaling pathway and encodes a transcription

- factor homologous to the human MBF family. *Cell* **81**, 781-790.
- Ashburner, M. (1989). Salivary gland chromosome squash technique. In *Drosophila: A Laboratory Handbook*. Cold Spring Harbor Laboratory Press. Cold Spring Harbor., pp 28-32.
- Ashburner, M. M Thompson, P., Roote, J., Lasko, P. F., and Grau, Y. (1990). The genetics of a small autosomal region of *Drosophila melanogaster* containing the structural gene for alcohol dehydrogenase. VII. Characterization of the region around the *snail* and *cactus* loci. *Genetics* **126**, 679-694.
- Ashe, H. L and Levine, M. (1999). Local inhibition and long-range enhancement of Dpp signal transduction by Sog. *Nature* **398**, 427-431.
- Aviezer, D., Hecht, D., Safran, M., Eisinger, M., David, G., and Yayon, A. (1994). Perlecan, basal lamina proteoglycan, promotes basic fibroblast growth factor-receptor binding, mitogenesis, and angiogenesis. *Cell* **79**, 1005-1013.
- Aza-Blanc, P., Ramirez-Weber, F. A., Laget, M. P., Schwartz, C., and Kornberg, T. B. (1997). Proteolysis that is inhibited by *hedgehog* targets *Cubitus interruptus* protein to the nucleus and converts it to a repressor. *Cell* **89**, 1043-1053.
- Azpiazu, N., and Frasch, M. (1993). *Tinman* and *bagpipe*: two homeobox genes that determine cell fates in the dorsal mesoderm of *Drosophila*. *Genes Dev.* **7**,1323-1340.
- Azpiazu, N., Lawrence, P. A., Vincent, J. P., and Frasch, M. (1996). Segmentation and specification of the *Drosophila* mesoderm. *Genes Dev.* **10**, 3183-3194.
- Baeg, G., Lin, X., Khare, N., Baumgartner, S., and Perrimon, N. (2001). Heparan sulfate proteoglycans are critical for the organization of the extracellular distribution of Wingless. *Development* **128**, 87-94.
- Baeg, G-H., and Perrimon, N. (2000). Functional binding of secreted molecules to heparan sulfate proteoglycans in *Drosophila*. *Curr. Opin. Cell Biol.* **12**, 575-580.
- Baker, N. E. (1987). Transcription of the segment polarity gene *wingless* in the imaginal discs of *Drosophila*, and the phenotype of a pupal-lethal *wg* mutation. *Development* **102**, 489-497.
- Basler, K., and Struhl, G. (1994). Compartment boundaries and the control of *Drosophila* limb pattern by *hedgehog* protein. *Nature* **368**, 208-214.
- Basler, K., and Burke, M. (1996). *Dpp* receptors are autonomously required for cell proliferation in the entire developing *Drosophila*. *Development* **122**, 2261-2269.
- Bate, M., and Martinez-Arias, A. (1991). The embryonic origin of imaginal discs in *Drosophila*. *Development* **112**, 755-761.
- Beachy, P. A., Cooper, M. K., Young, K. E., von Kessler, D. P., Park, W. J., Hall, T. M., Leahy, D. J., and Porter, J. A. (1997). Multiple roles of cholesterol in hedgehog protein biogenesis and

- signaling. *Cold Spring Harb. Symp. Quant. Biology* **62**, 191-204.
- Beiman, M., Shilo, B. Z., and Volk, T. (1996). *Heartless*, a *Drosophila* FGF receptor homolog, is essential for cell migration and establishment of several mesodermal lineages. *Genes Dev.* **10**, 2993-3002.
- Bejsovec, A., and Martinez-Arias, A. (1991). Roles of *wingless* in patterning the larval epidermis of *Drosophila*. *Development* **113**, 471-485.
- Bellaiche, Y., The, I., and Perrimon, N. (1998). *Tout-velu* is a *Drosophila* homolog of the putative tumour suppressor EXT-1 and is needed for Hh diffusion. *Nature* **394**, 85-88.
- Bellen, H. J., O'Kane, C. J., Wilson, C., Grossniklaus, U., Pearson, R. K., and Gehring, W. J. (1989). P-element mediated enhancer detection: a versatile method to study development in *Drosophila*. *Genes Dev.* **3**, 1288-1300.
- Belvin, M., Jin, Y., and Anderson, K. V. (1995). *Cactus* protein degradation mediates *Drosophila* dorsal-ventral signals. *Genes Dev.* **9**, 783-793.
- Ben-Ze'ev, A., Robinson, G. S., Bucher, N. L., and Farmer, S. R. (1988). Cell-cell and cell-matrix interactions differentially regulate the expression of hepatic and cytoskeletal genes in primary cultures of rat hepatocytes. *Proc. Natl. Acad. Sci. USA* **85**, 2161-2165.
- Berleth, T., Burri, M., Thoma, G., Bopp, D., Richstein, S., Frigerio, G., Noll, M., and Nusslein-Volhard, C. (1988). The role of localization of *bicoid* RNA in organizing the anterior pattern of the *Drosophila* embryo. *EMBO J.* **7**, 1749-1756.
- Bernfield, M. (1999). Functions of cell-surface heparan sulfate proteoglycans. *Annu. Rev. Biochem.* **68**, 729-777.
- Bernfield, M., and Hooper, K. C. (1991). Possible regulation of FGF activity by syndecan, an integral membrane heparan sulfate proteoglycan. *Ann. N. Y. Acad. Sci.* **638**, 182-194.
- Bernfield, M., and Hooper, K. C. (1993). Possible regulation of FGF activity by syndecan, an integral membrane heparan sulfate proteoglycan. *Cell* **73**, 182-194.
- Bernfield, M., Kokenyesi, R., Kato, M., Hinkes, M. T., Spring, J., Gallo, R. L., and Lose, E. J. (1992). Biology of the syndecans: A family of transmembrane heparan sulfate proteoglycans. *Annu. Rev. Cell Biol.* **8**, 365-393.
- Bernfield, M., Gotte, M., Park, P. W., Reizes, O., Fitzgerald, M. A., Lincecum, J., and Zako, M. (1999). Functions of cell-surface heparan sulfate proteoglycans. *Annu. Rev. Biochem.* **68**, 729-777.
- Bernfield, M., and Sanderson, R. D. (1990). Syndecan, a developmentally regulated cell-surface proteoglycan that binds extracellular matrix and growth factors. *Philos. Trans. Royal Soc. Lond. Biol. Sci.* **327**, 171-186.
- Bhanot, P., Brink, M., Samos, C. H., Hsieh, J. C., Wang, Y., Macke, J. P., Andrew, D., Nathans, J., and

- Nusse, R. (1996). A new member of the *frizzled* family from *Drosophila* functions as a *wingless* receptor. *Nature* **382**, 225-230.
- Biehs, B., Francois, V., and Bier, E. (1996). The *Drosophila short gastrulation* gene prevents Dpp from autoactivating and suppressing neurogenesis in the neuroectoderm. *Genes Dev.* **10**, 2922-2934.
- Bienz, M. (1994). Homeotic genes and positional signaling in the *Drosophila* viscera. *Trends Genet.* **10**, 22-26.
- Binari, R. C., Staveley, B. E., Johnson, W. A., Godavanti, R., Sasisekharan, R., and Manoukian, A. S. (1997). Genetic evidence that heparin-like glycosaminoglycans are involved in *wingless* signaling. *Development* **124**, 2623-2632.
- Bissell, M. J., and Hall, H. G. (1987). Form and function in the mammary gland. The role of extracellular matrix, In: *The mammary Gland*, edited by M.C. Neville and C.W. Daniel, Plenum Press, New York, pp. 97-146.
- Blackman, R. K., Sanicola, M., Raftery, L. A., Gillevet, T., and Gelbart, W. M. (1991). An extensive C-3-regulatory region directs the imaginal disc expression of *decapentaplegic*, a member of the TGF- β family in *Drosophila*. *Development* **111**, 657-665.
- Blair, S. S. (1992). *Engrailed* expression in the anterior lineage compartment of the developing wing blade of *Drosophila*. *Development* **115**, 21-33.
- Blair, S. S. (1995). *Hedgehog* digs up old friends. *Nature* **373**, 656-657.
- Blair, S. S. (1996) Compartments and appendage development in *Drosophila*. *BioEssays* **17**, 299-309
- Bodenmuller, H., and Schaller, H. C. (1981). Conserved amino acid sequence of a neuropeptide, the head activator, from coelenterates to humans. *Nature* **293**, 579-580.
- Bourin, M-C., and Lindahl, U. (1993). Glycosaminoglycans and the regulation of blood coagulation. *J. Biochem.* **289**, 313-330.
- Brand, A. H., and Perrimon, N. (1993). Targeted gene expression as a means of altering cell fates and generating dominant phenotypes. *Development* **118**, 401-415.
- Brand, A. H., and Perrimon, N. (1994). Raf acts downstream of the EGF receptor to determine dorsoventral polarity during *Drosophila* oogenesis. *Genes Dev.* **8**, 629-639.
- Brickell, P. M., and Tickle, C. (1989). Morphogens in chick limb development. *BioEssays* **11**, 145-149.
- Brook, W. J., and Cohen, S. M. (1996). Antagonistic interaction between *wingless* and *decapentaplegic* is responsible for dorsal-ventral pattern in the *Drosophila* leg. *Science* **273**, 1373-1377
- Brook, W. J., Diaz-Benjumea, F. J., and Cohen, S. M. (1996). Organizing spatial pattern in limb

- development. *Annu. Rev. Cell Dev. Biol.* **12**, 161-180.
- Brook, W. J. (1994). Gene expression in regenerating imaginal discs of *Drosophila melanogaster*. Ph.D. Thesis, Department of Genetics, University of Alberta, Edmonton, Alberta, Canada.
- Brook, W. J., Ostafichuk, L. M., Piorecky, J., Wilkinson, M. D., Hodgetts, D. J., and Russell, M. A. (1993). Gene expression during imaginal disc regeneration detected using enhancer-sensitive P-elements. *Development* **117**, 1287-1297.
- Brummel, T. J., Twombly, V., Marques, G., Wrana, J. L., Newfeld, S. J., Attisano, L., Massague, J., O'Connor, M. B., and Gelbart, W. M. (1994). Characterization and relationship of *dpp* receptors encoded by the *saxophone* and *thickveins* genes in *Drosophila*. *Cell* **78**, 251-261.
- Bryant, P. J. (1971). Regeneration and duplication following operations in situ on the imaginal discs of *Drosophila melanogaster*. *Dev. Biol.* **26**, 637-651.
- Bryant, P. J. (1975). Pattern formation in the imaginal wing disc of *Drosophila melanogaster*: fate map, regeneration, and duplication. *J. Exp. Zool.* **193**, 49-77.
- Bryant, P. J. (1976). Determination and pattern formation in the imaginal discs of *Drosophila*. *Curr. Top. Dev. Biol.* **8**, 41-80.
- Bryant, P. J. (1978). Cell interactions controlling pattern regulation and growth in epimorphic fields. *Birth Defects Orig. Artic. Ser.* **14**, 529-245.
- Bryant, P. J., Adler, P. N., Duranceau, C., Fain, M. J., Glenn, S., Hsei, B., James, A. A., Littlefield, C. L., Reinhardt, C. A., Strub, S., and Schneiderman, H. A. (1978). Regulative interactions between cells from different imaginal discs of *Drosophila melanogaster*. *Science* **201**, 928-230.
- Bryant, P. J., and Fraser, S. E. (1988). Wound healing, cell communication, and DNA synthesis during imaginal disc regeneration in *Drosophila*. *Dev. Biol.* **127**, 197-208.
- Bryant, S.V., French, V., and Bryant, P. J. (1981). Distal regeneration and symmetry. *Science* **212**, 993-1002.
- Bryant, S. V., and Gardiner, D. M. (1992). Retinoic acid, local cell-cell interactions, and pattern formation in vertebrate limbs. *Dev. Biol.* **152**, 1-25.
- Bryant, P. J., and Schneiderman, H. A. (1969). Cell lineage, growth, and determination in the imaginal leg discs of *Drosophila melanogaster*. *Dev. Biol.* **20**, 263-290.
- Bulik, D.A., Wei, G., Toyoda, H., Kinoshita-Toyoda, A., Waldrip, W.R., Esko, J. D., Robbins, P. W., and Selleck, S. B. (2000). *sqv-3*, *-7*, and *-8*, a set of genes affecting morphogenesis in *Caenorhabditis elegans*, encoded enzymes required for glycosaminoglycan biosynthesis. *Proc. Natl. Acad. Sci. USA* **97**, 10838-10843.
- Bullock, S. L., Fletcher, J. M., Bedding, R. S. P., and Wilson, V. A. (1998). Renal agenesis in mice homozygous for gene trap mutation in the gene encoding heparan sulfate 2-O-sulfotransferase.

Genes Dev. **12**, 1894-1906.

- Cadigan, K. M., Fish, M. P., and Nusse, R. (1998). *Wingless* repression of *Drosophila frizzled 2* expression shapes the *wingless* morphogen gradient in the wing. *Cell* **93**, 767-777.
- Campbell, G., and Tomlinson, A. (1999). Transducing the DPP morphogen gradient in the wing of *Drosophila* regulation of *dpp* targets by *brinker*. *Cell* **96**, 553-562.
- Campbell, G., and Tomlinson, A. (1998). The roles of the homeobox genes *aristaless* and *Distal-less* in patterning the legs and wings of *Drosophila*. *Development* **125**, 4483-4493.
- Campbell, G., and Tomlinson, A. (1995). Initiation of the proximodistal axis in insect legs. *Development* **121**, 619-628.
- Campbell, G., Weaver, T., and Tomlinson, A. (1993). Axis specification in the developing *Drosophila* appendage: the role of *wingless*, *decapentaplegic* and the homeobox gene *aristaless*. *Cell* **74**, 1113-1123.
- Capdevilla, J., and Belmonte, J. C. (1999). Extracellular modulation of the Hedgehog, Wnt and TGF- β signaling pathways during embryonic development. *Curr. Opin. Genet. Dev.* **9**, 427-433.
- Capdevilla, J., Estrada, M. P., Sanchez-Herrero, E., and Guerrero, I. (1994). The *Drosophila* segment polarity gene *patched* interacts with *decapentaplegic* in wing development. *EMBO J.* **13**, 71-82.
- Capdevilla, J., and Guerrero, I. (1994). Targeted expression of the signaling molecule Decapentaplegic induces pattern duplications and growth alterations in *Drosophila* wings. *EMBO J.* **13**, 4459-4468.
- Carey, D. J. (1997). Syndecans: multifunctional cell-surface co-receptors. *J. Biochem.* **327**, 1-16.
- Carrington, J. L., Chen, P., Yanagishita, M., and Reddi, A. H. (1991). Osteogenin (bone morphogenetic protein-3) stimulates cartilage formation by chick limb bud cells in vitro. *Dev. Biol.* **146**, 406-415.
- Celeste, A. J., Iannazzi, J. A., Taylor, R. C., Hewick, R. M., Rosen, V., Wang, E. A., and Wozney, J. M. (1990). Identification of transforming growth factor β family members present in bone-inductive protein purified from bovine bone. *Proc. Natl. Acad. Sci. USA* **87**, 9843-9847.
- Chan, L. N., and Gehring, W. (1971). Determination of blastoderm cells in *Drosophila melanogaster*. *Proc. Natl. Acad. Sci. USA* **68**, 2217-2221.
- Chang, S. C., Hoang, B., Thomas, J. T., Vukicevic, S., Luyten, F. P., and Ryban, N. J. P. (1994). Cartilage-derived morphogenetic proteins. *J. Biol. Chem.* **269**, 28227-28234.
- Chasan, R., and Anderson, K. V. (1989). The role of *easter*, an apparent serine protease, in organizing the dorsal-ventral pattern of the *Drosophila* embryo. *Cell* **56**, 391-400.

- Chasen, R., and Anderson, K. V. (1993). Maternal control of dorsal-ventral polarity and pattern in the embryo. In: *The Development of Drosophila melanogaster*. Bate, M. and Martinez Arias, A. eds. Cold Spring Harbor Lab Press, Plainview, New York, pp. 387-424.
- Chasen, R., Jin, Y., and Anderson, K. V. (1992). Activation of the easter zymogen regulated by five other genes to define dorsal-ventral polarity in the *Drosophila* embryo. *Development* **115**, 607-616.
- Cheifetz, S., Anders, J. L., and Massague, J. (1988). The Transforming Growth Factor- β receptor type III is a membrane proteoglycan. *J. Biol. Chem.* **263**, 16984-16991.
- Cheifetz, S., and Massague, J. (1989). Transforming growth factor- β (TGF- β) receptor proteoglycan. *J. Biol. Chem.* **264**, 12025-12028.
- Chen, L. H., and Bissell, M. J. (1989). A novel regulatory mechanism for whey acidic protein expression. *Cell Regulation* **1**, 45-54.
- Chen, L. H., and Bissell, M. J. (1987). Transferrin mRNA level in mouse mammary gland is regulated by pregnancy and extracellular matrix. *J. Biol. Chem.* **262**, 12918-12921.
- Chen, P., Carrington, J. L., Hammonds, R. G., and Reddi, A. H. (1991). Stimulation of chondrogenesis in limb bud mesodermal cells by recombinant human BMP-2B and modulation by TGF- β , and TGF- β 2. *Exp. Cell Res.* **195**, 509-515.
- Chen, Y., and Struhl, G. (1996). Dual roles for *patched* in sequestering and transducing *Hedgehog*. *Cell* **87**, 553-563.
- Chen, Y., and Struhl, G. (1998). *In vivo* evidence that Patched and Smoothed constitute distinct binding and transducing components of a *hedgehog* receptor complex. *Cell* **90**, 193-196.
- Chen, Y., Gallaher, N., Goodman, R. H., and Smolik, S. M. (1998). *Protein kinase A* directly regulates the activity and proteolysis of *Cubitus interruptus*. *Proc. Natl. Acad. Sci. USA* **95**, 2349-2354.
- Childs, S. R., Wrana, J. L., Arora, K., Attisano, L., O'Conner, M., and Massague, J. (1995). Identification of a *Drosophila* activin receptor. *Proc. Natl. Acad. Sci. USA* **90**, 9475-9479.
- Clark, W. C. (1976). Histological investigations of a temperature-sensitive cell-lethal mutant of *Drosophila melanogaster*. M. Sc. Thesis. University of Alberta, Edmonton, Alberta, Canada.
- Clark, W. C., and Russell, M. A. (1977). The correlation of lysosomal activity and adult phenotype in a cell-lethal mutant of *Drosophila*. *Dev. Biol.* **57**, 160-173.
- Clark, E. A., and Brugge, J. S. (1995). Integrins and signal transduction pathways: the road taken. *Science* **268**, 233-239.
- Cohen, S. M. (1990). Specification of limb development in the *Drosophila* embryo by positional cues from segmentation genes. *Nature* **343**, 173-177.

- Cohen, S. M. (1993). Development and patterning of the larval epidermis of *Drosophila*. In "The Development of *Drosophila melanogaster*." (ed. M. Bate and A. Martinez Arias), Cold Spring Harbor Laboratory Press, New York., pp. 747-892.
- Cohen, S. M., Bronner, G., Kuttner, F., Jurgens, G., and Jackle, H. (1989). *Distal-less* encodes a homeodomain protein required for limb development in *Drosophila*. *Nature* **338**, 432-434.
- Cohen, S., and Jurgens, G. (1991). *Drosophila* headlines. *Trends Genet.* **7**, 267-272.
- Cohen, B., Simcox, A. A and Cohen, S. M. (1993). Allocation of the thoracic imaginal primordia in the *Drosophila* embryo. *Development* **117**, 597-608.
- Condic, M. L., and Fristrom, D. (1991). Apical cell shape changes during *Drosophila* imaginal leg disc elongation: a novel morphogenetic mechanism. *Development* **111**, 23-33.
- Cooley, L., Kelly, R., and Spradling, A. (1988). Insertional mutagenesis of the *Drosophila* genome with single P-elements. *Science* **239**, 1121-1128.
- Couso, J. P., Bate, M., and Martinez-Arias, A. (1993). A *wingless* dependent polar coordinate system in *Drosophila* imaginal discs. *Science* **59**, 484-489.
- Couso, J. P., and Gonzalez-Gaitan, M. (1993). Embryonic limb development in *Drosophila*. *Trends Genet.* **9**, 371-373.
- Crick, F. H. C., and Lawrence, P. A. (1975). Compartments and polyclones in insect development. *Science* **189**, 340-347.
- Cumberledge, S., and Reichsman, F. (1997). Glycosaminoglycans and WNTs: just a spoonful of sugar helps the signal go down. *Trends Genet.* **13**, 421-423.
- Dale, L., and Bownes, M. (1980). Is regeneration in *Drosophila* the result of epimorphic regulation? *Wilhelm Roux's Arch. Dev. Biol.* **189**, 91-96.
- Dale, L., and Bownes, M. (1985). Pattern regulation in fragments of *Drosophila* wing discs which show variable wound healing. *J. Embryol. Exp. Morph.* **85**, 95-109.
- Dale, L., and Jones, C. M. (1999). BMP signaling in early *Xenopus* development. *BioEssays* **21**, 751-760.
- Dale, L., and Wardle, F. C. (1999). A gradient of BMP activity specifies dorsal-ventral fates in early *Xenopus* embryos. *Semin. Cell Dev. Biol.* **10**, 319-326.
- D'Amore, P. A. (1990). Heparin-endothelial cell interactions. *Haemostasis* **20** (Suppl 1), 159-165.
- David, G., Loriew, V., Decock, B., Marynen, P., Cassiman, J. J., and van den Berghe, H. (1990). Molecular cloning of a phosphatidylinositol-anchored membrane heparan sulfate proteoglycan from human lung fibroblasts. *J. Cell Biol.* **111**, 3165-3176.

- David, G. (1993). Integral membrane heparan sulfate proteoglycans. *FASEB J.* **7**, 1023-1030.
- Davidson, E. H. (1968). "Gene activity in early development". Academic Press Inc., New York.
- Dealy, C. N., Seghatoleslami, M. R., Ferrari, D., and Kosher, R. A. (1997). FGF-stimulated outgrowth and proliferation of limb mesoderm is dependent on syndecan-3. *Dev. Biol.* **184**, 343-350.
- De Cat, B., and David, G. (2001). Developmental roles of glypicans. *Cell Dev. Biol.* **12**, 117-125.
- Derynck, R., and Feng, X. H. (1997). TGF- β receptor signaling. *Biochim. Biophys. Acta.* **1333**, 105-150.
- Desplan, C., and Theis, J. (1985). The *Drosophila* developmental gene, *engrailed*, encodes a sequence specific DNA binding activity. *Nature* **318**, 630-635.
- Diaz-Benjumea, F. J., Cohen, B., and Cohen, S. M. (1994). Cell interactions between compartments establishes the proximal-distal axis of *Drosophila* legs. *Nature* **372**, 175-178.
- Diaz-Benjumea, F. J., and Cohen, S. M. (1993). Interaction between dorsal and ventral cells in the imaginal disc direct wing development in *Drosophila*. *Cell* **75**, 741-752.
- Diaz-Benjumea, F. J., and Cohen, S. M. (1994). *Wingless* acts through the *shaggy/zeste-white 3* kinase to direct dorsal-ventral axis formation in the *Drosophila* leg. *Development* **120**, 1661-70.
- Diaz-Benjumea, F. J., and Cohen, S. M. (1995). Serrate signals through Notch to establish a *wingless* dependent organizer at the dorsal/ventral compartment boundary of the *Drosophila* wing. *Development* **121**, 4215-4225.
- DiGabriele, A. D. (1998). Structure of a heparin-linked biologically active dimer of FGF. *Nature* **393**, 812-817.
- DiNardo, S., Sher, E., Heemskerk-Jongens, J., Kassis, J. A., and O'Farrell, P. H. (1988). Two-tiered regulation of spatially patterned *engrailed* gene expression during *Drosophila* embryogenesis. *Nature* **332**, 604-609.
- Doherty, J. P., Lindeman, R., Trent, R. J., Graham, M. W., and Woodcock, D. M. (1993). *Escherichia coli* host strains SURE and SRB fail to preserve a palindrome cloned in lambda phage: improved alternative host strains. *Gene* **124**, 29-35
- Dominguez, M., Brunner, M., Hafen, E., and Basler, K. (1996). Sending and receiving the *hedgehog* signal: control by the *Drosophila* Gli protein *Cubitus interruptus*. *Science* **272**, 1621-1625.
- Dosch, R., Gawantka, V., Delias, H., Blumenstock, C., and Niehrs, C. (1997). BMP4 acts as a morphogen in dorsal-ventral mesoderm patterning in *Xenopus*. *Development* **124**, 2325-2334.

- Dougherty, B. A., and van de Rijn, I. (1993). Molecular characterization of hasB from an operon required for hyaluronic acid synthesis in group A. *Streptococcus*. *J. Biol. Chem.* **268**, 7118-7124.
- Driever, W. J., Ma, J., Nusslein-Volhard, C., and Ptashne, M. (1989). Rescue of *bicoid* mutant *Drosophila* embryos by *bicoid* fusion proteins containing heterologous activating sequences. *Nature* **342**, 149-154.
- Driever, W., and Nusslein-Volhard, C. (1988a). The *bicoid* protein determines position in the *Drosophila* embryo in a concentration-dependent manner. *Cell* **54**, 95-104.
- Driever, W., and Nusslein-Volhard, C. (1988b). A gradient of *bicoid* protein in *Drosophila* embryos. *Cell* **54**, 83-93.
- Duncan, I. (1987). The *bithorax* complex. *Annu. Rev. Genet.* **21**, 285-319.
- Eaton, S., and Kornberg, T. B. (1990). Repression of *ci-D* in posterior compartments of *Drosophila* by *engrailed*. *Genes Dev.* **4**, 1068-1077.
- Eichele, G. (1989). Retinoids and vertebrate limb pattern formation. *Trends Genet.* **5**, 246-251.
- Entchen, E. V., Schwabedissen, A., and Gonzalez-Gaitian, M. (2000). Gradient Formation of the TGF β homolog Dpp. *Cell* **103**, 981-991.
- Ephrussi, B., and Beadle, G. W. (1936). A technique of transplantation for *Drosophila*. *Am. Naturalist* **70**, 218-225.
- Ernst, S., Langer, R., Cooney, C. L., and Sasisekharan, R. (1995). Enzymatic degradation of glycosaminoglycans. *Critical Rev. Biochem. Mol. Biol.* **30**, 387-444.
- Ernst, S., Venkataraman, G., Winkler, S., Godavarti, R., Langer, R., Cooney, C. L., and Sasisekharan, R. (1996). Expression in *E.coli*, purification and characterization of heparinase from *Flavobacterium heparinum*. *J. Biochem.* **315**, 589-597.
- Esko, J. D. (1991). Genetic analysis of proteoglycan structure, function and metabolism. *Current Opinion. in Cell Biology.* **3**, 805-816.
- Faham, S., Hilemann, R. E., Fromm, J. R., Linhardt, R. J., and Ress, D. C. (1996). Heparin structure and interactions with basic FGF. *Science* **271**, 1116-1120.
- Falcone, D. J., McCaffery, T. A., Haimovitz-Friedman, A., Vergilio, J. A., and Nicholson, A. C. (1993). Macrophage and foam cell release of matrix bound growth factors. Role of plasminogen activation. *J. Biol. Chem.* **268**, 11951-11958.
- Fan, C. M., and Tessier-Lavigne, M. (1994). Patterning of mammalian somites by surface ectoderm and notochord: evidence for sclerotome induction by a Hedgehog homolog. *Cell* **79**, 1175-1186.

- Felsenfeld, A. L., and Kennison, J. A. (1995). Positional signaling by *hedgehog* in *Drosophila* imaginal disc development. *Development* **121**, 1-10.
- Ferguson, E. L., and Anderson, K. V. (1991). Dorsal-ventral pattern formation in the *Drosophila* embryo: the role of zygotically active genes. *Curr. Top. Dev. Biol.* **25**, 17-43.
- Ferguson, E. L., and Anderson, K.V. (1992a). *Decapentaplegic* acts as a morphogen to organize dorsal-ventral pattern in the *Drosophila* embryo. *Cell* **71**, 451-461
- Ferguson, E. L., and Anderson, K. V. (1992b). Localized enhancement and repression of the activity of the TGF- β family member *decapentaplegic* is necessary for dorsal-ventral pattern formation in the *Drosophila* embryo. *Development* **114**, 583-597.
- Filmus, J., Shi, W., Wong, Z. M., and Wong, M. J. (1995). Identification of a new membrane-bound heparan sulfate proteoglycan. *J. Biochem.* **311**, 561-565.
- Finelli, A. L., Bossie, C. A., Xie, T., and Padgett, R. W. (1995). Mutational analysis of the *Drosophila tolloid* gene, a human BMP-1 homolog. *Protein Science* **4**, 1247-1261.
- FlyBase (1994). FlyBase the *Drosophila* database. *Nucleic Acids Res.* **22**, 3456-3458.
- Flybase (2001). Flybase <http://www.flybase.com>
- Folkman, J., Bashkin, S., Doctrow, M., Klagsbrun, C., Svahn, M., and Vlodavsky, I. (1989). Basic fibroblast growth factor binds to subendothelial extracellular matrix and is released by heparinase and heparin-like molecules. *Biochemistry* **28**, 1737-1743.
- Forsberg, E., Pejler, G., Ringwall, M., Lunderius, C., Tomasini-Johansson, B., Kusche-Gullberg, M., Eriksson, I., Ledin, J., Hellman, L., and Kjellen, L. (1999). Abnormal mast cells in mice deficient in a heparin-synthesizing enzyme. *Nature* **400**, 773-776.
- Forsten, K. E. Courant, N. A., and Nugent, M. A. (1997). Endothelial proteoglycans inhibit bFGF binding and mitogenesis. *J. Cell Physiol.* **172**, 209-220.
- Francois, V., Solloway, M., O'Neil, J. W., Emery, J., and Bier, E. (1994). Dorsal-ventral patterning of the *Drosophila* embryo depends on a putative negative growth factor encoded by the *short gastrulation* gene. *Genes Dev.* **8**, 2602-2616.
- Francois, V., and Bier, E. (1995) *Xenopus chordin* and *Drosophila short gastrulation* genes encode homologous proteins functioning in dorsal-ventral axis formation. *Cell* **80**, 19-29.
- Frasch, M. (1995). Induction of visceral and cardiac mesoderm by ectodermal *Dpp* in the early *Drosophila* embryo. *Nature* **374**, 464-467.
- Frasch, M., Hoey, T., Rushlow, C., Doyle, H., and Levine, M. (1987). Characterization and localization of the *even-skipped* protein of *Drosophila*. *EMBO J.* **6**, 749-759.

- French, V. (1976). Leg regeneration in the cockroach, *Blatella germanicall*. Regeneration from a non-congruent tibial graft/host junction. *J. Embryol. Exp. Morph.* **53**, 267-301.
- French, V., Bryant, P. J., and Bryant, S. V. (1976). Pattern regulation in epimorphic fields. *Science* **193**, 969-981.
- Gallo, R. L., Kim, C., Kokenyesi, R., Adzick, N. S., and Bernfield, M. (1996). Syndecans-1 and -4 are induced during wound repair of neonatal but not fetal skin. *J. Invest. Dermatol.* **107**, 676-683.
- Gallo, R. L., Ono, M., Povsic, T., Page, C., Eriksson, E., Klagsburn, M., and Bernfield, M. (1994). Syndecans, cell-surface heparan sulfate proteoglycans, are induced by a proline-rich antimicrobial peptide from wounds. *Proc. Natl. Acad. Sci. USA* **91**, 11035-11039.
- Garcia-Bellido, A., and Merriam, J. R. (1969). Cell lineage of the imaginal discs in *Drosophila* gynandromorphs. *J. Exp. Zool.* **170**, 61-75.
- Garcia-Bellido, A., and Merriam, J. R. (1971). Genetic analysis of cell heredity in imaginal discs of *Drosophila melanogaster*. *Proc. Natl. Acad. Sci. USA* **8**, 2222-2226.
- Garcia-Bellido, A., and Santamaria, P. (1972). Developmental analysis of the wing disc in the mutant *engrailed* of *Drosophila melanogaster*. *Genetics* **72**, 87-104.
- Garcia-Bellido, A., Ripoll, P., and Morata, G. (1973). Developmental compartmentalization of the wing disc of *Drosophila*. *Nature New Biology* **245**, 251-253.
- Garcia-Bellido, A., Ripoll, P., and Morata, G. (1976). Developmental compartmentalization in the dorsal mesothoracic disc of *Drosophila*. *Dev. Biol.* **48**, 132-147.
- Gardiner, D. M., Gaudier, C., and Bryant, S. V. (1992). Mouse limb bud cells respond to retinoic acid in vitro with reduced growth. *J. Exp. Zool.* **263**, 406-413.
- Gay, N. J., and Keith, F. J. (1991). *Drosophila* Toll and IL-1 receptor. *Nature* **351**, 355-356.
- Gehring, W. (1966). Cell heredity and changes of determination in cultures of imaginal discs in *Drosophila melanogaster*. *J. Embryol. Exp. Morph.* **15**, 77-111.
- Gehring, W. J. (1973). Genetic control of determination in the *Drosophila* embryo. *Symp. Soc. Dev. Biol.* **31**, 103-28.
- Geisler, R., Bergmann, A., Hiromi, Y., and Nusslein-Volhard, C. (1992). *cactus*, a gene involved in dorsoventral pattern formation of *Drosophila*, is related to the *I κ B* gene family of vertebrates. *Cell* **71**, 613-621.
- Gelbart, W. M. (1989). The *decapentaplegic* gene: a TGF- β homolog controlling pattern formation in *Drosophila*. *Development* **4** (Suppl.), 65-74.

- Gelbart, W. M., Irish, V. F., St Johnston, R. D., Hoffmann, F. M., Blackman, R. K., Segal, D., Posakony L. M., and Grimaldi, R. (1985). The *decapentaplegic* gene complex in *Drosophila melanogaster*. *Cold Spring Harb. Symp. Quant. Biol.* **50**, 119-25.
- Gertula, S., Jin, Y. S., and Anderson, K. V. (1988). Zygotic expression and activity of the *Drosophila Toll* gene, a gene required maternally for embryonic dorsal-ventral pattern formation. *Genetics* **119**, 123-133.
- Ghysen, A., and O'Kane, C. (1989). Neural enhancer-like elements as specific cell markers in *Drosophila*. *Development* **105**, 35-52.
- Girton, J. R. (1981). Pattern triplication produced by a cell lethal mutation in *Drosophila*. *Dev. Biol.* **84**, 164-172.
- Girton, J. R., and Russell, M. A. (1980). A clonal analysis of pattern duplications in a temperature-sensitive cell-lethal mutant of *Drosophila*. *Dev. Biol.* **77**, 1-21.
- Girton, J. R., and Russell, M. A. (1981). An analysis of compartmentalization in pattern duplications induced by a cell-lethal mutation in *Drosophila*. *Dev. Biol.* **85**, 55-64.
- Girton, J. R., and Kumor, A. L. (1985). The role of cell-death in the induction of pattern abnormalities in a cell-lethal mutation of *Drosophila*. *Dev. Genet.* **5**, 93-102.
- Gisselbrecht, S., Skeath, J. B., Doe, C. Q., and Michelson, A. M. (1996). *Heartless* encodes a FGF receptor (DRF1/DRF-R2) involved in the directional migration of early mesodermal cells in the *Drosophila* embryo. *Genes Dev.* **10**, 3003-3017.
- Godavarti, R., and Davis, M. (1996). Heparinase III from *Flavobacterium heparinum*: cloning and recombinant expression in *Escherichia coli*. *Biochem. Biophys. Res. Commun.* **225**, 751-758.
- Goldstein, L. S. B., and Fyrberg, E. A. (1994) Methods in Cell Biology "*Drosophila melanogaster*: Practical Uses in Cell and Molecular Biology", Academic Press v44, New York, pp. 445-487.
- Gonzalez, F., Swales, L., Bejsovec, A., Skaer, H., and Martinez-Arias, A. (1991). Secretion and movement of *wingless* protein in the epidermis of the *Drosophila* embryo. *Mech. Dev.* **35**, 43-54.
- Gonzalez-Gaitan, M. A., and Jackle, H. (1999). The range of *spalt*-activating *dpp* signaling is reduced in endocytosis defective *Drosophila* wing discs. *Mech. Dev.* **87**, 143-151.
- Goode, S., Wright, D., and Mahowald, A. P. (1992). The neurogenic locus *brainiac* cooperates with the *Drosophila* EGF receptor to establish the ovarian follicle and to determine its dorsal-ventral polarity. *Development* **116**, 177-192.
- Govind, S., and Steward, R. (1991). Dorsoventral pattern formation in *Drosophila*: signal transduction and nuclear targeting. *Trends Genet.* **7**, 1-7.

- Gray, S. Szymanski, P., and Levine, M. (1994). Short-range repression permits multiple enhancers to function autonomously within a complex promoter. *Genes Dev.* **8**, 1829-1838.
- Greco, V. Hannus, M., and Eaton, S. (2001). Argosomes: A potential vehicle for the spread of morphogens through epithelia. *Cell* **106**, 633-645.
- Green, J., and Smith, J. (1990). Gradient changes in dose of a *Xenopus* activin homolog elicit step wise transitions in embryonic cell fate. *Nature* **347**, 391-394.
- Green, J., New, H. V., and Smith, J. C. (1992). Responses of embryonic *Xenopus* cells to activin and FGF are separated by multiple dose thresholds and correspond to distinct axes of the mesoderm. *Cell* **71**, 731-739.
- Greider, N. C., Nellen, D., Burke, R., Basler, K., and Affolter, M. (1995). *Schnurri* is required for *Drosophila dpp* signaling and encodes a zinc finger protein similar to the mammalian transcription factor PRDII-BFI. *Cell* **81**, 791-800.
- Grimm, S., and Pflugfelder, G. O. (1996). Control of the gene *optomotor-blind* in *Drosophila* wing development by *decapentaplegic* and *wingless*. *Science* **271**, 1601-1604.
- Grossniklaus, U., Bellen, H. J., Wilson, C., and Gehring, W. J. (1989). P-element-mediated enhancer detection applied to the study of oogenesis in *Drosophila*. *Development* **107**, 189-200.
- Guan, J. L., Trevithick, J. E., and hynes, R. O. (1991). Fibronectin/integrin interaction induces tyrosine phosphorylation of a 120-kDa protein. *Cell Regulation* **2**, 951-640.
- Guimond, S., Maccarana, M., Olwin, B., Lindahl, U., and Rapraeger, A. C. (1993). Activating and inhibitory heparin sequences for FGF-2 (bFGF). Distinct requirements for FGF-1, FGF-2, and FGF-4. *J. Biol. Chem.* **268**, 23906-23914.
- Guo, Y., and Conrad, H. E. (1989). The disaccharide composition of heparins and heparan sulfates. *Anal. Biochem.* **176**, 96-104.
- Gurdon, J. (1998). Cell perception of position in a concentration gradient. *Cell* **95**, 159-162.
- Gurdon, J. B., Harger, P., Mitchell, A., and Lemaire, P. (1994). *Activin* signaling and response to a morphogen gradient. *Nature* **371**, 487-492.
- Gurdon, J. B., and Mitchell, A. (1996). An experimental system for analyzing response to a morphogen gradient. *Proc. Natl. Acad. Sci. USA* **93**, 9334-9338.
- Gurdon, J. B., Mitchell, A., and Mahoney, D. (1995). Direct and continuous assessment by cells of their position in a morphogen gradient. *Nature* **376**, 520-521.
- Gurdon, K., Ryan, F., Stennard, N., McDowell, A., Zorn, M., Crease, D. J., and Dyson, S. (1997). Cell response to different concentrations of a morphogen: activin effects on *Xenopus* animal caps. *Cold Spring Harb. Symp. Quant. Biol.* **62**, 151-158.

- Habuchi H., Habuchi, O., and Kimata, K. (1998). Biosynthesis of heparan sulfate and heparin. How are the multifunctional glycosaminoglycans built up? *Trends Glycosci. Glycotechnol.* **10**, 65-80.
- Hacker, U., Lin., X., and Perrimon, N. (1997). The *Drosophila sugarless* gene modulates *Wingless* signaling and encodes an enzyme involved in polysaccharide biosynthesis. *Development* **124**, 3565-3573.
- Hadorn, E. (1960). Developmental genetics and lethal factors. Methuen, London..
- Hadorn, E. (1965). Problems of determination and transdetermination. In Genetic Control of Differentiation. *Brookhaven Symp.* **18**, 148-161.
- Hadorn, E. (1969). Proliferation and dynamics of cell heredity in blastema cultures of *Drosophila*. *Natl. Cancer Inst. Monogr.* **31**, 351-364.
- Haerry, T. E., Heslip, T. R., Marsh, J. L., and O'Connor, M. B. (1997) Defects in glucuronate biosynthesis disrupt *wingless* signaling in *Drosophila*. *Development* **124**, 3055-3064.
- Haerry, T. E., Khalsa, O., O'Conner, M. B., and Wharton, K. A. (1998). Synergistic signaling by two BMP ligands through the SAX and TKV receptors controls wing growth and patterning in *Drosophila*. *Development* **125**, 3977-3987.
- Hama, C., Ali, Z., and Kornberg, T. B. (1990). Region specific recombination and expression are directed by portions of the *Drosophila engrailed* promoter. *Genes Dev.* **4**, 1079-1093.
- Hanahan, D., and Meselson, M. (1983). Plasmid screening at high colony density. *Methods Enzymol.* **100**, 333-3342.
- Harding, K., Rushlow, C., Doyle, H. J., Hoey, T., and Levine, M. (1986). Cross-regulatory interactions among pair-rule genes in *Drosophila*. *Science* **233**, 953-959.
- Hartenstein, V., and Jan, X. N. (1992). Studying embryogenesis with P-lacZ enhancer-trap lines. *Wilhelm Roux's Arch. Dev. Biol.* **201**, 192-220.
- Hashimoto, C., Hudson, K. L., and Anderson, K. V. (1988). The *Toll* gene of *Drosophila*, required for dorsal-ventral embryonic polarity, appears to encode a transmembrane protein. *Cell* **52**, 269-279.
- Haynie, J. L., and Bryant, P. J. (1976). Intercalary regeneration in imaginal wing discs of *Drosophila melanogaster*. *Nature* **259**, 659-662.
- Hecht, P. M., and Anderson, K. V. (1992). Extracellular proteases and embryonic pattern formation. *Trends Cell Biol.* **2**, 197-202.
- Hecht, P. M., and Anderson, K. V. (1993). Genetic characterization of *tube* and *pelle*, genes required for signaling between *toll* and *dorsal* in the specification of the dorsal-ventral pattern of the *Drosophila* embryo. *Genetics* **135**, 405-417.

- Hecht, J. T., Hogue, D., Strong, L. C., Hansen, M. F., and Blanton, S. H. (1995). Hereditary multiple exostosis and chondrosarcoma: linkage to chromosome II and 8. *Am. J. Hum. Genet.* **56**, 1125-1131.
- Held, L. I. J. (1993). Segment polarity mutations cause stripes of defects along a leg segment in *Drosophila*. *Dev. Biol.* **157**, 240-250.
- Held, L. I. J. (1995). Axes, boundaries and coordinates: the ABCs of fly leg development. *BioEssays*, **17**, 721-732.
- Held, L. I. J., Huep, M. A., Sappington, J. M., and Peters, S. D. (1994). Interactions of *decapentaplegic*, *wingless* and *Distal-less* in the *Drosophila* leg. *Wilhelm Roux's Arch. Dev. Biol.* **203**, 310-319.
- Held, L. I. J., and Hempf, M. A. (1996) Genetic mosaic analysis of *decapentaplegic* and *wingless* gene function in the *Drosophila* leg. *Dev. Genes Evol.* **206**, 180-194.
- Heldin, C-H. (1995). Dimerization of cell-surface receptors in signal transduction. *Cell* **80**, 213-223.
- Heldin, C. H., Miyazono, K., and ten Dijke, P. (1997). TGF- β signaling from cell membrane to nucleus through SMAD proteins. *Nature* **390**, 465-71.
- Hemple, J., Perozich, J., Romovacek, H., Kuo, I., and Feingold, D. S. (1994). UDP-glucose dehydrogenase from bovine liver: primary structure and relationship to other dehydrogenases. *Protein Science.* **3**, 1074-1080.
- Hemmati-Brivanlou, A., Kelly, O. G., and Melton, D. A. (1994). Follistatin, an antagonist of activin, is expressed in the Spemann organizer and displays direct neuralizing activity. *Cell* **77**, 283-295.
- Hepker, J., Wang, O. T., Motzny, C. K., Holmgren, R., and Orenic, T. V. (1997). *Drosophila cubitus interruptus* forms a negative feedback loop with *patched* and regulates expression of *hedgehog* target genes. *Development* **124**, 549-558.
- Herman, T., and Horvitz, H. R. (1999). Three proteins involved in *Caenorhabditis elegans* vulval invagination are similar to components of a glycoylation pathway. *Proc. Natl. Acad. Sci. USA* **96**, 974-979.
- Herman, T., Hartweig, E., and Horvitz, H. R. (1999). *sqv* mutants of *Caenorhabditis elegans* are defective in vulval epithelial invagination. *Proc. Natl. Acad. Sci. USA* **96**, 968-973.
- Herr, A. B., Ornitz, D. M., Sasisekharan, R., Venkataraman, G., and Waksman, G. (1997). Heparin-induced self-association of fibroblast growth factor-2. *J. Biol. Chem.* **272**, 16382-16389.
- Heslip, T. R., Theisen, H., Walker, H., and Marsh, J. L. (1997). *Shaggy* and *disheveled* exert opposite effects on *wingless* and *decapentaplegic* expression and on positional identity in imaginal discs. *Development* **124**, 1069-1078.

- Hicklin, J., and Wolpert, L. (1973). Positional information and pattern regulation in hydra: the effect of gamma-radiation. *J. Embryol. Exp. Morph.* **30**, 741-752.
- Hiroko, H., Osami, H., and Koji, K. (1998). Biosynthesis of Heparan Sulfate and Heparin. How are multifunctional glycosaminoglycans built up?. *Trends in Glycoscience and Glycotechnology* **10**, 65-80.
- Hirschberg, C. B., and Snider, M. D. (1987). Topography of glycosylation in the rough endoplasmic reticulum and Golgi apparatus. *Annu. Rev. Biochem.* **56**, 63-87.
- Hirschberg, C. B., Robbins, P. W., and Abeijon, C. (1998). Transporters of nucleotide sugars, ATP and nucleotide sulfate in the endoplasmic reticulum and Golgi apparatus. *Annu. Rev. Biochem.* **67**, 49-69.
- Ho, G., Sasisekharan, R., Venkataraman, G., and Waksman, G. (1997). Role of heparan sulfate proteoglycans in the uptake and degradation of tissue factor pathway inhibitor-coagulation factor Xa complexes. *J. Biol. Chem.* **272**, 16838-16844.
- Hogan, B. L. M. (1996). Bone morphogenetic proteins: multifunctional regulators of vertebrate development. *Genes Dev.* **10**, 1580-1594.
- Holley, S. A., Jackson, P. D., Sasai, Y., Lu, B., DeRobertis, E. M., Hoffmann, F. M., and Ferguson, E. L. (1995). A conserved system for dorsal-ventral patterning in insects and vertebrates involving *sog* and *chordin*. *Nature* **376**, 249-253.
- Holley, S. A., Neul, J. L., Attisano, I., Wrana, J. L., Sasai, Y., O'Conner, M. B., DeRobertis, E. M., Hoffmann, F. M., and Ferguson, E. L. (1996). The *Xenopus* dorsalizing factor Noggin ventralizes *Drosophila* embryos by preventing DPP from activating its receptor. *Cell* **86**, 607-617.
- Hong, C. C., and Hashimoto, C. (1995). An unusual mosaic protein with a protease domain, encoded by the *nudel* gene, is involved in defining embryonic dorsoventral polarity in *Drosophila*. *Cell* **82**, 785-794.
- Hoodless, P. A., Haerry, T., Abdollah, S., Stapleton, M., O'Conner, M. B., Attisano, L., and Wrana, J. L. (1996). MADR1, a MAD-related protein that functions in BMP2 signaling pathways. *Cell* **85**, 489-500.
- Hooper, J. E., and Scott, M. P. (1989). The *Drosophila patched* gene encodes a putative membrane protein required for segmental patterning. *Cell* **59**, 751-765.
- Hooper, J. E., and Scott, M. P. (1992). The molecular genetic basis of positional information in insect segments. *Results Probl. Cell Differ.* **18**, 1-48.
- Hoppler, S., and Bienz, M. (1995). Two different thresholds of *wingless* signaling with distinct developmental consequences in the *Drosophila* midgut. *EMBO J.* **14**, 5016-5026.

- Hopwood, J. J. (1989). Enzymes that degrade heparin and heparan sulfate. In heparin: Chemical and biological clinical applications. (D.A. Lane and U. Lindahl, eds) Boca Raton: CRC Press, pp 1-10.
- Hornebeck, W., Lafuma, C., Robert, L., Moczar, M., and Moczar, E. (1994). Heparin and its derivatives modulate serine proteinases (SERPS) serine proteinase inhibitors (SERPINS) balance. Physiopathological relevance. *Pathol. Res. Pract.* **190**, 895-902.
- Hsu, J-C., and Perrimon, N. (1994). A temperature-sensitive MEK mutation demonstrates the conservation of the signaling pathways activated by receptor tyrosine kinases. *Genes Dev.* **8**, 2176-2187.
- Huang, J-D., Schwyster, D. H., Shirokaw, J. M., and Courey, A. J. (1993). The interplay between multiple enhancer and silencer elements defines the pattern of *decapentaplegic* expression. *Genes Dev.* **8**, 694-704.
- Hudson, J. B., Podos, S. D., Keith, K., Simpson, S. L., and Ferguson, E. L. (1998). The *Drosophila Medea* gene is required downstream of *dpp* and encodes a functional homolog of human Smad4. *Development* **125**, 1407-1420.
- Humphries, D. E., Wong, G. W., Friend, D. S., Gurish, M. F., Qui, W. T., Huang, C., Sharpe, A. H., and Stevens, R. L. (1999). Heparin is essential for the storage of specific granule proteases in mast cells. *Nature* **400**, 769-772
- Huynh, T. V., Young, R. A., and Davis, R. W. (1985). Constructing and screening cDNA libraries in lambda gt10 and lambda gt11. In "DNA cloning: A practical approach" (ed. D., M.m Glover) vol. 1, IRL Press, Oxford, pp. 49-60.
- Ingber, D. E., and Folkman, J. (1989). How does extracellular matrix control capillary morphogenesis? *Cell* **58**, 803-805.
- Ingber, D. E. (1993). The riddle of morphogenesis: a question of solution chemistry or molecular cell engineering. *Cell* **75**, 1249-1252.
- Ingham, P. W. (1988). The molecular genetics of embryonic pattern formation in *Drosophila*. *Nature* **335**, 25-30.
- Ingham, P. W., and Martinez-Arias, A. (1992). Boundaries and fields in early embryos. *Cell* **68**, 221-229.
- Ingham, P. W., and Fietz, M. J. (1995). Quantitative effects of *hedgehog* and *decapentaplegic* activity on patterning of the *Drosophila* wing. *Curr. Biol.* **5**, 432-440.

- Inoue, H., and Tabata, T. (1998). Interplay of signaling mediators *Decapentaplegic* (Dpp): molecular characterization of *Mothers against dpp*, *Medea*, and *Daughters against dpp*. *Mol. Biol. Cell* **9**, 2145-2156.
- Iozzo, R. V. (1998). Matrix proteoglycans: from molecular design to cellular function. *Annu. Rev. Biochem.* **67**, 609-652.
- Ip, Y. T., Kraut, R., Levine, M., and Rushlow, C. A. (1991) The *dorsal* morphogen is a sequence-specific DNA-binding protein that interacts with a long-range repression element in *Drosophila*. *Cell* **68**, 439-446.
- Ip, Y. T., Park, R. E., Kosman, D., Yazdabakhsh, K., and Levine, M. (1992). *Dorsal-twist* interactions initiate mesoderm differentiation in the *Drosophila* embryo. *Genes Dev.* **6**, 1518-1530.
- Irish, V. F., and Gelbart, W. M. (1987). The *decapentaplegic* gene is required for dorsal-ventral patterning of the *Drosophila* embryo. *Genes Dev.* **1**, 868-879.
- Irvine, K., and Wieschaus, E. (1994). *fringe*, a boundary specific signaling molecule, mediates interactions between dorsal and ventral cells during *Drosophila* wing development. *Cell* **79**, 955-606.
- Israel, D. I., Nove, J., Kerns, K. M., Moutsatsos, I. K., and Kaufman, R. J. (1992). Expression and characterization of bone morphogenetic protein-2 in Chinese hamster ovary cells. *Growth Factors* **7**, 139-150.
- Jackson, R. L., Busch, S. J., and Cardin, A. D. (1991). Glycosaminoglycans: molecular properties, protein interactions, and role in physiological processes. *Physiol. Rev.* **71**, 481-539.
- Jackson, M., Nakato, H., Sugiura, M., Jannuzi, A., Oakes, R., Kaluza, V., Golden, C., and Selleck, S. B. (1997). *Dally*, a *Drosophila* glypican, controls cellular responses to the TGF- β related morphogen, DPP. *Development* **114**, 4113-4120.
- Jacobs, J. R., Hiromi, I., Patel, N. H., and Goodman, C. S. (1989). Lineage, migration and morphogenesis in *Drosophila* CNS as revealed by a lineage marker. *Neuron* **2**, 1625-1631.
- Jacobson, A. G., and Sater, A. K. (1988). Features of embryonic induction. *Development* **104**, 341-359.
- James, A. A., and Bryant, P. J. (1981). Mutations causing pattern deficiencies and duplications in the imaginal wing disk of *Drosophila melanogaster*. *Dev. Biol.* **85**, 39-54.
- Janning, W. (1978). Gynandromorph fate maps in *Drosophila*. *Results Probl. Cell Differ.* **9**, 1-28.
- Jazwinska, A., Kirov, N., Wieschaus, E., Roth, S., and Rushlow, C. (1999). The *Drosophila* gene *brinker* reveals a novel mechanism of Dpp target gene regulation. *Cell* **96**, 563-573.
- Jiang, J., Cai, H., Zhou, Q., and Levine, M. (1990). Conversion of a *dorsal*-dependent silencer into an enhancer: evidence of dorsal corepressors. *EMBO J.* **12**, 320-329.

- Jiang, J., Kosman, D. Ip, Y. T., and Levine, M. (1991). The *dorsal* morphogen gradient regulates the mesoderm determinant *twist* in early *Drosophila* embryo. *Genes Dev.* **5**, 1881-1891.
- Jiang, J., Rushlow, C. A., Zhou, Q., and Levine, M. (1992). Individual dorsal morphogen binding sites mediate activation and repression in the *Drosophila* embryo. *EMBO J.* **11**, 3147-3154.
- Jiang, J., and Levine, M. (1993). Binding affinities and cooperative interaction with bHLH activators delimit threshold responses to the *dorsal* gradient morphogen. *Cell* **72**, 741-752.
- Jiang, J., and Struhl, G. (1995). *Protein Kinase A* and *hedgehog* signaling in *Drosophila* limb development. *Cell* **80**, 563-572.
- Jiang, J., and Struhl, G. (1996). Complementary and mutually exclusive activities of *decapentaplegic* and *wingless* organize axial pattern during *Drosophila* limb development. *Cell* **86**, 401-409.
- Jones, C. M., Dale, L., Hogan, B. L., Wright, C. V., and Smith, J. C. (1996). BMP-4 acts during gastrula stages to cause ventralization of *Xenopus* embryos. *Development* **122**, 1545-1554.
- Jones, C. M., and Smith, J. C. (1998). Establishment of a BMP-4 morphogen gradient by long-range inhibition. *Dev. Biol.* **194**, 12-27.
- Kainulainen, V., Wang, H., Schick, A., and Bernfield, M. (1998). Syndecans, heparan sulfate proteoglycans, maintain the proteolytic balance of acute wound fluids. *J. Biol. Chem.* **273**, 11563-11569.
- Kan, M., Wang, F., Xu, J., Crabb, J. W., Hou, J., and McKeehan, W. L. (1993). An essential heparin-binding domain in the fibroblast growth factor receptor kinase. *Science* **259**, 1918-1921.
- Karlsson, J. (1980). Distal regeneration in proximal fragments of the wing disc of *Drosophila*. *J. Embryol. Exp. Morph.* **59**, 315-323.
- Karlsson, J. (1981). The distribution of regenerative potential in the wing disc of *Drosophila*. *J. Embryol. Exp. Morph.* **61**, 303-316.
- Karn, J., Brenner, S., Barnett, L., and Cesareni, G. (1980). Novel bacteriophage lambda cloning vector. *Proc. Natl. Acad. Sci. USA* **77**, 5172-5176.
- Karpen, G. H., and Schubiger, G. (1981). Extensive regulatory capabilities of a *Drosophila* imaginal disc blastema. *Nature* **294**, 744-747.
- Karthikeyan, L., and Maurel, P. (1992). Cloning of a major heparan sulfate proteoglycan from brain and identification as the rat form of glypican. *Biochem. Biophys. Res. Commun.* **188**, 395-401.
- Kassis, J. A., Noll, E., Vansickle, E. P., Odenwald, W. F., and Perrimon, N. (1992). Altering the insertional specificity of a *Drosophila* transposable element. *Proc. Natl. Acad. Sci. USA* **89**, 1919-1923.

- Kato, M., Wang, H., Kainulainen, V., Fitzgerald, M. L., Ledbetter, S., Ornitz, D. M., and Bernfield, M. (1998). Physiological degradation converts the soluble syndecan-1 ectodomain from an inhibitor to a potent activator of FGF-2. *Nature. Med.* **4**, 691-697.
- Khalas, O., Yoon, J. W., Torres-Schumann, S., and Wharton, K. A. (1998). TGF β /BMP superfamily members, Gbb-60A and Dpp, cooperate to provide pattern formation and establish cell identity in the *Drosophila* wing. *Development* **125**, 2723-2734.
- Khare, N., and Baumgartner, S. (2000). *Dally-like* protein, a new *Drosophila* glypican with expression overlapping with wingless. *Mech. Dev.* **99**, 199-202.
- Kidd, S. (1992). Characterization of the *Drosophila cactus* locus and analysis of interactions between *cactus* and *dorsal* proteins. *Cell* **71**, 623-635.
- Kim, J., Irvine, K. D., and Carroll, S. B. (1995). Cell recognition, signal induction and gene activation at the dorsal/ventral boundary of the developing *Drosophila* wing. *Cell* **82**, 795-802
- Kingsley, D. M. (1994). The TGF- β superfamily: new members, new receptors and new genetic tests of function in different organisms. *Genes Dev.* **8**, 133-146.
- Kiss, I., Bencze, G., Fekete, E., Fodor, A., Gausz, J., Maray, P., Szabad, J., and Szydonya, J. (1976). Isolation and characterization of X-linked lethal mutants affecting differentiation of the imaginal discs in *Drosophila melanogaster*. *Theor. Appl. Genet.* **48**, 217-226.
- Kirov, N., Zhelmin, L., Shah, J., and Rushlow, C. (1993). Conversion of a silencer into an enhancer: evidence for co-repressor in *dorsal-mediated* repression in *Drosophila*. *EMBO J.* **12.**, 3193-3199.
- Kirov, N., Childs, S., O'Conner, M., and Rushlow, C. (1994). The *Drosophila dorsal* morphogen represses the *tolloid* gene by interacting with a silencer element. *Mol. Cell. Biol.* **14**, 713-722.
- Kitagawa, H., Shimakawa, H., and Sugahara, K. (1999). The tumor suppressor EXT-like gene EXTL-2 encodes an alpha 1,4-N-acetylhexosamonyltransferase that transfers N-acetylgalactosamine and N-acetylglucosamine to the common glycosaminoglycan-protein linkage region. The key enzyme for the chain initiation of heparan sulfate. *J. Biol. Chem.* **274**, 13933-13937.
- Kjellen, L., and Lindahl, V. C. (1991). Proteoglycans: structures and interactions. *Annu. Rev. Biochem.* **60**, 443-475.
- Klambt, C., Glazer, L., and Shilo, B. Z. (1992). *breathless*, a *Drosophila* FGF receptor homolog, is essential for migration of tracheal and specific midline glial cells. *Genes Dev.* **10**, 2912-2921.
- Klagsburn, M., and Baird, A. (1991). A dual receptor system is required for basic fibroblast growth factor activity. *Cell* **67**, 229-231.
- Klein, G., Conzelmann, S., Beck, S., Timpl, R., and Muller, C.A. (1995). Perlecan in human bone marrow: agrowth-factor-presenting, but anti-adhesive, extracellular matrix component for hematopoietic cells. *Matrix Biology* **14**, 457-465.

- Klemm, J. D., Schreiber, S. L., and Crabtree, G. R. (1998). Dimerization as a regulatory mechanism in signal transduction. *Annu. Rev. Immunol.* **16**, 569-592.
- Koeing, B. B., Cook, J. S., Wolsing, D. H., Ting, J., Tiesman, J. P., Correa, P. E., Olson, C. A., Pecquet, A. L., Ventura, F., Grant, R. A., Chen, G. X., Wrana, J. L., Massague, J., and Rosenbaum, J.S. (1994). Characterization and cloning of a receptor for BMP-2 and BMP-4 from NIH 3T3 cells. *Mol. Cell Biol.* **14**, 5961-5974.
- Kojima, T., Leone, C. W., Marchildon, G. A., Marcum, T. A., and Rosenberg, R. D. (1992). Isolation and characterization of heparan sulfate proteoglycans produced by cloned rat microvascular endothelial cells. *J. Biol. Chem.* **267**, 4859-4869.
- Kojima, T., Michiue, T., Orihar, A. M., and Saigo, K. (1994). Induction of a mirror-image duplication of anterior wing structures by localized *hedghog* expression in the anterior compartment of *Drosophila melanogaster* wing imaginal discs. *Gene* **148**, 211-217.
- Konsolaki, M., and Schupbach, T. (1998). *windbeutel*, a gene required for dorsoventral patterning in *Drosophila*, encodes a protein that has homologies to vertebrate proteins of the endoplasmic reticulum. *Genes Dev.* **12**, 120-31.
- Kornberg, T. (1981). *Engrailed*: a gene controlling compartment and segment formation in *Drosophila*. *Proc. Natl. Acad. Sci. USA* **78**, 1095-1099.
- Kornberg, T., Siden, I., O'Farrell, P., and Simon, M. (1985). The *engrailed* locus of *Drosophila*: In situ localization of transcripts reveals compartment specific expression. *Cell* **40**, 45-53.
- Kornfeld, R., and Kornfeld, S. (1980). The biochemistry of Glycoproteins and Proteoglycans. Plenum Press, New York
- Kosman, D., Ip, Y.T., Levine, M., and Arora, K. (1991). Establishment of the mesoderm-neuroectoderm boundary in the *Drosophila* embryo. *Science* **254**, 118-122.
- Kretzschmar, M., and Massague, J. (1998). SMADs: mediators and regulators of TGF- β signaling. *Curr. Opin. Genet. Dev.* **8**, 103-111.
- Kuroiwa, A., Hafen, E., and Gehring, W. (1984). Cloning and transcriptional analysis of the segmentation gene *fushi tarazu* of *Drosophila*. *Cell* **37**, 825-831.
- Lander, A. D. (1999). Seeking the function of cell-surface heparan sulfate proteoglycans. In Cell surface proteoglycans in signaling and development. (Lander, A. D., Nakato, H., Selleck, S. B., Turnbull, J. E., and Cath, C. eds.) Strasbourg: Human Frontier Science Program, pp. 73-87.
- Lander, A. D., and Selleck, S. B. (2000). The elusive functions of proteoglycans: In vivo veritas. *J. Cell Biol.* **148**, 227-232.
- Lawrence, P. A. (1966). Gradients in the insect segment: the orientation of hairs in the milkweed bug *Oncopeltus fasciatus*. *J. Exp. Biol.* **44**, 607-620.
- Lawrence, P. A. (1972). The development of spatial patterns in the integument of insects. In

- “Developmental Systems: Insects”. (Waddington, C. H., Ed.). Academic Press, New York..
- Lawrence, P. A., and Morata, G. (1976). Compartments in the wing of *Drosophila*: a study of the *engrailed* gene. *Dev. Biol.* **50**, 321-337.
- Lawrence, P. A., and Morata, G. (1977). The early development of mesothoracic compartments in *Drosophila*. An analysis of cell lineage and fate mapping and an assessment of methods. *Dev. Biol.* **56**, 40-51.
- Lawrence, P. A., and Morata, G. (1994). Homeobox genes: their function in *Drosophila* segmentation and pattern formation. *Cell* **78**, 181-189.
- Lawrence, P. A., and Struhl, G. (1996). Morphogens, compartments and pattern: lessons from *Drosophila*. *Cell* **85**, 951-961.
- Lawrence, P. A., and Sanson, B. (1996). Compartments, *wingless* and *engrailed*: patterning the ventral epidermis of *Drosophila* embryos. *Development* **122**, 4095-103.
- LeBaron, R. G., Esko, J. D., Woods, A., Johansson, S and Hook, M. (1988). Adhesion of glycosamino glycan-deficient chinese hamster ovary cell mutants to fibronectin substrata. *J. Cell. Biol.* **106**, 945-952.
- Lecuit, T., Brook, W. J., Ng, M., Calleja, M., Sun, H., and Cohen, S. M. (1996). Two distinct mechanisms for long-range patterning by *decapentaplegic* in the *Drosophila* wing. *Nature* **381**, 387-393.
- Lecuit, T., and Cohen, S. M. (1997). Proximal-distal axis formation in the *Drosophila* leg. *Nature* **388**, 139-145.
- Lecuit, T., and Cohen, S. M. (1998). *Dpp* receptor levels contribute to shaping the DPP morphogen gradient in *Drosophila* wing imaginal disc. *Development* **125**, 4901-4907.
- Lee, J. J., von Kessler, D. P., Parker, S., and Beachy, P. A. (1992). Secretion and localized transcription suggest a role in positional signaling for products of the segmentation gene *hedgehog*. *Cell* **71**, 33-50.
- Lee, J. J., Ekker, S. C., von Kessler, D. P., Porter, J. A., Sun, B. I., and Beachy, P. A. (1994). Autoproteolysis in *hedgehog* protein biogenesis. *Science* **266**, 1528-1537.
- Lehninger, A. L., Nelson, D. L., and Cox, M. M. (1993). In “Principles of Biochemistry 2nd Edition”. (Horton, H. R., Moran, L. A., Ochs, R. S., Rawn, J. D. and Scrimgeour, K. G. Eds.). Prentice Hall, New Jersey, pp. 438-439.
- LeMosely, E. K., Kemmerl, D., and Hashimoto, C. (1998). Role of Nudel protease activation in triggering dorsal-ventral polarization of the *Drosophila* embryo. *Development* **125**, 1261-1267.

- Lepage, T., Cohen, S. M., Diaz-Benjumea, F. J., and Parkhurst, S. M. (1995). Signal transduction by cAMP-dependent *protein kinase A* in *Drosophila* limb patterning. *Nature* **373**, 711-715.
- Leptin, M. (1991). *twist* and *snail* as positive and negative regulators during *Drosophila* mesoderm development. *Genes Dev.* **5**, 1568-1576.
- Letsou, A., Alexander, S., and Wasserman, S.A. (1991). Genetic and molecular characterization of tube, a *Drosophila* gene maternally required for embryonic dorsoventral polarity. *Proc. Natl. Acad. Sci. USA* **88**, 810-814.
- Letsou, A., Arora, K., Wrana, J. L., Simin, K., Twombly, V., Jamal, J., Staehling-Hampton, K., Hoffman, F. M., Gelbart, W. M., Massague, J., and O'Connor, M. B. (1995). *Drosophila dpp* signaling is mediated by the *punt* gene product: a dual ligand-binding type II receptor of the TGF-B receptor family. *Cell* **80**, 899-908.
- Lewis, E. B. (1978). A gene complex controlling segmentation in *Drosophila*. *Nature* **276**, 565-570.
- Li, W., Ohlmeyer, J. T., Lane, M. E., and Kalderon, D. (1995). Function of *protein kinase A* in *hedgehog* signal transduction and *Drosophila* imaginal disc development. *Cell* **80**, 553-562.
- Lin, C. Q., and Bissell, M. J. (1993). Multi-faceted regulation of cell differentiation by extracellular matrix. *FASEB J.* **7**, 737-743.
- Lin, X., and Perrimon, N. (1999). *Dally* cooperates with *Drosophila frizzled-2* to transduce *wingless* signaling. *Nature* **400**, 281-284.
- Lin, X., Buff, E. M., Perrimon, N., and Michelson, A. M. (1999). Heparan sulfate proteoglycans are essential for FGF receptor signaling during *Drosophila* embryonic development. *Development* **126**, 3715-3723.
- Lind, T., Turfaro, F., McCormick, C., Lindahl, K., and Lidholt, K. (1998). The putative tumour suppressors EXT1 and EXT2 are glycosyltransferases required for the biosynthesis of heparan sulfate. *J. Biol. Chem.* **273**, 26265-26268.
- Lindahl, B., and Lindahl, U. (1997). Amyloid-specific heparan sulfate from human liver and spleen. *J. Biol. Chem.* **272**, 26091-26094.
- Lindahl, U., Kusche-Gullberg, M., and Kjellen, L. (1998). Regulated diversity of heparan sulfate. *J. Biol. Chem.* **271**, 17804-17810.
- Lindsley, D. L., and Zimm, G. G. (1992). The genome of *Drosophila melanogaster*. Academic Press, San Diego USA.
- Litwack, E. D., Stipp, C. S., Kumbasan, A., and Lander, A. D. C. (1994). Neuronal expression of glypican, a cell-surface glycosylphosphatidylinositol-anchored heparan sulfate proteoglycan, in the adult rat nervous system. *J. Neurosci.* **14**, 3713-3724.
- Locke, M. (1959). The cuticular pattern in an insect, *Rhodnius prolixus*. *J. Exp. Biol.* **3**, 459-477.

- Lopez-Casillas, F., and Cheifetz, S., Doody, J. Anders, J. L., Lane, W. S., and Massague, J. (1991). Structure and expression of the membrane proteoglycan betaglycan, a component of the TGF- β receptor system. *Cell* **67**, 785-795.
- Lopez-Casillas, F., Wrana, J. L., and Massague, J. (1993). Betaglycan presents ligand to the TGF- β signaling receptor. *Cell* **73**, 1435-1444.
- Lopez-Casillas, F., Payne, H. M., Andres, J. L., and Massague, J. (1994). Betaglycan can act as a dual modulator of TGF β access to signaling receptors: mapping of ligand binding and GAG attachment sites. *J. Cell. Biol.* **124**, 557-568.
- Luyten, N. S., Cunningham, S., Ma, N., Muthukumaran, R. G., Hammonds, W. B., Nevins, W., Woods, I., and Reddi, A. H. (1989). Purification and partial amino acid sequence of osteogenin, a protein initiating bone differentiation. *J. Biol. Chem.* **264**, 13377-13380.
- Lyons, R. M., Keski-Oja, J., and Moses, H. L. (1988). Proteolytic activation of latent transforming growth factors- β from fibroblast-conditioned medium. *J. Cell Biol.* **106**, 1659-1665.
- Lyon, M., Deakin, J. A., Mizuno, K., Nakamura, T., and Gallagher, J. T. (1994). Interaction of hepatocyte growth factor with heparan sulfate, elucidation of the major heparan sulfate structural determinants. *J. Biol. Chem.* **269**, 11216-11223.
- Ma, S., Chen, G., and Reddi, A. H. (1990). Collaboration between collagenase matrix and osteogenin is required for bone induction. *Ann. NY Acad. Sci.* **580**, 524-525.
- Maccarana, M., Casu, B., and Lindahl, U. (1993). Minimal sequence in heparin/heparan sulfate required for binding of basic fibroblast growth factor. *J. Biol. Chem.* **268**, 23898-23905.
- Macdonald, P. M., and Struhl, G. (1988). Cis-acting sequences responsible for anterior localization of *bicoid* mRNA in *Drosophila* embryos. *Nature* **336**, 595-598.
- MacWilliams, H. K., and Kafatos, F. C. (1968). Hydra viridis: inhibition by the basal disk. *Science* **159**, 1246-1247.
- Madhavan, M. M., and Schneiderman, A. A. (1977). Histological analysis of the dynamics of growth of imaginal discs and histoblast nests during the larval development of *Drosophila melanogaster*. *Wilhelm Roux's Arch. Dev. Biol.* **183**, 269-305.
- Mahaffey, J. W., and Kaufman, T. C. (1988). The homeotic genes of the *Antennapedia* complex and *bithorax* complex of *Drosophila*. In "Developmental genetics of higher organisms: A primer in developmental biology". (G. Malakinski Ed.). Macmillan Press, New York.
- Mahowald, A. P., and Kambysellis, M. P. (1980). Oogenesis, In *Genetics and Biology of Drosophila*, ed. M Ashburner, TRF Wright, Academic Press, New York, pp. 141-224.
- Mali, M., Elenius, K., Miettinen, H. M., and Jalkanen, M. (1993). Inhibition of basic FGF-induced growth promotion by over-expression of syndecan-1. *J. Biol. Chem.* **268**, 24215-24222.

- Mali, M., Andtfolk, H., Miettinen, H. M., and Jalkanen, M. (1994). Suppression of tumor cell growth by syndecan-1 ectodomain. *J. Biol. Chem.* **269**, 27795-27798
- Mandon, E. C., Milla, M. E., Kempner, E., and Hirschberg, C. B. (1994). Purification of the Golgi adenosine 3'-phosphate 5'-phosphosulfate transporter, a homodimer within the membrane. *Proc. Nat. Acad. Sci. USA* **91**, 10707-10711.
- Manoukian, A. S., and Krause, H. M. (1993). Control of segmental asymmetry in *Drosophila* embryos. *Development* **118**, 785-796.
- Manseau, L. J., and Schupbach, T. (1989). *cappuccino* and *spire*: two unique maternal-effect loci required for both the anterioposterior and dorsoventral patterns of the *Drosophila* embryo. *Genes Dev.* **3**, 1437-1452.
- Marigo, V., Davey, R. A., Zuo, Y., Cunningham, J. M., and Tabin, C. J. (1996). Biochemical evidence that *patched* is the *hedgehog* receptor. *Nature* **384**, 176-179.
- Marouf, A., Quayle, A., and Sloan, P. (1990). In vitro and in vivo studies with collagen/hydroxyapatite implants. *Int. J. Oral Maxillofac. Implants* **5**, 148-154.
- Marques, M., Musacchio, M. J., Shimell, K., Wunnenberg-Stapleton, K., Cho, W., and O'Connor, M. B. (1997). Production of a DPP activity gradient in the early *Drosophila* embryo through the opposing actions of the SOG and TLD proteins. *Cell* **91**, 417-426.
- Martinez-Arias, A. (1989). A cellular basis for pattern formation in the insect epidermis. *Trends Genet.* **5**, 262-267.
- Martinez-Arias, A., Baker, N. E., and Ingham, P. W. (1988). Role of segment polarity genes in the definition and maintenance of cell states in the *Drosophila* embryo. *Development* **103**, 157-170.
- Martinez Arias, A. (1993). Development and patterning of the larval epidermis of *Drosophila*. In "The Development of *Drosophila melanogaster*." (ed. M. Bate and A. Martinez Arias), Cold Spring Harbor Laboratory Press, New York., pp. 517-608.
- Mason, E. D., and Konrad, K. D. L. (1994). Dorsal midline fate in *Drosophila* embryos requires *twisted gastrulation*, a gene encoding a secreted protein related to human connective tissue growth factor. *Genes Dev.* **8**, 1489-1501.
- Massague, J. (1998). TGF β signal transduction. *Annu. Rev. Biochem.* **67**, 737-791.
- Massague, J., Hata, A., and Liu, F. (1997). TGF- β signaling through the Smad pathway. *Trends Cell Biol.* **7**, 187-191.
- Massucci, J. D., Millenberger, R. J., and Hoffman, F. M. (1990). Pattern specific expression of the *Drosophila decapentaplegic* gene in imaginal discs is regulated by 3' cis regulatory elements. *Genes Dev.* **4**, 2011-2022.

- Matrisan, L. M. (1990). Metalloproteinase and their inhibitors in matrix remodeling. *Trends Biochem.* **12**; 10-15.
- McCormick, C., Leduc, Y., Martindale, D., Mattison, K., Esford, L. E., Dyer, A. P., and Tufaro, F., (1998). The putative tumour suppressor EXT1 alters the expression of cell-surface heparan sulfate. *Nature Genet.* **19**, 158-161.
- McDonald, N. Q., and Hendrickson, W. (1993). A structural superfamily of growth factors containing a cystine knot motif. *Cell* **73**, 421-424.
- McDowell, A., Zorn, A. M., Crease, D. J., and Gurdon, J. B. (1997). Activin has direct long-range signaling activity and can form a concentration gradient by diffusion. *Curr. Biol.* **7**, 671-681.
- McCormick, C., Leduc, Y., Martindale, A., Mattison, K., and Esford, L. E. (1998). The putative tumour suppressor EXT1 alters the expression of cell-surface heparan sulfate. *Nature Genet.* **19**, 158-161.
- McPherson, J. M. (1992). The utility of collagenase-based vehicles in delivery of growth factors for hard and soft tissue wound repair. *Clinical Materials* **9**, 225-234.
- Meinhardt, H. (1983a). Cell determination boundaries as organizing regions for secondary embryonic fields. *Dev. Biol.* **96**, 375-385.
- Meinhardt, H. (1983b). A bootstrap model for the proximodistal pattern formation in vertebrate limbs. *J. Embryol. Exp. Morph.* **76**, 139-146.
- Meinhardt, H. (1984). Models for positional signaling, the threefold subdivision of segments and the pigmentation pattern of molluscs. *J. Embryol. Exp. Morph.* **83** (Suppl.), 289-311.
- Meinhardt, H. (1986). Hierarchical inductions of cell states: A model of segmentation in *Drosophila*. *J. Cell. Sci.* **4** (Suppl.), 357-381.
- Meinhardt, H. (1989). Models for positional signaling with application to the dorsoventral patterning of insects and segregation into different cell types. *Development* **107** (Suppl.), 169-180.
- Meinhardt, H., and Gierer, A. (1980). Generation and regeneration of sequence of structures during morphogenesis. *J. Theor. Biol.* **85**, 429-450.
- Method, N., and Basler, K. (1999). *Hedgehog* controls limb development by regulating the activities of distinct transcriptional activator and repressor forms of *cubitus interruptus*. *Cell* **96**, 819-831.
- Minami, M., Shimizu, S., Nose, T., Shimohigashi, Y., and Nakamura, T. (1999). *brinker* is a target of Dpp in *Drosophila* that negatively regulates Dpp-dependent genes. *Nature* **398**, 242-246.
- Misra, S., Hecht, P., Maeda, R., and Anderson, K. V. (1998). Positive and negative regulation of *easter*, a member of the serine protease family that controls dorsal-ventral patterning in the *Drosophila* embryo. *Development* **125**, 1261-1267.

- Mitchelson, A., Simonelig, M. M., William, C., and O'Hare, K. (1993). Homology with *Saccharomyces cerevisiae* RNA14 suggests that phenotypic suppression in *Drosophila melanogaster* by *suppressor of forked* occurs at the level of RNA stability. *Genes Dev.* **7**, 241-249.
- Miyazaki, Y., Shinomura, S., Higashiyama, S., Kanayama, Y., Higashimoto, S., Tsutsui, S., Zushi, N., Taniguchi, N., and Matsuzawa, Y. (1996). Heparin-binding EGF-like growth factor is an autocrine growth factor for rat gastric epithelial cells. *Biochem. Biophys. Res. Commun.* **223**, 36-41.
- Miyazawa, K., Shimomura, T., and Kitamura, N. (1996). Activation of hepatocyte growth factor in the injured tissues is mediated by hepatocyte growth factor activator. *J. Biol. Chem.* **271**, 3615-3618.
- Mizuno, K., Inoue, H., Hagiya, M., Shimizu, S., Nose, T., Shimohigashi, Y., and Nakamura, T. (1994). Hairpin loop and second kringle domain are essential sites for heparin binding and biological activity of hepatocyte growth factor. *J. Biol. Chem.* **269**, 1131-1136.
- Moerman, D. G., Hutter, H., Mullem, G. P., and Schnabel, R. (1996). Cell autonomous expression of perlecan and plasticity of cell shape in embryonic muscle of *Caenorhabditis elegans*. *Dev. Biol.* **173**, 228-242.
- Mohler, J., and Vani, K. (1992). Molecular organization and embryonic expression of the *hedgehog* gene involved in cell-cell communication in segmental patterning of *Drosophila*. *Development* **115**, 957-971.
- Moore, D. S., and McCabe, G. P. (1993). Inference for count data Chapter 8. In: Introduction to the practice of Statistics, 2nd Edition. W.H. Freeman and Company, New York, pp. 574-623.
- Morata, G., and Lawrence, P. A. (1975). Control of compartment development by the *engrailed* gene in *Drosophila*. *Nature* **255**, 614-617.
- Morata, G., and Garcia-Bellido, A. (1976). Developmental analysis of some mutants of the *bithorax* system of *Drosophila*. *Wilhelm Roux's Arch. Dev. Biol.* **179**, 125-143.
- Morisato, D., and Anderson, K. A. (1994). The *spatzle* gene encodes a component of the extracellular signaling pathway establishing the dorsal-ventral pattern of the *Drosophila* embryo. *Cell* **76**, 677-688.
- Mullen, G. P., Rogalski, T. M., Bush, J. A., Gorji, P. R., and Moerman, D. G. (1999). Complex patterns of alternative splicing mediate the spatial and temporal distribution of perlecan/UNC-52 in *Caenorhabditis elegans*. *Mol. Biol. Cell* **10**, 3205-3221.
- Mullins, M. C. (1994). Holy *Tolloido*: *Tolloid* cleaves SOG/Chordin to free DPP/BMP'S. *Trends Genet.* **8**, 23-33.

- Nace, J. D., and Tassava, R. A. (1995). Examination of fibronectin distribution and its sources in the regenerating newt limb by immunocytochemistry and in situ hybridization. *Dev. Dyn.* **202**, 153-164.
- Nakajima, T., Irimura, D., Di Ferrante, N., and Nicolson, G. L. (1983). Heparan sulfate degradation: relation to tumor invasive and metastatic properties of mouse B16 melanoma sublines. *Science* **220**, 611-613.
- Nakato, H., Futch, T. A., and Selleck, S. B. (1995). The *division abnormally delayed (dally)* gene: a putative integral membrane proteoglycan required for cell division patterning during postembryonic development of the nervous system in *Drosophila*. *Development* **121**, 3687-3702.
- Nash, D., and Bell, J. B. (1968). Larval age and pattern of DNA synthesis in polytene chromosome. *Can. J. Genet. Cytol.* **15**, 237-254.
- Neri, G., Gurrieri, F., Zanni, G., and Lin, A. (1998). Clinical and molecular aspects of the Simpson-Gobabi-Behmel syndrome. *Am. J. Med. Genet.* **79**, 279-283.
- Nellen, D., Affolter, M., and Basler, K. (1994a). The *Drosophila saxophone* gene: a serine-threonine kinase receptor of the TGF- β superfamily. *Science* **263**, 1756-1759.
- Nellen, D., Affolter, M., and Basler, K. (1994b). Receptor serine/threonine kinases implicated in the control of *Drosophila* body pattern by *decapentaplegic*. *Cell* **78**, 225-237.
- Nellen, D., Burke, R., Struhl, G., and Basler, K. (1996). Direct and long-range action of a DPP morphogen gradient. *Cell* **85**, 357-368.
- Neul, J. L., and Ferguson, E. L. (1998). Spatially restricted activation of the SAX receptor by SCW modulates DPP/TKV signaling in *Drosophila* dorsal-ventral patterning. *Cell* **95**, 483-494.
- Neuman-Silberberg, F. S., and Schupbach, T. (1994). Dorsventral axis formation in *Drosophila* depends on the correct dosage of the gene *gurken*. *Development* **120**, 2457-2463.
- Neumann, C. J., and Cohen, S. M. (1997a). Long-range action of *Wingless* organizes the dorsal-ventral axis of the *Drosophila* wing. *Development* **124**, 871-880.
- Neumann, C. J., and Cohen, S. M. (1997b). Morphogens and pattern formation. *BioEssays* **19**, 721-729.
- Newfeld, S., Chartoff, E., Graff, J., Melton, D., and Gelbart, W. (1996). *Mothers against dpp* encodes a conserved cytoplasmic protein required in Dpp/TGF- β responsive cells. *Development* **122**, 2099-2108.
- Newfeld, S. J., Mehra, A., Singer, M. A., Wrana, J. L., Attisano, L., and Gelbart, W. M. (1997). *Mothers against dpp* participates in a Dpp/TGF- β responsive serine-threonine kinase signal transduction cascade. *Development* **124**, 3167-3176.
- Nguyen, M., Park, S., Marques, G., and Arora, K. (1998). Interpretation of a BMP activity gradient in *Drosophila* embryos depends on synergistic signaling by two type I receptors, SAX and TKV.

Cell **95**, 495-506.

- Nothiger, R., and Schubiger, G. (1966). Developmental behavior of fragments of symmetrical and asymmetrical imaginal discs of *Drosophila melanogaster* (Diptera). *J. Embryol. Exp. Morph.* **16**, 255-268.
- Nugent, M. A., and Edelman, E. R. (1992). Kinetics of basic fibroblast growth factor binding to its receptor and heparan sulfate proteoglycan: a mechanism for co-operativity. *Biochemistry* **31**, 8876-8883.
- Nurcombe, V., Ford, M. D., Wildschut, J. A., and Bartlett, P. F. (1993). Developmental regulation of neural response to FGF-1 and FGF-2 by heparan sulfate proteoglycan. *Science* **260**, 103-106.
- Nusse, R., and Varmus, H. E. (1992). Wnt genes. *Cell* **69**, 1073-1087.
- Nusslein-Volhard, C., and Wieschaus, E. (1980). Mutations affecting segment number and polarity in *Drosophila*. *Nature* **287**, 795-801.
- Nusslein-Volhard, C., Frohnhof, H. G., and Lehmann, R. (1987). Determination of anterior-posterior polarity in *Drosophila*. *Science* **238**, 1675-1681.
- O'Connor, M. B., Haerry, T. E., Khalsa, O., and Wharton, K. A. (1998). Synergistic signaling by two BMP ligands through the SAX and TKV receptors controls wing growth and patterning in *Drosophila*. *Development* **125**, 3977-3987.
- O'Connor, M., and Haerry, T. E. (1999). Cell Surface Proteoglycans in Signaling and Development, vol VI (Lander, A., Nakato, H., Selleck, S.B., Turnbull, J.E., and Coath, C. eds) Human Frontier Science Program, pp.169-176. .
- Ohlmeyer, J. T., and Kalderon, D. (1998). *Hedgehog* stimulates maturation of *Cubitus interruptus* into a labile transcriptional activator. *Nature* **396**, 749-753.
- O'Kane, C., and Gehring, W. J. (1987). Detection in situ of genomic regulatory elements in *Drosophila*. *Proc. Natl. Acad. Sci. USA*, **84**, 9123-9127.
- Olwin, B. B., and Rapraeger, A. (1992). Repression of myogenic differentiation by FGF, bFGF and K-FGF is dependent on cellular heparan sulfate. *J. Cell. Biol.* **118**, 631-639.
- Ornitz, D. M. (2000). FGFs, heparan sulfate and FGFRs: complex interactions essential for development. *BioEssays* **22**, 108-112.
- Ornitz, D. M., Herr, A. B., Nilsson, M., Westman, J., Svahn, C., and Waksman, G. (1995). FGF binding and FGF receptor activation by synthetic heparan-derived di- and trisaccharides. *Science* **268**, 432-436.
- Ornitz, D. M., and Leder, P. (1992). Ligand specificity and heparin dependence of fibroblast growth factor receptors 1 and 3. *J. Biol. Chem.* **267**, 16305-16311.

- Ornitz, D. M., Yayon, A., Flanagan, J. G., Svahn, C. M., Levi, E., and Leder, P. (1992). Heparin is required for cell-free binding of basic fibroblast growth factor to a soluble receptor and for mitogenesis in whole cells. *Mol. Cell Biol.* **12**, 240-247.
- Osborne, T. E., and Rosenfeld, J. M. (1998). Related membrane domains in proteins of sterol sensing and cell signaling provide a glimpse to treasures still buried within the dynamic realm of intercellular metabolic regulation. *Curr. Opin. Lipidol.* **9**, 137-140.
- Ototani, N., Kikuchi, M., and Yosizawa, Z. (1981). Purification of heparinase and heparitinase by affinity chromatography on glycosaminoglycan-bound AH-Sepharose 4B. *Carbohydr. Res.* **88**, 291-303.
- Ototani, N., and Yosizawa, Z. (1981). Anticoagulant activity of heparin octasaccharide. *J. Biochem. (Tokyo)* **90**, 1553-1556.
- Ozkaynak, D., Rueger, D. C., Drier, E. A., Corbett, C., Ridge, R. J., Sampath, T. K., and Opperman, H. (1990). OP-1 cDNA encodes an osteogenic protein in the TGF- β family. *EMBO J.* **9**, 2085-2093.
- Padgett, R. W., St. Johnston, R. D., and Gelbart, W. M. (1987). A transcript from a *Drosophila* pattern gene predicts a protein homologous to the transforming growth factor- β family. *Nature* **325**, 81-84.
- Padgett, R. W., Wozney, J. M., and Gelbart, W. M. (1993). Human BMP sequences can confer normal dorsal-ventral patterning in the *Drosophila* embryo. *Proc. Natl. Acad. Sci. USA* **90**, 2905-2909.
- Pan, D., Huang, J.-D., and Courey, A. J. (1991). Functional analysis of the *Drosophila twist* promoter reveals a dorsal-binding ventral activator region. *Genes Dev.* **5**, 1892-1901.
- Pan, D., and Courey, A. J. (1992). The same *dorsal* binding sites mediate both activation and repression in a context-dependent manner. *EMBO J.* **11**, 1837-1842.
- Pan, D., and Rubin, G. M. (1995). cAMP-dependent protein kinase and *hedgehog* act antagonistically in regulating *decapentaplegic* transcription in *Drosophila* imaginal discs. *Cell* **80**, 543-552.
- Panganiban, G., and Nagy, L. (1994). The role of the *Distal-less* gene in the development and evolution of insect limbs. *Curr. Biol.* **4**, 671-675.
- Panganiban, G. E., Rashka, K. E., Neitzel, M. D., and Hoffmann, F. M. (1990a). Biochemical characterization of the *Drosophila dpp* protein, a member of the transforming growth factor beta family of growth factors. *Mol. Cell Biol.* **10**, 2669-2677.
- Panganiban, G. E., Reuter, R., Scott, M. P., and Hoffmann, F. M. (1990b). A *Drosophila* growth factor homolog, *decapentaplegic*, regulates homeotic gene expression within and across germ layers during midgut morphogenesis. *Development* **110**, 1041-1050.

- Pankratz, M. J., and Jackle, H. (1990). Making stripes in the *Drosophila* embryo. *Trends Genet.* **6**, 287-292.
- Pantoliano, M. W., Horlick, R. A., Springer, B. A., Van Dyk, D. E., Tobery, T., Wetmore, D. R., Lear, J. D., Nahapetian, A. T., Bradley, J. D., and Sisk, W. P. (1994). Multivalent ligand-receptor binding interactions in the fibroblast growth factor system produce a cooperative growth factor and heparin mechanism for receptor dimerization. *Biochemistry* **33**, 10229-10248.
- Paralkar, V. M., Nandedkar, A. K. N., Pionters, R. H., Kleinman, H. K., and Reddi, A. H. (1990). Interaction of osteogenin, a heparin binding bone morphogenetic protein, with type IV collagen. *J. Biol. Chem.* **265**, 17281-17284.
- Patel, N., and Goodman, C. (1992). Detection of *even-skipped* transcripts in *Drosophila* embryos with PCR/DIG-labeled DNA probes. In "Nonradioactive In Situ Hybridization Application Manual". Boehringer Mannheim GmbH, Biochemica, pp. 62-63.
- Peifer, M., Karch, F., and Bender, W. (1987). The *bithorax* complex: control of segment identity. *Genes Dev.* **1**, 891-898.
- Peifer, M., Rauskolb, C., Williams, M., Riggelman, B., and Wieschaus, E. (1991). The segment polarity gene *armadillo* interacts with the *wingless* signaling pathway in both embryonic and adult pattern formation. *Development* **111**, 1029-1043.
- Penton, A., Chen, Y., Staehling-Hampton, K., Wrana, J. L., Attisano, L., Szidonya, J., Casill, J. A., and Hoffman, F. M. (1994). Identification of two bone morphogenetic protein type I receptors in *Drosophila* and evidence that Brk25D is a *decapentaplegic* receptor. *Cell* **78**, 239-250.
- Penton, A., and Hoffman, F. M. (1996). *Decapentaplegic* restricts the domain of *wingless* during *Drosophila* limb patterning. *Nature* **382**, 162-165.
- Perrimon, N., Lanjuin, A., Arnold, C., and Noll, E. (1996). Zygotic lethal mutations with maternal effect phenotypes in *Drosophila melanogaster*. II. Loci on the second and third chromosomes identified by P-element induced mutations. *Genetics* **144**, 1681-1692.
- Perrimon, N., and Bernfield, M. (2000). Specificities of heparan sulfate proteoglycans in developmental processes. *Nature* **404**, 725-728.
- Perrimon, N., and Duffy, J. B. (1998). Developmental biology. Sending all the right signals. *Nature* **396**, 18-19.
- Phillips, R. G., Roberts, I. J. H., Ingham, P. W., and Whittle, J. R. S. (1990). The *Drosophila* segment polarity gene *patched* involved in a position-signaling mechanism in imaginal discs. *Development* **110**, 105-114.
- Piccolo, S., Sasai, Y., Lu, B., and DeRobertis, E. M. (1996). Dorsoventral patterning in *Xenopus*: inhibition of ventral signals by direct binding of chordin to BMP-4. *Cell* **86**, 589-598.
- Pilia, G., Hughes-Benzie, R.M., Huber, R. Neri, G., Cao, A., Forabosco, A., and Schlessinger, D.

- (1996). Mutations in GPC3, a glypican gene, cause the Simpson-Golabi-Behmel overgrowth syndrome. *Nature Genetics* **12**, 241-247.
- Plessow, S., Koster, M., and Knochel, W. (1991). cDNA sequence of *Xenopus laevis* bone morphogenetic protein-2 (BMP-2). *Biochim. Biophys. Acta.* **1089**, 280-282.
- Podos, S. D., and Ferguson, E. L. (1999). Morphogen gradients: new insights from DPP. *Trends Genet.* **15**, 396-402.
- Poodry, A., Bryant, P. J., and Schneiderman, H. A. (1971). The mechanism of pattern reconstruction by dissociated imaginal discs of *Drosophila melanogaster*. *Dev. Biol.* **26**, 464-477.
- Porter, J. A., von Kessler, D. P., Ekker, S. C., Young, K. E., Lee, J. J., Moses, K., and Beachy, P. A. (1995). The product of *hedgehog* autoproteolytic cleavage active in local and long-range signaling. *Nature* **374**, 363-366.
- Porter, J. A., Young, K. E., and Beachy, P. A. (1996). Cholesterol modification of Hedgehog signaling proteins in animal development. *Science* **274**, 255-259.
- Posakony, A., Raftery, L. A., and Gelbart, W. M. (1990). Wing formation in *Drosophila melanogaster* requires *decapentaplegic* gene function along the anterior-posterior compartment boundary. *Mech. Dev.* **33**, 69-82.
- Postlethwait, J. H., Poodry, C. A., and Schneiderman, H. A. (1971). Cellular dynamics of pattern duplication in imaginal discs of *Drosophila melanogaster*. *Dev. Biol.* **26**, 125-132.
- Postlethwait, J. H., and Schneiderman, H. A. (1973). Pattern formation and determination in imaginal discs of *Drosophila melanogaster* after irradiation of embryos and young larvae. *Dev. Biol.* **32**, 345-360.
- Prydz, K., and Dalen, K. T. (2000). Synthesis and sorting of proteoglycans. *J. Cell Sci.* **113**, 193-205.
- Raftery, L. A., Sanicola, M., Blackman, M., and Gelbart, W. M. (1991). The relationship of *decapentaplegic* and *engrailed* expression in *Drosophila* imaginal discs: do these genes mark the anterior-posterior compartment boundary? *Development* **113**, 27-33.
- Raftery, L. A., Twombly V., Wharton, K., and Gelbart, W. M. (1995). Genetic screens to identify elements of the *decapentaplegic* signaling pathway in *Drosophila*. *Genetics* **139**, 241-254.
- Ramirez-Weber, F. A., and Kornberg, T. B. (1999). Cytonemes: cellular processes that project to the principle signaling center in *Drosophila* imaginal discs. *Cell* **97**, 599-607.
- Rapraeger, A. C., Krufka, A., and Olwin, B. B. (1991). Requirement of heparan sulfate for bFGF-mediated fibroblast growth and myoblast differentiation. *Science* **252**, 1705-1708.
- Rapraeger, A. C. (2001). Molecular interactions of syndecans during development. *Curr. Opin. Cell Dev. Biol.* **12**, 107-116.
- Rapraeger, A. C. (1993). The coordinated regulation of heparan sulfate, syndecans and cell behavior.

Curr. Opin. in Cell Biol. **5**, 844-853.

- Ray, R. Arora, K., Nusslein-Volhard, C., and Gelbart, W. M. (1991). The control of cell fate along the dorsal-ventral axis of the *Drosophila* embryo. *Development* **11**, 35-54.
- Reichsman, F., Smith, L., and Cumberledge, S. (1996). Glycosaminoglycans can modulate extracellular localization of the *wingless* protein and promote signal transduction. *J. Cell Biol.* **135**, 819-827.
- Reinhardt, C. A., Hodgkin, N. M., and Bryant, P. J. (1977). Wound healing in the imaginal discs of *Drosophila*. I. Scanning electron microscopy of normal and healing wing discs. *Dev. Biol.* **60**, 238-257.
- Reinhardt, C. A., and Bryant, P. J. (1981). Wound healing in the imaginal discs of *Drosophila*. II. Transmission electron microscopy of normal and healing wing discs. *J. Exp. Zool.* **216**, 45-61.
- Riddle, R. D., Johnson, R.L., Laufer, E., and Tabin, C. (1993). *Sonic hedgehog* mediates the polarizing activity of the ZPA. *Cell* **75**, 1401-1416.
- Rijsewijk, F., and Schuermann, M. (1987). The *Drosophila* homolog of the mouse mammary oncogene *int-1* is identical to the segment polarity gene *wingless*. *Cell* **50**, 649-57.
- Ripamonti, U. (1996). Osteoinduction in porous hydroxyapatite implanted in heterotopic sites of different animal models. *Biomaterials* **17**, 31-5.
- Ripamonti, U.; Van den Heever, B., Sampath, T. K., Tucker, M. M., Rueger, D C., and Reddi, A. H. (1996). Complete regeneration of bone in the baboon by recombinant human osteogenic protein-1 (hOP-1, bone morphogenetic protein-7). *Growth Factors* **13**, 273-89.
- Roark, E. F., and Greer, K. (1994). Transforming growth factor beta and bone morphogenetic protein-2 act by distinct mechanisms to promote chick limb cartilage differentiation in vitro. *Dev. Dyn.* **200**, 103-116.
- Roberts, R., Gallegher, J., Spooncer, E., Allen, T .D., Bloomfield, F., and Dexter, T. M. (1988). Heparan sulfate bound growth factors: a mechanism for stromal cell mediated haemopoiesis. *Nature* **332**, 376-378.
- Rogalski, T. M., Williams, B. D., Mullen, G. P., and Moerman, D. G. (1993). Products of the *unc-52* gene in *Caenorhabditis elegans* are homologous to the core protein of the mammalian basement membrane heparan sulfate proteoglycan. *Genes Dev.* **7**, 1471-1484.
- Roghani, M., Mansukhani, A., Dell'era, P., Bellosta, P., Basilico, C., Rifkin, D. B., and Moscatelli, D. (1994). Heparin increases the affinity of basic fibroblast growth factor for its receptor but is not required for binding. *J. Biol. Chem.* **269**, 3976-3984.
- Rosenberg, R. D., Spooncer, E., Allen, T. D., Bloomfield, F. (1997). Heparan sulfate proteoglycans of the cardiovascular system. Specific structures emerge but how is synthesis regulated? *J. Clin. Invest.* **100**, 67-75.

- Roth, S., Stein, D., and Nusslein-Volhard, C. (1989). A gradient of nuclear localization of the *dorsal* protein determines dorsoventral pattern in the *Drosophila* embryo. *Cell* **59**, 1189-1202.
- Roth, S., Hiromi, Y., Godt, D., and Nusslein-Volhard, C. (1991). *cactus*, a maternal gene required for proper formation of the dorsoventral morphogen gradient in *Drosophila* embryo. *Development* **112**, 371-388.
- Roth, S. (1994). Proteolytic generation of a morphogen. *Curr. Biol.* **4**, 755-757.
- Roth, S., Neuman-Silberberg, F. S., Barcell, G., and Schupbach, T. (1995). *cornichon* and the EGF receptor signaling process are necessary for both anterior-posterior and dorsal-ventral pattern formation in *Drosophila*. *Cell* **81**, 967-978.
- Ruberte, E., Marty, T., Nellen, D., Affolter, M., and Basler, K. (1995). An absolute requirement for both the type II and type I receptors, *punt* and *thickveins*, for *dpp* signaling in vivo. *Cell* **80**, 889-897.
- Ruohola-Baker, H., Jan, L. Y., and Jan, Y. N. (1994). The role of gene cassettes in axis formation during *Drosophila* oogenesis. *Trends Genet.* **10**, 898-94.
- Ruoslahti, E., Yamaguchi, Y., Hildebrand, A., and Border, W. A. (1992). Extracellular matrix/growth factor interactions. *Cold Spring Harbor Symp. Quant. Biol.* **57**, 309-315.
- Ruppert, R., Hoffmann, E., and Sebald, W. (1996). Human bone morphogenetic protein 2 contains a heparin-binding site which modifies its biological activity. *Eur. J. Biochem.* **237**, 295-302.
- Rushlow, C. A., Han, K., Manley, J. L., and Levine, M. (1989). The graded distribution of the *dorsal* morphogen is initiated by selective nuclear transport in *Drosophila*. *Cell* **59**, 1165-1177.
- Russell, M. A. (1974). Pattern formation in the imaginal discs of a temperature sensitive cell lethal mutant of *Drosophila melanogaster*. *Dev. Biol.* **40**, 24-39.
- Russell, M. A. (1985). Positional information in insect segments. *Dev. Biol.* **108**, 269-283.
- Russell, M. A., Girton, J. R., and Morgan, K. (1977). Pattern formation in a ts cell lethal mutant of *Drosophila*: The range of phenotypes induced by larval heat treatments. *Wilhelm Roux's Arch. Dev. Biol.* **183**, 41-59.
- Russell, M. A., Ostafichuk, L., and Scanga, S. (1998). Lethal P-lacZ insertion lines expressed during pattern respecification in the imaginal discs of *Drosophila*. *Genome* **41**, 7-13.
- Saharinene, J., Taipale, J., and Keski-Oja, J. (1996). Association of the small latent transforming growth factor- β with an eight-cysteine repeat of its binding protein LTBP-1. *EMBO J.* **15**, 245-253.
- Salmivirta, M., Lidholt, K., and Lindahl, U. (1996). Heparan sulfate: a piece of information. *FASEB. J.* **10**, 1270-1279.
- Sambrook, J., Fritsch, E. F., and Maniatis, T. (1989). "Molecular Cloning: A laboratory manual". Cold

Spring Harbor Laboratory, Cold Spring Harbor, New York.

- Sampath, T. K., and Reddi, A. H. (1981). Dissociative extraction and reconstitution of extracellular matrix components involved in local bone differentiation. *Proc. Natl. Acad. Sci USA* **78**, 7599-7603.
- Sampath, T. K., Rashka, K. E., Doctor, J. S., Tucker, R. F., and Hoffmann, F. M. (1993). *Drosophila* transforming growth factor beta superfamily proteins induced endochondral bone formation in mammals. *Proc. Natl. Acad. Sci. USA* **90**, 6004-6008.
- Sang, J. H. (1984). Genetics and Development (Langman and Pledi Ed.) Longman House Inc., New York, pp. 230-234.
- Sang, J. H., and Simcox, A. A. (1983). When does determination occur in *Drosophila* embryos? *Dev. Biol.* **97**, 212-221.
- Sander, K. (1975). Pattern specification in the insect embryo. *Ciba Found Symp.* **10**, 241-263.
- Sanicola, M., and Sekelsky, J. (1995). Drawing a stripe in *Drosophila* imaginal disks: negative regulation of *decapentaplegic* and *patched* expression by *engrailed*. *Genetics* **139**, 745-756.
- Sasai, Y., Lu, B., Steinbeisser, H., Geissert, D., Gont, L. K. De Robertis, E. M. (1994). *Xenopus chordin*: a novel dorsalizing factor activated by organizer-specific homoeobox genes. *Cell* **79**, 779-790.
- Sasisekharan, R. (1993). Cloning and expression of heparinase III gene from *Flavobacterium heparium*. *Proc. Natl. Acad. Sci. USA* **90**, 3660-3664.
- Sasisekharan, R., Ernst, S., and Venkataraman, G. (1997). On the regulation of fibroblast growth factor activity by heparin-like glycosaminoglycans. *Angiogenesis* **1**, 45-54.
- Saunders, S., and Bernfield, M. (1988). Cell surface proteoglycan binds mouse mammary epithelial cells to fibronectin and behaves as a receptor for interstitial matrix. *J. Cell. Biol.* **106**, 423-430.
- Saxena, U., Klein, M. G., and Goldberg, I. J. (1990). Metabolism of endothelial cell-bound lipoprotein lipaes. Evidence for heparan sulfate proteoglycan-mediated internalization and recycling. *J. Biol. Chem.* **265**, 12880-12886.
- Schaller, H. C. (1976). Action of the head activator as a growth hormone in hydra. *Cell Differ.* **5**, 1-11.
- Schaller, H. C. (1978). Action of a morphogenetic substance from hydra. *Symp. Soc. Dev. Biol.* **35**, 231-41.
- Schlessinger, J. (1994). SH2/SH3 signaling proteins. *Curr. Opin. Genet. Dev.* **4**, 25-30.
- Schlessinger, J., Lax, I., and Lemmon, M. (1995). Regulation of growth factor activation by proteoglycans: what is the role of the affinity receptors? *Cell* **83**, 357-360.

- Schultz-Cherry, S., and Murphy-Ullrich, J. E. (1993). Thrombospondin causes activation of latent transforming growth factor- β secreted by endothelial cells by a novel mechanism. *J. Cell. Biol.* **122**, 923-932.
- Schmidt, T., and Schaller, H. C. (1976). Evidence for a foot-inhibiting substance in hydra. *Cell Differ.* **5**, 151-599.
- Schneider, D. S., Hudson, K. L., Lin, T. Y., and Anderson, K. V. (1991). Dominant and recessive mutations define functional domains of *Toll*, a transmembrane protein required for dorsal-ventral polarity in the *Drosophila* embryo. *Genes Dev.* **5**, 797-807.
- Schneider, D. S., Jin, Y., Morisato, D., and Anderson, K. V. (1994). A processed form of the *Spatzle* protein defines dorsal-ventral polarity in the *Drosophila* embryo. *Development* **120**, 1243-1250.
- Schubiger, G. (1971). Regeneration, duplication and transdetermination in fragments of leg disc of *Drosophila melanogaster*. *Dev. Biol.* **26**, 277-283.
- Schubiger, G., and Hadorn, E. (1968). Auto- and allotypic differentiation in in vivo cultivated foreleg blastemas of *Drosophila melanogaster*. *Dev. Biol.* **17**, 584-602.
- Schubiger, G., and Karpen, G. (1983). Blastema formation in regenerating disc fragments of *Drosophila melanogaster*. In "Limb development and regeneration". Alan Liss, Inc., New York.
- Schubiger, G., and Schubiger, M. (1978). Distal transformation in *Drosophila* leg imaginal disc fragments. *Dev. Biol.* **67**, 286-295.
- Schupbach, T. (1987). Germ line and soma cooperate during oogenesis to establish the dorsoventral pattern of eggshell and embryo in *Drosophila melanogaster*. *Cell* **49**, 699-707.
- Schupbach, T., and Wieschaus, E. (1989). Female sterile mutations on the second chromosome of *Drosophila melanogaster*. I. Maternal effect mutations. *Genetics* **121**, 101-107.
- Schupbach, T., Clifford, R. J., Manseau, L. J., and Price, J. V. (1991). Dorso-ventral signaling processes in *Drosophila* oogenesis. *Symp. Soc. Dev. Biol.* **4**, 502-507.
- Schupbach, T., and Roth, S. (1994). Dorsoventral patterning in *Drosophila* oogenesis. *Curr. Opin. Genet. Dev.* **4**, 502-507.
- Schwartz, C., Locke, J., Nishida, C., and Kornberg, T. B. (1995). Analysis of *cubitus interruptus* regulation in *Drosophila* embryos and imaginal disks. *Development* **121**, 1625-1635.
- Selleck, S. B. (2000). Proteoglycans and pattern formation. *Trend. Genet.* **16**, 206-212.
- Selleck, S. B. (2001). Genetic dissection of proteoglycan function in *Drosophila* and *C. elegans*. *Cell and Dev. Biol.* **12**, 127-134.
- Sen, J., Goltz, J. S., Stevens, L., and Stein, D. (1998). Spatially restricted expression of *pipe* in the *Drosophila* egg chamber defines embryonic dorsal-ventral polarity. *Cell* **95**, 471-481.

- Segarini, P. R., and Seyedin, S. M. (1988). The high molecular weight receptor to transforming growth factor-beta contains glycosaminoglycan chains. *J. Biol. Chem.* **263**, 8366-8370.
- Sharma, R. P., and Chopra, V. L. (1976). Effect of the *wingless* (*wg*) mutation on wing and haltere development in *Drosophila melanogaster*. *Dev. Biol.* **48**, 461-465.
- Shearn, A., Rice, T., Garen, A., and Gehring, J. (1971). Imaginal disc abnormalities in lethal mutants of *Drosophila*. *Proc. Natl. Acad. Sci. USA* **68**, 2594-2598.
- Shearn, A., and Garen, A. (1974). Genetic control of imaginal disc development in *Drosophila*. *Proc. Natl. Acad. Sci. USA* **71**, 1393-1397.
- Shearn, A. (1977). Mutation analysis of imaginal disc development in *Drosophila melanogaster*. *Amer. Zool.* **17**, 585-594.
- Shelton, C. A., and Wasserman, S. A. (1993). *pelle* encodes a protein kinase required to establish dorsoventral polarity in the *Drosophila* embryo. *Cell* **72**, 515-525.
- Shieh, M. T., WuDunn, D., Montgomery, R. I., Esko, J. D., and Spear, P. G. (1992). Cell surface receptors for herpes simplex virus are heparan sulfate proteoglycans. *J. Cell. Biol.* **116**, 1273-1281.
- Shimell, M. J., Ferguson, E. L., Childs, S. R., and O'Connor, M. B. (1991). The *Drosophila* dorsoventral patterning gene *tolloid* is related to human bone morphogenetic protein I. *Cell* **67**, 469-481.
- Shimomura, T., Miyazawa, K., Komiyama, Y., Hiraoka, H., Naka, D., Morimoto, Y., and Kitamura, N. (1995). Activation of hepatocyte growth factor by two homologous proteases, blood coagulation factor XIIIa and hepatocyte growth factor activator. *Eur. J. Biochem.* **229**, 257-261.
- Siegfried, E., and Perrimon, N. (1994). *Drosophila wingless*: a paradigm for the function and mechanism of Wnt signaling. *BioEssays* **16**, 395-404.
- Siegfried, E., Wilder, E. L., and Perrimon, N. (1994). Components of *wingless* signaling in *Drosophila*. *Nature* **367**, 76-80.
- Simcox, A. A., and Sang, J. H. (1982). Cell determination in *Drosophila melanogaster* embryos. *Prog. Clin. Biol. Res.* **8**, 349-361.
- Simcox, A. A., Roberts, I. J. H., Hersperger, E., Gribbin, M. C., Shearn, A., and Whittle, J. R. S. (1989). Imaginal discs can be recovered from embryos mutant for the segment polarity genes *engrailed*, *naked*, and *patched* but not from *wingless*. *Development* **107**, 715-722.
- Simmonds, A. J., Brook, W. J., Cohen, S. M., and Bell, J. B. (1995). Distinguishable functions for *engrailed* and *invected* in anterior-posterior patterning in the *Drosophila* wing. *Nature* **376**, 424-427.

- Simpson, P., and Morata, G. (1980). The control of growth in the imaginal discs of *Drosophila*. *Basic Life Sci.* **16**, 129-139.
- Singer, M. A., Penton, A., Twombly, V., Hoffmann, F. M., and Gelbart, W. M. (1997). Signaling through both type I DPP receptors is required for anterior-posterior patterning of the entire *Drosophila* wing. *Development* **124**, 79-89.
- Slack, J. M. (1987). Morphogenetic gradients: past and present. *Trends Biochem. Sci.* **12**, 200-204.
- Slack, J. M. (1991). *From Egg to Embryo* (2nd ed.). Cambridge University Press, Cambridge.
- Smith, J. C., Price, B. M., Van Nimmen, K., and Huyelebroeck, D. (1990). Identification of a potent *Xenopus* mesoderm-inducing factor as a homolog of *activin A*. *Nature* **345**, 729-731.
- Smith, W. C., and Harland, R. M. (1992). Expression cloning of *noggin*, a new dorsalizing factor localized to the Spemann organizer in *Xenopus* embryos. *Cell* **70**, 829-840.
- Smith, C. L., and DeLotto, R. (1994). Ventralizing signal determined by protease activation in *Drosophila* embryogenesis. *Nature* **368**, 548-551.
- Smith, C. L., Giordano, H., Schwartz, M., and DeLotto, R. (1995). Spatial regulation of *Drosophila* snake protease activity in the generation of dorsal-ventral polarity. *Development* **121**, 4127-4135.
- Spemann, H. (1938). *Embryonic Development and Induction*. Yale University Press. Conn
- Spencer, F. A., Hoffmann, F. M., and Gelbart, W. M. (1982). *decapentaplegic*: A gene complex affecting morphogenesis in *Drosophila melanogaster*. *Cell* **28**, 451-461.
- Spivak-Kroizman, T., Lemmon, M. A., Dick, I., Ladbury, J. E., Pinchasi, D., Huang, J., Jaye, M., Crumley, G., Schlessinger, J., and Lax, I. (1994). Heparin-induced oligomerization of FGF molecules is responsible for FGF receptor dimerization, activation, and cell proliferation. *Cell* **79**, 1015-1024.
- Sporn, M. B., and Roberts, A. B. (1990). The transforming growth factor-betas: past, present, and future. *Ann. N. Y. Acad. Sci.* **593**, 1-6.
- Spradling, A. C., Stern, D. M., Kiss, I., Roote, J., Lavery, T., and Rubin, G. M. (1995). Gene disruptions using P transposable elements: an integral component of the *Drosophila* genome project. *Proc. Natl. Acad. Sci. USA* **92**, 10824-10830.
- Spring, J., Paine-Saunders, S. E., Hynes, R. O., and Bernfield, M. (1994). *Drosophila* syndecan: conservation of a cell-surface heparan sulfate proteoglycan. *Proc. Natl. Acad. Sci. USA* **91**, 3334-3338.
- Stachling-Hampton, K., Hoffmann, F. M., Baylies, M. K., Rushton, E., and Bate, M. (1994). *Dpp* induces mesodermal gene expression in *Drosophila*. *Nature* **372**, 783-786.

- Stark, P., Gates, P. B., Brockes, J. P., and Ferretti, P. (1998). *Hedgehog* family member is expressed throughout regenerating and developing limbs. *Dev. Dyn.* **212**, 352-63.
- Stein, D., and Nusslein-Volhard, C. (1992). Multiple extracellular activities in *Drosophila* egg perivitelline fluid are required for establishment of embryonic dorsal-ventral polarity. *Cell* **68**, 429-440.
- Steinfeld, R., van den Berghe, H., and David, G. (1996). Stimulation of fibroblast growth factor receptor-1 occupancy and signaling by cell surface-associated syndecans and glypican. *J. Cell Biol.* **133**, 405-416.
- Steiner, E. (1976). Establishment of compartments in developing leg imaginal discs of *Drosophila melanogaster*. *Wilhelm Roux's Arch. Dev. Biol.* **180**, 9-30.
- Stern, C. (1968). *Genetic mosaics and other essays*. Harvard University Press, Cambridge Mass.
- Steward, R. (1987). *Dorsal*, an embryonic polarity gene in *Drosophila*, is homologous to the vertebrate proto-oncogene, *c-rel*. *Science* **238**, 692-694.
- Steward, R., and Govind, S. (1993). Dorsal-ventral polarity in the *Drosophila* embryo. *Curr. Opin. Genet. Dev.* **3**, 556-561.
- Stickens, D., Clines, G., Burbee, D., and Thomas, S. (1996). The EXT2 multiple exostoses gene defines a family of putative tumour suppressor genes. *Nature Genet.* **14**, 25-32.
- St. Johnston, R. D., and Gelbart, W. M. (1987). *Decapentaplegic* transcripts are localized along the dorsal-ventral axis of the *Drosophila* embryo. *EMBO J.* **6**, 2785-2791.
- St. Johnston, D., Driever, W., Berleth, T., Richstein, S., and Nusslein-Volhard, C. (1989). Multiple steps in the localization of *bicoid* RNA to the anterior pole of the *Drosophila* oocyte. *Development* **107**(Suppl), 13-19.
- St. Johnston, D., and Nusslein-Volhard C. (1992). The origin of pattern and polarity in the *Drosophila* embryo. *Cell* **68**, 201-209.
- Stone, D. M., Hynes, M., Armanini, M., Swanson, T. A., Gu, Q., Johnson, R. L., Scott, M. P., Pennica, D., Goddard, A., and Phillips, H. (1996). The tumor-suppressor gene *patched* encodes a candidate receptor for *Sonic hedgehog*. *Nature* **384**, 129-134.
- Struhl, G., and Basler, K. (1993). Organizing activity of *wingless* protein in *Drosophila*. *Cell* **72**, 527-540.
- Struhl, G., Struhl, K., and Macdonald, P. M. (1989). The gradient morphogen *bicoid* is a concentration-dependent transcriptional activator. *Cell* **57**, 1259-1273.
- Stumpf, H. (1966). Mechanism by which cells estimate their location within the body. *Nature* **212**, 430-431.

- Stumpf, N., Koike, N., Hayakawa, K., Tokuda, K., Nishimiya, Y., Tsuchiya, J., Hirate, A., Okazaki, A., and Kumaki, K. (1994). 1,25-Dihydroxyvitamin D3 and 22-oxa-1,25-dihydroxyvitamin D3 in vivo nuclear receptor binding in developing bone during endochondral and intramembranous ossification. *Histochemistry* **102**, 183-94.
- Su, M., Burrell, D. E., Hill, J., Gyuris, R., Brent, R., Wiltshire, J., Trent, B., Vogelstein, B., and Kinzler, K. W. (1995). APC binds to the novel protein EB1. *Cancer Res.* **55**, 2972-2877.
- Subramanian, M. L., Fitzgerald, M., and Bernfield, M. (1997). Regulated shedding of syndecan-1 and -4 ectodomains by thrombin and growth factor receptor activation. *J. Biol. Chem.* **272**, 14713-14720.
- Szabad, J., Simpson, P., and Nothiger, R. (1979). Regeneration and compartments in *Drosophila*. *J. Embrol. Exp. Morph.* **49**, 229-241.
- Tabata T., Eaton, S., and Kornberg, T. B. (1992). The *Drosophila hedgehog* gene is expressed specifically in posterior compartment cells and is a target of *engrailed* regulation. *Genes Dev.* **6**, 2635-2645.
- Tabata, T., and Kornberg, T. (1994). *Hedgehog* is a signaling protein with a key role in patterning *Drosophila* imaginal discs. *Cell* **76**, 89-102.
- Tabata, T., Schartz, C., Gustavson, E., Ali, Z., and Kornberg, T. (1995). Creating a *Drosophila* wing de novo, the role of *engrailed*, and the compartment border hypothesis. *Development* **121**, 3359-3365.
- Taipale, J., Miyazono, K., Heldin, C-H., and Keski-Oja, J. (1994). Latent transforming growth factor- β 1 associates to fibroblast extracellular matrix via latent TGF- β binding protein. *J. Cell Biol.* **124**, 171-181.
- Taipale, J., Lohi, J., Saarinen, J., Kovanen, P. T., and Keski-Oja, J. (1995). Human mast cell chymase and leukocyte elastase release latent transforming growth factor- β 1 from the extracellular matrix of cultured human epithelial and endothelial cells. *J. Biol. Chem.* **270**, 4689-4696.
- Taipale, J. and Keski-Oja, J. (1997). Growth factors in the extracellular matrix. *FASEB J.* **11**, 51-59.
- Tang, A. H., and Tu, C. P. (1994). Biochemical characterization of *Drosophila* glutathione S-transferases D1 and D21. *J. Biol. Chem.* **269**, 27876-27884.
- Tang, S., Woodhal, R. W., Shen, Y. J., deBellard, M. E., Saffell, J. L., Doherty, P., Walsh, F. S., and Filbin, M. T. (1997). Soluble myelin-associated glycoprotein (MAG) found in vivo inhibits axonal regeneration. *Mol. Cell Neurosci.* **9**, 333-346.
- Tautz, D. (1988). Regulation of the *Drosophila* segmentation gene *hunchback* by two maternal morphogenetic centres. *Nature* **332**, 281-284.

- Tautz, D., and Pfeifle, C. (1989). A non-radioactive insitu hybridization method faor the localization of specific RNAs in *Drosophila* embryos reveals translational control of the segmentation gene *hunchback*. *Chromosoma*, **98**, 81-85.
- Terracol, R., and Lengyel, J. A. (1994). The *thickveins* gene of *Drosophila* is required for dorso-ventral polarity of the embryo. *Genetics* **138**, 165-178.
- Thaller, C., and Eichele, G. (1987). Identification and spatial distribution of retinoids in the developing chick limb bud. *Nature* **327**, 625-628.
- The, I., Bellaiche, Y., and Perrimon, N. (1999). *Hedgehog* movement is regulated through *tout velu*-dependent synthesis of a heparan sulfate proteoglycan. *Mol. Cell* **4**, 633-639.
- Theisen, H., Haerry, T. E., O'Connor, M. B., and Marsh, J. L. (1996). Developmental territories created by mutual antagonism between *Wingless* and *Decapentaplegic*. *Development* **122**, 3939-3948.
- Teleman, A. A., and Cohen, S. M. (2000). Dpp Gradient Formation in the *Drosophila* Wing Imaginal Disc. *Cell* **103**, 971-980.
- Tephly, T. R., and Burchell, B. (1990). UDP-glucuronosyltransferases: a family of detoxifying enzymes. *Trends Pharmacol. Sci.* **11**, 276-279.
- Thisse, C., Perrin-Schmitt, F., Stoetzel, C., and Thisse, B. (1991). Sequence-specific trans-activation of the *Drosophila twist* gene by the dorsal gene product. *Cell* **65**, 1191-1201.
- Tickle, C. D., Summerbell, D., and Wolpert, L. (1975). Positional signaling and specification of digits in chick limb morphogenesis. *Nature* **254**, 199-202.
- Tickle, C. B., Alberts, B., Wolpert, L., and Lee, J. (1982). Local application of retinoic acid to the limb bud mimics the action of the polarizing region. *Nature* **296**, 564-566.
- Tickle, C. B., Yang, Y., Drossopoulou, G., Chuang, P. T., Duprez, D., Marti, E., Bumcrot, D., Vargesson, N., Clark, J., Niswander, L., and McMahon, A. (1997). Relationship between dose, distance and time in Sonic Hedgehog-mediated regulation of anterioposterior polarity in the chick limb. *Development* **124**, 4393-4404.
- Tomlinson, A. (1988). Cellular interactions in the developing *Drosophila* eye. *Development* **104**, 183-193.
- Toriumi, D. H., Kotler, H. S., Luxenberg, D. P., Holtrop, M. E., and Wang, E. A. (1991). Osteoinductive biomaterial for medical implantation. *J. Long Term Eff. Med. Implants* **1**, 53-77.
- Toyoda, H., Kinoshita-Toyoda, A., Fox, B., and Selleck, S. B. (2000). Structural analysis of glycosaminoglycans in animals bearing mutations in *sugarless*, *sulfateless*, and *tout-velu*. *Drosophila* homologs of vertebrate genes encoding glycoaminoglycan biosynthetic enzymes. *J. Biol. Chem.* **275**, 21856-21861.
- Toyoda, H., Kinoshita-Toyoda, A., and Selleck, S. B. (2000). Structural analysis of GAGs in *Drosophila* and *C. elegans* and demonstration that *tout velu*, a *Drosophila* gene related to EXT

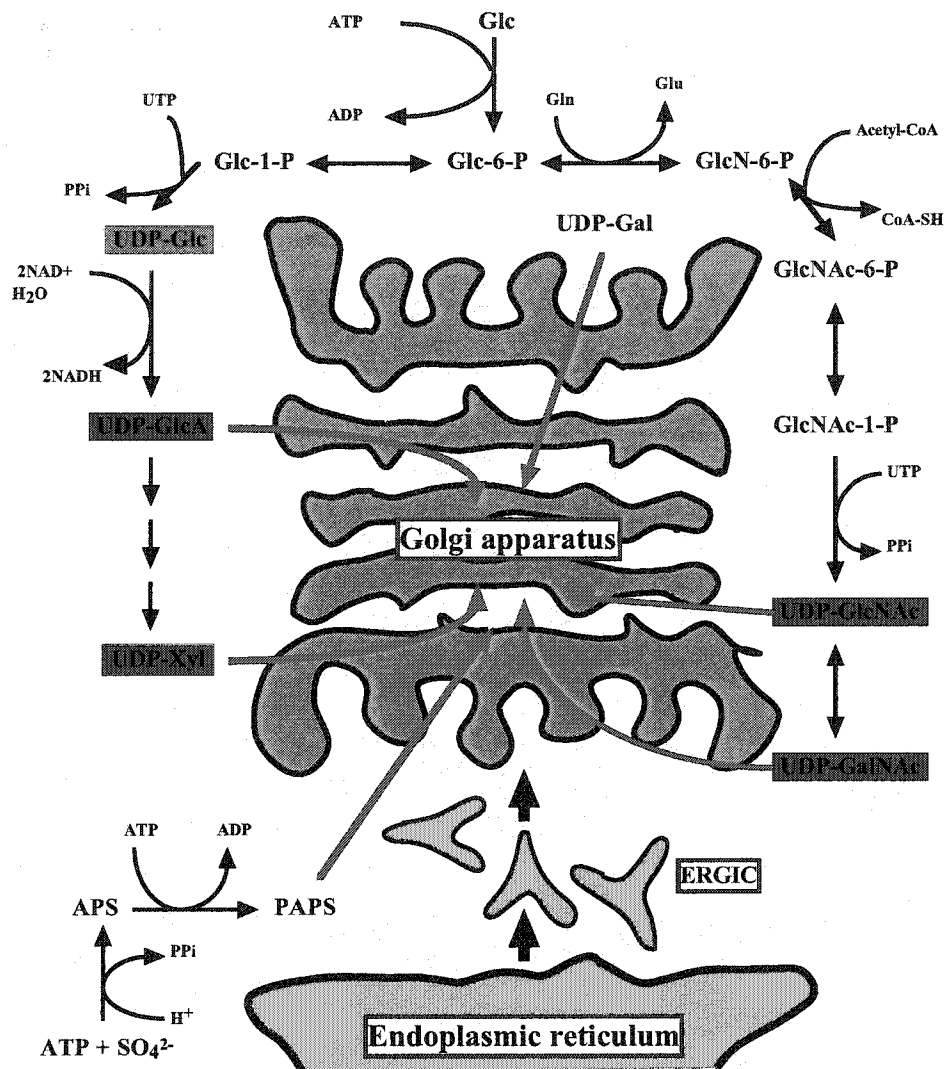
- tumor suppressors, affects heparan sulfate in vivo. *J. Biol. Chem.* **275**, 2269-2275.
- Treisman, J. E., Lai, Z. C., and Rubin, G. (1995). *Shortsighted* acts in the *decapentaplegic* pathway in *Drosophila* eye development and has homology to a mouse TGF-beta-responsive gene. *Development* **121**, 2835-2845.
- Treisman, J. E., and Rubin, G. M. (1995). *wingless* inhibits morphogenetic furrow movement in the *Drosophila* eye disc. *Development* **121**, 3519-3527.
- Tsuda, K., Kamimura, H., Nakato, M., Archer, W., Staatz, B., Fox, M., Humphrey, S., Olson, T., Futch, V., Kaluza, E., Siegfried, E., Stam, L., and Selleck, S. B. (1999). The cell-surface proteoglycan *Dally* regulates *Wingless* signaling in *Drosophila*. *Nature* **400**, 276-80.
- Tsuneizumi, K., Nakayama, T., Kmoshida, Y., Kornberg, T. B., Christian, J. L., and Tabata, T. (1997). *Daughters against dpp* modulates *dpp* organizing activity in *Drosophila* wing development. *Nature* **389**, 627-631.
- Turing, A. (1952). The chemical basis of morphogenesis. *Philos. Trans. R. Soc. London Ser.* **B237**, 37-72.
- Ursprung, H. (1967). In vivo culture of *Drosophila* imaginal discs. In "Methods in developmental Biology". F. Witt and N. Wessels (eds.). Academic Press, New York.
- van der Geer, P., Hunter, T. Lindberg, R. A. (1994). Receptor protein-tyrosine kinases and their signal transduction pathways. *Annu. Rev. Cell Biol.* **10**, 251-337.
- van den Heuvel, M., Nusse, R., Johnston, P., and Lawrence, P. A. (1989a). Distribution of the *wingless* gene product in *Drosophila* embryos: a protein involved in cell-cell communication. *Cell* **59**, 739-749.
- van den Heuvel, L. P., van den Born, J., van de Velden, T. J., Veerkamp, J. H., Monnens, L. A., Schroder, C. H., and Berden, J. H. (1989b). Isolation and partial characterization of heparan sulfate proteoglycan from the human glomerular basement membrane. *J. Biochem.* **264**, 457-465.
- van den Heuvel, M., and Ingham, P. W (1996). *smoothed* encodes a receptor-like serpentine protein required for hedgehog signaling. *Nature* **382**, 547-551.
- Vincent, J.P. (1994). Morphogens dropping like flies? *Trends Genet.* **10**. 383-385.
- Vincent, J. P., and O'Farrell, P. H. (1992). The state of *engrailed* expression is not clonally transmitted during early *Drosophila* development. *Cell* **68**, 923-931.
- Vincent, J. P., and Lawrence, P. A. (1994). Developmental genetics. It takes three to distalize. *Nature* **372**, 132-133.
- Viviano, A., and Brockes, J. P. (1996). Is retinoic acid an endogenous ligand during urodele limb

- regeneration? *Int. J. Dev. Biol.* **40**, 817-22.
- Vlodavsky, R., Bar-Shavit, R., Ishai-Michaeli, P., Bashkin, P., and Fuks, Z. (1991a). Extracellular sequestration and release of fibroblast growth factor: a regulatory mechanism? *Trends Biochem. Sci.* **16**, 268-271.
- Vlodavsky, P., Bashkin, R., Ishai-Michaeli, T., Chajek-Shaul, R., Bar-Shavit, A., Haimovitz-Friedman, M., Klagsbrun, M., and Fuks, Z. (1991b). Sequestration and release of basic fibroblast growth factor. *Ann. N. Y. Acad. Sci.* **638**, 207-220.
- VonKalm, L., Fristrom, D., and Fristrom, J. (1995). The making of a fly leg: a model for epithelial morphogenesis. *BioEssays* **17**, 693-699.
- Waddington, C. H. (1959). "An Introduction to Modern Genetics, 4th ed." George Allen and Unwin Ltd., London.
- Walsh, E. C., and Stainier, D. Y. (2001). UDP-glucose dehydrogenase required for cardiac valve formation in *zebrafish*. *Science* **293**, 1670-1673.
- Wang, E. A., Rosen, V., D'Alessandro, J.S., Bauduy, M., Cordes, P., Harada, T., Israel, D. I., Hewick, R. M., Kerns, K. M., LaPan, P., Luxenberg, D. H., McQuid, D., Moutsas, J. K. Nove, J., and Wozney, J. M. Recombinant human bone morphogenetic protein induces bone formation. *Proc. Natl. Acad. Sci. USA* **87**, 2220-2224.
- Wang, X-F., Herbert, Y. L. Ng-Eaton, E., Downward, J. Lodish, H. F and Weinberg, R. A. (1991). Expression cloning and characterization of TGF- β Type III receptor. *Cell* **67**, 797-805.
- Wasserman, S. A. (1993). A conserved signal transduction pathway regulating the activity of the *rel*-like proteins Dorsal and NF- κ B. *Mol. Biol. Cell* **4**, 767-771.
- Watanabe, K., Yamada, H., and Yamaguchi, Y. (1995). K-glypican: a novel GPI-anchored heparan sulfate proteoglycan that is highly expressed in developing brain and kidney. *J. Cell. Biol.* **130**, 1207-1218.
- Webster, G., and Wolpert, L. (1966). Studies on pattern regulation in hydra. I. Regional differences in time required for hypostome determination. *J. Embryol. Exp. Morph.* **16**, 91-104.
- Werb, Z. (1997). ECM and Cell Surface Proteolysis: Regulating Cellular Ecology. *Cell* **91**, 439-442.
- Whalen, A. M., and Steward, R. (1993). Dissociation of the *dorsal-cactus* complex and phosphorylation of the *dorsal* protein correlate with nuclear localization of *dorsal*. *J. Cell. Biol.* **123**, 523-534.
- Wharton, K. A., Ray, R. P., and Gelbart, W. M. (1993). An activity gradient of *decapentaplegic* is necessary for the specification of dorsal pattern elements in the *Drosophila* embryo. *Development* **117**, 807-822.
- Wieschaus, E. (1980). A combined genetic and mosaic approach to the study of oogenesis in *Drosophila*. *Basic Life Sci.* **16**, 85-94.

- Wieschaus, E., and Gehring, W. J. (1976). Clonal analysis of primordial disc cells in the early embryos of *Drosophila melanogaster*. *Dev. Biol.* **50**, 249-263.
- Wieschaus, E., and Nusslein-Volhard, C. (1986). Looking at embryos. In *Drosophila: A practical approach* (ed. D.B. Roberts), IRL Press, Oxford, England, pp. 199-228.
- Wilder, E. L., and Perrimon, N. (1995). Dual functions of *wingless* in the *Drosophila* leg imaginal disc. *Development* **121**, 477-88.
- Wilkins, A. S., and Gubb, D. (1991). Pattern formation in the embryo and imaginal discs of *Drosophila*: what are the links? *Dev. Biol.* **145**, 1-12.
- Williams, J. A., Paddock, S. W., Vorwerk, K., and Carroll, S. B. (1994). Organization of wing formation and induction of a wing-patterning gene at the dorsal/ventral compartment boundary. *Nature* **368**, 299-305.
- Wilson, C., Pearson, R. K., Bellen, H. J., O'Kane, C. J., Grossniklaus, U., and Gehring, W. J. (1989). P-element-mediated enhancer detection: an efficient method for isolating and characterizing developmentally regulated genes in *Drosophila*. *Genes Dev.* **3**, 1301-1313.
- Wisotzkey, R. G., Mehra, A., Sutherland, D. J., Dobens, L. L., Liu, X., Dohrmann, C., Attisano, L., and Raftery, L. A. (1998). *Medea* is a *Drosophila Smad 4* homolog that is differentially required to potentiate DPP responses. *Development* **125**, 1433-1445.
- Wodarz, A., and Nusse, R. (1998). Mechanisms of Wnt signaling in development. *Annu. Rev. Cell Dev. Biol.* **14**, 59-88.
- Wolpert, L. (1969). Positional information and the spatial pattern of cellular differentiation. *J. Theoret. Biol.* **25**, 1-47.
- Wolpert, L. (1989). Positional information revisited. *Development* **107** (Suppl.), 3-12.
- Wolpert, L. (1996). One hundred years of positional information. *Trends Genet.* **12**, 359-364.
- Woods, A., Couchman, J. R., Johansson, S., and Hook, M. (1986). Adhesion and cytoskeletal organization of fibroblast in response to fibronectin fragments. *EMBO J.* **5**, 665-670.
- Woods, A., and Couchman, J. (1998). Syndecans: synergistic activators of cell adhesion. *Trends Cell Biol.* **8**, 189-192.
- Wozney, J. M. (1998). The bone morphogenetic protein family: multifunctional cellular regulators in the embryo and adult. *Eur. J. Oral Sci.* **1** (Suppl), 160-166.
- Wozney, J. M., and Rosen, V. (1998). Bone morphogenetic protein and bone morphogenetic protein gene family in bone formation and repair. *Clin. Orthop.* **11**, 26-37.
- Wrana, J. L., Carcamo, J., Attisano, L., Cheifetz, S., Zentella, A., Lopez-Casillas, F., and Massague, J. (1992). The type II TGF- β receptor signals diverse responses in cooperation with the type I receptor. *Cold Spring Harb. Symp. Quant. Biol.* **57**, 81-86.

- Wrana, J. L., Attisano, L., Wieser, R., Ventura, F., and Massague, J. (1994a). Mechanism of activation of the TGF- β receptor. *Nature* **370**, 341-347.
- Wrana, J. L., Tran, H., Attisano, L., Arora, K., Childs, S. R., Massague, J., and O'Conner, M. B. (1994b). Two distinct transmembrane serine/threonine kinases from *Drosophila melanogaster* from an activin receptor complex. *Mol. Cell Biol.* **14**, 944-950.
- Wright, D. A., and Lawrence, P. A. (1981). Regeneration of the segment boundary in *Oncopeltus*. *Dev. Biol.* **85**, 317-327.
- Wu Dunn, D., and Spear, P. G. (1989). Initial interaction of herpes simplex virus with cells is binding to heparan sulfate. *J. Virology* **63**, 52-58.
- Xie, L., Finelli, A. L., and Padgett, R. W. (1994). The *Drosophila saxophone* gene: a serine-threonine kinase receptor of the TGF- β superfamily. *Science* **263**, 1756-1759.
- Xu, T., and Rubin, G. (1993). Analysis of genetic mosaics in developing and adult *Drosophila* tissues. *Development* **117**, 1223-1229.
- Yanagishita, M., and Hascall, V. C. (1992). Integral membrane heparan sulfate proteoglycans. *J. Biol. Chem.* **267**, 9451-9454.
- Yayon, A., Klagsburn, M., Esko, J. D., Leder, P., and Ornitz, D. M. (1991). Cell surface, heparin-like molecules are required for binding of basic FGF to its high affinity receptor. *Cell* **64**, 841-848.
- Zecca, M., Basler, K., and Struhl, G. (1995). Sequential organizing activities of *engrailed*, *hedgehog* and *decapentaplegic* in the *Drosophila* wing. *Development* **121**, 2265-2278.
- Zecca, M., Basler, K., and Struhl, G. (1996). Direct and long-range action of *Wingless* morphogen gradient. *Cell* **8**, 833-844.
- Zimmerman, J. B., De Jesus-Escobar, J. M., and Harland, R. M. (1996). The Spemann organizer signal *noggin* binds and inactivates BMP-4. *Cell* **86**, 599-606.
- Zusman, S. B., Francois, V., and Bier, E. (1988). *Short gastrulation*, a mutation causing delays in stage-specific shape changes during gastrulation in *Drosophila melanogaster*. *Dev. Biol.* **129**, 417-427.

Appendix I. Synthesis pathways for the formation of UDP-sugars (Prydz and Dalen, 2000)



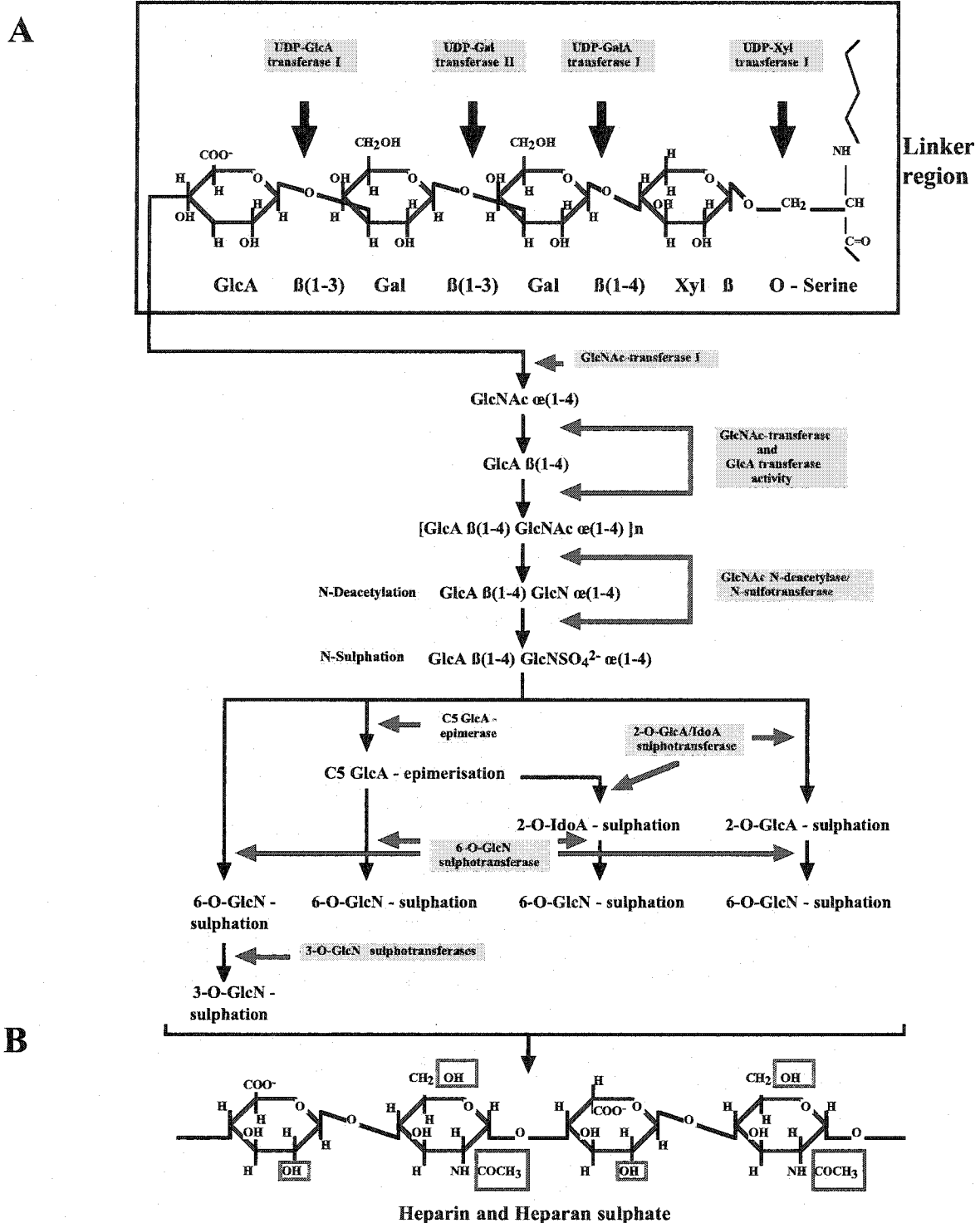
Synthesis pathways for the formation of UDP-sugars and PAPS required for the synthesis of proteoglycans. Each UDP-sugar and PAPS is actively transported from the cytosol into the Golgi lumen, by a corresponding transporter. **Abbreviations:** APS, Adenosine-5-phosphosulfate; ERGIC, ER-Golgi Intermediate Compartment; Gal, Galactose; GalNAc, N-acetyl-Galactosamine; Glc, Glucose; GlcA, Glucuronic acid; GlcN, N-Glucosamine; GlcNAc, N-acetyl-Glucosamine; IdoA, Iduronic acid; PAPS, 3'-Phosphoadenosine-5'-phosphosulfate; Xyl, Xylose.

Appendix II. The structure of disaccharide residues of different glycosaminoglycan chains (Prydz and Dalen, 2000)

GAG	Hexuronic or Iduronic acid	Galactose	Hexosamine	Disaccharide composition
Heparan sulphate / Heparin	D-glucuronic acid (GlcA) L-iduronic acid (IdoA)		D-glucosamine (GlcNAc)	<p>GlcA β(1-4) GlcNAc α(1-4) IdoA α(1-4) GlcNAc α(1-4)</p>
Keratan sulphate		D-galactose (Gal)	D-glucosamine (GlcNAc)	<p>GalA β(1-4) GlcNAc β(1-3)</p>
Chondroitin sulphate	D-glucuronic acid (GlcA)		D-galactosamine (GalNAc)	<p>GlcA β(1-3) GalNAc β(1-4)</p>
Decoran sulphate	D-glucuronic acid (GlcA) L-iduronic acid (IdoA)		D-galactosamine (GalNAc)	<p>IdoA β(1-3) GalNAc β(1-4)</p>
Hyaluronic acid	D-glucuronic acid (GlcA)		D-glucosamine (GlcNAc)	<p>GlcA β(1-3) GlcNAc β(1-4)</p>

The structure of the repeating disaccharides in the different types of GAG chains. The sulfation modifications are not shown.

Appendix III. The heparin and heparan sulfate biosynthetic pathway (review Lander et al., 1999)



(A). The different steps in the synthesis of heparin and heparan sulfate GAG chains of the GlcA-Gal-Gal-Xyl-linker region. (B) The different sulfation positions in each GAG are marked in blue.

TGTTT TACTAGTAATCATT TGATA TTTAGCCAGACCTACAAA ACTCCAAGT AAGT TTT CGCGCAGT GTA GT CCGTCTT CACTTGAA CAACGCT

GCCTGT CCGGCATTCTACT AGACTTCAGGT GCTTAACGCACCTTGGCCACAA CAAGGTCAATGGT CAGTCCATT AGTCACT CAAAAT AAAOC

ATGAAAAGCGCGCAGAGCCGTTTGATTGCTGAAATATGATT CGGAA CGGAAAAGT AGAGTGGGAATCGATTTTACTTCCAGACT GCGTGAC

CATCGGCGTCCCTCCATTAGGCCTAAAATTCCAGATACTACAAAATGCGCCAAA CGAAGCCARAA GGTGCAA GCGGATTGCCTCCCATCCAC

CACACCACTGGCGCATTTCOGT CCTGGCTTCCGCCGCTCATTTCCCACTGTACATATGT CGAGCTAACCACTCTTCTTATCGGCTCTGCG

CCAAAACAAAGTCTCGGGT CGAGATAAGCTCGCTGGGCATGGCGTTTCTTATATTTT TGGTTT ACCGACCGCACATTAGTTGGA AATTG

TCCAAT TACCCACGT TCTCGACAAACAGCCAGTATCTCTGGT GAAAAAAAAGCACCGAATAGAAAGTATGTACAATCAGCCAAA CACTCAGTA

TATATGTTT GTTTCTAT TAGACAATAATTTGGTATTTGTAT CCTATAGCAGT AGTAATCAGTTAAAA ACCATACATTTGGAAAGATGGT

ATAGGGCATATATTAAGCTCAT TCTTATCGCCCTACTATTGTATCCCTAAAAATAGT TAAAA CCCATTAAGAAAATACACTATTGACTGCA

GCCTAGAA GCTTATCGATACCGTCGACCTCGAGGGGGG

The nucleotide sequence of the *A64* (1-1) 3L 1.8 kbp genomic flanking region rescued from the P-element insertion line A64. A 5' initiation codon at position 297 corresponds to the translation start site of the UDP-GlcDH gene of *Drosophila*. The ORF extends 835 bp downstream of the 5' start site, encoding the first 273 amino acids of the enzyme.